"*Science is not a body of knowledge nor a system of belief; it is just a term which describes humankind's incremental acquisition of understanding through observation. Science is awesome.*" – Tim Minchin, Australian musician, actor, comedian and writer

Promotor

Prof. dr. ir. Korneel Rabaey

Center for Microbial Ecology and Technology (CMET),

Department of Biochemical and Microbial Technology,

Faculty of Bioscience Engineering, Ghent University

Members of the examination committee

Prof. dr. ir. Lars Angenent

Center for Applied Geosciences, University of Tübingen, Germany

Department of Biological and Environmental Engineering, Cornell University, USA

Prof. dr. ir. Annemiek Ter Heijne

Department of Environmental Technology, Wageningen University, The Netherlands

Prof. dr. ir. Pascal Boeckx

Department of Applied Analytical and Physical Chemistry, Faculty of Bioscience Engineering, Ghent University

Prof. dr. ir. Marjan De Mey

Department of Biochemical and Microbial Technology, Faculty of Bioscience Engineering, Ghent University

Prof. dr. ir. Monica Höfte

Department of Crop Protection, Faculty of Bioscience Engineering, Ghent University

Dean of the faculty of Bioscience Engineering, Ghent University

Prof. dr. ir. Marc Van Meirvenne

Rector of Ghent University

Prof. dr. Anne De Paepe

Technology and tools for bioelectrochemical production of short- and medium-chain carboxylic acids from CO_2

Ir. Sylvia Gildemyn

Thesis submitted in fulfillment of the requirements for the degree of Doctor (PhD) in Applied Biological Sciences: Environmental Technology

Dutch translation of the title

Technologie en technieken voor de bio-elektrochemische productie van korte-en middellange-keten carbonzuren uit CO_2

Citing this PhD:

Gildemyn, S. (2016). Technology and tools for bioelectrochemical production of short- and medium-chain carboxylic acids from CO_2. PhD thesis, Ghent University, Belgium

ISBN 978-90-5989-923-0

The work presented in this thesis was performed at the Center for Microbial Ecology and Technology, in the Faculty of Bioscience Engineering at Ghent University (Gent, Belgium), and at the Angenent Lab, in the Department of Biological and Environmental Engineering at Cornell University (Ithaca, NY, USA). This work was supported by the Special Research Fund (Bijzonder Onderzoeksfonds) of Ghent University.

Cover illustration

Cédric Vanhoeck

Notation Index

AEM	Anion exchange membrane
ATP	Adenosine triphosphate
BES	Bioelectrochemical system
BPM	Bipolar membrane
CCS	Carbon capture and storage
CCU	Carbon capture and utilization
CE	Coulombic efficiency
CEM	Cation exchange membrane
COD	Chemical oxygen demand
CV	Cyclic voltammetry
CZV	Chemische zuurstofvraag
DET	Direct electron transfer
ED	Electrodialysis
GRS	Growth reference system
HRT	Hydraulic residence time
MCCA	Medium-chain carboxylic acid
ME	Membrane electrolysis
MEC	Microbial electrolysis cell
MES	Microbial electrosynthesis / Microbiële elektrosynthese
MET	Microbial electrochemical technology
MFC	Microbial fuel cell

OCP	Open circuit potential
OLR	Organic loading rate
RED	Reverse electrodialysis
SCCA	Short-chain carboxylic acid
SHE	Standard hydrogen electrode
SRT	Sludge residence time
toe	ton oil equivalent
vs.	versus
γ	Degree of reduction
$\Delta G_e^{0'}$	Gibbs energy per electron
$E^{0'}$	Theoretical cell voltage of a reaction at biochemical standard conditions
F	Faraday's number (96485.3 C/mol)

Table of Contents

CHAPTER 1 – GENERAL INTRODUCTION: ELECTRICITY AS A DRIVER FOR MICROBIAL PROCESSES

1. The carbon economy

The world economy is highly dependent on fossil fuel resources. Fossil fuels are used for production of both energy and chemicals. Through energy production and industrial processes fossil fuel resources are transformed from a reduced product to carbon dioxide (CO_2), the most oxidized form of carbon, and an important greenhouse gas. Climate change caused by the use of fossil fuels is the main problem of our current carbon-based economic model, not the announced depletion of fossil fuels. The current economic model is often called a carbon economy. It is characterized by an important interrelationship between the source of energy and the building blocks for production of chemicals.

1.1 Our consumption pattern relies on fossil fuels

Global primary energy consumption increases yearly. In the period 2004-2014, consumption increased at an average of 2.1%, reaching 12930 million ton oil equivalents (toe) in 2014 (BP, 2015). More than 86% of this energy was obtained from fossil fuel resources (oil, natural gas and coal) (BP, 2015). A vast majority of these fossil fuel resources were used for energy production, while only 5%-10% were used for production of chemicals (Deloitte, 2014). Flanders consumed a total of 35000 ktoe in 2014 and only 5.7% of this energy was obtained from renewable resources. Nuclear heat accounted for 11% of Flanders' energy production. Although nuclear energy is not obtained from fossil fuel resources, it remains is a non-renewable resource (VITO, 2015). Worldwide emissions of greenhouse gases associated with consumption of fossil fuel resources are as high as 50 Gton CO_2-equivalents per year, while Flanders emits 74.1 Mton CO_2-equivalents. About 70% of these emissions are actual CO_2 and other greenhouse gases complete the balance (EPA, 2014; MIRA-VMM, 2016).

Primary energy is used in different industrial sectors and emissions can thus be distributed amongst those (Table 1.1) (IPCC, 2014; MIRA-VMM, 2016). Flanders is a densely populated industrialized area, which explains the higher contribution of industry and transportation to greenhouse gas emissions. About half of the emissions are derived from point sources (energy and industry), while other sectors such as transportation contribute to diffuse emissions. To decrease greenhouse gas emissions, a different mitigation strategy is necessary for these two types of emissions. Concentrated carbon emissions could be captured at point sources and sequestered or used as a carbon source for production (Markewitz et al., 2012). Diffuse sources are, however, characterized by low concentration emissions, making mitigation more challenging.

Table 1.1 – Distribution of greenhouse gas emissions per sector (%) for the world and Flanders.

Sector	Worldwide emissions (%)	Emissions in Flanders (%)
Energy	26	24
Industry	19	27
Forestry, agriculture and land use	31	5
Transport	13	21
Other	11	23

It is a common misconception that the future lack of fossil fuel resources is the driver for the implementation of sustainable technologies. A transition toward the use of renewable resources is in fact not an urgent matter when considering the known stocks of fossil fuels (Shafiee & Topal, 2009). Current carbon reserves, and coal in particular, allow to secure the energy demand for longer than the coming century. However, the emissions associated with the use of these stocks and the subsequent increase in global temperature, form the core problem. To keep the temperature increase below 2°C with 75% certainty, a maximum of 1100 Gton CO_2-equivalents can be emitted in the period 2000-2050 (McGlade & Ekins, 2015). Considering the increasing demand for energy during this period, a business-as-usual scenario would lead to the emission of 1790 Gton CO_2-equivalents by 2050 (BP, 2012). As a result, to achieve the objectives regarding temperature mitigation, a decrease and a shift in utilization of fossil fuel resources is needed. Transitioning toward a carbon-free economy would mean that most of the known fossil fuel stocks have to remain untouched. As we also highly depend on fossil fuels for production of our daily-use materials (plastics, cosmetics, clothing, building materials), a rapid ban of all carbon seems unlikely. A possible scenario is the transition toward a carbon-neutral economy, where not the use of carbon, but its emission into the atmosphere is avoided (Hunt et al., 2010).

1.2 A transition toward renewable resources for energy and chemicals

Fossil fuels are convenient sources of energy because of their high energy density, about 45 MJ/kg for liquid fuels (DOE, 2016). They can be used both for electricity production, as transportation fuel and for production of chemicals and materials. The economy of scale is a crucial advantage of the carbon economy and the petrochemical industry. Transitioning away from fossil fuels requires a diversification of the energy and chemical market. In the future carbon-neutral economy a wide variety of technologies will replace fossil fuel resources.

For electricity production, several alternatives to fossil fuels are already implemented at large scale. Nuclear power provides electricity at low emission levels, but due to the non-renewable nature of the energy generation it is not considered as a sustainable alternative. The sun's energy and gravity are the source of most renewable energy (Table 1.2) (Albrecht & Laleman, 2015). Renewable electricity is strictly-speaking not carbon-neutral because equipment, transport and materials require an input of fossil fuel resources. Carbon dioxide emissions are,

however, significantly lower than fossil fuel derived electricity. Electricity production from natural gas, the cleanest fossil fuel, emits at least 6 times more CO_2 than any form of renewable electricity production. By using renewable resources for electricity production, a large number of point sources of CO_2 emissions, electricity plants, will disappear. A downside of renewable energy is that the production is in many cases more difficult to control. A gap between production and demand can exist, both at a geographical level and at a time level. An efficient and large-scale system to store the peak electricity will be needed to transition to a carbon-neutral or fossil fuel-free society (Dunn et al., 2011).

Table 1.2 – Emissions (CO_2/kWh) for different types of electricity. Electricity production from natural gas (the cleanest type fossil fuel) is given as a benchmark. n.d.: not determined.

Electricity type	Origin	Emissions (CO_2/kWh)
Natural gas	Solar	600
Biomass	Solar	100
Wind	Solar	20
Photovoltaic	Solar	100
Nuclear	Nuclear fission	50
Tidal	Gravity	n.d.
Hydropower	Solar + gravity	30

In the case of transportation, alternative fuels are needed to eliminate diffuse CO_2 emissions. Electric cars are promoted as sustainable mean of transportation. Electric vehicles are at least three times more energy-efficient than gasoline powered cars, based on the energy content of gasoline and an equivalent amount of electrical energy (DOE, 2016). To store the electrical energy efficient batteries are needed. These batteries require expensive and rare metals and are accompanied by issues of scarcity, recycling and geopolitical supply problems (Graedel et al., 2015).

Another renewable alternative is the use of biofuels such as bioethanol and biodiesel. Their production is, however, characterized by a large input of land, nutrients and water resources. Bioethanol production in the U.S. for example, requires about 3 m² land and 570 L water per L ethanol produced. Considering that about 35 billion L ethanol is produced yearly in the U.S, this increases the pressure on food production and land management (Dominguez-Faus et al., 2009). Second generation biofuels that use lignocellulosic biomass can only be produced with a large input of chemicals to purify the cellulose from this biomass (Havlík et al., 2011; Liao et al., 2016). In additions, biomass derived fuels suffer from transport requirements of biomass toward a central production facility.

Biomass could also be converted to methane (CH_4) in a delocalized manner, as this is already a highly distributed fuel. Hydrogen (H_2) can be produced from renewable electricity through water electrolysis at 99% electron efficiency, and approximately 80% energetic efficiency. It only

produces water upon combustion, but its storage and transportation remain problematic (Li et al., 2015). Catalysis and electrocatalysis of CO_2 for the production of reduced C1-compounds such as methane and methanol is also being investigated as a safer alternative to H_2. Methanol has good fuel properties and can be further processed to hydrocarbons with longer carbon chains. Methanol thus bridges CO_2 based catalysis and the petrochemical production processes (Lim, 2015). Alternative fuel sources for cars start being spread, but for other transportation means such as aviation and nautical transport fossil fuels currently remain the sole option (De Guzman, 2011).

Production of chemicals and materials from renewable resources such as biomass faces the same problems as fuel production. Many carbon fuels and products that are produced from renewable resources are essentially simple molecules (alcohols, esters) that can act as building blocks for the production of other materials. Chemical transformation processes are usually well established as part of the petrochemical industry. Besides the direct use of fossil fuels for materials production, fossil fuels can be required indirectly during the production process. The indirect use of fossil fuel as energy vector for stainless steel production, for example, will also lead to point source emissions (Molitor et al., 2016). Utilizing the carbon that is emitted at these point sources to produce chemicals and materials would contribute to a carbon-neutral economy. This strategy is defined as “carbon capture and utilization” (CCU, (Markewitz et al., 2012)). Besides exhaust gas purification, an additional energy input is required to reduce CO_2 to a useful form. This reduction process can be both chemical and biological and contributes to carbon-neutrality when renewable electricity is used as a driver (Hunt et al., 2010).

In this work, the issues discussed above are brought together: it was investigated how electricity can drive microbial processes to capture CO_2 and CO in added value chemicals. By implementing technologies that capture and reuse CO_2, the targeted emission reduction can be achieved, which is the main driver for this work. Many point sources of carbon emissions are available, as well as clean, renewable forms of electricity. Bacterial metabolism is essentially the exchange of electrons, a feature that has been exploited in the bioelectrochemical systems (BESs). In the coming sections, it is explained how electricity can be a driver of three processes occurring in BESs: anodic oxidations, cathodic reductions and ionic transport processes (Figure 1.1).

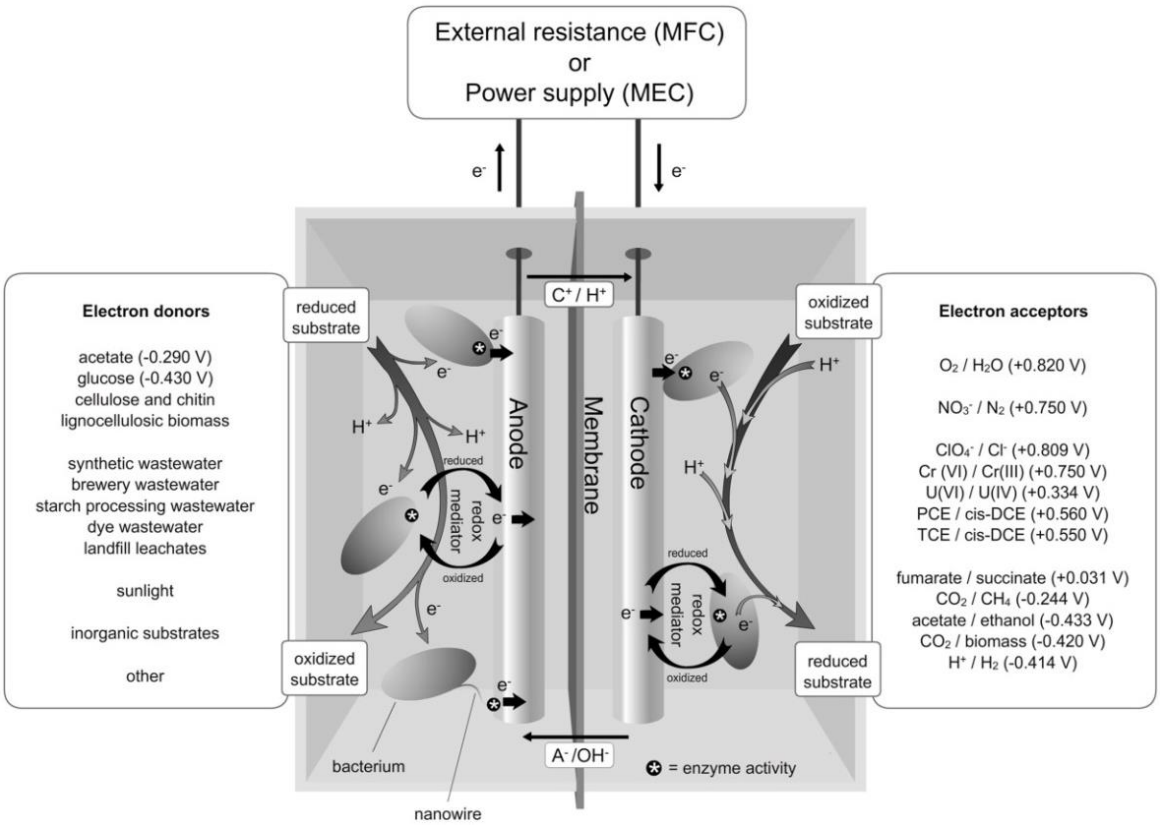

Figure 1.1 - In a bioelectrochemical system, microbial metabolism can drive the anodic oxidation and/or the cathodic reduction. Ions are transported over an ion exchange membrane to restore the charge balance. *A-: anion; C+: cation; e-: electron.* When operated as microbial fuel cell (MFC), electrical power is produced; in microbial electrolysis cell (MEC) mode invested electrical power drives a cathodic reduction reaction. Sunlight is mentionned as indirect electron donor as it can drive water electrolysis at the anode. Copied from Arends et al. (2012).

2. Microorganisms and electricity

2.1 The anode as solid electron acceptor

Biochemical processes are associated with a change in electric potential. This conclusion was already drawn in the early 20th century and was illustrated, among other experiments, by the development of a voltage between two platinum electrodes in a solution containing bacteria fermenting sugars (Potter, 1911). It was shown later that bacteria can interact directly or indirectly with solid electron acceptors (Lovley & Phillips, 1988; Myers & Nealson, 1988). In anaerobic environments the absence of dissolved electron acceptors forces bacteria to reduce minerals such as manganese and iron to obtain energy for their growth. This unique feature of bacterial metabolism resulted in the development of microbial fuel cell (MFC) technology, a term later broadened to bioelectrochemical systems (BESs). BESs are a type of electrochemical cell in which at least one of the two electrode reactions is biologically catalyzed, in contrast to chemical fuel and electrolysis cells. The spatial separation between the oxidation and reduction reaction is a key feature of electrochemical cells.

Extracellular electron transfer to generate electricity from waste

Microorganisms that can transport electrons in and out of their cell to sustain their metabolism are known as microbial electrocatalysts. Unlike real catalysts they derive part of the energy for their growth. The microorganisms grow as a biofilm on the electrode, using the substrate provided as electron donor and the electrode as electron acceptor (Schröder, 2007). A wide variety of substrates can be used by the electrocatalysts, ranging from carboxylic acids to wastewater. Three mechanisms of electron transfer are possible: i) *via* soluble electron redox mediators known as shuttles; ii) *via* direct contact between the outer membrane cytochromes and the solid electron acceptor; and iii) *via* contact with the electrode through so-called pili or nanowires. These electron transfer mechanisms can be combined simultaneously in one biofilm. The use of nanowires and electron shuttles allows the formation of thicker biofilms, up to 50 µm (Pham et al., 2009).

Several molecules have been identified as shuttles in microbial biofilms. These molecules are reversely redox-active and have a mid-point potential between the equilibrium potential of the electron donor (the substrate) and electron acceptor (the electrode) (Hernandez & Newman, 2001). *Pseudomonas aeruginosa* produces phenazines such as pyocyanin and *Shewanella oneidensis* synthesizes quinones that act as redox shuttles (Newman & Kolter, 2000; Rabaey et al., 2005). Certain species that do not have the capability to produce the shuttles themselves can utilize them when they are externally provided or produced by other microorganism (Rabaey et al., 2007).

Cytochromes seem to play a crucial role in direct electron transfer (DET). They are the final element in the respiratory electron transport chain and are located in the outer cell membrane (Richardson, 2000). Genetic analysis of *Geobacter sulfurreducens*, which is an organism often enriched on bioanodes, confirmed the role of outer-membrane cytochromes (Holmes et al., 2006), while also the role of cytochromes in DET in *S. oneidensis* has been elucidated (Bretschger et al., 2010). Additionally, both organisms produce bacterial nanowires to conduct electrons. In the case of *G. sulfurreducens*, these are pili, while for *S. oneidensis* these appendices are an extension of the outer membrane (Reguera et al., 2005; Gorby et al., 2006; Subramanian et al., 2016). The mechanisms through which electrons are transferred in the pili and whether these pili show metallic-like conductivity, electron hopping, or another mechanism, remains a subject of debate (Snider et al., 2012; Lovley & Malvankar, 2015).

The transfer of electrons to the electrode is inherently subjected to losses, both in generated current and generated potential (Clauwaert et al., 2008a). The coulombic efficiency (CE) is calculated as the percentage of electrons from the substrate that is measured as current. As part of the electrons is used to sustain biomass growth, a 100% CE cannot be achieved on a continuous basis. Losses in generated potential are due to cellular losses, electrode overpotentials and resistances in the system (*e.g.* the membrane). Some of these losses are irreversible losses. Slow electrode kinetics for example, decrease the cell voltage through activation overpotentials (Schröder & Harnisch, 2010). It is also critical to avoid a pH-gradient buildup between the anode and cathode, which occurs when protons are not efficiently transferred over the cation exchange membrane (CEM) to balance the charge. The use of an anion exchange membrane (AEM) has been proposed to partially decrease those losses (Cheng & Logan, 2007). As a result of these losses, the open circuit potential (OCP) is not measured during operation of the cell (Figure 1.2 (Logan, 2009)). Figure 1.2 also illustrates how bacteria that can operate close to the thermodynamic limit can outcompete other species in mixed culture systems, given their growth rate is sufficiently high: a lower anodic overpotential means that less Gibbs free energy is available for ATP formation, which is a competitive advantage for a species that can thrive in such energy-limited conditions. Minimizing losses in BESs is crucial to create value and enable applications. Certain strategies however, such as the use of highly buffered electrolytes to reduce resistance, bring the MFC technology far from the real environments where the technology could be applied.

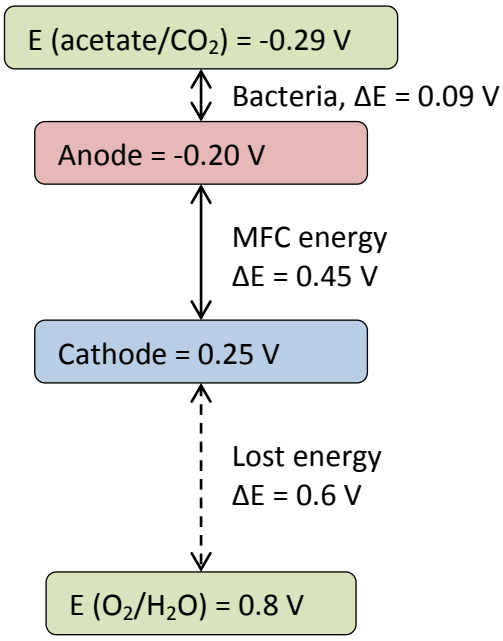

Figure 1.2 - The energy gained from an operating MFC compared to the losses occurring in the system. For an MFC operating on acetate the difference between the equilibrium potential of the acetate/CO_2 couple and the actual anode potential is the maximal energy gain for the bacteria. Figure adapted from Logan (2009).

Bioanodes for technologic applications

The performance of MFCs has been evaluated based on the generated current density and power density. The large variety in system configurations and the lack or standardized way of reporting makes comparison of performance difficult (Harnisch & Rabaey, 2012; Sharma et al., 2014; Patil et al., 2015b). Power densities in the range of 2-3 $W/m^2_{projected\ electrode\ area}$ are usually achieved under ideal conditions. Wastewater MFCs usually produce power densities up to 0.5 W/m^2 because of the lower degradability of the organics, the lower conductivity and lower buffer capacity (Logan & Rabaey, 2012). Optimization of the anode material has often been tested as strategy to boost the current production (Pham et al., 2009). Carbon materials are usually used because of their biocompatibility, but the relatively low conductivity can cause problems when scaling up the system. The chemical properties of the (carbon) anode can be altered through pretreatment of the electrode material (Guo et al., 2014b) or addition of functional groups that favor the microbial attachment (Picot et al., 2011). Adapting the structure and the design of the anode to create a 3D electrode has also been proven to be a successful strategy (Logan et al., 2007; Chen et al., 2012).

The initial application that was envisioned for the MFC technology was wastewater treatment, as power can be produced by treating the water, unlike through the classic energy-demanding aerobic treatments. Looking critically at the performance of MFCs for wastewater treatment, the present energy recovery is too low to make the technology economically feasible for large scale, mainstream applications. Less than 5% of the energy inherently present in the

wastewater is usually recovered as power output (Heidrich et al., 2010; Hays et al., 2011). Niche applications in wastewater treatment, or applications creating added value, such as the recovery of nutrients, therefore, seem more promising (Puig et al., 2011; Kuntke et al., 2012). Even though some companies are developing MFC technology for wastewater treatment, established technologies such as anaerobic digestion have a competitive advantage due to more efficient energy generation (Angenent et al., 2004; Arends & Verstraete, 2012).

The use of MFCs in remote areas to power sensing devices or remove pollutants might be a more successful niche application. MFCs can, thereby, act as biosensing devices, to measure specific contaminants present in water, such as arsenite (Webster et al., 2014). In another application, a sediment MFC was designed to power a temperature sensor (Donovan et al., 2013). Removal of pollutants such as hydrocarbons from groundwater and sediments has been shown to be feasible but would require very large electrode surface areas upon implementation (Zhang et al., 2010).

After almost 20 years of research and technological improvements, MFCs are limited to niche applications. While the questions on electron transfer between organisms and the electrode remain scientifically interesting, the high cost of materials hampers the technological development (Rozendal et al., 2008a; Rosenbaum & Franks, 2013). The focus of research has, therefore, moved to creation of added value in cathodic processes, through bioremediation or bioproduction.

2.2 Bioproduction using the cathode as a source of reducing power

Reductive processes can either be driven by a biological or chemical anode. Certain applications generate electricity (MFCs) while others require an additional energy input (microbial electrolysis cells (MECs)). With the development of MEC systems, the focus has shifted from energy production to value creation. The first BESs with biocathodes for the generation of added value were systems for the reduction of oxidized contaminants. The second, and now most-studied application, is the production of chemicals and bioproducts at a (bio)cathode.

The cathode as solid electron donor

Bioremediation of oxidized substances requires an electron donor. By using the electrons from an electrode to stimulate microbial metabolism, additions of organics or chemicals can be avoided. Cathode-driven reductive metabolism was first demonstrated with the reduction of nitrate to nitrite, both with a pure culture of *Geobacter metallireducens* and an enriched mixed culture that was formerly functioning as bioanode (Gregory et al., 2004; Clauwaert et al., 2007a). Another pure culture (*Geobacter lovleyi*) was used as microbial electrocatalyst for the reduction

of tetrachloroethene to *cis*-dichloroethene (Strycharz et al., 2008). A wide variety of toxic compounds, such as perchlorate or trichloroethene, can now be reduced at biocathodes (Gregory & Lovley, 2005; Thrash et al., 2007; Aulenta et al., 2010; Huang et al., 2011).

Production of biochemicals through cathodic reductions

The second application of cathodic reductions in BESs is the production of chemicals. Three configurations can be designed: i) a bioanode combined with a chemical cathode; ii) a chemical anode combined with a biocathode; or iii) a bioanode combined with a biocathode. The focus will be on production through the first two configurations, as studies with the combination of two bioelectrodes are limited (Geelhoed & Stams, 2011; Gong et al., 2012).

Production of chemicals at the cathode, driven by a bioanode (configuration i), was first demonstrated in two independent studies producing H_2 in a MEC (Liu et al., 2005c; Rozendal et al., 2006b). This is not a biocathodic reaction, but because organic matter is oxidized at the anode by microbial electrocatalyst, H_2 can be generated at a lower energy-input compared to a system with water oxidation. To reduce overpotentials at the cathode, catalysts such as platinum are preferred materials (Logan et al., 2008). Production yields up to 93% have been reported, while other studies could lower the energy input to as low as 1 kWh/m² H_2 produced, which is more than 5 times less than the energy required for H_2 production *via* water electrolysis (Logan et al., 2008). Compared to other BES technologies, H_2 production in an MEC generates added value (Rozendal et al., 2008a). The same strategy of a bioanode linked to a chemical anode has been applied to the production of hydrogen peroxide and caustic. In both cases wastewater treatment is, thereby, coupled to the production of a low-cost disinfectant (Rozendal et al., 2009; Rabaey et al., 2010).

Biocathodes for bioproduction (configuration ii) were first used in combination with a chemical anode as a storage strategy for peak renewable electricity. Hydrogen production and CH_4 production from CO_2 have been studied in this perspective (Rozendal et al., 2008b; Cheng et al., 2009; Villano et al., 2011). The disadvantage of this production strategy is the pressurization required for gas storage. Methane production with hydrogen from electrolysis is now being developed as full scale technology. For example, the company Electrochaea (www.electrochaea.com) is producing methane from CO_2 and H_2 with the latter being produced with an abiotic cathode from an electrolyzer. In the future, the technology could benefit by using biocathodes into one system.

The reductive power of a biocathode can also be used to drive the microbial metabolism for the conversion of organic products. This way low value organics can be transformed into added-value fuels and chemicals. The conversion of acetic acid to ethanol by a mixed culture has as

such been studied (Steinbusch et al., 2010). The addition of the mediator methyl viologen (MV) was necessary to increase production rates. It was, however, unclear if the MV only acted as inhibitor of methanogens and chain elongating bacteria, thus favoring the reduction of acetic acid to ethanol, or if the MV effectively shuttled electrons.

Electricity as reducing power can also alter microbial metabolism. The reduction of glycerol to 1,3-propanediol, propionic acid, and valeric acid was possible using electricity as source of reducing power, but not when supplied with H_2. The high partial pressures of H_2 in the vicinity of the cathode possibly favored the reduction process, but the exact reduction mechanisms are not yet fully understood (Dennis et al., 2013). In another case, *Geobacter sulfurreducens* was used for the reduction of fumarate to succinate. This organism is a known anodic microbial electrocatalyst and has the ability to reverse the electron transfer chain to receive electrons from a cathode (Gregory et al., 2004).

Microbial electrosynthesis from CO_2

The most-studied process using biocathodes is microbial electrosynthesis (MES). MES is defined as the microbially catalyzed reduction of CO_2 to multicarbon organics using electrons as source of reducing power (Rabaey et al., 2011). It allows the production of biochemicals almost independently from land use, using renewable energy. Other advantages over the biorefinery route are the higher efficiency of solar panels compared to plants to capture solar energy and the direct synthesis of products rather than biomass that requires more intensive processing (Nevin et al., 2010; Desloover et al., 2012b).

The first report on MES concerned the production of acetic acid using a pure culture of *Sporomusa ovata*, which is a known homoacetogenic organism, with a carbon electrode poised at -400 mV *vs.* the standard hydrogen electrode (SHE). The coulombic efficiency (CE), here defined as the percentage of electrons delivered by the electrode recovered in the final product, reached 86% (Nevin et al., 2010). MES of acetic acid was soon after described with other pure cultures and a mixed culture (Nevin et al., 2011; Marshall et al., 2012). Besides the use of either pure or mixed cultures, various other conditions have been tested and optimized for MES, including the mode of operation (fixed potential *vs.* fixed current) and the electrode materials. The high variability in designs and reported performance parameters makes comparisons between studies difficult, especially regarding production rates (Table 1.3) (Patil et al., 2015b).

Acetic acid is the main product of MES. Acetic acid has a variable value, currently $370/ton, and is used, *inter alia*, as precursor for the production of polymers and solvents (Marshall et al., 2013a). Most acetic acid is produced from fossil fuel resources (90%), the remaining is produced via ethanol oxidation. In MES, acetic acid production primarily relies on homoacetogenic

organisms that use the Wood-Ljungdahl pathway to reduce CO_2 to acetic acid. Mixed cultures for MES are usually obtained from anaerobic fermentative environments such as anaerobic digesters or syngas fermenters (Ganigué et al., 2015). Methane production has regularly been reported in MES, unless inhibitors are added or a pre-enrichment of the culture eliminated the methanogens (Jiang et al., 2013; Marshall et al., 2013b; Patil et al., 2015a). Longer chain carboxylic acids, such as butyric acid, have also been produced from CO_2 in MES (Ganigué et al., 2015). This is not a surprising finding as butyric acid can either be produced through the Wood-Ljungdahl pathway or through chain elongation, which is a metabolic pathway typically present in anaerobic mixed cultures (Spirito et al., 2014). Details regarding metabolic pathways are given in the next section.

Unlike bioanodic electron transfer, which has been thoroughly studied and for which mechanisms are now well understood, there is currently no mechanistic explanation on how bacteria receive electrons from the cathode during MES (Lovley, 2011; Rosenbaum et al., 2011). For most MES studies it is concluded that, as no H_2 was produced in abiotic control experiments, a direct transfer of electrons took place from the electrode to the microorganisms in the biofilm. An increased catalysis and shift in the onset potential of the H_2 evolution reaction to more positive potentials has regularly been noted for biocathodes (Marshall et al., 2012; Patil et al., 2015a). Two possible explanations for the different behavior of abiotic cathodes and colonized cathodes can now be given. First, the sorption of hydrogenase enzymes on the cathode could facilitate H_2 evolution. The role of the enzymes was elucidated using genetically modified organisms lacking hydrogenases and through electrochemical experiments with cell-free medium (Deutzmann et al., 2015). A second mechanism to enhance H_2 evolution can be the modification of the electrode surface through precipitation of metal nanoparticles. Metals such as copper are usually present in growth media used for MES. It was found that microorganism can induce the precipitation of the copper on the electrode, thereby enhancing the catalysis (Jourdin et al., 2016b). In both cases the presence of a biofilm on the electrode combined with a rapid uptake of the abiotically produced H_2 can explain why H_2 is usually not detected in MES experiments. Early reports of DET at biocathodes might be because of indirect electron transfer *via* H_2 after all.

Table 1.3 - Key production parameters for selected studies on MES of acetic acid. Adapted from Patil et al. (2015a). WW: wastewater; WWTP: wastewater treatment plant; n.d.: not defined.

Microbial inoculum/Reactor operation			$J_{applied/produced}$ (A/m^2)[a]	$E_{cathode}$ (V vs. SHE)	Volumetric production rate mM/day	Surface based rate ($g/m^2_{cathode}/day$)[a]	Max. product titer (g/L)	Coulombic efficiency in acetic acid	Reference
Pure cultures	Continuous	*Sporomusa ovata*	-0.208	-0.4	0.17	1.3	0.063[b]	85%	Nevin et al. (2010)
		Sporomusa ovata	-0.63	-0.4	1.13	3.38	0.094[b]	82 ± 14 %	Nie et al. (2013)
		Sporomusa sphaeroides	-0.017	-0.4	0.01	0.06	0.003[b]	84%	Nevin et al. (2011)
		Moorella thermoacetica	-0.009		0.01	0.10	0.005[b]	84%	
		Sporomusa ovata	-0.25 ± 0.06[c]	-0.68	0.45 ± 0.02	38 ± 2	1.875[b]	79 ± 6 %	Giddings et al. (2015)
Mixed cultures		AD sludge and fresh cow manure	n.d.	-0.6	0.165	n.d.	0.008[b]	30.7 ± 7.6 %[d]	Batlle-Vilanova et al. (2015)
	Batch or Fed-Batch	Brewery wastewater sludge	n.d.	-0.590	4	n.d.	1.71	67 % (includes H_2)	Marshall et al. (2012)
		Adapted brewery WW sludge	n.d.	-0.590	17.25[e]	n.d.	10.5	69%	Marshall et al. (2013b)
		Domestic WWTP sludge	-2.96	-0.903	2.35	10	4.7	90%	Su et al. (2013)
		Domestic WWTP sludge	~ -19	- 0.953	6.58	19	0.095	15%	Jiang et al. (2013)
		Enriched culture (Sediment from a bog)[f]	-0.03±0.006	-0.4	0.05	0.063±0.008	0.02±0.0025	35.2 ± 4.4 %	Zaybak et al. (2013)
		Pond sediments and anaerobic WWTP sludge	-2.91 ± 0.004	-0.85	0.47 ± 0.07	15[g]	1.65[h]	79%	Jourdin et al. (2014)[i]
			-6.28	-0.85	5.5	42[g]	n.d.	100 ± 1 %	Jourdin et al. (2016a)
		Enriched culture (Labscale anode and algae UASB sludge)	-5.0	-1.0±0.15	1.0±0.45	18±8	1.25±0.3	48±8 %	Patil et al. (2015a)

a: calculated per projected electrode surface unless stated differently
b: estimated based on linear production rate and reported flow rate
c: Membraneless MES, one of the three tested conditions represented (2.2V)
d: Only period 3 of the experiment considered
e: 24 h production test
f: estimated based on the data reported in the paper for autotrophic bioproduction (stoichiometric calculations based on consumed electrons)
g: calculated based on total surface area of the 3D material. For Jourdin et al. (2016) the material with the largest pore size was considered for the calculations.
h: data provided by L. Jourdin
i: data based on the last phase of the batch experiments (38 days/140 days)

Microbial pathways: carbon fixation through the Wood-Ljungdahl pathway

MES of acetic acid from CO_2 relies on homoacetogenic organisms. These are chemolithoautotrophic bacteria that use H_2 as source of electrons and Gibbs free energy and CO_2 as carbon source (Heijnen, 1999; Ragsdale & Pierce, 2008). The reductive Acetyl-CoA pathway (Figure 1.3) that they use for carbon fixation, also called Wood-Ljungdahl pathway, is probably closely related to the first microbial pathway for autotrophic CO_2 fixation (Martin, 2012). The pathway is present in both bacterial and archaeal species and can only function in anaerobic conditions, as several of the enzymes are extremely oxygen-sensitive. It is the most energetically favorable pathway of all 6 CO_2-fixation pathways that have been identified in bacteria and archaea (Berg et al., 2010). The fact that other carbon fixation pathways exist opens perspectives for the production of chemicals from CO_2 that are not derived from Acetyl-CoA, but these options have not yet been studied in the context of MES.

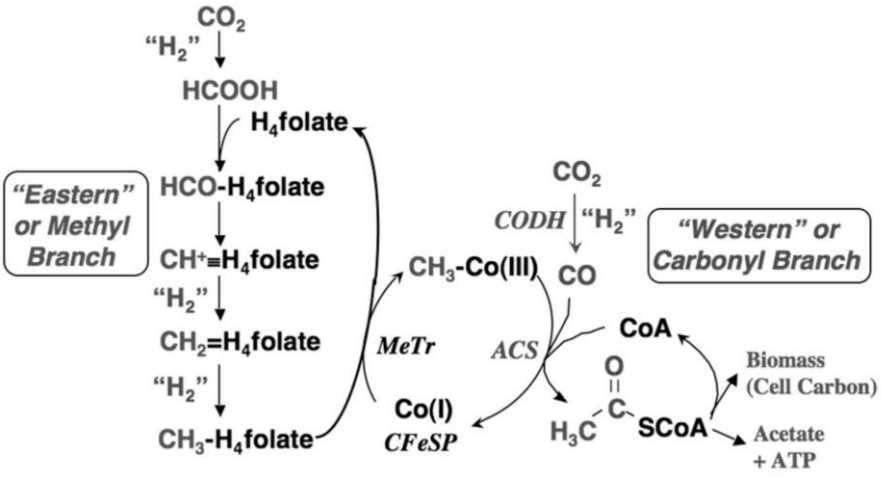

Figure 1.3 - Carbon fixation by homoacetogens takes place *via* the Wood-Ljungdahl pathway. The methyl and carbonyl branch deliver precursors for the formation of Acetyl-CoA, through which biomass and acetic acid are synthesized. Copied from Ragsdale and Pierce (2008). CODH: CO dehydrogenase; ACS: Acetyl-CoA synthase; MeTr: Methyltransferase.

The Wood-Ljungdahl pathway is a linear pathway that consists of two branches, the methyl-branch and the carbonyl-branch. In the methyl branch, CO_2 is first reduced to formate and subsequently converted through several steps to a methyl-group of a protein-bound Co-methylcorrinoid. This conversion requires 1 ATP. In case only CO is available, as can be the case in syngas fermentation, it will be oxidized to CO_2 in the methyl branch *via* a water-gas shift reaction (Ljungdahl, 1986; Drake et al., 2008). The reaction in the carbonyl-branch consists of the reduction of CO_2 to CO by the enzyme acetyl-CoA synthase. This same enzyme then catalyzes the formation of acetyl-CoA from CO and the methyl-group obtained in the methyl-branch (Wood, 1991). The acetyl-CoA can either be used in anabolic reactions or can be converted to acetic acid *via* acetyl-phosphate. This last reaction yields 1 ATP, making the sum of ATP obtained by substrate-level phosphorylation zero. Electrons for the reduction reactions in the methyl and

carbonyl branch are either obtained from H_2 *via* hydrogenases or through oxidation of CO to CO_2. The Wood-Ljungdahl pathway can, therefore, be used for H_2/CO_2 fermentations (Reaction 1) or CO-fermentations (Reaction 2). This last aspect is an important feature for the syngas platform (Latif et al., 2014; Bertsch & Müller, 2015).

$$4\ H_2 + 2\ CO_2 \rightarrow 1\ CH_3COO^- + 1\ H^+ + 2\ H_2O \qquad \Delta G^{0'} = -\ 95\ kJ/mol \qquad (1)$$

$$4\ CO + 2\ H_2O \rightarrow 1\ CH_3COO^- + 1\ H^+ + 2\ CO_2 \qquad \Delta G^{0'} = -\ 175\ kJ/mol \qquad (2)$$

The Wood-Ljungdahl pathway does not result in net ATP formation. Three chemi-osmotic energy conservation mechanisms have been identified in homoacetogens, all of them relying on the creation of an ion gradient over the cell membrane (Müller, 2003; Köpke et al., 2010). A first mechanism is the formation of a H^+-gradient through the use of quinones and cytochromes. This transmembrane proton potential then leads to ATP generation *via* an H^+-dependent ATPase. *Moorella thermoacetica* is studied as model organism for this energy conservation mechanism. A second mechanism relies on the formation of a Na^+-gradient and consequent ATP generation *via* an Na^+ translocating ATPase. *Acetobacterium woodii* utilizes this energy conservation mechanism and is unable to grow in media with Na^+ concentrations below 2.5 mM (Heise et al., 1989). A third energy conservation mechanism was only recently discovered through sequencing of the genome of *Clostridium ljungdahlii*. This organism also utilizes a H^+-gradient, but the gradient is formed through an Rnf complex. ATP generation takes place *via* an H^+-dependent ATPase (Köpke et al., 2010; Tremblay et al., 2013).

Homoacetogens are a diverse group of bacteria. About 100 different species from 21 different genera have been described. The bacteria are mainly mesophilic or thermophilic and have been isolated from a wide spectrum of environments, ranging from sediments and sludge to fecal samples from termites and rabbits (Drake et al., 2008). The term “homoacetogen” is used to distinguish them from those microorganisms that do not use the Wood-Ljungdahl pathway for acetic acid synthesis. Acetic acid synthesis is, however, not the only process that can result in energy conservation and growth in these microorganisms. Ethanol production or synthesis of lactic acid, butyric acid, or butanol are other possible pathways (Drake et al., 2006). The alternative synthesis pathways differ amongst homoacetogens and are dependent on the cultivation conditions. For example, the absence of nutrients and vitamins, a low pH environment and a high partial pressure of CO favors production of ethanol over acetic acid, resulting in higher ethanol/acetic acid ratios. This is a desired outcome for syngas fermentation (Köpke et al., 2011a; Dürre & Eikmanns, 2015; Richter et al., 2016).

From short carboxylic acids to longer chain products: the reverse β-oxidation pathway

The short-chain products obtained *via* the Wood-Ljungdahl pathway, acetic acid and ethanol, can be further elongated to short- and medium-chain carboxylic acids (butyric, caproic and caprylic acid). These products have a higher energy density and are more easily separated because of their lower solubility. Conversion of acetic acid and ethanol takes place *via* reverse β-oxidation, with ethanol as source of Gibbs free energy, electrons, and carbon. In contrast to the linear Wood-Ljungdahl pathway, chain elongation is a cyclic process (Figure 1.4). *Clostridium kluyveri* is a model-organism for this process (Thauer et al., 1968; Spirito et al., 2014; Angenent et al., 2016).

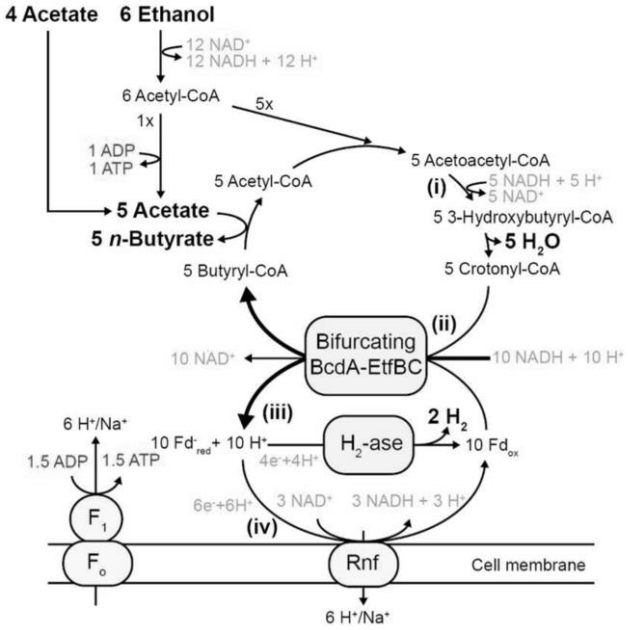

Figure 1.4 - The reverse β-oxidation pathway results in elongation of carboxylic acids with ethanol as source of electrons and carbon. The pathway for high substrate concentrations is represented. Copied from Angenent et al. (2016).

The cycle starts with the production of acetyl-CoA from ethanol. This acetyl-CoA is coupled to another acetyl-CoA to form acetoacetyl-CoA. Further transformation to butyryl-CoA finally results in the formation of *n*-butyric acid. A similar cycle with ethanol and *n*-butyric acid results in the formation of hexanoyl-CoA and thus caproic acid (Thauer et al., 1968). Depending on the concentration of substrates, different ratios of ethanol and carboxylic acids are metabolized in the cycle. A model has been developed for this (Angenent et al., 2016).

Energy conservation takes places through a combination of substrate-level phosphorylation and transport-coupled phosphorylation. Oxidation of ethanol to acetic acid *via* Acetyl-CoA yields 1 ATP. Additional ATP is obtained when reduced ferredoxin forms H_2, generating a Na^+/H^+ gradient (Schoberth & Gottschalk, 1969; Angenent et al., 2016). In mixed cultures it is imperative

to keep the H_2 partial pressure high enough to avoid re-oxidation of the produced carboxylic acids (Agler et al., 2014). Thermodynamic models have shown that chain elongation with H_2 as sole electron source is energetically not possible. When chain elongation takes places in MES, this must first take place *via* ethanol as intermediate (Gonzalez-Cabaleiro et al., 2013).

Microbial caproic acid production is currently a niche application, as medium-chain carboxylic acids (MCCAs) are usually obtained from hydrolyzed palm and coconut oils (TMR, 2016). They can be used as anti-microbial in animal feed, to replace antibiotics.

Microbial electrosynthesis technology: state-of-the art

The design and operation of MES reactors is largely based on knowledge gained from MFC technology. Similar to MFCs, an MES reactor contains three basic components: the anode, membrane and cathode. Chemical anodes are mostly used and the anolyte solution is usually highly buffered or highly conductive to promote water electrolysis. Stable anode materials are used to avoid deterioration over time. The use of a CEM between the anode and cathode compartment is standard practice (Patil et al., 2015b).

The electrochemical operation of the reactors can differ. Usually a fixed cathode potential is applied, but the use of a fixed current has also been reported. The fixed potential approach is usually chosen to favor DET, although different cathode potentials have also been tested within one study to compare production rates with and without H_2 evolution (Blanchet et al., 2015; Jourdin et al., 2016a). With a fixed current the aim is to not limit the microbial electrocatalyst in reducing equivalents (Dennis et al., 2013; Patil et al., 2015a; Molenaar et al., 2016).

Several cathode materials have been tested for MES to develop a low-cost, scalable and well-conductive material (Desloover et al., 2012b). Carbon materials such as carbon felt or graphite granules offer a good 3D-structure and are easy-to-handle at laboratory scale but their limited conductivity hampers scale-up (Guo et al., 2014a). A chemical modification of the electrode surface has been a successful strategy for bioanodes and also resulted in an increase of production rates for MES up to 6 times for treated *vs.* untreated carbon cloth (Zhang et al., 2013c). Functionalization with chitosan, which is an inexpensive biopolymer, holds promise, whereas the use of metal nanowires and nanoparticles might increase the material cost too much despite their successful operation (Nie et al., 2013). Another approach to improve the biocathode properties is the use of 3D-materials. Jourdin and co-workers have developed two reticulated vitreous carbon materials with a carbon nanotube coating. A combination of macroscale pores and nanoscale roughness enhanced mass transfer and bacteria-electrode interaction, resulting in high volumetric and surface based production rates (Table 1.3) (Jourdin et al., 2014; Jourdin et al., 2015). Surface based production rates are a key parameter to

consider for scale-up of MES systems. High surface-to-volume ratios will most likely be implemented and the necessary electrode surface will largely impact the overall cost.

MES reactors can be operated either in batch or continuous mode. Operation in batch mode can be combined with a continuous supply of CO_2 as carbon source. The operation mode influences the product concentration and pH, therefore impacting the production rates. Acetic acid accumulation in parallel to a decrease in pH is often observed during batch mode operation. Accumulation of short-chain carboxylic acids (SCCAs), such as acetic acid, at low pH can inhibit the microbial metabolism due to toxicity of the protonated form. While at pH 7 less than 1% of the acetic acid is present as undissociated acetic acid, this increases to 36% at pH 5 (pKa acetic acid: 4.76). Depending on the total concentration of product, this can negatively affect the culture (LaBelle et al., 2014). Control of the pH above 6 to avoid product toxicity can thus be necessary, even though this entails the addition of chemicals. Continuous mode operation is less frequently reported, but can be a strategy to keep the product concentrations and pH in the desired range (Nevin et al., 2010; Nevin et al., 2011; Batlle-Vilanova et al., 2015). A consequence of continuous mode operation is that the product gets diluted. Lower product concentrations will negatively affect its recovery efficiency.

Product recovery is not considered yet in the development of MES technology. The focus of developing MES technology has been the improvement of production rates and efficiencies, through material design and microbial catalyst selection. As product inhibition and product dilution need to be avoided, an efficient *in-situ* product recovery technique should be considered for MES.

2.3 Electricity-driven transport of ions

The movement of electrons in an electrochemical cell, or current, results in a charge imbalance if other charged species are not moved in the system as well. For each electron reaching the cathode, either a negative charge has to move toward the anode, or a positive charge must move toward the cathode. In BESs it is often crucial to physically separate the anodic oxidation and cathodic reduction to avoid cyclical reactions. This would for example be the case if oxygen produced at the cathode of an MFC would be used as electron acceptor by the anodic biofilm instead of the electrode (Clauwaert et al., 2008a). The physical separation barriers used are ion exchange membranes. These allow for a selective transport of either cations or anions in the electrochemical cell. The membranes consist of a polymer matrix to which negatively charged groups (for a CEM) or positively charged groups (for an AEM) are bound (Xu, 2005). A third possibility is the use of a bipolar membrane (BPM) where water splitting is induced on the membrane surface due to the creation of a potential difference (Harnisch et al., 2008). The transport of ions over the membrane can be used solely to restore the charge

balance, but can also be designed specifically to create added value. Electricity-driven transport of ions is already implemented at industrial scale in the electrodialysis process.

Electrodialysis: a large-scale application of electricity-driven ionic transport

Electrodialysis (ED) is used mainly for water desalination. The concentrated saline wastewater or seawater stream is sent through a stack of electrochemical units consisting of series of AEMs and CEMs (Figure 1.5). When an electrical potential is applied, the anions migrate toward the anode through the AEM while the cations will migrate in the opposite direction to the cathode, through a CEM. The ions will consequently be blocked by the next membrane, a CEM in the case of anions and an AEM in the case of cations. The original solution is thus depleted from its electrons while a concentrated brine solution is obtained in the adjacent compartment (Strathmann, 2010). One cell pair consists of a diluate containing cell, an AEM, a concentrate containing cell and a CEM. At industrial scale, up to 200 cell pairs are stacked between the anode and cathode.

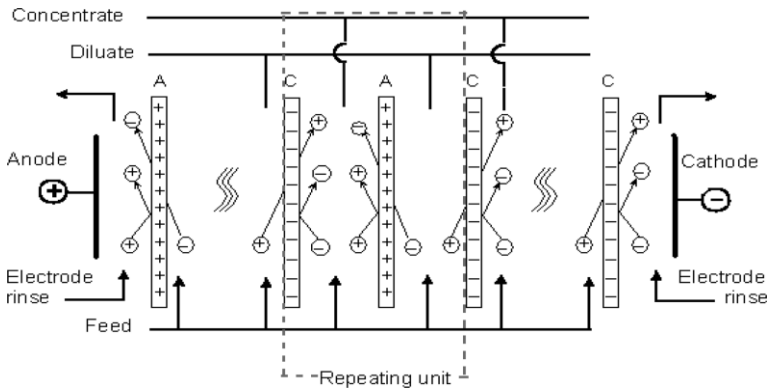

Figure 1.5 - Wastewater and seawater can be desalinated in an electrodialysis cell as the ions are driven through the anion exchange membrane and cation exchange membrane, resulting in a diluate and concentrate stream. Figure copied from Strathmann et al. (2013).

In reverse electrodialysis (RED) the opposite process is studied: seawater and river water are mixed with the concurrent generation of electrical power. The difference in salinity between the two streams represents a difference in potential energy that can be harvested. RED could be applied anywhere a river flows into the sea. The high cost of membranes currently does not make RED a competitive form of renewable energy (Długołęcki et al., 2008; Yip et al., 2014).

The desalination of brackish water and seawater has historically been the most used application of ED. Uncharged molecules and viruses are, however, not eliminated through ED, which is the case for other technologies such as reverse osmosis. This has resulted in competition between the two technologies, especially when low salt concentrations need to be achieved. (Ghyselbrecht et al., 2013). At the membrane surface the ion concentration can reach almost 0 in the diluate stream, due to concentration polarization. In this situation an increase of

the cell potential does not lead to an increased current; the limiting current density was reached. The high membrane surface required to desalinate down to low salt concentrations significantly increases the capital cost of ED installations (Lee et al., 2002).

To increase the process value, ED can be combined with BPMs to produce acids and bases from the salt streams. The cell pair then consists of a BPM, an acid stream, an AEM, the dilute stream, a CEM, a base stream and a second BPM. Due to the higher voltage drop over a BPM, the number of units in a stack is limited to 100. Electrodialysis with BPMs can be used in combination with fermentation technology, which has been demonstrated for the production of itaconic acid. Fermentations require a high acid and base input during fermentation and separation of the products. By recovering the charged product through ED, the base produced can be used to adjust the pH of the fermentation process while the concentrated stream with itaconic acid is sent to a crystallizer for product recovery (Xu, 2005). A similar process has been designed for lactic acid production. Large scale implementation of ED with BPMs is still rare, mainly due to the low stability of the membranes at high acid and base concentrations (Strathmann, 2010).

Membrane electrolysis

In BESs the active use of membrane processes to create added value has also been proposed through the concept of membrane electrolysis (ME). A concentrate stream is obtained through the transport of a charged species through one membrane, a CEM in case a selective transport of a positively charged product is targeted, and AEM for negatively charged species. In contrast to ED, the electrodes in ME are in direct contact with the treated streams and only one membrane is used. Two examples of ME are shortly elaborated on: i) the recovery of ammonium from an anaerobic digester to mitigate ammonia toxicity; and ii) the recovery of short- and medium-chain carboxylic acids from a fermenter. Both are examples of a secondary microbial electrochemical technology, as defined by Schröder et al. (2015). The electrochemical cell is connected to the electrolyte and supports the microbial process. Yet, no electron transfer, direct or mediated, is taking place between the electrodes and the microorganisms.

The first example is ammonium recovery from NH_4^+-rich streams such as digestates. This could lead to production of fertilizers at a lower energy input than through the Haber-Bosch process (Desloover et al., 2012a). Additional added value can be created if this recovery process simultaneously decreases toxicity in the anaerobic digestion process (Desloover et al., 2015). An electrochemical cell coupled to an anaerobic digester positively affected CH_4 production through several mechanisms. First, NH_4^+ was extracted through the CEM of the cell. The applied potential drives the transport of the charged NH_4^+ over the membrane. In the cathode compartment this NH_4^+ was converted to NH_3 due to the high pH obtained through water electrolysis. The NH_3 can

be recovered as $(NH_4)_2SO_4$ in a stripping and absorption unit. Secondly, sulfide that was present in the digester was oxidized at the anode of the electrochemical cell, reducing sulfide toxicity in the anaerobic digestion process.

A second example of ME is the extraction of carboxylates from a fermentation broth using an electrochemical cell with an AEM. The carboxylates are transported from the cathode to the anode compartment, where they are protonated due to the low pH (Andersen et al., 2014). The fermentation products are as such recovered as a clean acidic concentrate, which allows further processing, for example to esters. The removal of the product positively affects the fermentation process by decreasing product toxicity. Furthermore, the hydroxide ions that are formed at the cathode take away the need for chemical pH control of the fermentation process (Andersen et al., 2015). The extraction efficiency of the different carboxylates is closely linked to the molar concentration of the different species in the fermenter broth and their hydrophilicity, limiting the selectivity of the extraction (Andersen et al., 2014). To improve the selectivity of the extraction process, a combination of ME with another extraction technique, membrane-based liquid-liquid extraction (pertraction) has been proposed (Xu et al., 2015). Pertraction relies on the use of a hydrophobic solvent as extraction medium in a first extraction module, therefore favoring the extraction of the longer chain carboxylic acids from the fermenter into the solvent. These carboxylic acids are then extracted into a high-pH stripping solution in a second extraction module (Agler et al., 2012). In the combined approach with ME, this stripping solution is in fact the catholyte of an electrochemical cell, kept at pH 9 due to water electrolysis instead of chemical pH control. The applied current drives the dissociated carboxylates through the AEM into the low pH anolyte. Due to the low solubility of the longer chain carboxylic acids (caproic acid 10.82 g/L and caprylic acid 0.68 g/L), these phase-separate spontaneously in the anolyte, allowing their recovery. Shorter chain products such as butyric acid increased in concentration in the anolyte, but their extraction leveled off over time, with the maximum concentration reached remaining below their solubility limit (Xu et al., 2015). This phase-separation of carboxylic acids with carbon chain length ≥ 6 should also allow the ME process to be selective by itself.

Electrodialysis and membrane electrolysis technology: state-of-the art

Large-scale ED plants have been implemented for desalination and water treatment in the food, chemical, and biotechnology industry. Advances in process technology focus on the application of ED at lower salinities and the creation of added value, for example using BPMs. Electrodialysis has several advantages over other physicochemical water treatment techniques such as reverse osmosis. Desalination with ED is not limited by osmotic pressure, resulting in higher brine concentrations. Pre-treatment of the streams is not necessary because, as no pressure is used, membrane fouling and scaling is limited. By temporarily reversing the polarity

of the electrodes the membranes can be cleaned. This leads to membrane life-times ranging between 5 and 8 years for most ED applications. The capital and operational cost can be estimated based on the number of ions to be removed from the solution (Strathmann, 2010).

Membrane electrolysis still requires technology development before being implemented at larger scale. Only lab-scale studies have been executed thus far, but the first pilot scale study is underway. A major concern is the life-time of the membranes in ME. As ME is applied to fermentation and digestion technologies, the membranes are in contact with broths high in suspended solid concentrations. Problems such as scaling and fouling could thus be of higher importance compared to ED. Scaling could potentially be solved using the same strategy as for ED, by switching the polarity of the electrodes. For an MEC treating sewage, this has been shown to be a feasible approach to remove scaling and restore the cell potential (Pikaar et al., 2011). Reversing polarity is, however, not possible with all stable anodes used in ME, as the electrode coating can be damaged (Bagastyo et al., 2011). Membrane fouling and solids build-up on the membrane surface can account for approximately one third of the applied potential during extraction of carboxylates from a fermentation broth (Andersen et al., 2015). Increasing the distance between the membrane and electrode affected the mixing positively and decreased the resistance in the system. Similar high cell potentials were obtained by Xu et al. (2015), even though the electrolysis system was not in direct contact with the fermentation broth, but with the stripping solution containing carboxylates. A strategy to clean the membranes, such as improved flow design, will be critical to allow longer term use of the membranes. Even though the membrane surface area is limited in ME compared to ED, it still represents a substantial cost. Based on a 5-year life-time it was estimated that membranes would account for 20% of the reactor cost of BESs, but reaching this life-time seems unlikely for ME (Rozendal et al., 2008a).

Selectivity of membranes toward the extraction of the product of interest has regularly been mentioned as a crucial aspect of technology development. Improving selectivity requires a better understanding of the electrochemical transport of organic molecules in ion exchange membranes. In solutions with an elevated salt concentration and low concentrations of organics, *e.g.* trace contaminants, the transport of the organic molecules is mainly diffusion driven because of their low concentration compared to other charged species. Charged organics were partially driven by the applied potential (Vanoppen et al., 2014). In fermentation studies the ratio of organic products is much higher and their transport is, thus, potential driven. Development of membranes specifically for ME applications is required as the transport of larger organic molecules is inherently different to the transport processes occurring in ED.

3. Objectives and outline of this work

Electricity-driven bioproduction and purification have the potential to fulfill part of the demand in sustainable chemicals and fuels. Carbon dioxide and carbon monoxide can serve as carbon sources for this production process, especially *via* decentralized production systems at emission point sources. Critical aspects to obtain a mature technology are improvements in production rates and product purities, as well as decreased production costs. Several knowledge gaps have been identified and worked on in this thesis (Figure 1.6).

Understanding the thermodynamic implications of (electricity-driven) production from CO_2 and CO is a critical aspect to improve the technology. A thermodynamic assessment of microbial electrocatalysis and gas fermentations was thus conducted. Bioanodic and biocathodic processes were compared based on overpotentials and biomass formation. Cathodic reductions and gas fermentations were compared based on Gibbs free energy changes. These results were used to evaluate differences in production rates between the different systems. It was furthermore investigated which lessons can be learned from thermodynamics when designing systems for bioproduction. The results of this theoretical assessment are given in **Chapter 2**.

Chapter 3 focusses on one of the bioproduction systems, microbial electrosynthesis of acetic acid from CO_2. In the present systems the obtained acetic acid concentrations are low, the process requires pH control and because of the low product concentrations the purification of the acetic acid is costly and challenging. A new reactor technology was thus proposed to integrate acetic acid production, extraction and concentration. This technology was based on membrane electrolysis, using an anion exchange membrane in the reactor configuration instead of the usual cation exchange membrane. A proof-of-concept for this reactor technology is first given. It is followed by an evaluation of the performance of the new technology *vs.* the systems without extraction based on critical performance parameters.

Acetic acid and ethanol, either produced *via* microbial electrosynthesis or syngas fermentation, are feedstocks for chain elongation. Production of medium-chain carboxylic acids (caproic and caprylic acid) from acetic acid and ethanol results in a higher value product that can be more easily separated. Mixed cultures have shown potential to upgrade the C2 products from microbial electrosynthesis and syngas fermentation. In **Chapter 4** it is investigated if a pure culture of *Clostridium kluyveri* can be used as biocatalyst for the production of caproic and caprylic acid from syngas fermentation effluent. Production of caprylic acid by *C. kluyveri* has not yet been reported. Continuous reactor experiments, both with and without in-line product extraction, were designed and evaluated.

Following these chapters with experimental results, a general discussion is provided in **Chapter 5**, together with suggestions for future research.

In the **Addenda**, two technical notes describe methods for: i) enrichment of homoacetogenic microorganisms from mixed cultures; and ii) nitrogen removal from nitrogen-rich streams such as urine, using both an electrochemical and bioelectrochemical system. While the results obtained do not directly link to the work presented in the main chapters, important conclusions were nonetheless drawn and integrated into the general discussion.

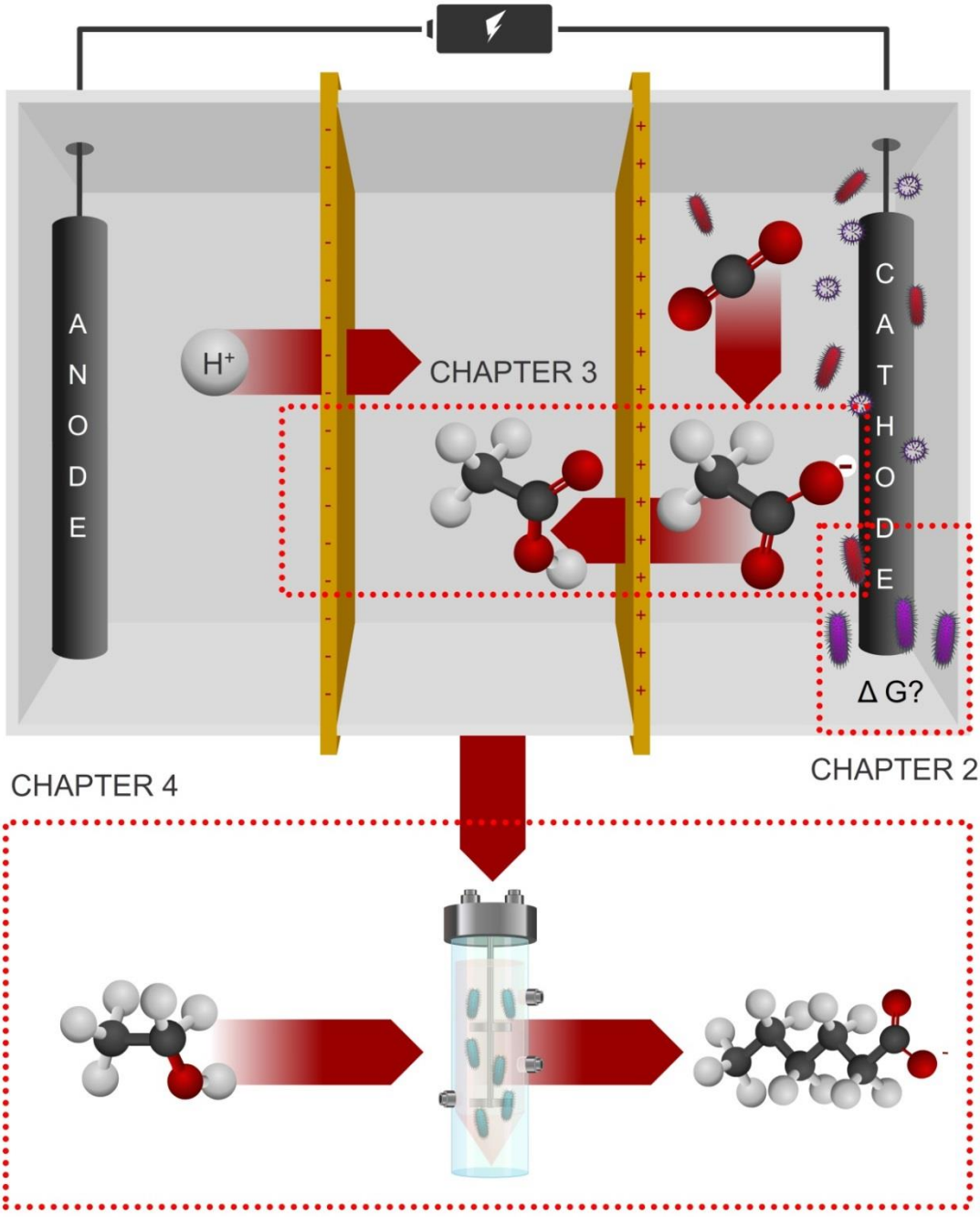

Figure 1.6 - Overview of the experimental chapters in this PhD thesis

CHAPTER 2 - A THERMODYNAMIC ASSESSMENT OF MICROBIAL ELECTROCATALYSIS

This chapter has been redrafted after:

Gildemyn S., Rozendal, R., Rabaey, K. 2016. A Thermodynamic Assessment of Microbial Electrocatalysis. Submitted to Trends in Biotechnology.

Abstract

The use of electrochemically active microorganisms for electrode reactions has led to a plethora of possible applications in the context of bioremediation, biosensing, bioproduction, and bioenergy. Electrochemically active microorganisms interact with electrodes by donating or receiving electrons to/from electrode surfaces, while consuming substrates and/or excreting bioproducts. To understand the electrochemical performance of these microbially catalyzed electrode reactions, it is essential to properly understand the reaction thermodynamics. Here, we first elaborate on the *Growth Reference System* (Heijnen, 1999), simplifying thermodynamic calculations in the aforementioned context and showing that cathodic bioprocesses generally suffer from higher overpotentials than anodic processes. For none of the cathodic microbial electrosynthesis processes described, thus far, the *in-situ* production of H_2 can be thermodynamically excluded. We also assessed the thermodynamic efficiency of both anodic and cathodic processes as well as gas fermentations. With this approach, it is also feasible to make predictions for maximum biomass production correlated to electron flow, which are in line with observations. We have included a comprehensive set of thermodynamic and electrochemical data, including CO_2-based production, to support a wide array of other calculations relevant for the field of microbial electrocatalysis.

1. Introduction

A century after the first description of electrical effects associated with microbial degradation (Potter, 1911), microbial electrocatalysis has become the key driver for a host of processes in BESs (Schröder, 2011; Arends & Verstraete, 2012). While initially the main research focus was on electricity production in MFCs (Logan et al., 2006), emphasis has now shifted toward the development of bioremediation and bioproduction processes in MECs (Rabaey et al., 2007; Logan et al., 2008). Microbially generated electrons from an anode enable bioremediation processes for the removal of persistent pollutants (Mu et al., 2009b; Feng et al., 2010), denitrification (Clauwaert et al., 2007a; Virdis et al., 2009), perchlorate reduction (Thrash et al., 2007; Butler et al., 2010), dehalogenation (Aulenta et al., 2009), decolorization (Mu et al., 2009a), and heavy metal removal/recovery (Gregory & Lovley, 2005; Ter Heijne et al., 2010). In addition, bioelectrochemical production processes driven by bioanodes have been developed for the generation of H_2, H_2O_2 and caustic soda (Liu et al., 2005c; Rozendal et al., 2006b; Logan et al., 2008; Rozendal et al., 2009; Rabaey et al., 2010).

Microbial electrocatalysts were also used on a cathode for the production of H_2, CH_4, ethanol, and SCCAs (Park et al., 1999; Clauwaert et al., 2008b; Rozendal et al., 2008b; Cheng et al., 2009; Nevin et al., 2010; Steinbusch et al., 2010; Marshall et al., 2012; Ganigué et al., 2015). The latter was first shown through the cathodic bioproduction of acetic acid and 2-oxobutyrate using a pure culture of the acetogenic microorganism *S. ovata* with CO_2 as the carbon source (Nevin et al., 2010). The production of organic chemicals using whole microorganisms receiving electrons from electrodes is now widely known as microbial electrosynthesis (MES) (Rabaey & Rozendal, 2010). Developments over the last five years have resulted in a wider product spectrum (e.g. glycerol and butyric acid production from CO_2) (Soussan et al., 2013; Ganigué et al., 2015), increased production rates (up to 51 g/m²/d for acetic acid) (Jourdin et al., 2016a) and increased titers (up to 13.5 g/L acetic acid) (Gildemyn et al., 2015b), but the production rates and concentrations will need to further increase several orders of magnitude to compete with existing bioproduction pathways (Rabaey et al., 2011).

A key aspect of process development and performance assessment is the relationship between *input* and *output*. In the case of anodic reactions, the input represents the type of substrate/product and concentration and the electrochemical performance is the output of the system, while this is the opposite for cathodic production processes. This requires an understanding of the thermodynamics of the system, which is rarely studied. A general method to conduct at thermodynamic state analysis of environmental systems has been proposed (Kleerebezem & Van Loosdrecht, 2010). Here, we present a method that simplifies thermodynamic calculations in the context of microbial electrocatalysis. This method is based on

the *Growth Reference System* (GRS) as designed by J.J. Heijnen in 1999 (Heijnen, 1999). Our method allows the calculation of reaction potentials and electrode overpotentials to assess the thermodynamic efficiency of microbial electrocatalysis processes. Differences between anodic and cathodic catalysis can as such be identified. The method also allows to support statements concerning DET, especially in the context of MES. Biomass production and biofilm development can furthermore be linked to the substrate type and thermodynamic overpotentials. This calculation method opens perspectives for a deeper understanding of the thermodynamics of the widely studied BESs.

2. The Growth Reference System

The most important feature of the GRS is the fact that, compared to the conventional thermodynamic system, it chooses a different reference for all thermodynamic data (Heijnen, 1999). Whereas the conventional thermodynamic system is defined in such way that the Gibbs energy of formation is zero for the elements in their most stable state (e.g., $H_2(g)$, $O_2(g)$, $N_2(g)$, C(s), etc.) at standard conditions (1 bar, 298.15 K, 1 mol/L, pH 0), the GRS is defined in such a way that the Gibbs energy is zero for the end products typically occurring in microbial systems ($HCO_3^-(aq)$, $SO_4^{2-}(aq)$, $NO_3^-(aq)$, H_2O, $H^+(aq)$, etc.) at biochemical standard conditions (1 atm, 298.15 K, 1 mol/L, pH 7). In addition, the GRS defines three simple numbers for each chemical compound: (i) degree of reduction, γ; (ii) Gibbs energy per electron; and (iii) enthalpy per electron. These numbers further simplify calculations. In the context of BESs, the degree of reduction and Gibbs energy per electron are particularly relevant as they define the limits to the coulombic yields and the potential; the enthalpy per electron is further not discussed.

Degree of reduction. For each component participating in an electrochemical reaction, the GRS defines a degree of reduction, which can be calculated using Table 2.1. The interesting feature of this definition is that the degree of reduction is zero for the following typical end products in microbial systems: bicarbonate (HCO_3^-), sulfate (SO_4^{2-}), nitrate (NO_3^-), water (H_2O), and protons (H^+). These compounds are also referred to as reference compounds. For instance, the degree of reduction of bicarbonate is calculated as 1 (H) + 4 (C) + 3×-2 (O) + 1 (negative charge) = 0.

All other compounds have a degree of reduction different from zero. For instance, acetate ($C_2H_3O_2^-$) has a positive degree of reduction of 2×4 (C) + 3×1 (H) + 2×-2 (O) +1 (negative charge) = 8, while oxygen gas, which is a typical electron acceptor in microbial systems, has a negative degree of reduction of 2×-2 (O) = -4. In the context of BESs, the value of the degree of reduction is equal to the electron content of a specific compound. This thus corresponds to the number of electrons an electron donor can donate or an electron acceptor can accept per mole of

compound, for it to be completely oxidized or reduced to reference compounds. The degree of reduction can, therefore, be straightforwardly used for calculation of coulombic efficiencies as detailed in Logan et al. (2006) and Logan et al. (2008).

Table 2.1. - Degree of reduction (γ) of atoms and charge as defined in the Growth Reference System (after Heijnen (1999)).

Atom/Charge	γ
C	4
H	1
O	-2
N	5
S	6
Halogen (F, Cl, Br, I) [a]	-1
Positive charge	-1
Negative charge	+1

[a] Added by the authors.

One additional advantage of the definition of the degree of reduction of compounds in the GRS is that it simplifies the calculation of reaction stoichiometry, especially also in the context of BESs. The reason for this is that the degree of reduction is equivalent to the electron content of a specific compound. Moreover, in most half reactions there are only few compounds that have a degree of reduction other than zero. Therefore, an electron balance can be made easily. Using this electron balance, the reaction stoichiometry can be easily solved using simple sequential steps. A calculation example for both a half reaction and a complete reaction stoichiometry can be found in Text Box 1, at the end of this chapter.

In anaerobic fermentation processes, the degree of reduction is usually expressed per mole carbon (γ/C-mol), to express the oxidation state of a substrate or product. As such, although methane and acetate both have a degree of reduction of 8, expressed per C-mol one can see that methane is more reduced (methane: 8; acetate: 4). This is also illustrated by the reaction for acetoclastic methanogenesis, in which acetate splitting results in a more reduced product, methane, and a more oxidized product, carbon dioxide (bicarbonate).

Gibbs energy per electron. The GRS also defines a Gibbs energy value *per electron* for each specific compound. This new value is easily calculated from the Gibbs energy of formation data in conventional thermodynamic tables in two simple steps. First, a reference half reaction is written out, which is the production reaction of a specific compound from reference compounds (e.g., HCO_3^-(aq), SO_4^{2-}(aq), NO_3^-(aq), H_2O, H^+(aq), etc.) and electrons. E.g. for acetate:

$$2\ HCO_3^- + 9\ H^+ + 8\ e^- \rightarrow C_2H_3O_2^- + 4\ H_2O \qquad (1)$$

Secondly, using the conventional thermodynamic tables (e.g., from (Thauer et al., 1977; Heijnen, 1999; Amend & Shock, 2001; Alberty, 2003)), the Gibbs energy of this specific reference reaction is calculated at biochemical standard conditions and subsequently divided by the amount of electrons (i.e., the degree of reduction γ) involved in the reaction:

$$\Delta G_e^{0'} = \frac{\Delta G_{ref}^{0'}}{\gamma} \quad (2)$$

In which $\Delta G_e^{0'}$ is the Gibbs energy value *per electron* present in a specific compound at biochemical standard conditions and $\Delta G_{ref}^{0'}$ is the Gibbs energy change of the reference reaction of this specific compound at biochemical standard conditions. E.g., calculating the $\Delta G_e^{0'}$ for acetate (thermodynamic data from Thauer et al. (1977)):

$$\Delta G_{ref}^{0'} = -2 \times \Delta G_{f\_HCO_3^-}^{0'} - 9 \times \Delta G_{f\_H^+}^{0'} + \Delta G_{f\_C_2H_3O_2^-}^{0'} + 4 \times \Delta G_{f\_H_2O}^{0'} \quad (3a)$$

$$\Delta G_{ref}^{0'} = -2 \times \text{-}586.85 - 9 \times \text{-}39.87 + \text{-}369.41 + 4 \times \text{-}237.18 = 214.4\ \text{kJ/mol} \quad (3b)$$

$$\Delta G_e^{0'} = \frac{214.4}{8} = 26.80\ \text{kJ/e - mol} \quad (3c)$$

The values for γ and $\Delta G_e^{0'}$ for chemical compounds relevant in the context of existing bioelectrochemical conversions are listed in Table App. 2.1. A very important note of caution is thermodynamic values listed in Table App. 2.1 should never be used in combination with conventional thermodynamic data due to the different reference used (i.e., standard conditions *vs.* biochemical standard conditions; see above), as this unavoidably results in miscalculations. The SHE is used as reference electrode for all calculations based on the GRS.

3. Simplifying bioelectrochemical calculations

At first glance, the GRS might appear to be a highly elaborate recalculation of already existing data. However, when using the system, it quickly becomes clear that it can simplify thermodynamic calculations in microbial systems, particularly also for BESs. Electrode potentials and cell voltages are calculated from the Gibbs energy change of a reaction (Text Box 2), which can be calculated from the tabulated data in the GRS according to:

$$\Delta G_r^{0'} = \sum \left(\nu_X \times \gamma_X \times \Delta G_{e,X} \right) \quad (4)$$

with ν_X is the stoichiometric reaction coefficient of compound X involved in the reaction (positive for products and negative for reactants). The most important advantage of using the GRS is that most of the compounds involved in a bioelectrochemical reaction are reference compounds, which can be eliminated from the calculations, as the value of γ and $\Delta G_e^{0'}$ for these compounds is zero per definition. For instance, the reaction equation of an MFC operated on acetate only contains two compounds that are not a reference compound (i.e., acetate and oxygen). Therefore, the theoretical cell voltage of this reaction at biochemical standard conditions can be easily calculated according to (according to Text Box 2; thermodynamic data from Table App. 2.1):

$C_2H_3O_2^- + 2\ O_2 \rightarrow 2\ HCO_3^- + H^+$ (5)

$$\Delta G_r^{0'} = -1 \times \gamma_{C_2H_3O_2^-} \times \Delta G_{e\_C_2H_3O_2^-}^{0'} - 2 \times \gamma_{O_2} \times \Delta G_{e\_O_2}^{0'} + 2 \times \gamma_{HCO_3^-} \times \Delta G_{e\_HCO_3^-}^{0'} + 1 \times \gamma_{H^+} \times \Delta G_{e\_H^+}^{0'} \quad (6a)$$

$$\Delta G_r^{0'} = -1 \times 8 \times 26.801 - 2 \times -4 \times -78.719 + 0 + 0 = -844.16 \text{ kJ/mol} \quad (6b)$$

$$E^{0'} = -\frac{\Delta G_r^{0'}}{nF} = -\frac{-844.16}{8 \times 96.4853} = 1.09 \text{ V} \quad (6c)$$

This advantage is even more evident when calculating the equilibrium potentials of half reactions, as many half reactions have only one compound that is not a reference compound. According to the IUPAC convention, equilibrium potentials for half reactions involving a certain electron acceptor/electron donor couple are calculated from the reduction reaction (i.e., the electron consuming reaction with the electron acceptor in the left side of the equation and the electron donor in the right side of the equation (e.g., Eq. (1) for acetate)). Similar to above, the equilibrium potential of the half reaction for acetate oxidation to bicarbonate is then calculated according to (based on Eq. (1) according to Eq. (4) and Text Box 2; thermodynamic data from Table App. 2.1):

$$\Delta G_r^{0'} = -2 \times \gamma_{HCO_3^-} \times \Delta G_{e\_HCO_3^-}^{0'} - 9 \times \gamma_{H^+} \times \Delta G_{e\_H^+}^{0'} + 1 \times \gamma_{C_2H_3O_2^-} \times \Delta G_{e\_C_2H_3O_2^-}^{0'} + 4 \times \gamma_{H_2O} \times \Delta G_{e\_H_2O}^{0'} \quad (7a)$$

$$\Delta G_r^{0'} = 0 - 0 + 1 \times 8 \times 26.801 + 0 = 214.4 \text{ kJ/mol} \quad (7b)$$

$$E^{0'} = -\frac{\Delta G_r^{0'}}{nF} = -\frac{214.41}{8 \times 96.485} = -0.278\ \text{V} \quad (7c)$$

Or, if the half reaction only contains one compound that is not a reference compound, the equilibrium potential of the half reaction can just simply be calculated from the Gibbs energy value *per electron* according to:

$$E^{0'} = -\frac{\Delta G_e^{0'}}{F} \quad (8)$$

Again, in the example of the half reaction for acetate oxidation to bicarbonate:

$$E^{0'} = -\frac{\Delta G_{e\_C_2H_3O_2^-}^{0'}}{F} = -\frac{26.801}{96.485} = -0.278\ \text{V} \quad (9)$$

Or for the half reaction for oxygen reduction to water:

$O_2 + 4\ H^+ + 4\ e^- \rightarrow 2\ H_2O$ (10)

$$E^{0'} = -\frac{\Delta G_{e\_O_2}^{0'}}{F} = -\frac{-78.719}{96.485} = 0.815\ \text{V} \quad (11)$$

Based on the Gibbs energy change and the equilibrium potential of specific half reactions at biochemical standard conditions calculations for BESs can easily be made. Thermodynamic data for selected half reactions involving bicarbonate as the electron acceptor are listed in Table App. 2.2. Thermodynamic data for selected half reactions involving an organic electron acceptor can be found in Table App. 2.3. The thermodynamic data for selected half reactions involving an inorganic electron acceptor (other than bicarbonate) are listed in Table App. 2.4.

Equilibrium potentials of half reactions can conveniently be used for calculating the theoretical cell voltage by subtracting the equilibrium potential of the anode reaction from that of the cathode reaction. E.g., for an MFC operated on acetate:

$$E_{cell}^{0'} = E_{cathode}^{0'} - E_{anode}^{0'} = 0.815 - (-0.278) = 1.09\ \text{V} \quad (12)$$

Evidently, this will give the same result as Eq. 6.

4. Concentration effects

The thermodynamic data of the GRS, and thus the numbers in Table App. 2.2, 2.3 and 2.4, are reported at biochemical standard conditions, which are defined as 1 atm, 298.15 K, 1 mol/L, and

pH 7. A real system is rarely operating at biochemical standard conditions. Therefore, the Gibbs energy change and equilibrium potential need to be corrected for the effect of partial pressure, temperature, concentration, and pH. For the half reaction:

$$\nu_A A + \nu_B B + \nu_H H^+ + n\ e^- \rightarrow \nu_C C + \nu_D D \tag{13}$$

in which compound A, B, and protons are converted into compound C and D, consuming n electrons and with ν_i being the reaction coefficient of the specific reactants, protons, and products, the Gibbs energy change of the half reaction can be corrected for the effect of the pressure, temperature, concentration, and pH using the Nernst equation:

$$\Delta G_r = \Delta G_r^{0'} + RT\,ln(\Pi) - RT\,ln\left(\left[\frac{10^{-pH}}{10^{-7}}\right]^{\nu_H}\right) \tag{14}$$

The last term in Eq. 14 is a consequence of the chosen reference of pH 7 in the GRS. Π is defined as:

$$\Pi = \frac{a_C{}^{\nu_C} a_D{}^{\nu_D}}{a_A{}^{\nu_A} a_B{}^{\nu_B}} \approx \frac{[C]^{\nu_C}[D]^{\nu_D}}{[A]^{\nu_A}[B]^{\nu_B}} \tag{15}$$

With a_i the activity of a specific of a specific compound and $[i]$ the concentration (in mol/l) or partial pressure (in atm) of a specific compound i. In dilute systems, which is often the case in microbial systems, calculations can be conveniently simplified by estimating the activities as concentrations or partial pressures.

Accordingly, the equilibrium potential of the half reaction can be corrected for the effect of the pressure, temperature, concentration, and pH using the following equation (i.e., Eq. 14 divided by -*nF*):

$$E_r = E_r^{0'} - \frac{RT}{nF} ln(\Pi) + \frac{RT}{nF} ln\left(\left[\frac{10^{-pH}}{10^{-7}}\right]^{\nu_H}\right) \tag{16}$$

Due to the exponential nature of the pH scale, the pH value can have a very strong effect on the equilibrium potential when $\nu_H > 0$, which is demonstrated in Figure App. 2.1 for half reactions that involve as many protons involved in the reaction as electrons (i.e., ν_H=n).

The equilibrium potential of half reaction $\nu_A A + \nu_B B + \nu_H H^+ + n\,e^- \rightarrow \nu_C C + \nu_D D$ (i.e., involving protons as reactants) *decreases* by about $\left[\frac{\nu_H RT}{nF}\right] ln(10)$ V per pH unit *increase* and *increases* by about $\left[\frac{\nu_H RT}{nF}\right] ln(10)$ V per pH unit *decrease*. At a temperature of 298.15 K, this means that the equilibrium potential *decreases* by about $\left[\frac{\nu_H}{n}\right]$ times 0.059 V per pH unit *increase* and *increases* by about $\left[\frac{\nu_H}{n}\right]$ times 0.059 V per pH unit *decrease*.

The pH related voltage loss can become very important in BESs with ion exchange membranes or other separators dividing the anode and cathode compartment (Rozendal et al., 2006a; Rozendal et al., 2008d), as this usually leads to decreasing anode pH and increasing cathode pH because of incomplete H^+ or OH^- migration in the presence of other ions. The decreasing pH in the anode causes the anode equilibrium potential to increase, whereas the rising pH in the cathode causes the anode equilibrium potential to decrease. Overall, this results in significant energy losses as the cell voltage that can be generated in MFCs decreases and the applied voltage required for MECs increases.

Similarly, also concentrations/partial pressures can have a considerable effect on the equilibrium potential (Figure 2.1). In general, the equilibrium potential of half reaction $\nu_A A + \nu_B B + \nu_H H^+ + n\,e^- \rightarrow \nu_C C + \nu_D D$ increases by about $\left[\frac{\nu_i RT}{nF}\right] ln(10)$ V per 10 fold increase of reactants A or B and decreases by about $\left[\frac{\nu_i RT}{nF}\right] ln(10)$ V per 10 fold increase of products C or D. At a temperature of 298.15 K, this means that the equilibrium potential increases by $\left[\frac{\nu_i}{n}\right]$ times 0.059 V per 10 fold increase of reactants A or B and decreases by $\left[\frac{\nu_i}{n}\right]$ times 0.059 V per 10 fold increase of products C or D.

The extent of this concentration effect on the equilibrium potential highly depends on the type of reactant/products involved in the reaction. At a constant pH, the effect of a changing acetate concentration on the equilibrium potential of acetate oxidation is relatively low in the typical concentration range occurring in microbial systems (10^{-3}-10^{1} M), which is, indeed, what is observed for most electron donors in BESs (Figure 2.1A). Most electron donors have a high degree of reduction (i.e., n is high), so $\left[\frac{\nu_i}{n}\right]$ is low. For example, for acetate $\left[\frac{\nu_i}{n}\right]$ equals 1/8

and, therefore, the equilibrium potential only decreases by about 0.0074 V per 10 fold increase of the acetate concentration (T= 298.15 K).

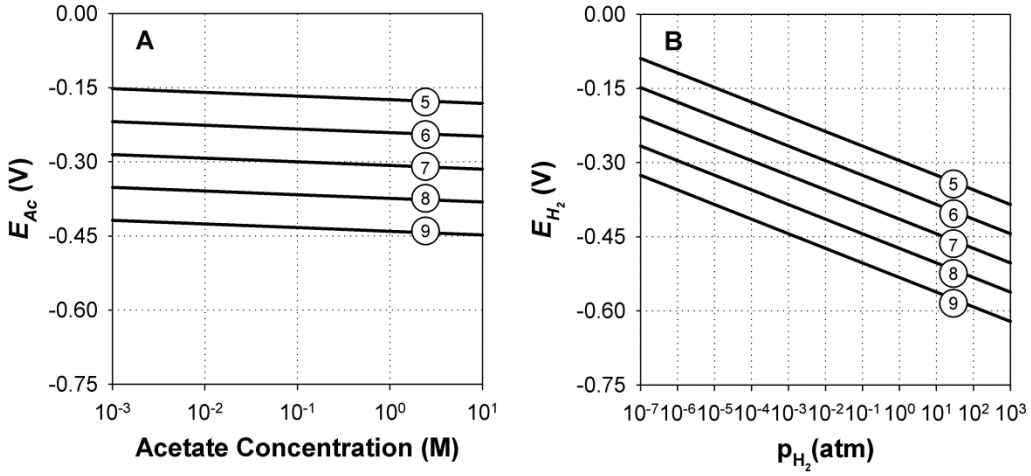

Figure 2.1 - The effect of concentration/partial pressure on the equilibrium potential of half reactions highly depends on the number of electrons involved in the reaction and can be calculated according to equation 16: (A) effect of acetate concentration on the equilibrium potential of the half reaction 2 HCO_3^- + 9 H^+ + 8 e^- ⇆ Acetate + 4 H_2O in the pH range 5 to 9 (298.15 K; 0.01 M HCO_3^-), (B) effect of hydrogen partial pressure on the equilibrium potential of the half reaction 2 H^+ + 2 e^- ⇆ H_2 in the pH range 5 to 9 (298.15 K).

For H_2, however, a larger shift in equilibrium potential can be observed because it only has a degree of reduction of 2 (i.e., n is low, so $\left[\frac{\nu_i}{n}\right]$ is high). The shift in equilibrium potential is about 0.03 V per 10 fold change in partial pressure (T= 298.15 K). In addition, H_2 is known for its wide range of partial pressures that can occur in microbial systems (10^{-7}-10^{3} atm). This can cause a large shift in equilibrium potential (Figure 2.1). The latter is also of particular importance when discussing whether H_2 is a possible intermediate in microbially catalyzed cathode reactions (Villano et al.; Cheng et al., 2009; Nevin et al., 2010; Blanchet et al., 2015). At pH 7, H_2 can already start evolving from about -0.33 V if the H_2 partial pressure is kept below 10^{-3} atm, which is indeed a typical H_2 partial pressure that can be observed in syntrophic methanogenic populations (Schink, 1997). Thus, a potential above -0.41 V *vs.* SHE, the potential at biochemical standard conditions, or an H_2 concentration below the detection limit of a standard gas chromatograph, is not necessarily proof that H_2 is not an intermediate.

An important note of caution with the above calculations is that they do not take acid-base speciation into account. The thermodynamic effects of acid-base speciation are generally very small, but can be of importance in some biological systems where thermodynamic gains are small (approximately -20 kJ/mol per reaction), such as in syntrophic methanogenic populations (Schink, 1997; Stams et al., 2006; Dolfing, 2014) or the alcohol production through the reduction of SCCAs with H_2 as the electron donor (Steinbusch et al., 2008; Steinbusch et al., 2009). Under those conditions, acid-base speciation should be included in thermodynamic calculations as

described by Dolfing and coworkers (Dolfing et al., 2010). Several metabolic models have shown the importance of ionic strength and acid-base speciation for the prediction of the feasibility of reactions, and have included an additional term to take this into account (Alberty, 2006; Henry et al., 2007). For instance, Dolfing and co-workers calculated that if the Gibbs energy data of the most dominant species (i.e., the weak acid/base *vs.* the conjugated base/acid) present under the actual working conditions is used for calculations, the maximum error of neglecting acid-base speciation is about 1.72 kJ/mol (Dolfing et al., 2010). This value is indeed 2 to 3 orders of magnitude smaller than the actual Gibbs energies of the specific half reactions tabulated in Table App. 2.2, 2.3, and 2.44. In BESs overpotentials are usually much larger than the possible thermodynamic effect of acid-base speciation, and these effects can thus usually be neglected.

5. From theory to practice: evaluating the performance of bioelectrochemical systems

A range of microbially catalyzed half reactions was investigated in specific literature studies, and the corresponding equilibrium potentials calculated for the conditions of the study (Table 2.2). Based on this information and the observed OCP, the associated overpotentials at zero current can be calculated, which is an indicator of the efficiency of catalysis. Interestingly, based on what is seen from literature thus far, microbially catalyzed cathodic systems under open circuit conditions generally seem to exhibit higher overpotentials than microbially catalyzed anodic systems (Table 2.2). Still, for fermentable substrates such as glucose the observed anodic overpotential is quite substantial. This suggests that glucose oxidation occurs through intermediates, such as acetic and butyric acid, with higher equilibrium potentials (Freguia et al., 2008), although direct catalysis has also been observed in pure culture systems (Chaudhuri & Lovley, 2003).

The calculations to determine electrode potentials as shown above are all based on equilibrium conditions and, thus, only give theoretical operating boundaries. In practice, however, the operating potential and also the OCP can deviate significantly from the equilibrium values as a result of various types of electrode overpotentials (Bard & Faulkner, 2001). In addition, with microbially catalyzed electrode reactions, the required biochemical pathways might be non-existent and, therefore, catalysis might not be efficient enough to operate close to equilibrium potentials. Thermodynamics only provide theoretical boundaries and can, thus, not be uncoupled from kinetics. A modeling approach could unify insights from both thermodynamic and kinetic studies, as has now done already, mainly for metabolic studies outside the field of BESs (Henry et al., 2007; Rodríguez et al., 2008; Kracke & Krömer, 2014). Because bacteria are not true catalysts (they derive energy for growth), overpotentials are intrinsically part of the system. The specific equilibrium potentials of the electron transfer molecules, whether

membrane-bound (e.g. cytochrome) or soluble (e.g. phenazine), also influence the overall reaction thermodynamics (Liu et al., 2011). Nevertheless, the ability to calculate an equilibrium potential gives the researcher the ability to assess the extent of the overpotentials.

The performance of BESs can be further investigated using other parameters. First, a method to assess the energetic efficiency of a BES has been proposed (Patil et al., 2015b). The calculation tool takes into account the energetic efficiency of half-reactions alone, or the full system, which allows comparison of BES performance independently from the design or counter-electrode reaction. Second, besides investigating the efficiency of catalysis under open circuit conditions, the efficiency of catalysis can be assessed by studying the dynamic behavior between the calculated overpotential and obtained current density, as with chemically catalyzed electrodes, current density generally increases with overpotential. For biological anodes, this relationship between overpotential and current density has been investigated and modeled by several research groups (Marcus et al., 2007; Picioreanu et al., 2007; Hamelers et al., 2010). The anodic overpotentials can for example be used as a tool to stimulate kinetics of electrogenic bacteria over methanogens (Sleutels et al., 2016). There is, however, no clear correlation between increased overpotential, which theoretically results in more energy available for the microbial electrocatalyst, and overall BES performance (Wagner et al., 2010).

Table 2.2. - Equilibrium potentials, observed open circuit potential, calculated overpotential of microbially catalyzed half reactions in specific literature studies.

Half cell reactions	Equilibrium potential [a] (V)	Observed open circuit potential (V)	Calculated Overpotential (V)	Reference
Anodic reactions				
Acetate + 4 H_2O ⇆ 2 HCO_3^- + 9 H^+ + 8 e^-	-0.29 [b]	-0.28	0.01	(Liu et al., 2005b)
Butyrate + 10 H_2O ⇆ 4 HCO_3^- + 23 H^+ + 20 e^-	-0.23 [c]	-0.28	0.05	(Liu et al., 2005b)
Glucose + 12 H_2O ⇆ 6 HCO_3^- + 30 H^+ + 24 e^-	-0.39 [d]	-0.22	0.17	(Freguia et al., 2008)
Wastewater COD ⇆ x HCO_3^- + y H^+ + z e^-	-0.26 [e]	-0.29	0.03	(He et al., 2016)
Cathodic reactions				
O_2 + 4 H^+ + 4 e^- ⇆ H_2O	0.81 [f]	0.50	0.31	(Clauwaert et al., 2007b)
*NO_3^- + 6 H^+ + 5 e^- ⇆ 0.5 N_2 + 3 H_2O	0.71 [g]	0.0	0.66	(Clauwaert et al., 2007a)
2 H^+ + 2 e^- ⇆ H_2	-0.41 [h]	-0.65 [i]	0.24	(Rozendal et al., 2008b)
HCO_3^- + 9 H^+ + 8 e^- ⇆ Methane + 4 H_2O	-0.25 [j]	-0.6 [k]	0.35	(Cheng et al., 2009)

[a] Calculated under the operating conditions as specified in the literature studies.

[b] Acetate concentration 800 mg/L (≈0.014 M); assumed HCO_3^- concentration 0.01 M; assumed pH 7; temperature 313.15 K.

[c] Butyrate concentration 800 mg/L (≈0.009 M); assumed HCO_3^- concentration 0.01 M; assumed pH 7; temperature 313.15 K.

[d] Assumed glucose 0.001 M; assumed HCO_3^- concentration 0.01 M; pH 6.4; temperature 295.15 K.

[e] COD concentration 1010 mg/L (assuming acetate COD: 0.016 M); assumed HCO_3^- concentration 0.01 M; pH 7; temperature 293.15 K.

[f] Assumed oxygen partial pressure 0.2 atm; assumed pH 7; assumed temperature 295.15 K.

* This reaction consists of 4 reactions, each with a different equilibrium potential. The average is calculated here. The bottleneck reaction is considered to be NO_2^- + e^- + 2H^+ → NO + H_2O (Clauwaert et al., 2007a). For calculations of partial reactions, see (Gregory et al., 2004; Desloover et al., 2011).

[g] Assumed nitrate concentration ~0.001 M; assumed nitrogen partial pressure 1 atm; assumed pH 7; temperature 295.15 K.

[h] Assumed H_2 partial pressure 1 atm; pH 7; temperature 303.15 K.

[i] Cathode potential at the onset of cathodic current generation during polarity reversal (Figure S3 of Rozendal et al. (2008c))

[j] Assumed CH_4 partial pressure 1 atm; assumed HCO_3^- concentration 0.01 M; pH 7; temperature 303.15 K.

[k] Cathode potential at the onset of cathodic current generation during linear sweep voltammetry (Figure 1 of Cheng et al. (2009))

The example calculations outlined in Table 2.2 deal with pure compounds, which makes it possible to do exact calculations. In many practical situations, however, the electron donor or acceptor will be a mix of several compounds and often of unknown composition and concentrations. Wastewaters for example contain a broad range of organic electron donors, such as carboxylic acids, carbohydrates, proteins (amino acids), of which the exact composition is unknown. In wastewater treatment this uncertainty in composition is generally solved by aggregating the organic loading of the wastewater as Chemical Oxygen Demand (COD), which describes the amount of oxygen needed to oxidize all organics present in the wastewater to CO_2 (Tchobanoglous et al., 2003). This COD value is also a convenient number in the context of bioelectrochemical wastewater treatment (Rozendal et al., 2008a) as it can be used to calculate the maximum amount of electrons that can produced per liter of wastewater (i.e., 1 g COD = 0.125 mol e^-; see also Textbox 1). What is unknown, however, is the equilibrium potential for COD, as its composition, and thus energy content, varies. Thus far a wide range of electron donors, such as carboxylic acids, (Bond & Lovley, 2003; Liu et al., 2005b) carbohydrates (sugars) (Chaudhuri & Lovley, 2003; Rabaey et al., 2003; Freguia et al., 2008), and proteins (amino acids) (Logan et al., 2005), have been used as feedstock for BESs. Interestingly, oxidation of the most commonly occurring organic components in wastewater feature a narrow range of equilibrium potentials (-0.34 ± 0.06 V, 37 compounds listed in Table App. 2.2) The lowest equilibrium potential is -0.544 V (oxalate) and the highest equilibrium potential -0.238 V (CH_4). Even though not all these compounds have been shown to be possible electron donors, this is indeed the typical range of observed anode potentials in BESs operated on wastewater (e.g., (Katuri & Scott, 2010; He et al., 2016)). In fact, for bioelectrochemical wastewater treatment this can be narrowed even further as in most circumstances complex substrates, such as proteins, carbohydrates, and fats are hydrolyzed and fermented to form the SCCAs acetic acid, propionic aicd, and butyric acid (Angenent et al., 2004) of which the equilibrium potential averages at -0.279 ± 0.001 V. For example, even when glucose, which is a substrate with theoretical equilibrium potential of -0.412 V (Table App. 2.2), is used as an anodic electron donor in BESs, OCPs are close to that of SCCAs (Liu & Logan, 2004; Freguia et al., 2008), As indicated earlier, the reason for this is that glucose is usually fermented to intermediates, such as SCCAs. The OCP therefore evolves as a mixed potential of the more oxidized fermentation products such as SCCAs. Hence, without an accurate knowledge of the exact composition of wastewater, we suggest to estimate the equilibrium potential of COD by using the average theoretical equilibrium potential of SCCAs (-0.279 ± 0.001 V).

6. Bioproduction: the Growth Reference System applied to microbial electrosynthesis and syngas fermentation

Production of chemicals from CO_2 is now widely being studied as sustainable alternative to the use of fossil fuels. Electrochemical and gas fermentation production systems compete for this market of CO_2-based products. The cathode overpotential will influence the operational cost of a process as it determines to a large extend the energy loss of the system. Kinetics and production rates, on the other hand, impact the capital costs of a process. Four different processes of interest are elaborated upon: i) the electrochemical production of formic acid; ii) the bioelectrochemical production of acetic acid (acetate); iii) the production of acetic acid from H_2/CO_2 in a pressurized system; and iv) syngas fermentation to acetic acid and ethanol (Table 2.3).

Electrochemical reduction of CO_2 has the potential to become a high-rate production technology, as current densities applied are usually several orders of magnitude higher than for BESs (> 1000 A/m² *vs.* 5 to 10 A/m²) (Qiao et al., 2014; Patil et al., 2015a). The use of highly conductive electrolytes decreases overpotentials, and thus operating cost. Formate production at 90% selectivity was recently obtained using atomically thin layers of partially oxidized cobalt as cathode material (Gao et al., 2016). This material development allows efficient production at a limited cathodic overpotential (0.24 V) for a current density of 100 A/m². Selectivity was often regarded as one of the main bottlenecks of electrochemical reductions compared to bioelectrochemical reduction, but the use of advanced electrode materials is greatly eliminating this problem (Yoo et al., 2015; Gao et al., 2016).

Electrochemical reduction of CO_2 seems nonetheless limited to single carbon compounds thus far, and generally requires the use of expensive catalysts (Costentin et al., 2013). This opens perspectives for BESs that use microbial electrocatalysts with the metabolic ability to produce more complex organics. Acetic acid production at the cathode by homoacetogenic microorganisms is the most studied pathway. Differences between the equilibrium potential and measured potential between 0.125 and 1.0 V have been reported for those systems, with a higher overpotential for studies using a fixed current (galvanostatic) approach instead of a fixed cathode potential (potentiostatic approach)(Table 2.3). In several MES studies both low and high cathode potentials have been tested, resulting in systems with and without H_2 production under abiotic conditions. The more negative cathode potential resulted in higher production rates (Blanchet et al., 2015; Jourdin et al., 2016a). A higher overpotential is not necessarily negative from an engineering point of view if a higher production rate is obtained under these conditions, and efficiencies remain high (Gildemyn et al., 2015b). An important note on the overpotential values in Table 2.3 is that these were calculated based on the cathode potential during the

experiment, not the OCP. For processes that potentially occur *via* indirect electrons transfer due to H_2 production, this is however a better approach as it takes into account the thermodynamic conditions during operation.

The exact mechanism for acetic acid production at a cathode is not yet fully understood. Certain studies claim a form of DET must take place, as no H_2 was detected neither in the biotic nor in the abiotic experiments. The electrode surface and mode of catalysis can, however, change as the biofilm develops, lowering the overpotential for the hydrogen evolution reaction. Modification with enzymes or biologically induced copper reduction combined with a rapid uptake of the produced H_2 by the microbial catalyst has been put forward as an explanation for the absence of H_2 in those experiments (Deutzmann et al., 2015; Jourdin et al., 2016b). Hydrogen can thus most likely be produced at the electrode in most MES studies. This would also partially explain the higher overpotentials observed at cathodes, as H_2 evolution should be considered as half-reaction instead. As discussed in section 4, the rapid uptake of H_2 by the biofilm can result in very low partial pressures at the electrode, enabling H_2 evolution at a higher potential than in abiotic conditions. The absence of H_2 in an abiotic control is thus not proof for DET. The electron transfer mechanism also impacts the calculation of the Gibbs free energy change. If one would assume DET, this can be calculated from the overpotential based on the reduction half-reaction (Table 2.3). This is a maximal value for $\Delta G_r^{0'}$ as it also partially consists of dissipated heat (Schink, 1997). Assuming MES *via* H_2 formation, the Gibbs energy change can be calculated from the H_2 partial pressure and total reaction. This allows a more fair comparison with other bioproduction techniques. Indeed, as most studies probably rely on indirect electron transfer *via* H_2, this makes the use of BESs for acetic acid production comparable to H_2/CO_2 fermentations. The low solubility of H_2 is an often mentioned problem, which could be circumvented by using electrodes. Partial pressures of H_2 in the direct vicinity of the electrode have, however, not been measured yet. In H_2/CO_2 fermentations the low solubility of H_2 gas requires improved gas mixing and when possible, the use of pressurized reactor systems. The latter does not only enhance the solubility, it also improves the energy gain for the microbial catalyst. The Gibbs free energy change increases by 20% when the partial pressure of H_2 increases with a factor 10 (-106 kJ/mol *vs.* -129 kJ/mol at pH 7 and T=298.15 K). High production rates and concentrations, up to 7.4 g/L/d and 44 g/L have been obtained in pressurized systems (Demler & Weuster-Botz, 2011).

Gas solubility also plays an important role in syngas fermentation. The presence of CO in syngas, however, distinguishes it from H_2/CO_2 fermentation: the Gibbs energy gain from CO conversion is higher (-165 kJ/mol acetic acid for CO-based fermentation *vs.* -106 kJ/mol acetic acid for H_2/CO_2 based fermentation under biochemical standard conditions). Values for MES

systems are situated in an even lower range (Table 2.3). When the microbial catalysts' kinetics are not limiting, the higher value for CO-based fermentation results in higher production rates for acetate (~10 g/L/d) and higher ATP production, and thus a distinct advantage over other production system that only rely on CO_2 at an industrial scale (Martin et al., 2015). For MES to become a competitive production strategy, volumetric production rates have to increase several orders of magnitude, to the level of H_2/CO_2 based fermentations. A strategy to improve the productivity could be the combination of the use of a biofilm on the cathode with controlled H_2 evolution and thus increased availability of H_2 in the attached biofilm (i.e. a galvanostatic approach as demonstrated by Gildemyn et al. (2015b) and Patil et al. (2015a)), as well as the use of pressurized cathodes (Fornero et al., 2008). In any case CO based fermentations have the advantage that the Gibbs energy gain is higher under conditions typical for microbial systems. The technical feasibility of the above-mentioned processes is, however, independent from the calculated thermodynamic parameters.

Table 2.3 - Equilibrium potentials, observed potential, calculated overpotential and Gibbs energy gain for the four discussed strategies for productions of chemicals from CO_2.

Reaction	Equilibrium potential [a] (V)	Observed/ Applied potential (V)	Calculated Overpotential (V)	Maximal Gibbs energy gain $\Delta G^{0'}$ (kJ/mol)	Reference
Electrochemical CO_2 reduction					
$HCO_3^- + 2\ H^+ + 2\ e^- \leftrightarrows$ Formate + H_2O	-0.37	-0.61	0.24	na	(Gao et al., 2016)
Microbial electrosynthesis					
$HCO_3^- + 9\ H^+ + 8\ e^- \leftrightarrows$ Acetate + 4 H_2O	-0.27[b]	-0.4	0.13	-96.1[g]	(Nevin et al., 2010)
$HCO_3^- + 9\ H^+ + 8\ e^- \leftrightarrows$ Acetate + 4 H_2O	-0.20[c]	-0.59	0.39	n.d.	(Marshall et al., 2013b)
$HCO_3^- + 9\ H^+ + 8\ e^- \leftrightarrows$ Acetate + 4 H_2O	-0.19[d]	-1.26	1.07	n.d.	(Patil et al., 2015a)
$HCO_3^- + 9\ H^+ + 8\ e^- \leftrightarrows$ Acetate + 4 H_2O	-0.38[e]	-1.14	0.75	-73.6[h]	(Gildemyn et al., 2015b)
$HCO_3^- + 9\ H^+ + 8\ e^- \leftrightarrows$ Acetate + 4 H_2O	-0.29[f]	-0.85	0.56	n.d.	(Jourdin et al., 2014)
H_2/CO_2-based fermentation					
4 H_2 + 2 HCO_3^- + $H^+ \leftrightarrows$ Acetate + 4 H_2O	na	na	na	-99.8[i]	(Zhang et al., 2013a)
4 H_2 + 2 HCO_3^- + $H^+ \leftrightarrows$ Acetate + 4 H_2O	na	na	na	-110.9[j]	(Demler & Weuster-Botz, 2011)
Syngas fermentation with CO					
4 CO + 4 $H_2O \leftrightarrows$ Acetate + 2 HCO_3^- + 3 H^+	na	na	na	-150[k]	(Martin et al., 2015)

[a] Calculated under the operating conditions as specified in the literature studies.

[b] Assumed $HCO3^-$ concentration 4 g/L (≈0.048 M); assumed acetate concentration 0.063 g/L (Patil et al., 2015a); assumed pH 7; temperature 303.15 K. I = 0.208 A/m²

[c] $HCO3^-$ concentration 2.5 g/L (≈0.30 M) in medium; acetate concentration 10.5 g/L; pH 5.5; temperature 298.15 K. I = n.d.

[d] $HCO3^-$ concentration 2.5 g/L (≈0.30 M) in medium; acetate concentration 1.29 g/L; pH 5.5; temperature 301.15 K. I = 5 A/m²

[e] $HCO3^-$ concentration 2.5 g/L (≈0.30 M) in medium; acetate concentration 2 g /L; pH 8.4; temperature 294.15 K. I = 5 A/m²

[f] $HCO3^-$ concentration 2 g/L (≈0.24 M) in medium; assumed acetate concentration 1.65 g/L (Patil et al., 2015a); assumed pH 7; temperature 308.15 K. I = 2.91 A/m²

[g] Calculated based on the overpotential of 0.13 V

[h] Calculated for full reaction assuming H_2 partial pressure of 0.17%

[i] $HCO3^-$ concentration 0.01 M in medium; acetate concentration 0.06 M; pH 4.5; temperature 308.15 K; H_2 partial pressure 0.6 atm

[j] $HCO3^-$ concentration 0.12 M in medium; acetate concentration 0.017 M; pH 7; temperature 303.15 K; H_2 partial pressure 1.7 bar

[k] Assumed $HCO3^-$ concentration 0.1 M; acetate concentration 0.17 M; pH 5.5; temperature 308.15 K; CO partial pressure 0.6 atm

n.d.: not determined, na: not applicable.

7. Biomass production

In his pioneering work on microbial bioenergetics, Heijnen was also able to derive empirical equations to estimate the maximum biomass yields in microbial systems as function of Gibbs energy dissipation (Heijnen, 1999). These equations were based on measurements in real microbial systems and found to be applicable to a wide range of electron donors and operating conditions:

For heterotrophic growth:

$$\frac{1}{Y_{GX}^{m}} = 200 + 18(6 - C)^{1.8} + exp\left[\left(\left(3.8 - \frac{\gamma_C}{C}\right)^2\right)^{0.16}(3.6 + 0.4C)\right] \quad (17a)$$

For autotrophic growth when reversed electron transport (RET)(Berg et al., 2010) is not required for growth:

$$\frac{1}{Y_{GX}^{m}} = 1000 \quad (17b)$$

For autotrophic growth when RET is required for growth:

$$\frac{1}{Y_{GX}^{m}} = 3500 \quad (17c)$$

With $\frac{1}{Y_{GX}^{m}}$ the Gibbs energy production required for biomass production in kJ/C-mol of biomass, C the number of carbon atoms per molecule of carbon source (e.g., 2 for acetate, 1 for bicarbonate), and γ_C the degree of reduction per molecule of carbon source (e.g., 8 for acetate, 0 for bicarbonate; Table App. 2.1). The predictions from these equations were found to be ± 10 - 20% accurate under a wide range of microbial conditions and for very diverse microbial systems (Heijnen, 1999). Therefore, these equations can be an interesting starting point for estimating the maximum biomass yield in BESs as well. The latter is then approximated by assuming that the overpotential (i.e. the potential difference between the electrode potential and theoretical potential of electron donor/acceptor couple), represents the maximum amount of energy available for the microorganisms. This means that at an overpotential of zero it is assumed that no energy is available. In such situation only catalysis and no growth is occurring in the system. At an overpotential of 1 V for example it is assumed that the maximum amount of energy available for the microorganisms is 1 J/C (or 96.5 kJ/mol e^-). As expected, the theoretical

maximum biomass production is higher when more easily assimilable compounds, such as acetate and glucose, are used as the carbon donor (Figure 2.2A, based on equation 17a). Under the conditions prevailing in active cells it is assumed that ATP-synthesis requires about 50 kJ/mol, not taking into account energy losses (Thauer et al., 1977). Less biomass is thus produced when bicarbonate is used as the carbon donor, particularly when RET is required for assimilating the bicarbonate (Figure 2.2A).

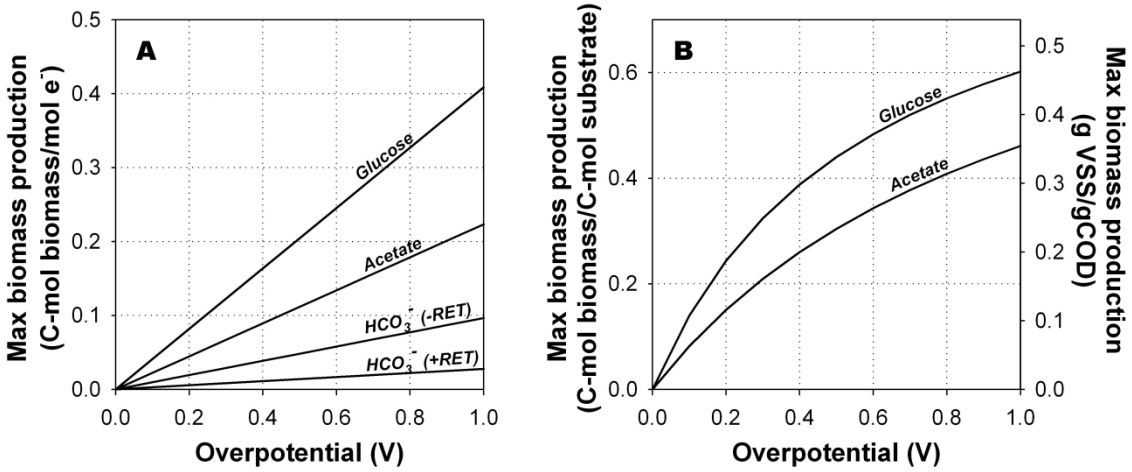

Figure 2.2 - Maximum biomass production increases with an increased overpotential. (A) Maximum biomass production expressed as C-mol biomass/mol e^- transferred by the microorganisms to/from the electrode for glucose, acetate, bicarbonate without reversed electron transport (RET), and bicarbonate with RET as the carbon donor (according to Eq. 17); (B) Maximum biomass production expressed as C-mol biomass/C-mol substrate and g VSS/g COD for glucose and acetate as the substrate (electron donor) at the anode. This includes both the substrate required for generating the electrons (catabolic) and the substrate required for building up biomass (anabolic) assuming a biomass composition of $CH_{1.8}O_{0.5}N_{0.2}$ ((Heijnen, 1999)) and ammonium as the nitrogen source (anabolic reaction for glucose: 0.175 glucose + 0.2 NH_4^+ → 1 C-mol biomass + 0.05 HCO_3^- + 0.4 H_2O + 0.25 H^+; anabolic reaction for acetate: 0.525 acetate + 0.2 NH_4^+ + 0.275 H^+ → 1 C-mol biomass + 0.05 HCO_3^- + 0.4 H_2O).

Figure 2.2B shows the maximum biomass production, but now expressed as C-mol biomass/C-mol substrate and g VSS/g COD. This graph includes both the substrate required for generating the electrons (catabolic) and the substrate required for building up biomass (anabolic). As shown in Figure 2.2B, Eq. 17 predicts that for an overpotential ranging from 0 to 1.0 V, the biomass yield for glucose will be in range of 0 to 0.60 C-mol biomass/C-mol substrate (0 to 0.46 g VSS/g COD), whereas the biomass yield for acetate will be in range of 0 to 0.46 C-mol biomass/C-mol substrate (0 to 0.35 g VSS/g COD). For comparison, in more conventional microbial systems (i.e., non-bioelectrochemical), the biomass yield is typically in the range 0.01 to 0.7 C-mol biomass/C-mol substrate (Heijnen, 1999).

The predictions in Figure 2.2B are in line with the limited data available in literature on biomass yield in BESs. For instance, using a balance calculation, Freguia and coworkers determined the biomass yield in glucose and acetate fed MFCs (Freguia et al., 2007). For the glucose fed MFC, a biomass yield of 0.48 C-mol biomass/C-mol substrate (0.37 g VSS/g COD) was

observed at an external resistance of 20 Ω, whereas a biomass yield of 0.54 C-mol biomass/C-mol substrate (0.41 g VSS/g COD) was observed at an external resistance of 5 Ω. For the acetate fed MFC, a biomass yield of 0.24 C-mol biomass/C-mol substrate (0.18 g VSS/g COD) was observed at an external resistance of 20 Ω, whereas a biomass yield of 0.29 C-mol biomass/C-mol substrate (0.22 g VSS/g COD) was observed at an external resistance of 5 Ω. These observations are in the range of the prediction in Figure 2.2B. Moreover, it confirms that glucose, as predicted by Eq. 17, gives a higher biomass yield than acetate, as glucose oxidation results in a larger Gibbs energy change compared to acetate. It also verifies that at higher overpotentials (which occur at lower resistance) higher biomass yields are observed for both glucose and acetate. Finally, Eq. 17 also explains why thinner biofilms are observed on biocathodes (using bicarbonate as C-source) compared to bioanodes despite the higher overpotentials (Virdis et al., 2011; Jourdin et al., 2014).

An important note of caution is that Eq. 17a predicts a *maximum* biomass yield and should therefore be treated this way. In practice, the true values for biomass yields can be expected to be lower than these predicted values. The main reason for this is that part of the measured overpotential is not available for the microorganism, but dissipated as heat in the electron transfer process. In addition, as with any other biological process, a proportion of the energy available to the microorganism is dedicated to maintenance rather than growth (Heijnen, 1999). As mentioned in section 5, the overpotential can be used as a tool steer the presence of electrocatalysts over methanogens in the biofilm. The control of the overpotential to avoid biomass growth and favor catalysis by electrogens has not been studied yet. Finally, the fact that a certain amount of energy is available does not necessarily mean that the microbial pathways are indeed available to utilize this energy and form ATP. Nevertheless, the prediction calculated by Eq. 17 and Figure 2.2 form a good starting point when trying to estimate the biomass formation potential in BESs.

8. Concluding Remarks

Based on the GRS as developed by J.J. Heijnen, we here presented an approach that can simplify thermodynamic calculations for bioelectrochemical conversions. We highlighted some important findings regarding overpotentials and bioproduction that can improve the understanding of BESs. An important note of caution when using this method is that the values calculated are theoretical values, that furthermore rely on empirical equations in the case of biomass production, and, therefore, represent thermodynamic limits. Microbial metabolic pathways and kinetics will eventually determine whether specific bioelectrochemical reactions are feasible or not.

Text Boxes

Text Box 1. Calculation examples for determining reaction stoichiometry using the Growth Reference System

In the anode half reaction for acetate oxidation to bicarbonate and electrons, acetate is the only compound that has a degree of reduction other than zero (i.e., 8 e^-). All other compounds involved in this reaction, i.e., bicarbonate, water, and protons, all have a zero degree of reduction and do not influence the balance of the degree of reduction. Therefore, by using the balance of degree of reduction, one can instantly derive that the amount of electrons generated in the anode reaction is eight:

$C_2H_3O_2^- \rightarrow 8\ e^-$

Then, by sequentially solving carbon balance using bicarbonate;

$C_2H_3O_2^- \rightarrow 2\ HCO_3^- + 8\ e^-$

the oxygen balance using water;

$C_2H_3O_2^- + 4\ H_2O \rightarrow 2\ HCO_3^- + 8\ e^-$

and the hydrogen balance using protons:

$C_2H_3O_2^- + 4\ H_2O \rightarrow 2\ HCO_3^- + 9\ H^+ + 8\ e^-$

one can quickly derive the complete stoichiometry of a half reaction. As a final check, one can then verify that the charge is equal on both sides of the equation.

Equally simple as for half reactions, also the complete reaction stoichiometry can be determined. For example, for the reaction stoichiometry of an MFC operated on acetate at biochemical standard conditions, the only compounds that have a degree of reduction other than zero are acetate (i.e., 8 e^-) and oxygen (i.e., -4 e^-). Therefore, by using the balance of degree of reduction, one can instantly derive that acetate and oxygen react in a 1/2 ratio:

$C_2H_3O_2^- + 2\ O_2 \rightarrow$

Then, by sequentially solving carbon balance using bicarbonate;

$C_2H_3O_2^- + 2\ O_2 \rightarrow 2\ HCO_3^-$

the oxygen balance using water;

$C_2H_3O_2^- + 2\ O_2 \rightarrow 2\ HCO_3^-$ (no water involved)

and the hydrogen balance using protons:

$C_2H_3O_2^- + 2\ O_2 \rightarrow 2\ HCO_3^- + H^+$

one can quickly derive the stoichiometry of the complete reaction. Note that determining the electron donor to oxygen ratio is also a rapid method for determining the COD value of a certain compounds (Heijnen, 1999). E.g. for the above case: 1 mol of acetate requires 2 moles of oxygen. Multiplied by the molecular weight of oxygen gas this gives 2×32=64 g COD, or thus 1.08 g COD/g acetate.

Text Box 2. Gibbs energy, cell voltage, and electrode potentials

Gibbs energy (ΔG) is a thermodynamic property that represents the maximum amount of useful work that can be produced from a specific chemical reaction or the minimum amount of work that needs to be delivered to make a specific chemical reaction happen. If Gibbs energy change of a reaction is negative, work can be produced from the system and the reaction is referred to as exergonic. In the context of BESs this means that electrical energy can be produced (i.e., MFC). If the Gibbs energy change of a reaction is positive, work needs to be delivered to the system and the reaction is referred to as endergonic. In the context of BESs this means that electrical energy needs to be invested to drive the reaction (i.e., MEC). The Gibbs energy change of a (half) reactions can be easily converted into cell voltage and potentials using the following equation:

$$E = -\frac{\Delta G}{nF}$$

In which *E* is the electrode potential resulting from a certain (half) reaction, ΔG is Gibbs energy change of that specific (half) reaction, *n* the amount of electrons involved in the specific (half) reaction, and *F* Faraday's number (96485.3 C/mol).

Acknowledgements

S.G. is supported by the Special Research Fund (BOF) from Ghent University. K.R. acknowledges support by the European Research Council grant ELECTROTALK. Equipment used was supported *via* "BOF Basisinfrastructuur 01B05912". The authors thank Peter Clauwaert, Jan B.A. Arends and Kun Guo for critically reading and commenting on the manuscript.

CHAPTER 3 - A REACTOR TECHNOLOGY FOR INTEGRATED PRODUCTION, EXTRACTION AND CONCENTRATION OF ACETIC ACID THROUGH MICROBIAL ELECTROSYNTHESIS

This chapter has been redrafted after:

Gildemyn, S., Verbeeck, K., Slabbinck, R., Andersen, S.J., Prévoteau, A., Rabaey, K. 2015. Integrated Production, Extraction, and Concentration of Acetic Acid from CO_2 through Microbial Electrosynthesis. Environmental Science & Technology Letters, 2(11), 325-328.

Gildemyn, S.*, Verbeeck, K.*, Jansen, R., Rabaey, K. 2016. The type of ion selective membrane determines stability and production levels of microbial electrosynthesis. Submitted to Bioresource Technology. * Equal contributions

Abstract

Using CO_2 for bioproduction combines decreased greenhouse gas emissions with a decreased dependence on fossil carbon for production of multicarbon products. Microbial electrosynthesis (MES) enables coupling such a process to renewable energy to drive the reduction of CO_2 at the cathode of an electrochemical cell. To date, low product concentrations preclude cost-effective extraction during MES. Here, we present an approach that couples production and recovery of acetic acid in a single, three-chamber reactor system. Acetic acid was produced at 61% coulombic efficiency (CE) and fully recovered as an acidified stream containing up to 13.5 g/L (225 mM) acetic acid, the highest concentration obtained thus far in MES. In a second study, a direct comparison was made between a reactor system with *in-situ* extraction, and two reactor types with a single ion selective membrane without *in-situ* extraction. The study showed that pH stabilization in the catholyte played an important role to maintain a higher production efficiency in the reactor with *in-situ* product extraction (41% CE with extraction *vs.* a maximum of 30% CE in a reactor without extraction). Using the improved reactor design with extraction, a single separated acidic product was generated through *in-situ* membrane electrolysis, enabling further upgrading.

1. Introduction

Carbon dioxide is ubiquitously available as a carbon source, particularly at hotspots such as cement kilns, steel factories and power plants. Converting this oxidized form of carbon to useful building blocks for chemical and fuel production lowers emissions of greenhouse gases to the atmosphere and decreases the dependence on fossil fuel derived chemicals (see Chapter 1). MES has emerged as an attractive bioproduction route to convert CO_2 to organic products using electricity as the driving force. It combines the advantages of electrocatalysis - electricity as source of reducing power, bringing more reducing conditions than for example H_2 under atmospheric conditions (Dennis et al., 2013) - with those of biology - the production of multicarbon products at high specificity (Rabaey & Rozendal, 2010). Acetic acid was the dominant product of this cathodic process in the first studies with pure cultures (Nevin et al., 2010; Nevin et al., 2011). Higher concentrations (up to 175 mM, 10 g/L) were obtained in experiments with mixed cultures, at a somewhat lower CE compared to that of pure culture studies (Marshall et al., 2013b). MES studies thus far typically use of a two-compartment setup, separating water oxidation at the anode and CO_2 reduction at the cathode by a CEM (Marshall et al., 2013b; Jourdin et al., 2014; Ganigué et al., 2015).

It is known from MFC operation that the membrane type influences the process output, by influencing the overpotentials. Limiting overpotentials can, amongst other strategies, be achieved by avoiding the buildup of a pH gradient between the anode and cathode compartment, as well as ensuring an efficient charge balancing through the membrane (Clauwaert et al., 2008a). Even though systems with an AEM showed a better MFC performance, the use of CEMs remains the state-of-the art, also for MES (Rozendal et al., 2008d; Sleutels et al., 2009). A major drawback of the use of a CEM for MES is that products cannot easily be recovered at the obtained titers, leading to possible product diversification and inhibition besides high costs for product recovery. An expensive post-treatment would be needed to concentrate and acidify the products to recover them from the microbial broth.

Andersen and co-workers described the extraction of carboxylates *via* ME, across an AEM (see Chapter 1; (Andersen et al., 2014)). The crossing carboxylates are protonated and recovered as carboxylic acids in a clean acidic anolyte. In the study described in this chapter we directly coupled the production of acetic acid with extraction in a single, three-chamber reactor system. This system includes an AEM separating the cathode from a saline extraction compartment, and a CEM between the saline extraction compartment and the anode compartment to avoid chlorination of acetic acid at the anode. The electrical current thus simultaneously drives two processes: the reduction of CO_2 into organic products *via* homoacetogenesis and the extraction of the latter into the extraction solution (Figure 3.1). The first study described in this chapter

shows that the overall process design with *in-situ* extraction allowed stable production unhindered by product inhibition and production of acetic acid above 13 g/L (220 mM) as a single organic acid in an extraction liquid. To further elucidate the advantages and disadvantages of a reactor system with *in-situ* extraction, a second series of experiments directly compared the performance of a reactor system with extraction (three-compartment reactor with AEM and CEM) and two systems without extraction, using either a single CEM or BPM. A CEM is the most commonly used ion selective membrane. Bipolar membranes have not yet been used for MES, and the effectiveness of particularly OH^- balancing in such systems is unknown. To avoid O_2 crossover and anodic Cl^- oxidation, the use of membrane(s) as separation barrier between anode and cathode appears preferred over setups without membrane (Harnisch & Schröder, 2009). In the context of this chapter, carboxylic acids are reported in the acid form, even though these are fully or partially dissociated in reality. When specifically describing the charged species crossing the AEM, that form (e.g. acetate) will be used.

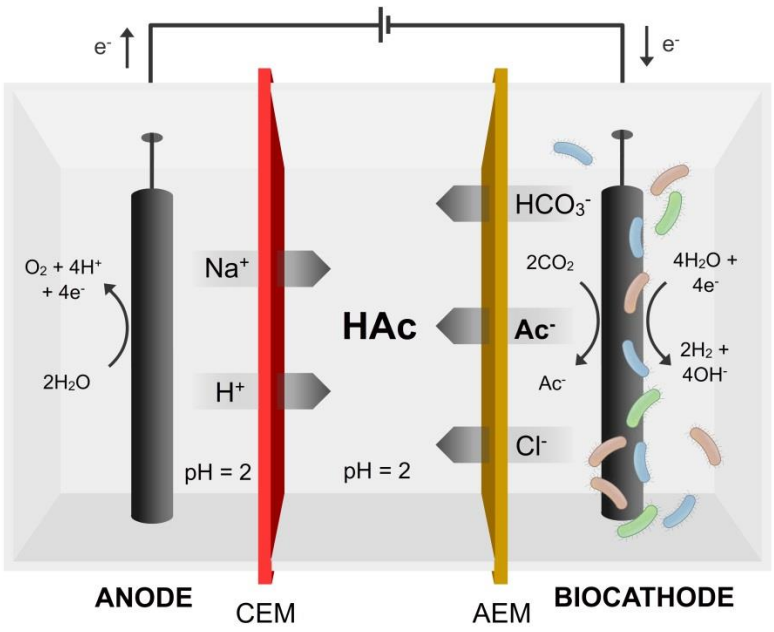

Figure 3.1 - Reactor concept for simultaneous biological production and extraction of acetate from CO_2 and electrical current. An anion exchange membrane (AEM) separates the cathode and extraction compartment. A cation exchange membrane (CEM) separates the anode and extraction compartment. The middle compartment serves as the extraction compartment for recovery of acetate as acetic acid.

2. Materials and Methods

2.1 Reactor setups and operation

For the first experiment, a three-compartment bioelectrochemical cell was constructed using Perspex frames (Figure 3.2). All reactor compartments had a working volume of 200 mL (5 × 20 × 2 cm^3). An AEM (Fumasep FAB, Fumatech, Germany) separated the cathode and extraction compartment. A CEM (Fumasep FKB, Fumatech, Germany) was used between the extraction and

anode compartment. Carbon felt (thickness 3.18 mm, Alfa Aesar, USA) was used as cathode material. The felt was soaked subsequently in 1 M NaOH and 1 M H_2SO_4, both for 24h, and rinsed with demineralized water before being placed in the reactor, where a stainless steel frame current collector contacted the edges of the felt. The anode material was a dimensionally stable titanium-coated TiO_2/IrO_2 (35/65%) mesh (Magneto Special Anodes BV, The Netherlands). All electrodes and membranes had a projected surface area of 100 cm². The initial volume of solution in each compartment was 350 mL, which includes a buffer vessel in the liquid recirculation loop. All compartments were operated in batch mode with a recirculation rate of 31 ± 0.6 mL/min.

In the second experiment three reactor setups were compared. The first reactor was a three-compartment reactor as described above. The second reactor was a two-compartment reactor built with the same materials, and a CEM (Fumasep FKB, Fumatech, Germany) separating the anode and cathode compartment. The third reactor was a two-compartment reactor with a BPM (Fumasep FBM, Fumatech, Germany) positioned according to the manufacturer's instructions, with the cation exchange layer directed towards the cathode and the anion exchange layer directed towards the anode. The liquid recirculation rates of all three reactors were doubled compared to the first experiment to increase mixing.

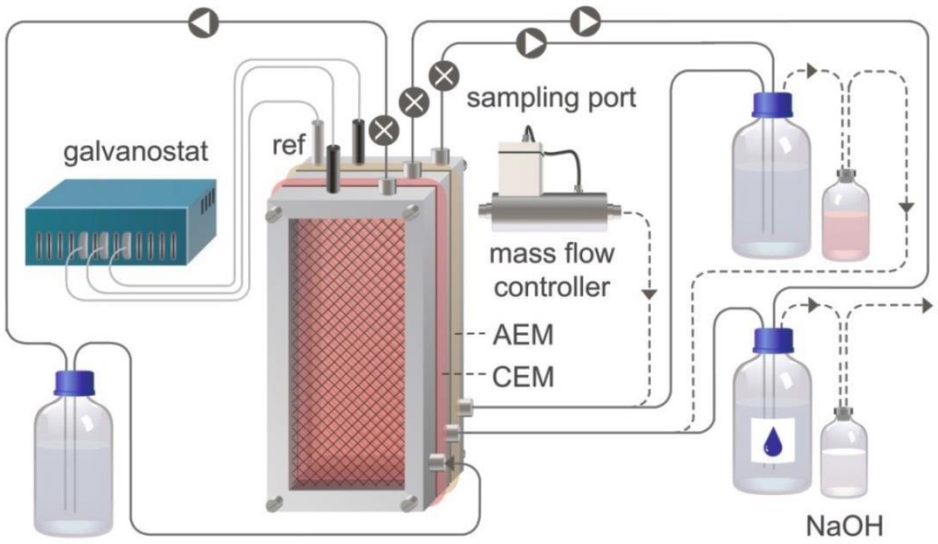

Figure 3.2 - Reactor setup for simultaneous biological production and extraction of acetate from CO_2 and electrical current. Full black lines show liquid streams, dotted lines gas streams (from mass flow controller N_2/CO_2 – 90%/10%) and gray lines electrical connections. Anodic and cathodic compartments are represented on the foreground and background of the reactor, respectively. The middle compartment serves as extraction compartment for recovery of acetate as acetic acid. AEM: anion exchange membrane; CEM: cation exchange membrane; ref: reference electrode.

In both experiments the catholyte consisted of an anaerobic homoacetogenic growth medium with a 30 mM bicarbonate buffer at pH 7.7, lacking all organic carbon sources (Table 3.1). A 50 mM Na_2SO_4 solution adjusted at pH 2 using 1 M H_2SO_4 was used as the anolyte. For

the reactors with extraction the initial solution of the extraction compartment (middle compartment) consisted of a 4-fold concentrated salt solution containing the same salts as the catholyte, initially adjusted to pH 2 using 1 M H_2SO_4.

Table 3.1 - Composition of the basal medium (homoacetogenic medium) used as catholyte in reactor experiments. The composition of the trace metal solution (*), vitamin solution (**) and tungstate-selenium solution (***) is given in Appendix 3. Medium adapted from Leclerc et al. (1997).

Component	Concentration
K_2HPO_4	0.2 g/L
NH_4Cl	0.25 g/L
KCl	0.5 g/L
$CaCl_2.2H_2O$	0.15 g/L
$MgCl_2.6H_2O$	0.6 g/L
NaCl	1.2 g/L
$NaHCO_3$	30 mL from 1M stock
Trace metal solution*	1 mL/L
Vitamin solution**	2.5 mL/L
Tungstate-selenium solution***	0.1 mL/L

A N_2/CO_2 (90%/10%) gas flow ensured anaerobic conditions in both the production and extraction compartment, CO_2 excess for autotrophic production and buffering of the catholyte. In the three-compartment reactors the gas stream bubbled through the catholyte first and consequently through the extraction compartment. In the two-compartment reactors the gas stream was passed through the catholyte and anolyte respectively. Possible volatilization of SCCAs was monitored using a 1 M NaOH trap after the gas outlet. Antibiotics were added weekly in the anodic and, if applicable, extraction compartment as a precaution to avoid contamination and the associated consumption of organics (Table 3.2). Gas and liquid samples were taken three times per week from each compartment and an equal volume of the respective solutions was added from a sterile anaerobic stock. The pH was corrected after sampling with 1 M anoxic NaOH if the pH had dropped below 6.

Table 3.2 - Composition of the antibiotic mix used to avoid consumption of the extracted acetic acid

Antibiotic	Final concentration (mg/L)
Tetracycline	10
Amoxicillin	40
Ciprofloxacin hydrochloride	40

In the first experiment the reactor was inoculated up to a cell density of 3.4×10^6 viable cells/$mL_{catholyte}$ with a pre-enriched mixed microbial community. The same pre-cultured inoculum was used in the second study, at a final cell density of 3.0×10^6 cells/$mL_{catholyte}$. The culture had been previously enriched at 28 °C from the effluent of a bioanode and anaerobic digester in

serum flasks using the homoacetogenic growth medium and a H_2/CO_2 atmosphere (Patil et al., 2015a). Through serial dilution and rapid transfers in fresh medium, an autotrophic acetate-producing community dominated by *Clostridiales*, that produced no CH_4 even in the absence of methanogenic inhibitors, was obtained. The culture was maintained by weekly transfers in fresh homoacetogenic growth medium and incubation at 28 °C. A quality check of the culture (absence of CH_4 in headspace and acetic acid concentration above 1 g/L) was performed before inoculation. The culture was not further characterized by sequencing or other molecular techniques. It was assumed that culturing conditions and operational conditions in the reactor would provide sufficient selective pressure to maintain the functionality of the culture. The reactor experiments took place at room temperature (21 ± 2 °C). The first experiment consisted of 2 consecutive cycles of 43 days. The second study comparing reactor systems with and without extraction consisted of 1 cycle of 43 days. For experiment 1 control outcomes (noninoculated with applied current and inoculated without applied current) and a biological replicate are reported in Appendix 3. The control experiments are also applicable to the second study.

2.2 Analytical Techniques

For pH measurements a Consort SP10B pH-electrode connected to a Consort C532 multimeter analyzer (Consort, Turnhout, Belgium) was used. Conductivity was measured with a Consort C833 multi-channel analyzer with an EC-electrode (Consort, Turnhout, Belgium). Both probes were calibrated with their respective calibration solutions before analysis of a batch of samples.

Total organic acids were analyzed using a 930 Compact IC Flex (Metrohm, Switzerland) ion chromatography system with in-line bicarbonate removal (MCS). Separation was done on a Metrosep organic acids (250/7.8) column at 35 °C behind a Metrosep organic acids (4.6) guard column. The eluent was 1 mM H_2SO_4 and the flow rate 0.5 mL/min. An 850 IC Conductivity Detector was used for detection of eluted components. Detection was enhanced using a chemical suppression module to replace protons with Li-cations (MSM with 0.5 M LiCl). The sample aspiration needle was cleaned with acetone between each analysis. The lower limit of quantification was 1 mg/L. Based on the total concentration of a specific organic acid and the pH, the concentration of undissociated carboxylic acids was calculated.

Inorganic anions (Cl^-, NO_2^-, NO_3^-, PO_4^{3-} and SO_4^{2-}) were determined using ion chromatography (930 Compact IC, Metrohm, Switzerland) equipped with a conductivity detector. The device was equipped with a Metrosep A Supp 5 - 150 column and Metrosep A Supp 4/5 guard column. The eluent was 1.0 mM $NaHCO_3$, 3.2 mM Na_2CO_3 and the flow rate was 0.7 mL/min. Sodium, potassium, magnesium and calcium were determined on a 761 Compact

Ion Chromatograph (Metrohm, Switzerland) using a conductivity detector. The device was equipped with a Metrosep C6 – 250/4 column and a Metrosep C4 Guard/4.0 guard column. The eluent was 1.7 mM HNO_3 and 1.7 mM dipicolinic acid at a flow rate of 1.2 mL/min.

Ammonium was measured according to standard Nessler method (Greenberg et al., 1992). Samples were filtered and diluted 20 times in demineralized water to fit in the working range of the method (0.1-5 mg NH_4^+-N/L*).* The color change from the Nessler's reagent was colorimetrically monitored at a wavelength of 425nm over a 1 cm path length using a spectrophotometer (Biochrom WPA Biowave, UK).

Alcohols were analyzed using a 930 Compact IC Flex (Metrohm, Switzerland) ion chromatography system with a Metrosep Carb 2 (250/4.0) column and an amperometric detector. The eluent was 20 mM NaOH, at a flow rate of 0.8 mL/min.

Gas samples were analyzed using a Compact GC (Global Analyser Solutions, Breda, The Netherlands), equipped with a Porabond precolumn and a Molsieve SA column. Concentrations of CH_4, O_2, N_2, CO_2 and H_2 were determined using a thermal conductivity detector with a lower detection limit of 1 ppmv for each gas component.

In the first experiment biomass growth was monitored *via* flow cytometry. Samples were diluted 100 times in 0.22 µm filtered drinking water (Evian) and stained with SYBR Green I and propidium iodide, followed by 10 min incubation in the dark at 37 °C (De Roy et al., 2012; Van Nevel et al., 2013). The stained samples were measured using an Accuri C6 flow cytometer (BD Biosciences), equipped with an autoloader. Cell counts were done by measuring the number of particles in a set volume after gating on green *vs.* red fluorescence plots in the BD CSampler software. Quality control with respect to absolute cell counting was done on a daily basis with standardized beads. Samples were taken from the bulk phase of the catholyte and are independent of the putative biomass retention on the cathode electrode surface.

2.3 Electrochemical operation

The reactors were operated as a three-electrode setup using the cathode as working electrode. A reference electrode (Ag/AgCl, 3 M KCl, + 210 mV *vs.* SHE, BASi) was placed in the catholyte. All potentials are reported *vs.* the SHE. The reactor was polarized for 24h at – 0.1 A/m² before the experiment started. After inoculation, a current density of – 5 A/m² was applied to the cathode using a potentiostat (VSP, BioLogic, France). This would lead to a maximal acetic acid production rate of 33.6 g/m²/d at 100% CE assuming 8 electrons consumed per acetic acid molecule produced. For calculations of the CE, products accumulated in all reactor compartments of one reactor are considered, as anolyte concentrations were minimal in the

case of the reactor with CEM and BPM, and the concentrations in the reactor with AEM evolved to a steady-state in the cathode and anode compartment. A cyclic voltammetry (CV; scan rate 2 mV/s) was run before and immediately after inoculation, and once per week during experimental operation.

3. Results and Discussion

3.1 Proof-of-concept for simultaneous production and extraction of acetic acid

A first experiment was started with the aim of simultaneously producing and extracting acetic acid in a single MES reactor. Production of SCCAs by the pre-enriched homoacetogenic mixed microbial community started on day 3 after inoculation (Figure 3.3). In MES, CO_2 is reduced to SCCAs as the main product likely *via* the Wood-Ljungdahl pathway (Nevin et al., 2010). Besides acetic acid production we observed H_2 evolution at the cathode.

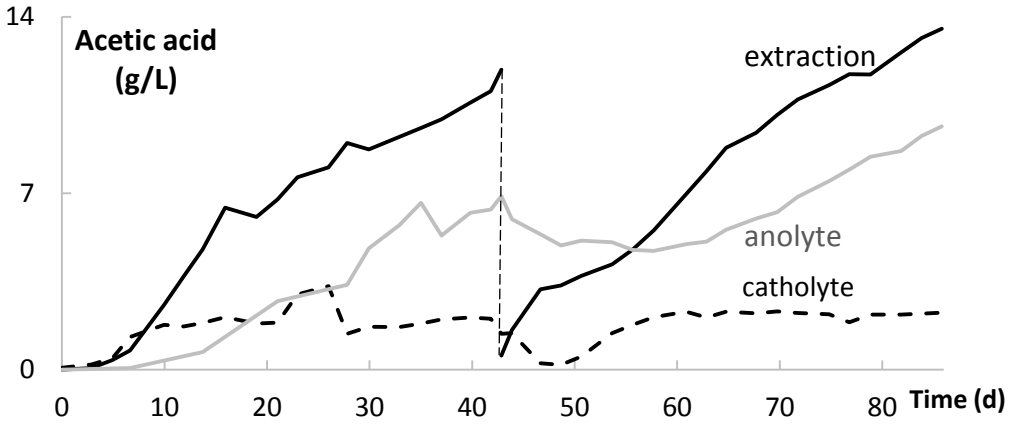

Figure 3.3 - The acetic acid concentration (g/L) in the extraction compartment steadily increased for a stable concentration in the cathode compartment. Concentrations in the catholyte (black dotted line), extraction compartment (full black line) and anolyte (gray line) are represented for the two cycles of the first experiment. The vertical dotted line shows the start of the second cycle for the extraction compartment.

Acetic acid was predominantly produced in this first experiment, accounting for 96.2 and 98.4% of all SCCAs present at the end of the first and second cycles, respectively (as carbon, see Appendix 3). The remainder were small amounts of formic and propionic acid. From day 10 the concentration of acetic acid in the catholyte reached a plateau at 2.0 ± 0.5 g/L (34 ± 8 mM) while the concentration in the extraction compartment steadily rose to reach 11.9 g/L (200 mM) on day 43. The solution from the extraction compartment was exchanged with fresh solution to assess reproducibility of the process, starting the second cycle for extraction. The acetic acid concentration in the extraction compartment similarly increased, to 13.5 g/L (225 mM) at the end of the second cycle (Figure 3.3), while the concentration in the catholyte remained stable. This is the highest concentration of acetic acid reported thus far for MES, and in this case due to

its purity and low pH, the product was already in a stream available for process use or upgrading, through esterification for example (Andersen et al., 2016). Overall 17.5 g of acetic acid was produced over an 86 day time period, resulting in a CE for production of 60.8%. When only the stable operation periods are taken into account the CE for cycles 1 and 2 was 72.6% and 67.0% respectively (Table 3.3). Ethanol concentrations did not exceed 35 mg/L. Electrons were lost as H_2 in the gas effluent (see further) and part of the carbon and electrons were used to sustain biomass growth, as the cell density in the catholyte increased from ~ 3.4×10^6 cells/$mL_{catholyte}$ to ~ 5.5×10^9 cells/$mL_{catholyte}$ after 82 days of operation. Limiting biomass growth and enhancing the catalytic effect of the microorganisms could lead to a further increase of the CE, which could be the case at a lower cathodic overpotential (Chapter 2; (Rabaey & Rozendal, 2010)). No organic products were detected in control experiments conducted in the absence of either inoculum or current, showing that both the cathodic process and the enriched mixed culture are required for the system to function. An independent biological replicate furthermore had a similar production pattern, proving the technology to be reproducible (see Appendix 3).

Table 3.3 - Coulombic efficiency (CE), production rate (per electrode surface area) and extraction rate (per membrane surface area) for both cycles during stable operation.

	Cycle 1 (day 10 – day 43)	Cycle 2 (day 54 – day 86)
Production rate (g/L/d)*	0.70	0.64
Production rate (g/m²/d)	24.3	22.4
CE (%)	72.6	67.0
Extraction rate (g/m²/d)	24.2	21.2
Extraction efficiency (%)*	99.5	94.3

* The volumetric production rates are calculated for a catholyte volume of 350 mL. The extraction efficiency is the ratio between extraction and production rate. A mass-based graph for production is available in Appendix 3 for interpretation of the calculated values, as water displacement took place from the cathode to the extraction compartment.

During the 86 day biocathode operation the pH of the catholyte remained stable at 8.4 ± 0.5. This contrasts with two-compartment MES setups using a CEM where a decreasing pH is mostly observed when SCCAs are produced and accumulated, an effect enhanced by migration of H^+ over the CEM (Marshall et al., 2013b; Ganigué et al., 2015). We hypothesize that the system with extraction favors a stable pH environment, provided the catholyte is continuously sparged with CO_2. At the start of cycle 2 the N_2/CO_2 bubbling stopped because of a technical failure. This resulted in a pH increase of the catholyte to 11.2 on day 47. The CO_2 gas flow was restored and 1 mL of 1 M HCl was dosed into the catholyte, to bring the pH below 8.5. During this intervention the production of carboxylic acids temporarily stopped though extraction continued, resulting in acetic acid concentrations as low as 194 mg/L in the catholyte on day 49. The functionality of the

bacterial community and acetic acid production rates recovered from the pH shock 4 days after the pH correction.

Microbial electrosynthesis was likely driven by indirect H_2 electron transfer. In the abiotic tests preceding the inoculation of experiment 1, H_2 was detected as the sole product of electrochemical reduction (– 5 A m^{-2}), for a cathode potential of approximately – 1.05 V *vs.* SHE. After inoculation a rapid consumption of H_2 by the microorganisms took place, as H_2 was not consistently detected in the headspace gas samples over time. A cathode potential of – 1.14 ± 0.04 V *vs.* the SHE was recorded during the experiment. Recovery of electrons in the form of H_2 measured in the headspace accounted for ~ 6% of the electrons provided during the MES experiment. No statements about the role of a biofilm can be made (see Appendix 3). Biofilm formation does constitute an advantage when developing continuous processes, thus avoiding washout of the microbial electrocatalyst. In contrast, an active microbiome could be sustained during a long period of time under stable conditions using the approach presented here, including product extraction. The absence of product build-up in the catholyte enabled the use of a batch mode operation for this compartment without the strict need for an electroactive biofilm and without the occurrence of product inhibition or product diversification.

The direct extraction of acetate as acetic acid constitutes the core mechanism of the technology presented here. The extraction, termed membrane electrolysis (Andersen et al., 2014), allows a stable and continuous production by the microorganisms. The extraction efficiencies (ratio of extraction rates to production rates) during stable operation were above 94% (Table 3.3). The stable concentration of acetic acid in the catholyte is a confirmation of the efficient extraction. Acetate accounted for 8.1 ± 0.8% of the charge passing through the AEM. It must be noted that as 8 electrons are needed for the production of one acetic acid molecule, the extraction of acetate can account for a maximum of 12.5% of the ions crossing the membrane. Other anions present in the catholyte (mainly HCO_3^-, Cl^- and OH^-) and the backflux of H^+ through the AEM balanced the rest of the charge. This backflux is due to the non-ideal permselectivity of ion exchange membranes (Varcoe et al., 2014) and the pH difference between the extraction and cathode compartment (average of 1.7 ± 0.2 *vs.* 8.4 ± 0.5 in the catholyte). It however remains unclear how this extraction of acetate and other ions affects the overall process efficiency. It is therefore necessary to compare the performance of systems with and without product extraction.

3.2 Acetic acid production in systems with and without in-situ *product extraction*

To distinguish the effect of electrochemical steering and extraction separately, MES of acetic acid was directly compared in three reactor types. One reactor was an exact copy of the system

used in experiment 1. The other two reactors were two-compartment reactors with either a CEM or a BPM. *In-situ* extraction was thus not possible in these reactors. The performance was evaluated based on several critical performance parameters described below.

Acetic acid production started soon after inoculation, as for the first experiment. In the reactor with CEM production started on day 3, while the lag-phase was about 2 days longer for the reactor with BPM and AEM (extraction) (Figure 3.4). Total acetic acid production was higher for the reactor with extraction. Acetic acid was the main SCCA produced in all three reactor setups, but in contrast to the previous experiment, the reactor with AEM (extraction) also showed increased concentrations of formic acid in the middle compartment (Appendix 3). Production of formic acid in the reactor with extraction stopped after 10 days. Formic acid is an intermediate of the Wood-Ljungdahl pathway and is often detected as a transient product in autotrophic fermentations and MES (Peters et al., 1999; Nevin et al., 2011). The activation of formic acid in the methyl branch, for production of acetyl-CoA requires 1 ATP. Enzymes in this pathway are Ni and Mn-dependent and the ATP has to be produced *via* chemi-osmotic energy conservation (See Chapter 1; (Drake et al., 2006)). As formic acid production took place at the beginning of the experiment only, when fresh medium was used, an inefficient chemi-osmotic ATP production could have resulted in formic acid production (Schuchmann & Müller, 2013).

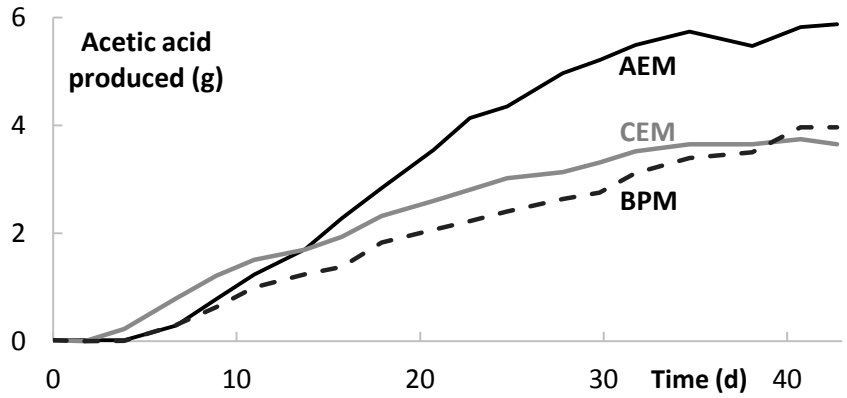

Figure 3.4 - The total mass of acetic acid produced was higher for the reactor with anion exchange membrane (AEM, black line) compared to the two reactors without extraction (cation exchange membrane: CEM (gray line); and bipolar membrane: BPM (black dotted line)).

From day 9 on all three reactors produced acetic acid at a relatively stable rate, which resulted in an acetic acid accumulation of 4.96 g, 2.44 g, and 2.77 g by day 35 for the reactor with extraction, the reactor with CEM, and the reactor with BPM respectively. This corresponds to a CE of 57%, 28%, and 32% during stable operation, respectively (Table 3.4). After day 35, the production rates and efficiencies decreased for all three reactors. The acetic acid production resulted in increased concentrations in the middle compartment of the reactor with extraction (up to 9 g/L), and in the catholyte of the reactor with CEM (10.5 g/L) and BPM (8.3 g/L). These

concentrations do not reflect the efficiency of the systems because of water displacement between the compartments. Indeed, as for experiment 1, water displacement was observed from the cathode to the middle compartment of the reactor with AEM (extraction). This took place at an average rate of 0.05 mL/cm²/d. No water displacement was observed in the reactor with CEM or BPM. Water displacement across membranes is driven by the salinity-gradient and intrinsic membrane properties (Nagarale et al., 2006). The 4-fold concentrated salt solution used as medium in the middle compartment is intended to favor extraction of acetate over other salts but likely also contributes to water displacement. The use of electrolytes with a similar salinity should be tested.

The electron balance can be further closed with the abiotic H_2 production, the presence of other SCCA and other losses such as biomass production (Appendix 3). Biomass production was not closely monitored in this second experiment. Methane was not detected in the gas effluent. Overall the behavior of the reactors was similar to the extraction reactor in experiment 1. The lower productivity of the culture could potentially be attributed to a loss of productivity due to the large number of transfers in serum flasks between the start of experiment 1 and 2, which would indicate that the growth medium or growth conditions are currently sub-optimal to conserve the functionality of the culture over a long period of time.

Table 3.4 - Critical performance parameters for the three reactor types: Coulombic efficiency (CE) for acetic acid production (overall and for the stable operation period day 9 - 35), production rates, addition of base per mass of acetic acid produced and product recovery (as extraction efficiency). stdev: standard deviation; na: not applicable.

Parameter	Extraction	CEM	BPM
Overall CE for acetic acid (%)	40.9	25.4	27.7
CE stable operation (%)	57.2	28.1	31.9
Production rate (g/m²/d)	13.8	8.5	9.3
Production rate stable operation (g/m²/d)	19.2	9.5	10.7
Production rate stable operation (g/L/d)	0.55	0.27	0.31
pH catholyte (average ± stdev)	8.15 ± 0.15	6.58 ± 0.62	6.44 ± 0.75
NaOH addition (g/g acetic acid)	0	0.50	0.69
Power input stable operation (kWh/kg produced)	26.5	44.3	30.7
Extraction efficiency (%)	97.5	na	na

The productivity of the reactor with extraction was generally higher than for the reactors without extraction, as hypothesized during experiment 1. The pH of the catholyte in the reactor with AEM (extraction) remained stable and high throughout the experiment (8.15 ± 0.15), while drops in pH took place in the reactors with CEM and BPM, which probably negatively affected the culture (Figure 3.5 and Table 3.4). A low pH has an inhibitory effect on homoacetogenic acetic acid production due to end-product inhibition (Menzel & Gottschalk, 1985). The drop on day 11 to pH 5.4, for example, was associated with concentrations of undissociated acetic acid of

740 mg/L and 470 mg/L for the CEM and BPM reactor, respectively. For the CEM reactor this also corresponded to the maximal undissociated acetic acid concentration throughout the experiment. The maximal undissociated acetic acid concentration in the BPM reactor (1800 mg/L; 30 mM) was measured on day 28 of the test. This concentration of undissociated acetic acid corresponds to the levels measured by LaBelle et al. (2014) at which no further acetic acid production was observed, but H_2 production peaked instead. In the catholyte of the reactor with extraction the concentration of undissociated acetic acid never exceeded 1 mg/L. This was due to the combined effect of the higher pH and the extraction that results in low catholyte dissociated acetic acid concentrations. Using the design with AEM, the pH is regulated by a balance between the different processes that either decrease (CO_2 buffering, backflux of H^+) or increase the pH (reduction of H_2O, acetic acid synthesis). In the comparison study (experiment 2) the drops in pH in the CEM and BPM reactor were compensated by dosage of 1M NaOH in the reactor after each sampling. Production of acetic acid was maintained, but at lower levels than the reactor with extraction, and at the cost of base addition. Product diversification to ethanol or longer chain carboxylic acids was not observed, while this was the case in other studies were the pH was not controlled (Appendix 3; (Ganigué et al., 2015)). Also for H_2/CO_2 gas fermentations, pH control is an important strategy to avoid decreased productivities due to undissociated acetic acid buildup. This has resulted in acetic acid concentrations as high as 44 g/L at pH 7 in pressurized reactors (Demler & Weuster-Botz, 2011). In this perspective the reactor with extraction seems more promising to obtain high-rate production and higher product concentrations without dosage of chemicals.

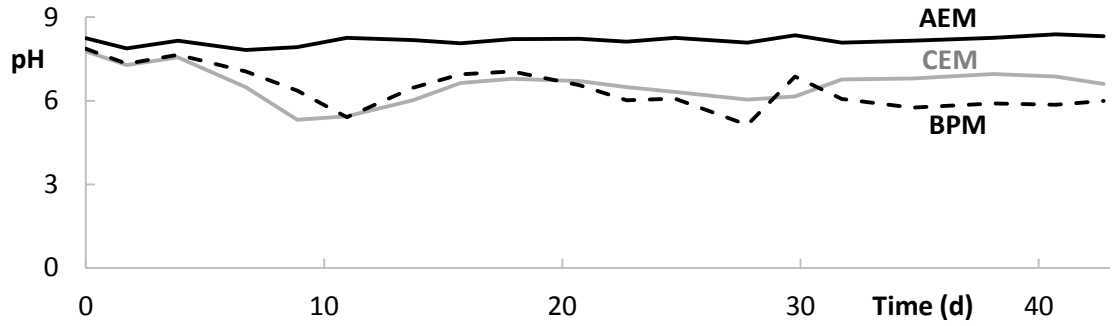

Figure 3.5 - The pH in the reactor with anion exchange membrane (AEM, black line) remained stable while drops in pH were observed for the reactors without extraction (cation exchange membrane (CEM, gray line) and bipolar membrane (BPM, black dotted line)) during experiment 2.

3.3 Ion balances: crucial role of HCO_3^-

Electrochemical systems require charge balancing, which is steered by the use of ion selective membranes. In total 1.9 moles of electrons were transported as current as a result of water electrolysis in each reactor of this experiment. Ion balances were made in experiment 2. For these balances, Cl^-, SO_4^{2-}, PO_4^{3-}, Na^+ and K^+ -transport was taken into account, besides transport

of H^+, OH^- and HCO_3^-. This last ion, HCO_3^-, acts as a buffer in the catholyte. At low pH, the carbonate system equilibrium shifts towards CO_2 and, therefore, the impact of HCO_3^- on charge balancing is difficult to quantify.

Different charge balances were expected for each reactor type. In principle, AEMs allow anions to cross, CEMs cations, and BPMs induce water splitting. Studies with MECs already showed that in practice, ions with the opposite charge can also cross the membrane, and back-diffusion of H^+ or OH^- ions can take place (Harnisch & Schröder, 2009). In all three reactors of experiment 2, the conductivity of the catholyte stabilized by the end of the experiment, implying that mainly H^+/OH^- and HCO_3^- were responsible for charge balancing, rather than other ions (Figure 4) (Sleutels et al., 2009). The increase in conductivity in the CEM and BPM reactor between day 10 and 30 is mainly due to NaOH dosing to counter the pH decrease.

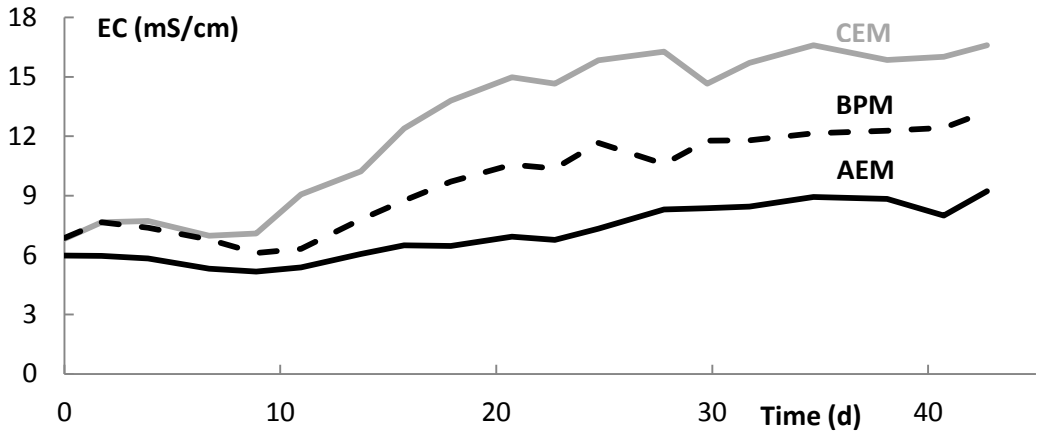

Figure 3.6 - Conductivity (EC, mS/cm) of the catholyte of the three reactor types (anion exchange membrane (AEM, full black line); cation exchange membrane (CEM, gray line) and bipolar membrane (BPM, black dotted line)) stabilized over time, indicating that H^+/OH^- and buffer species were mainly involved in charge balancing.

In the reactor with AEM , acetate transport from the cathode to the middle compartment accounted for only 5.0% of the charge balancing: 95.5 mmoles acetate was extracted, for a total of 1.9 moles electrons as current. Other anion salts balanced only 1.6% of the total charge during the 43 day-experiment. Cl^- was preferably transported in the first hours of the test, despite the higher molar concentration of HCO_3^-, which is related to the lower electrical mobility of this last ion compared to Cl^- (Block & Spiegler, 1963). The immediate transport of Cl^- from the medium might have caused the slower startup and formic acid production, as the medium composition differed from growth medium during preculturing. The concentration of Cl^- remained below 2.4 mM from day 2 on, and most likely HCO_3^- (> 50 mM) played a major role in charge balancing between the cathode and middle compartment for most of the experimental period (data not shown). The molar concentration of HCO_3^- in the catholyte was more than 30,000 times higher than the OH^- concentration. The concentration of HCO_3^- remained relatively stable in the catholyte despite the continuous CO_2 sparging and high pH (8.16 ± 0.15), which

indicates that HCO_3^- was transported through the membrane. In preliminary experiments (data not shown), an increased CO_2 concentration in the off gas of the extraction compartment compared to the catholyte off-gas had been measured as a result of CO_2 stripping. The total amount of protons in the middle compartment increased over time, which also supports the hypothesis that HCO_3^- was preferably transported compared to OH^-.

In the CEM setup, the results indicate that H^+-transport was responsible for most of the charge balancing. Na^+ transport could account for a maximum of 1.7% of the charge balancing, based on measurements of the anolyte Na^+-concentration, while based on pH measurements H^+ transport was responsible for 98% of the charge balancing. Taking into account measurement errors, this charge balance can be considered closed. Especially in the second half of the experimental run, the high concentration of H^+ (~100 mM) in the anode compared to other cations (Na^+ below 40 mM; data not shown), combined with a higher mobility for H^+, likely resulted in preferential transport of H^+ (Okada et al., 1998). The role of HCO_3^- in the charge balance is unclear in this case. Transport of this anion over the CEM should in principle be limited. However, there is also dissolved CO_2 present in the cathode which can diffuse. The concentration of HCO_3^- in the catholyte remained relatively stable over time, and probably there was a balance between losses through stripping when the catholyte pH decreased and additional dissolving when the pH increased. Diffusion of HCO_3^- towards the anolyte, followed by stripping, was not measured.

In the reactor with BPM, transport of ions was minimal, with Na^+ transport accounting for 0.8% of the charge balancing. Transport of salt ions was mainly concentration-driven, with minimal amounts of SO_4^{2-} and Na^+ moving towards the cathode and Cl^- towards the anode. Water splitting on the BPM was thus the dominant process. The increase of the H^+ concentration in the anolyte due to water splitting corresponded to only 1.0% of the charge generated, showing that OH^- production at the BPM was efficient. Regarding HCO_3^- transport, the conclusions made for the CEM reactor are also valid for the BPM reactor. Both in the CEM and BPM reactor, the H^+ transport/generation to the cathode compartment contributed to the catholyte acidification, augmenting the acidifying effect of acetic acid production *via* MES.

Overall, the use of HCO_3^- as buffer *via* CO_2 sparging is an advantageous strategy. As acetate can only account for a maximum of 12.5% of charge balancing, the presence of another anion at elevated concentration is required to sustain the fixed current. HCO_3^- transport allows efficient charge balancing in the reactor with AEM while the catholyte pH can be kept at a physiological pH. For long term reactor experiments the use of other buffers, such as $HPO_4^{2-}/H_2PO_4^-$, in combination with an AEM would not be feasible. This would require a continuous addition of salts, which ultimately leads to more complex wastewater treatment (Lefebvre & Moletta,

2006). Also for MFCs, CO_2/HCO_3^- has been shown to be an efficient buffer, by limiting the pH imbalance between the anolyte and catholyte, and by increasing the conductivity of the electrolytes without the addition of phosphate salts (Fornero et al., 2010). Usage of CO_2/HCO_3^- as buffer and for charge balancing, besides carbon source, does imply that the CO_2 conversion efficiency can never reach 100%. To obtain a high conversion rate, which is a prerequisite for an economically feasible MES process, a surplus of CO_2 would in any case be needed to drive reaction thermodynamics. Through the HCO_3^- transport over the AEM and consequent stripping of CO_2, purification of this gas is in fact also obtained, which might lead to additional applications and increased sequestration efficiencies.

3.4 Important process parameters for technology development

Production rates and power input are crucial parameters for technology development. In experiment 1, the operation of the reactor at – 5 A/m² lead to overall acetic acid production rates of 0.58 $g/L_{catholyte}/d$ or 20.4 $g/m^2_{projected\ cathode\ surface}/d$, and extraction rates of 19.7 $g/m^2_{membrane\ surface}/d$. The 2 cycles show a good reproducibility (Table 3.3). Production rates in the second study were lower, with the best results for the reactor with extraction during stable operation (19.22 g/m²/d or 0.55 g/L/d, Table 3.4). Patil et al. (2015a) obtained similar surface-based production rates with the same inoculum, but in a different reactor type (glass reactor with CEM). The difference in production rate between experiment 1 and 2 could possibly be attributed to the activity of the culture, as mentioned before. The different production rates between system designs in test 2 are most probably due to the pH effect, which inhibited the homoacetogenic culture in the reactor with CEM and BPM. The lower overall CE for these reactor types is directly related to the lower productivities. A comparison with other MES studies is difficult due to the high variability of MES designs and versatility of operational parameters (Chapter 1; (Patil et al., 2015a)). For operation at an industrial scale the rates obtained in both experiments are low. Bioethanol production for example achieves production rates of 70 g/L/d, but this process starts from a relatively pure, sugar-rich organic substrate such as corn starch (Graves et al., 2006). Recently however, acetic acid production rates of 148 g/L/d have been obtained in a H_2/CO_2 based fermentation with *Acetobacterium woodii*, showing that homoacetogenisis can lead to high rate bioproduction (Kantzow et al., 2015). Operation of the MES reactors at a higher current density would increase the availability of reducing equivalents and increase the production rates, provided that the kinetics of the culture are not the limiting factor.

In the second study, the acetic acid production rates decreased by the end of the 43-day production cycle (after day 35). Methane and ethanol were not produced and no increase in O_2 levels was measured. Oxygen toxicity, which would affect the highly sensitive enzymes of the

Wood-Ljungdahl pathway, can thus be excluded (Drake et al., 2008). A limitation of nutrient availability might have caused the decreased productivity even though after sampling an equal volume of fresh medium was added in the reactors. Despite these additions the concentration of NH_4^+ had decreased to 10 mg/L for the reactor with extraction, and less than 1 mg/L for the reactor with CEM and BPM at the end of experiment 2. Growth media for homoacetogens usually contain 100 to 130 mg/L NH_4^+ to not limit growth (Drake et al., 2006). Ammonium concentrations were not monitored in experiment 1, but we hypothesize that due to biomass production the concentrations of NH_4^+ would also have decreased to similar or lower levels. In that first experiment productivities were not affected. The impact on both experiments is thus uncertain, but we recommend a close monitoring of nutrient availability and addition of more concentrated medium after sampling during batch mode operation.

Maintaining high productivities at a low power input is critical for the process economics. In experiment 1 the process could be sustained at a constant cell voltage of 3.6 ± 0.2 V during stable operation, indicating the robustness of the process. The specific energy inputs per kilogram of acetic acid produced and extracted during stable operation were 18.5 kWh/kg and 19.0 kWh/kg, respectively. The energy input was calculated on the basis of the power input and the amount of acetic acid produced or extracted for each cycle. In experiment 2, the power input for the reactor with extraction was higher (26.5 kWh/kg). This is partially due to the lower production rate, but also results from the higher operating voltage in this experiment (4.2 ± 0.2 V). A similar conclusion can be drawn for the CEM reactor (44.3 kWh/kg for 3.5 ± 0.2 V) and BPM reactor (30.1 kWh/kg for 2.7 ± 0.05 V). A higher operating voltage can be expected for the reactor with extraction due to the presence of two membranes. The higher operating voltage for the CEM compared to the BPM reactor is surprising. Bipolar membranes typically require a larger input due to the water splitting reaction on the membrane (Harnisch et al., 2008) and the conductivity of the electrolytes was higher for the CEM reactor (data not shown). Total ohmic losses of the CEM reactor must have been higher (Clauwaert et al., 2008a).

Acetic acid is the product of interest in this study because it can be produced at high rates *via* homoacetogenesis, in contrast to other carboxylic acids, such as butyric acid, that require chain elongation (Ganigué et al., 2015). Coupling direct extraction to MES in a single, three-chamber reactor allows pure product recovery, possibly at a concentration higher than that with a typical two-compartment reactor. The extracted acetic acid was obtained as a clean product in a salt solution. Operating the reactor with a smaller volume of extraction liquid would lead to a further increase of the acetic acid concentration which opens perspectives for valorization of the acetic acid, as was demonstrated by the esterification to ethyl acetate in an ionic liquid (Andersen et al., 2016). The technology presented here could contribute to a selective esterification process,

in contrast to fermentation technology in which a mixture of organic products is obtained (Agler et al., 2011; Schievano et al., 2016).

Part of the extracted acetic acid was lost due to transfer to the anolyte. The CEM blocks negatively charged compounds but the small, uncharged acetic acid molecules were able to diffuse to the anolyte (Vanoppen et al., 2014). Calculated on a mass basis, 30% of the extracted acetic acid was present in the anolyte by the end of the second cycle of experiment 1 (Appendix 3). In experiment 2, transfer was limited to 12% because the concentration in the middle compartment was lower and the experiment was shorter. It thus remains unclear to what extent the transfer can cause important losses for further processing steps. As no oxidants other than O_2 were present in the anolyte and IrOx-coated electrodes have high overpotentials toward the oxidation of organics (Bagastyo et al., 2011), the diffusion did not result in notable conversion of acetic acid. Because of the diffusive nature of this process, the concentration of acetic acid in the anode will not exceed the concentration in the extraction compartment and thus, upon prolonged operation this fraction will become limited relative to overall acetic acid production.

4. Future perspectives

The reactor design can play a key role in the development of the MES technology. The product titer increase and product purification step are two features inherently present in the reactor with extraction. The power input for this more complex design was lower per mass of acetic acid produced compared to reactors without extraction. This was mainly due to the low productivity of the reactors with CEM and BPM. The power input of the system should however be decreased to obtain acetic acid production at a reasonable operating cost. This could for example be obtained with the use of more conductive electrolytes (see Chapter 5). At an equal production efficiency the integrated product purification, rather than the energy input, is a more suitable argument for the use of *in-situ* extraction as it takes away the need for post-purification from a dilute acetic acid stream. The acetate extraction is now limited to 12.5% of the charge balancing. An improved design were acetate production from an external H_2 source is linked to an extraction reactor providing only 12.5% of the electrons could improve the extraction efficiency at a lower power input. In any case the production and extraction rates will have to increase to obtain a more attractive process. This can be obtained by increased current densities, but the fragile pH equilibrium in the catholyte will have to be closely monitored. Pure CO_2 could potentially be used for sparging to provide more buffer capacity.

The use of a reactor with *in-situ* extraction offers new perspectives from a technology development point of view. The more complex design and associated operation render its use for investigation of more fundamental aspects of the MES technology, such as electron transfer

mechanisms, less useful. The classic reactors with CEM remain the most practical design, given a good surface-to-volume ratio is chosen: high to maximize volumetric production rates, low to minimize the acetate accumulation effects.

5. Conclusion

This is the first study presenting MES in the framework of a complete bioproduction pipeline, furthermore enabling a zero-chemical-input process, except for the CO_2. The possibility of operating the cathode under very stable circumstances while simultaneously extracting and concentrating the product as acetic acid is a key factor in the development of this technology. Future research should focus on increased production rates without neglecting optimized reactor design.

Acknowledgements

S.G. is supported by the Special Research Fund (BOF) from Ghent University. K.V. is supported by FWO Vlaanderen through a PhD scholarship. K.R. and S.J.A. are supported by the Ghent University Multidisciplinary Research Partnership (MRP) - Biotechnology for a sustainable economy (01 MRA 510W). K.R. and A.P. are supported by the European Research Council (ERC Starter Grant ELECTROTALK). Equipment used was supported *via* "BOF Basisinfrastructuur 01B05912". The input of Jan Arends, Paul Gildemyn and Pieter Naert on the manuscript was much appreciated. The authors thank Lars T. Angenent for scientific discussions, Jan Arends and Jana De Bodt for providing the enriched culture, and Tim Lacoere for designing the reactor scheme.

CHAPTER 4 - UPGRADING SYNGAS FERMENTATION EFFLUENT USING *Clostridium kluyveri* IN A CONTINUOUS FERMENTATION

This chapter has been redrafted after:

Gildemyn, S., Molitor, B., Usack, J., Nguyen, M., Rabaey, K., Angenent, L.T. 2016. Upgrading syngas fermentation effluent using *Clostridium kluyveri* in a continuous fermentation. In preparation for Biotechnology for Biofuels.

Abstract

Syngas fermentation with pure microbial cultures currently results in ethanol/acetic acid mixtures as product. Ethanol has a low market value and is traditionally purified through an energy-intensive distillation, which reduces overall profitability when waste heat is not available. These issues could be circumvented by implementing a biological platform that converts the dilute ethanol/acetic acid mixtures to longer, easier to extract products that attract higher value. Chain elongation has been studied using reactor microbiomes that convert complex organic waste streams to medium-chain carboxylic acids (MCCAs). Only few studies exist with pure microbial cultures as a biotechnology production platform. The upgrading of syngas fermentation effluent with pure cultures has not yet been shown. Here, we focus on the use of pure cultures of *Clostridium kluyveri* to convert ethanol/acetic acid mixtures to MCCAs. We describe the operation of two continuous bioreactors and factors influencing the productivity of the culture, such as organic loading rate (OLR), presence or absence of in-line product extraction, and pH. Increased loading rates resulted in proportionally higher volumetric production rates of *n*-caproic acid, up to 40 mM/d (4.64 g/L/d). Also caprylic acid production was observed for the first time with *C. kluyveri* (up to 2.19 ± 0.34 mM in batch). The use of real effluent from syngas fermentation, without added yeast extract, did not decrease productivities. The metabolism of *C. kluyveri* was, however, inhibited at the low pH values (5.50) that reactor microbiomes were successfully elongating. Overall, we show that syngas fermentation effluent can be converted to MCCAs under defined conditions, but several challenges remain for the use of *C. kluyveri* as a production strain.

1. Introduction

The sustainable production of biochemicals as alternatives to fossil fuel-based chemicals is gaining momentum. Not the predicted depletion of fossil fuels, but increased awareness that their use leads to climate change and air pollution, has resulted in the development of several bioproduction routes (Liao et al., 2016). Three major platforms have emerged: i) the sugar platform; ii) the syngas platform; and iii) the carboxylate platform (Agler et al., 2011).

With the sugar platform, the use of starch and sugar crops to produce bioethanol currently forms one of the biggest markets for biochemicals. Ethanol production rates of over 60 g/L/d are reported for commercial bioproduction strains and more than 100 million tons bioethanol are produced per year worldwide (Deloitte, 2014; Lam et al., 2014). This route is, however, controversial as crop cultivation requires a high input of land, water, and nutrients. Cultivation of these crops for fuel production may also compete with the production of food. Alternatively, the use of lignocellulosic biomass can be considered. This, however, requires addition of chemicals and process energy to pretreat the biomass to make the sugars available for fermentation, while a large percentage of the biomass remains unused (Liao et al., 2016).

With the syngas platform, conversion of lignocellulosic biomass to syngas (H_2/CO/CO_2 gas mixtures) and subsequent autotrophic fermentation of these gases to liquid products could tackle these issues (Munasinghe & Khanal, 2010). The syngas platform has potential because besides lignocellulosic biomass and other organic waste streams, also point-sources of syngas are widely available, for example the off-gasses from steel manufacturing (Daniell et al., 2012; Liew et al., 2016; Molitor et al., 2016). The use of industrial gaseous off streams can lead to decreased greenhouse gas emissions coupled to the production of multicarbon products, with ethanol currently being the dominant product. The conversion is carried out by anaerobic autotrophic bacteria such as *Clostridium ljungdahlii* and *Clostridium autoethanogenum*. These bacteria utilize the Wood-Ljungdahl pathway for carbon fixation (Latif et al., 2014; Dürre & Eikmanns, 2015). The main product of the autotrophic metabolism is acetic acid (Ragsdale & Pierce, 2008). When the intracellular, undissociated acetic acid concentration reaches a threshold, the metabolism is redirected toward ethanol production to decrease toxicity and increase the number of reducing equivalents per mole of product formed (Richter et al., 2016). Ethanol production rates exceeding 200 g/L/d are now obtainable with commercial strains (Molitor et al., 2016).

With the carboxylate-platform, treatment of organic waste is coupled to bioproduction *via* anaerobic fermentation processes. The carboxylate platform mainly involves the production of gases, such as H_2 and CO_2, and short-chain carboxylic acids (SCCAs) using mixed microbial

cultures (Holtzapple & Granda, 2009; Agler et al., 2011). Inhibition of methanogenesis, the last step in biogas production, results in the buildup of SCCAs in the fermentation broth. Chain elongation *via* the reverse β-oxidation pathway then leads to the MCCAs in the same microbiome (Angenent et al., 2004; Marshall et al., 2013a). Among the end-products, *n*-caproic acid and *n*-caprylic acid are two desirable MCCA bioproducts, but they are characterized by a higher product toxicity at low pH (pKa ~4.8). To circumvent product toxicity, a continuous removal of the produced carboxylic acids, *via* extraction or by applying high dilution rates, or process control at a neutral pH, is necessary to obtain high-rate fermentation (Agler et al., 2012; Grootscholten et al., 2013b). At high dilution rates, *n*-caproic acid production rates up to 55 g/L/d have been obtained (Grootscholten et al., 2013d).

Additional value could be created by coupling different production platforms to upgrade side streams or produce higher value chemicals. For example, syngas fermentation only leads to a marketable product when the ethanol is separated and extracted from the fermentation broth. Distillation of the dilute ethanol (6% w/v) is an energy-intensive process that results in a relatively low-value product. Mixtures of ethanol and acetic acid, in particular those with high ethanol/acetic acid ratios, could also be further biologically converted *via* chain elongation to MCCAs (Angenent et al., 2016). One of the main questions is whether or not growth factors, such as trace elements or yeast extract, would have to be added to enable the chain elongation process, or if those present in the effluent would suffice to support growth. Addition of growth factors would greatly increase the process cost. In a first proof-of-concept study that coupled chain elongation to syngas fermentation, several growth factors such as yeast extract were added to the syngas fermenter effluent. The necessity of these additions was, however, not studied (Vasudevan et al., 2014).

The chain elongation process and its underlying thermodynamics are now well understood (Thauer et al., 1968; Gonzalez-Cabaleiro et al., 2013; Angenent et al., 2016). Several microorganisms are known to convert ethanol/acetic acid mixtures *via* the reverse β-oxidation pathway, with *Clostridium kluyveri* being the most frequently studied. This organism has the ability to produce *n*-butyric and *n*-caproic acid from ethanol and acetic acid (Barker & Taha, 1942). It has regularly been found in mixed cultures converting either synthetic or real organic waste streams to MCCAs (Steinbusch et al., 2011; Agler et al., 2012). Except for one study that determined substrate utilization, pure culture continuous bioreactor studies with *C. kluyveri* are lacking (Kenealy & Waselefsky, 1985). A pure culture fermentation would allow a more controlled chain elongation process. Furthermore this would allow a study of the influence of different process parameters on the productivity of the culture. From thermodynamic models and mixed culture studies it is known that: i) a higher ethanol/acetic acid ratio drives the chain elongation reaction toward longer carbon chain carboxylic acids, including caprylic acid (Smith et

al., 1985; Angenent et al., 2016); and ii) selective in-line extraction of the longer chain products results in higher production rates of these carboxylic acids and a clean product (Agler et al., 2014; Angenent et al., 2016). Mixed culture studies will likely focus on obtaining high-rate caprylic acid production, because of its higher value than *n*-caproic acid, but this product has not yet been detected in pure *C. kluyveri* cultures.

To address the aforementioned concerns, we have conducted experiments using a pure culture of *C. kluyveri* in bioreactors to investigate whether syngas fermentation effluent can be directly used as growth medium for *C. kluyveri*. We report, for the first time, *n*-caprylic acid production by a pure culture of *C. kluyveri*. We elaborate on key challenges to obtain high-rate MCCA production from syngas fermentation effluent in reactors with and without in-line product extraction. In the context of this chapter, "carboxylic acids" is used as the general term for the products obtained. Depending on the pH of the processes described, these carboxylic acids are fully or partially present in their dissociated form.

2. Materials and Methods

2.1 Culture and media

A *Clostridium kluyveri* ATCC 8527 (DSM555) culture was obtained from ATCC (Manassas, VA, USA) and cultured according to the standard DSMZ protocols in DSMZ52 medium. Only 1 mM cysteine was used as reducing agent. The culture was incubated in serum flasks at 35°C without shaking. For reactor experiments, the $MgSO_4$ was omitted from the medium and replaced by an equimolar concentration of $MgCl_2.6H_2O$, while the cysteine concentration was increased to 4 mM. In addition, the ethanol and acetic acid concentrations were adapted to obtain the desired ratio of ethanol/acetic acid (10/1, later 3/1) and loading rate (Table 4.1). For the batch experiments two types of syngas fermentation effluent were tested. The first effluent type was obtained from the second stage of a 2-stage syngas fermenter operated as described by Richter et al. (2013b). The influent of the syngas fermenter consisted of 2 x concentrated P7 medium (see Appendix 4, (Datar et al., 2004)). The second effluent type was collected from a single stage syngas fermenter running on mineral medium adapted from Mock et al. (2015) (see Appendix 4). The second effluent was used for reactor experiments. The collected effluent was kept frozen (-20°C). Before use, the effluent was filtered using a 20 µm vacuum filter to obtain a sterile influent for the *C. kluyveri* experiments. The concentrations of ethanol and acetic acid were determined on the filtered feed, ethanol was supplemented to obtain the desired concentration (Table 4.2). Trace-elements, vitamins and selenite-tungstate solutions (as for DSMZ52 medium) were added after filtration; yeast extract was omitted.

Table 4.1 – Theoretical composition of the feed (ethanol and acetic acid) during reactor operation for the reactor with pertraction (R1) and without pertraction (R2). Ethanol has a COD content of 96 g COD/mol, acetic acid has a COD content of 64 g COD/mol. Values in italic indicate the use of real syngas fermentation effluent. COD: chemical oxygen demand; HRT: hydraulic residence time.

Day (Phase)	loading R1 (g COD/L/d – mM-C/d)	loading R2 (g COD/L/d – mM-C/d)	HRT (d)	Ethanol/Acetic acid ratio
1 – 18 (I)	12 – 257	12 – 257	2	10
18 – 28 (II)	6 – 129	6 – 129	4	10
28 – 37 (III)	10 – 215	6 – 215	2	10
37 – 48 (IV)	10 – 215	10 – 215	2	10
48 – 74 (V)	15 – 322	15 – 322	2	10
74 – 85 (VI)	15 – 340	15 – 340	2.3	3
86 – 95 (VII)	*15 – 340*	*15 – 340*	*2.3*	*3*

Table 4.2 – Composition of the media tested in the batch experiments. The test was carried out as three separate experiments, each time with DSMZ52 medium (DSMZ) as control. Each medium contained the same COD concentration. Additions were made based on the DSMZ52 medium. Ethanol and acetic acid concentrations depicted here are the theoretical concentration. (*)

Condition	Ethanol (mM)	Acetic acid (mM)	Vitamins	Trace elements	Selenite-tungstate	Yeast extract	Bicarbonate
DSMZ	343	101	Y	Y	Y	Y	Y
SGP-	315	144	N	N	N	N	Y
SGPT-	315	144	Y	Y	Y	N	Y
SGPT+	315	144	Y	Y	Y	Y	Y
SGM-	343	101	N	N	N	N	Y
SGMT-	343	101	Y	Y	Y	N	Y
P-	343	101	Y	Y	Y	N	Y
M-	343	101	N**	N**	N**	N	Y

*N: not added; Y: added; vitamins: vitamins of the DSMZ52 medium; trace: trace element solution of the DSMZ52 medium; YE: yeast extract; ** the vitamins and trace elements for the 2x Mock medium were used.

2.2 Batch growth experiment on syngas fermentation effluent

Growth and production of *C. kluyveri* was tested in 8 different media with and without various chemical additions to evaluate the use of syngas fermentation effluent as growth medium for a *C. kluyveri* bioreactor (Table 4.2). The eight different media used in the batch test were: i) DSMZ52 *C. kluyveri* medium (DSMZ); ii) P7 syngas fermentation effluent with only bicarbonate added (SGP-); iii) P7 syngas fermentation effluent with trace elements, vitamins, selenite-tungstate, and bicarbonate added (SGPT-); iv) P7 syngas fermentation effluent with trace elements, vitamins, selenite-tungstate, and bicarbonate, as well as yeast extract added (SGPT+); v) Mock syngas fermentation effluent with only bicarbonate added (SGM-); vi) Mock syngas fermentation effluent with trace elements, vitamins, selenite-tungstate, and bicarbonate

added (SGMT-); vii) 2 x concentrated P7 medium with only bicarbonate added (P-); and viii) 2 x concentrated Mock medium with only bicarbonate added (M-). Trace-elements, vitamins and selenite-tungstate solutions were prepared and added according to the DSMZ52 medium recipe.

The combined COD from ethanol and acetic acid was the same for each medium. In the five media based on the syngas effluent, ethanol was added to obtain the same total COD as the DSMZ52 medium, as no ethanol was measured in the effluent after thawing and filtering. The 2 x P7 medium was prepared using the mineral solution of the P7 medium, with additions according to the DSMZ52 medium and the COD and ethanol/acetic acid ratio of the DSMZ52 medium. The 2 x Mock medium was prepared as described in Appendix 4, with only ethanol and acetic acid added before transfer of *C. kluyveri*. The experiment was carried out in three separate batches, each time with the DSMZ52 medium as control. An active *C. kluyveri* culture growing in DSMZ52 medium was used as inoculum, and transferred in each specific medium for two growth cycles to dilute the original DSMZ52 medium and to allow adaptation of the culture. A triplicate bottle test was subsequently carried out. Incubation (without shaking) of the triplicate bottle test took place at 30°C, which was the same temperature used for reactor operation (see below). The pH of the media was not controlled during the experiment (See Appendix 4).

2.3 Reactor setup for continuous production experiments

Two BioFlo310 Benchtop fermenters (New Brunswick Scientific Co, USA), with a 2.5 L vessel (operating volume 1.5 L) were used for the reactor experiments. The headplate of each reactor was equipped with a sampling port, gas sparger, exhaust condenser, mixing system (200 rpm), a pH probe (Mettler Toledo 405-DPAS-SC, Mettler Toledo, USA), an inlet for influent, acid and base, an outlet for both recirculation and effluent, and an inlet for the recirculated broth. The temperature was controlled at 30°C using the built-in water jacket. Each reactor system included an external recirculation pump (Masterflex, USA). Reactor broth was recirculated at 120 mL/min over a hollow fiber membrane (Minikros Sampler, 20 cm, poresize 0.2 µm, PES, Spectrumlabs, USA) to retain all cells in the reactor. The cell-free medium obtained from the hollow fiber unit was pumped out as effluent at a rate of 750 mL/d. The same volume of influent medium was pumped in daily, resulting in an HRT of ~2 days. The reactors were continuously sparged with anaerobic gas, consisting of 20 mL/min N_2 and 5 mL/min CO_2, at a flow rate of ~25 mL/min. The flow rates of the two gases were manually controlled using flow meters (65-mm Correlated Flowmeter with valve, aluminum, Cole-Parmer, USA). Both reactors were initially controlled at pH 7, using 2 M KOH and 2 M HCl.

2.4 Pertraction system

One of the two bioreactors (R1) was also equipped with a membrane-based liquid-liquid extraction system (pertraction), consisting of a forward and backward extraction module (Figure 4.1). The system was started on day 11 of the bioreactor experiment. This system extracts carboxylic acids into a solvent based on their hydrophobicity and subsequently into an alkaline stripping solution, based on a pH gradient between the reactor and the stripping solution (Agler et al., 2012). The cell-free filtrate leaving the hollow fiber unit (cellguard) was pumped at 90 mL/min into the shell side of the forward extraction module (2.5 x 8 Liqui-Cel Membrane Contactor, Membrana, USA). There it contacted the hydrophobic solvent, which consisted of mineral oil containing 30 g/L tri-*n*-octylphosphine oxide (TOPO; Sigma Aldrich, USA). The mineral oil was recirculated on the tube side between the two extraction modules at a flow rate of 7.5 mL/min. In the backward module the mineral oil contacted the stripping solution, which was recirculated at 75 mL/min. The stripping solution consisted of 300 mM $Na_2B_4O_7$, which was controlled at pH 9.0 using 5 M NaOH. The stripping solution was regularly refreshed to keep the total carboxylate concentration below 120 mM.

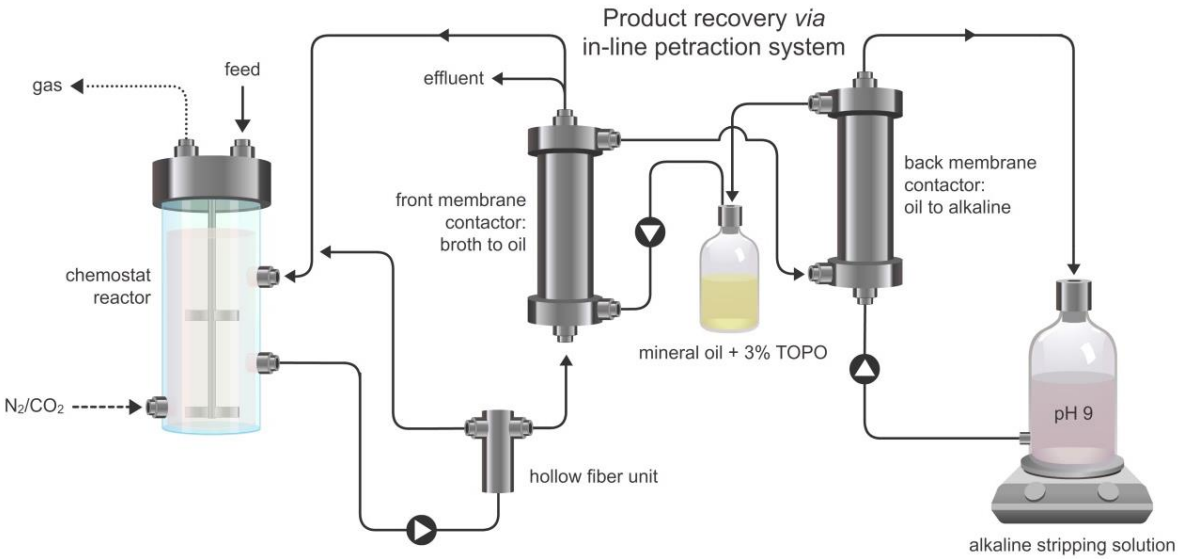

Figure 4.1 - Reactor setup for fermentation with in-line product extraction (pertraction). The reactor broth is sent through a hollow fiber unit to obtain a cell-free effluent and broth for the pertraction system.

Four technical problems decreased the efficiency of the pertraction system: i) mineral oil leakages took place on day 20 and 38; ii) the actual mineral oil recirculation rate was lower than the setpoint from day 30 to 76; iii) reactor broth was lost due to a tubing breakage in the pump line on day 87 and 95; and iv) a short-circuit in the broth flow was identified and remedied on day 89. In (iv), reactor broth containing biomass was siphoned into the cell-free broth feeding the effluent line. After the second incident involving reactor broth loss on day 95, both reactors were discontinued.

2.5 Reactor startup and operation

The reactors were filled with medium, autoclaved, and sparged with sterile N_2/CO_2 at a flowrate of ~25 mL/min for 24 h. Liquid samples were taken before inoculation. Each reactor was inoculated at a 7.5% (v/v) concentration using serum flask-cultures of *C. kluyveri*. In the bioreactor experiments described next, continuous mode was started after 12 h in batch mode. In initial runs, continuous mode operation was started when the OD was above 1, or, in a later run, this was done as soon as the OD was higher than 0.3 (data not shown). The loading rate applied upon transitioning to continuous mode was 2 g COD/L/d in the initial runs, and was later increased to 8 g COD/L/d. The faster transition and increased loading rate were chosen because the culture had shown sporulation behavior (visual observation with a phase contrast microscope, Nikon Labophot, Nikon, Melville, USA). The concentration of ethanol and acetic acid varied in the feed, based on the required COD loading rate and ethanol/acetic acid ratio (Table 4.1). The loading rate was gradually increased. Liquid samples were taken at least 4 times per week. Gas flow rate and composition, effluent volume, and volume of dosed acid and base were also measured during sampling. Possible losses of ethanol *via* the exhaust gas were not quantified, although these could have taken place despite the use of an exhaust condenser (Duboc & von Stockar, 1998).

2.6 Analytical procedures

The optical density (OD) was measured at 600 nm using a spectrophotometer (Spectronic 1201, Milton Roy, USA; quartz cuvette, Starna Cells, USA). Phosphate buffer (50 mM, pH 6.8) was used to dilute the samples, if necessary. For the batch experiment 200 µL broth was analyzed using a 96-well plate in a plate reader (BioTek Synergy 4, BioTek, USA).

The reading of the pH probes in the reactors was controlled at least 4 times/week by measuring the pH with an external pH probe, calibrated using buffers at pH 4, 7, and 10 (Orion Star A329, Thermo Fischer Scientific, USA).

Gas samples were analyzed on a Gow Mac gas chromatograph (GOW-MAC Instrument Co., USA) equipped with a Supelco column (Supelco, USA) at 25°C (1.8m; 80/100 Hayesep Q packing material), using helium as carrier gas. The ratio of the integrated peak areas for N_2 and CO_2 was determined using Peak Simple software. Ethanol concentrations were determined using an HPLC (Waters, USA) equipped with an Aminex HPX-87H analytical column at 65°C (Bio-Rad, USA) and a RI detector. Sulfuric acid (5 mM, flowrate 0.6 mL/min) was used as eluent. Concentrations of carboxylic acids (C2-C8) were measured using a gas chromatograph (HP5890, Hewlett Packard, USA), equipped with a 7683 autoinjector and flame ionization detector. Columns (capillary GC column (Nukol); 15m x 0.53mm internal diameter (Supelco) were purchased from Sigma Aldrich,

Inc. (USA). The flow rates of hydrogen, air, and helium were 21.4, 350, and 35 mL/min, respectively. The temperature was first set to 70°C for 2 min, and then ramped up to a final temperature of 200°C at 12°C/min, where the temperature was held for 2 min. The injection port temperature and detector temperature were 200°C and 275°C, respectively.

3. Results and Discussion

3.1 Addition of yeast extract is not required when using syngas fermenter effluent for C. kluyveri

Growth of *C. kluyveri* can be sustained without addition of yeast extract to syngas fermentation effluent. This was shown in a batch test with 8 different media. Yeast extract is often added to enhance growth and production rates of *C. kluyveri* although it is known that it can be substituted by biotin and p-aminobenzoic acid (Tomlinson & Barker, 1954; Grootscholten et al., 2013c). This is a favorable outcome for the further development of this reactor platform, as yeast extract has a large contribution to the cost of the culture medium (Richter et al., 2013a). The culture in the original DSMZ52 medium (DSMZ), and the culture on Mock syngas fermentation effluent with trace elements, vitamins, and selenite-tungstate added (SGMT-), showed the fastest growth, highest OD and highest concentration of *n*-caproic acid produced after 2 weeks (Figure 4.2). P7 syngas effluent-based medium with additional vitamins, trace-elements, and selenite-tungstate (SGPT-) resulted in faster growth than the same medium with additional yeast extract added (SGPT+). In a mixed culture study on chain elongation with syngas fermentation effluent addition of yeast extract, trace elements and vitamins was performed (Vasudevan et al., 2014). From our results, we concluded that the addition of yeast extract is not necessary when coupling the carboxylate platform and the syngas platform. The use of raw syngas fermentation effluent is however not advised, as growth in this condition was limited for the P7-based effluent (P-). Certain trace elements or vitamins, possibly biotin and p-aminobenzoic acid, are missing in the raw syngas effluent, that only contains cell material from dead cells or excretion products from the syngas fermentation. The syngas fermentation effluent should be characterized in detail and future experiments could determine the effect of the composition on the *C. kluyveri* culture.

3.2 Clostridium kluyveri *can produce caprylic acid*

In 7 out of 8 conditions (all except 2 x P7), *n*-caprylic acid was detected, with the highest concentrations occurring with Mock syngas fermentation effluent (2.19 ± 0.34 mM after 14 days). *n*-Caprylic acid production had been reported for mixed cultures, including mixed cultures with a high abundance of *C. kluyveri* (Steinbusch et al., 2011; Agler et al., 2012; Grootscholten et

al., 2013a), but this is the first time production of *n*-caprylic acid is reported for a pure culture of *C. kluyveri*.

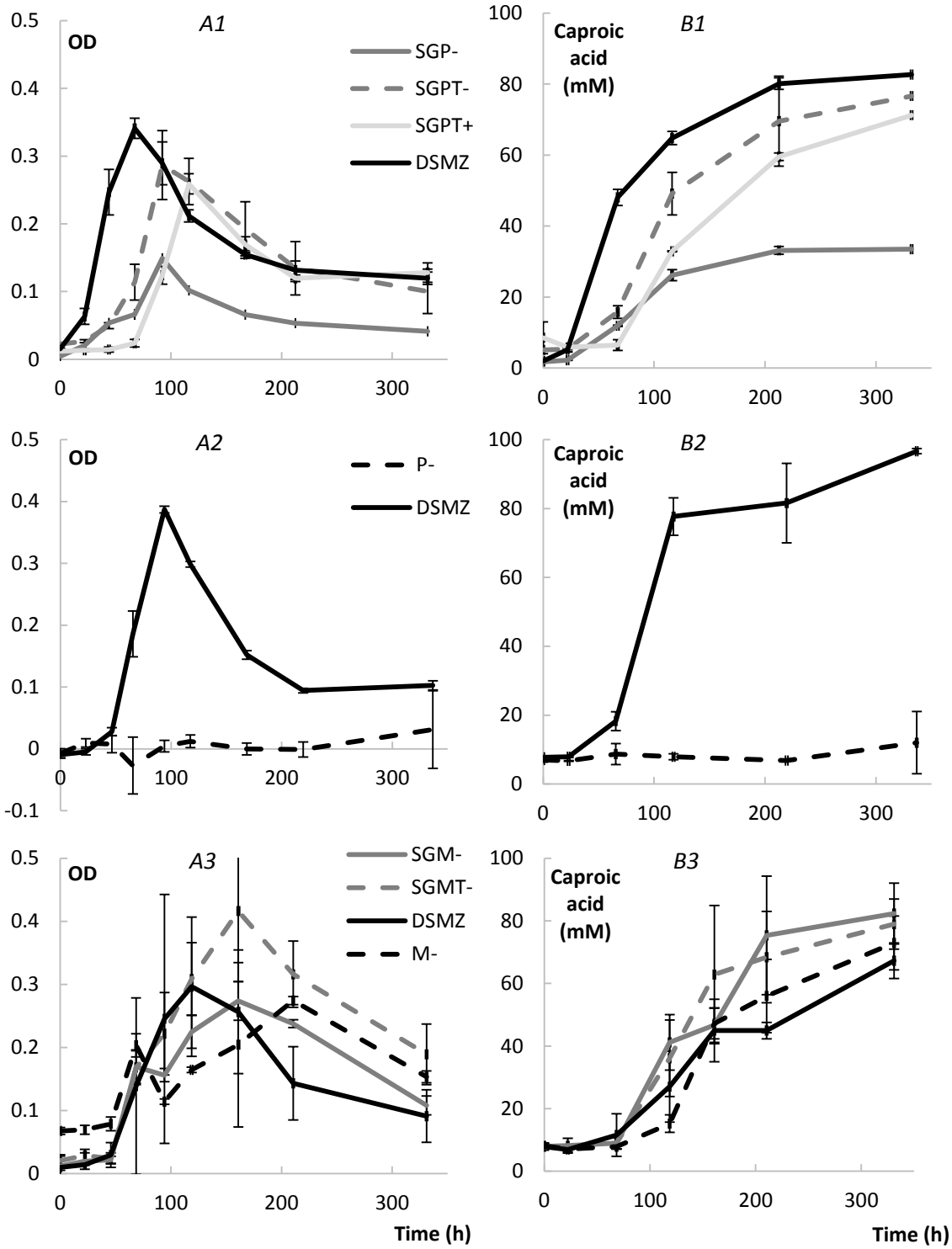

Figure 4.2 – Growth and production of *Clostridium kluyveri* in batch experiments. The test was carried out as three separate experiments, each time with DSMZ52 medium (DSMZ) as control. A. Growth (as OD) was highest for the standard DSMZ medium (DSMZ) and the Mock medium syngas fermentation effluent with added growth factors, but no yeast extract (SGMT-). B. Production of caproic acid was usually the highest in the standard DSMZ52 medium, but comparable results were obtained with syngas fermentation effluent with additions (SGMT-; SGPT-). Data represent the mean (n=3), error bars the standard deviation.

Chain elongation takes place through the reverse β-oxidation pathway, which is a cyclic process. In the first step, two acetyl-CoA molecules are combined to form butyryl-CoA, which may be reduced to *n*-butyric acid. Alternatively, butyryl-CoA may enter a second round of chain elongation where it is coupled to another acetyl-CoA forming hexanoyl-CoA which may then be reduced to *n*-caproic acid. Most likely, *C. kluyveri* has the capacity to produce *n*-caprylic acid through a similar cycle, coupling acetyl-CoA to hexanoyl-CoA under more reduced conditions (Steinbusch et al., 2011; Spirito et al., 2014). Carboxylic acids generally become more toxic with increasing chain length. Besides the availability of reducing equivalents and an adequate quantification method, this toxicity is a possible explanation for the absence of *n*-caprylic acid detection in previous experiments.

3.3 Continuous mode fermentation with C. kluyveri *requires a specific start-up procedure*

Two pure culture reactors were successfully started after initial attempts to start the continuous reactors on synthetic medium did not succeed due to: i) contamination of the reactor; and ii) sporulation of the culture. The reactors became contaminated by sulfate-reducing bacteria (SRB) despite all measures to maintain axenic conditions. SRB reduce sulfate using H_2 or acetate as electron donor (Widdel et al., 1992). Hydrogen gas is produced by *C. kluyveri* during chain elongation and sulfate is the sulfur source contained in the DSMZ52 medium used for this study. To prevent contamination, sulfate was replaced by cysteine as the sulfur source. The concentration of cysteine in the medium was increased from 1 mM to 4 mM to avoid sulfur limitation. It was hypothesized that this would not affect *C. kluyveri* as this organism is endowed with cysteine degradation genes (Seedorf et al., 2008). Growth of the culture was not affected by the change from sulfate to cysteine as sulfur source and contamination by SRB was successfully avoided in the subsequent reactor runs.

We had started our bioreactor in batch mode in initial runs, transitioning to continuous mode operation once the culture had reached the exponential growth phase. Visual observation with a phase contrast microscope showed sporulation of the culture (Appendix 4). We hypothesized that sporulation was triggered by a lack of carbon source or nutrients at the end of the exponential growth phase or beginning of the continuous mode operation (Dürre, 2014). A faster transition from batch to continuous mode or higher loading rate could not avoid sporulation, however. Therefore, the reactors were started in continuous mode directly, with a loading rate of 12 g COD/L/d. The use of the hollow fiber unit to retain cells in the reactor in fact made the start-up in batch mode unnecessary. Using this operation strategy, the culture also sporulated, and sporulation was initiated even faster compared to batch mode operation (day 3 instead of day 5). The spores however germinated within 2 days, forming thinner *C. kluyveri*

cells, compared to the cells from the initial culture (Appendix 4). The culture regained its original appearance over time. Germination was probably not detected in earlier runs because these were stopped directly when sporulation was observed.

Pure culture fermentations are often executed in batch fermentations rather than in the continuous mode operation demonstrated here. Our results suggest that continuous mode operation might be more advantageous. The batch growth experiment and Phase VI of the reactor process can be compared as similar ratios of ethanol and acetic acid were used (3/1). In the continuous process the conversion efficiencies, selectivity toward *n*-caproic acid and production rate were always higher (see section 3.5), which is expected from a thermodynamic point of view (Angenent et al., 2016). The sporulation behavior of the culture during continuous mode operation did not negatively affect process outcomes on the long term.

3.4 Reactor startup was characterized by metabolic oscillations

Both reactors showed similar behavior in the 10 days after start-up in continuous mode (Figure 4.3). The optical density increased within 3 days, dropped when sporulation occurred and increased again when the cells germinated (Appendix 4). Production of *n*-butyric and *n*-caproic acid followed the growth pattern, with the highest *n*-caproic acid concentration obtained on day 3 (33 mM for R1, 31 mM for R2; Figure App 4.4 and App 4.5). The drop in production between day 3 and 6 follows the drop in OD due to sporulation. The production in the reactor without pertraction (R2) then followed a cyclic pattern, with either the substrate concentrations (ethanol and acetic acid) or the product concentrations (*n*-butyric and *n*-caproic acid) peaking (Appendix 4). This pattern was less pronounced in R1 after day 11, when the pertraction was started, since products were being continuously removed. Such metabolic oscillations coupled to sporulation have been previously reported for solventogenic Clostridia (Jones & Woods, 1986; Clarke et al., 1988; Gapes et al., 1996; Richter et al., 2012). We could not link these metabolic oscillations to sporulation after day 6 in the case of the continuous *C. kluyveri* culture. The cyclic behavior disappeared when the loading rate was decreased to 6 g COD/L/d on day 17 (Phase II). Further investigations are needed to understand why these metabolic oscillations occurred, as both ethanol and caproic acid product concentrations remained below inhibitory levels (maximal ethanol concentration of 250 mM; Appendix 4). Growth of *C. kluyveri* has even been reported at ethanol concentrations of 700 mM, and a mixed culture could perform chain elongation at 435 mM ethanol (Weimer & Stevenson, 2012; Lonkar et al., 2016).

Table 4.3 – Overview of critical performance parameters* for the reactor with pertraction (R1, pH 6) and the reactor without pertraction (R2, pH 7) for the different operational phases as defined in Table 4.1 (average ± stdev). Production rates for the three products (*n*-butyric, *n*-caproic and *n*-caprylic acid) are given.

	Phase	OLR	OLR	*n*-butyric	*n*-caproic	*n*-caprylic	Select. C6	Select. C8	Carbon conversion	Extr. C6	Extr. C8
		mM C/d	g COD/L/d	mM/d	mM/d	mM/d	%	%	%	%	%
	II - III	151.9 ± 31.4	7.0 ± 0.4	0.9 ± 0.7	8.4 ± 8.4	0.2 ± 0.1	88.5 ± 10.1	3.7 ± 2.9	38.9 ± 17.4	80.4 ± 10.5	100.0 ± 0.0
	IV	255.2 ± 7.4	10.9 ± 0.4	1.3 ± 0.2	16.2 ± 5.4	0.6 ± 0.4	90.9 ± 2.0	3.9 ± 2.2	41.9 ± 2.5	64.8 ± 13.7	94.4 ± 6.6
R1	V	298.3 ± 9.6	14.2 ± 1.0	1.7 ± 0.4	19.1 ± 6.6	1.0 ± 0.4	87.7 ± 3.9	6.4 ± 3.0	38.5 ± 12.6	37.8 ± 27.2	65.0 ± 26.5
	VI	370.0 ± 9.7	16.3 ± 0.4	9.4 ± 0.7	39.9 ± 0.9	1.4 ± 0.2	83.0 ± 1.0	4.0 ± 0.4	79.9 ± 2.0	42.7 ± 6.9	77.0 ± 4.5
	VII	244.6 ± 74.4	10.7 ± 3.3	7.8 ± 0.11	25.0 ± 3.1	0.65 ± 0.3	80.3 ± 0.8	2.7 ± 1.0	86.1 ± 29.0	70.0 ± 40	101 ± 2.7
	II	122.5 ± 31.7	6.9 ± 0.2	1.0 ± 0.3	11.1 ± 2.7	0.8 ± 0.2	86.5 ± 0.5	8.1 ± 0.2	65.9 ± 17.4		
	III - IV	233.0 ± 7.9	10.9 ± 0.4	1.7 ± 0.3	15.7 ± 0.5	1.2 ± 0.1	85.5 ± 1.2	8.5 ± 0.4	47.5 ± 2.5		
R2	V	241.0 ± 28.4	11.3 ± 1.2	1.5 ± 0.2	18.6 ± 2.9	1.8 ± 0.3	84.7 ± 1.5	10.8 ± 1.2	54.7 ± 6.5		
	VI	296.5 ± 0.7	13.0 ± 0.03	7.8 ± 0.7	37.6 ± 1.6	2.6 ± 0.01	81.4 ± 0.5	7.4 ± 0.3	93.6 ± 4.4		
	VII	279.7 ± 27	12.3 ± 1.2	5.7 ± 0.7	35.3 ± 2.7	2.14 ± 0.4	84.2 ± 1.0	6.7 ± 0.7	90.1 ± 0.7		

* Averages are taken for the steady state periods (starting 3 HRTs after a change in condition), and for n ≥ 3. OLR: organic loading rate; COD: chemical oxygen demand; C6: *n*-caproic acid; C8: *n*-caprylic acid; Select.: selectivity for C6 or C8 production; Extr.: extraction efficiency.

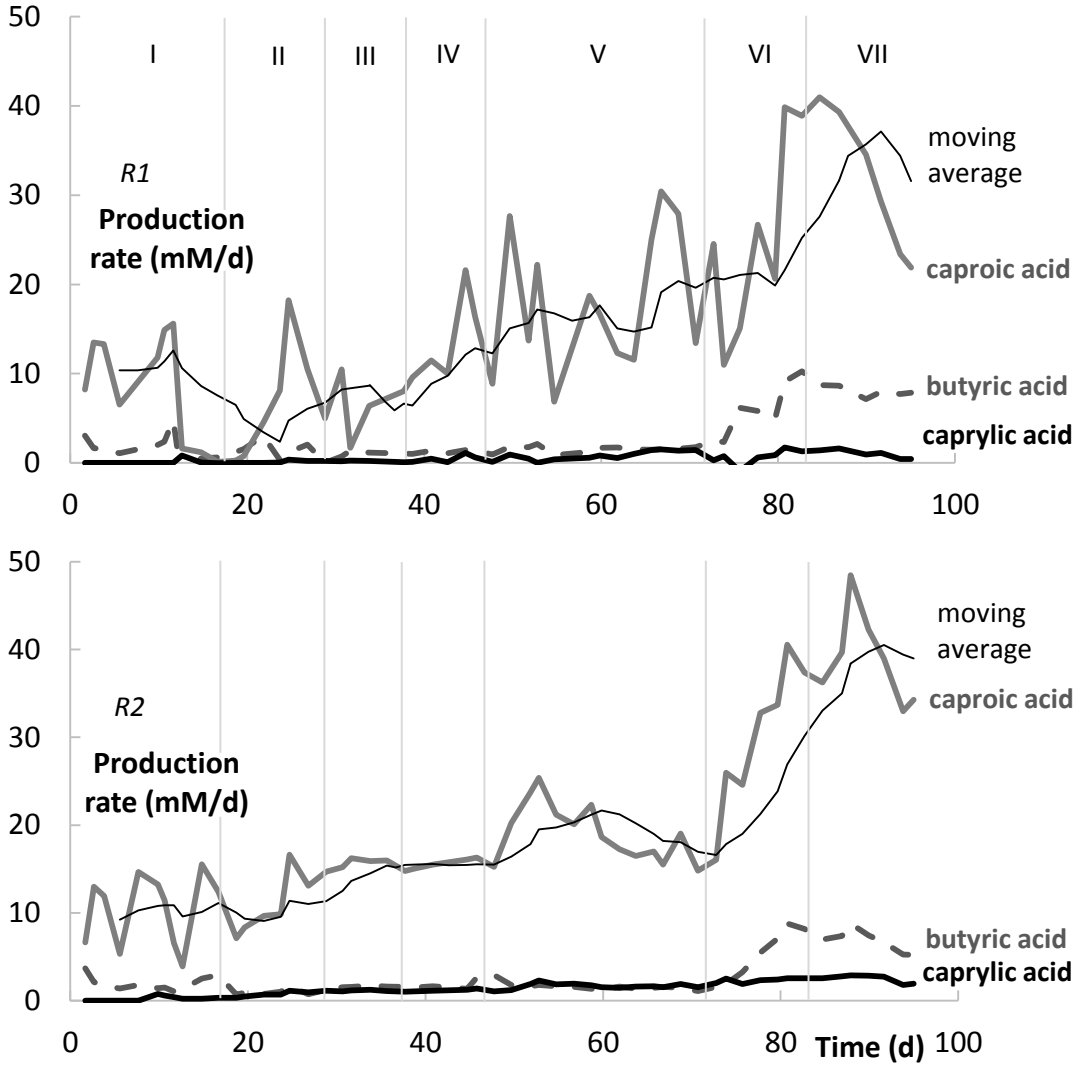

Figure 4.3 - Production rates of *n*-butyric acid (gray dotted line), *n*-caproic acid (gray line) and *n*-caprylic acid (black line) during continuous mode operation of the reactor with pertraction (R1, top, operating pH 6) and without pertraction (R2, bottom, operating pH 7). The moving average (n = 7) for the caproic acid concentration is provided. The 7 operational periods (Table 4.1) are marked with vertical lines.

3.5 The low pH required for in-line extraction is not favorable for C. kluyveri

The pH of the reactor with pertraction (R1), was decreased to 5.50 on day 11. This lower pH is necessary to obtain efficient extraction of the produced carboxylic acids, as only the undissociated species can be extracted. All caproic acid present in the reactor broth was extracted after the pH decrease but the production of MCCAs ceased (Figure 4.3) and the OD decreased. In early work on *C. kluyveri*, the pH range allowing growth was found to be between 6 and 7.50, with an optimum later defined at 6.40 (Barker & Taha, 1942; Kenealy & Waselefsky, 1985). A recent isolate of *C. kluyveri* from bovine rumen, however, was able to grow at a pH as low as 4.80 (Weimer & Stevenson, 2012), and a co-culture of *C. autoethanogenum* and *C. kluyveri* was functional at a pH of 5.50 (Diender et al., 2016). Mixed culture bioreactors, both

with and without pertraction, have operated at a pH of 5 to 5.50 without noticeable problems (Agler et al., 2012; Vasudevan et al., 2014), but enrichments of *C. kluyveri* were not detected in those systems, in contrast to reactors operating at neutral pH and higher dilution rates (Steinbusch et al., 2011). The toxicity of the MCCAs was always put forward as the reason for the growth inhibition in mixed cultures at low pH (Steinbusch et al., 2011; Agler et al., 2012). As all MCCA were extracted from the broth in the present study, clearly the acidic condition itself was detrimental for *C. kluyveri*. In future experiments a more gradual decrease to pH 5.50 could be tested as an operational strategy, but possibly the low pH would interfere with the proton motive force and energy metabolism of *C. kluyveri* (Seedorf et al., 2008). To restart production, the pH was increased to 6.0 on day 20 and additional biomass was spiked into the reactor. Production of *n*-caproic acid resumed but during Phase II production rates and carbon conversion efficiencies remained lower for R1 than for the reactor without pertraction (R2) at pH 7 (Appendix 4).

3.6 Production rate increases with loading rate

During Phase III, IV, and V the OLR was gradually increased (Table 4.1 and 4.3). The increase was slower in the reactor with pertraction following the pH shock. The theoretical OLR of 10 g COD/L/d resulted in *n*-caproic acid production rates of 16.2 ± 5.4 mM/d (1.9 g/L/d; 4.2 g COD/L/d) in the reactor with pertraction. *n*-Caproic acid was produced at a similar rate of 15.7 ± 0.5 mM/d (1.8 g/L/d; 4.0 g COD/L/d) in the reactor without pertraction (R2; Figure 4.3). These production rates are in line with mixed culture studies converting complex substrates at similar loading rates and with pertraction (Ge et al., 2015). The larger variation for the reactor with pertraction in this case, is possibly due to the aforementioned problems with the mineral oil recirculation in the pertraction system. On day 48, the OLR was increased to a theoretical loading rate of 15 g COD/L/d; however, after measurement, these loading rates were found to be lower (14.2 and 13.0 g COD/L/d; Table 4.3). *n*-Caproic acid production rates during this steady state period (day 55 – 74) were 19.1 ± 6.6 mM/d (2.21 g/L/d; 4.9 g COD/L/d) and 18.6 ± 2.9 mM/d (2.16 g/L/d; 4.8 g COD/L/d) for the reactor with and without pertraction, respectively.

In both reactors *n*-caproic acid was the main product, accounting for 90.9 ± 2.0 % and 85.5 ± 1.2 % of all carbon in products (here defined as selectivity for *n*-caproic acid; other products are *n*-butyric and *n*-caprylic acid) in the reactor with and without pertraction, respectively, at 10 g COD/L/d. *n*-Caprylic acid production was limited to 3.9 ± 2.2% of the carbon for the system with pertraction and 8.5 ± 0.4% for the system without pertraction. Higher selectivities for *n*-caprylic acid production have been obtained in mixed culture studies, albeit at a very low OLR (Zhang et al., 2013b). The selectivity for *n*-caproic acid remained similar at increased OLR, as long as the ethanol/acetic acid ratio in the feed was 10/1 (Table 4.3).

During Phase III and IV a carbon conversion efficiency of 47.5 ± 2.5 % was reached in the system without pertraction. Despite the lower production rate this is higher than the carbon conversion in the system with pertraction during Phase IV (41.9 ± 2.5%) due to the different actual OLR (Table 4.3). Conversion efficiencies remained similar during Phase V (Table 4.3). Conversion efficiencies were calculated based on the input carbon (ethanol and acetic acid) and carbon in products (butyric acid, caproic acid, caprylic acid). Carbon conversion to biomass or ethanol losses *via* evaporation were not quantified. For the production of carboxylic acids from syngas fermentation effluent a high conversion efficiency to products is desirable. The loss of substrate, which is not a low-value organic waste stream in this case, increases downstream processing costs and decreases overall profitability.

During Phase VI, the ethanol/acetic acid ratio in the synthetic feed was decreased to 3/1 to match the ratio in the real syngas fermentation effluent that was available. The carbon conversion efficiency increased for both reactors following this change (79.9 ± 2 % with pertraction (R1), 93.6 ± 4.4 % without pertraction (R2, Table 4.3)). Ethanol was completely consumed in the reactor without pertraction (Appendix 4). Production rates for all three carboxylic acids increased in both reactors. *n*-Caproic acid production rates reached 39.9 ± 0.9 (4.6 g/L/d; 10.2 g COD/L/d) and 37.6 ± 1.6 (4.4 g/L/d; 9.7 g COD/L/d) for the reactor with and without pertraction, respectively. The selectivity for *n*-caproic acid remained relatively stable, but proportionally more *n*-butyric acid was formed at the lower ratio, and, thus, the proportion of carbon in *n*-caprylic acid decreased. This was expected, as a high ethanol/acetic acid ratio is beneficial to obtain longer chain products. More ATP is produced when the ethanol/acetic acid ratio consumed is higher (Barker et al., 1945; Smith et al., 1985; Angenent et al., 2016). ATP is formed *via* substrate-level phosphorylation, in addition to transport-coupled phosphorylation, when the ethanol oxidation reaction is coupled to biological chain elongation (Gonzalez-Cabaleiro et al., 2013; Spirito et al., 2014). The higher substrate conversion efficiency might, thus, have been a mechanism to compensate for the decreased ATP production, when ethanol oxidation decreased due to the higher availability of acetic acid (Gonzalez-Cabaleiro et al., 2013). At the 3/1 ratio in this experiment, more ATP was formed, because the conversion increase was higher than needed to compensate for lost ATP production.

As we did not want to overload the bioreactors before or while testing syngas fermentation effluent, high loading rates have not been tested, yet this process parameter is worth studying further. During Phase VI, the concentration of undissociated *n*-caproic acid was already 3.5 ± 0.4 mM in the reactor with pertraction (pH 6), which is within the concentration range typically reported to be toxic for pure and mixed cultures, depending on the concentration of other undissociated carboxylic acids (0.66 mM – 7.5 mM; (Weimer & Stevenson, 2012; Ge et al., 2015; Diender et al., 2016)). For the reactor without pertraction, running at pH 7, *n*-caproic acid

accumulation was limited to 0.54 ± 0.07 mM. At a higher loading rate, even at pH 7, the accumulation of *n*-caproic and *n*-caprylic acid might negatively affect the culture, making an in-line extraction system essential, unless operation at a higher dilution rate is used.

3.7 The syngas platform can be coupled to the carboxylate platform

Real syngas fermentation effluent was used as influent for both bioreactors from day 86 onwards (Phase VII). *n*-Caproic acid was produced at a rate of 35.3 ± 2.7 mM/d (4.1 g/L/d; 9.0 g COD/L/d) in the reactor without pertraction, corresponding to a selectivity of 84.2 ± 1.0% (Table 4.3). Influent carbon was converted at an efficiency of 90.1 ± 0.7%. There was thus no decrease in productivity or conversion when real syngas fermentation effluent was used. A two-step process for the conversion of syngas fermentation effluent to MCCAs was successfully implemented, without addition of yeast extract for the chain elongation process. No conclusions can be drawn for the reactor with pertraction, because steady state was not yet reached when the experiment was terminated on day 95 due to an accident.

A direct conversion of syngas to *n*-caproic acid is possible (Diender et al., 2016), but a two-stage system allows better steering of process conditions, for example, by controlling the ethanol/acetic acid ratio obtained in syngas fermentation. Also, the pH values can be maintained for each bacterium or culture, because in one reactor a pH discrepancy exists. The effect of CO on *C. kluyveri* should also be further investigated. A co-culture of *C. autoethanogenum* and *C. kluyveri* produced a mixture of MCCAs and higher alcohols (butanol and hexanol) with CO and acetic acid as substrates (Diender et al., 2016). At low biomass levels coupled to mixing conditions, the CO inhibited the metabolism of *C. kluyveri* in a co-culture and as pure culture. The presence of CO in syngas could have an effect on the energy metabolism of *C. kluyveri* through inhibition of the hydrogenases (Buckel & Thauer, 2013). This could be beneficial, if proportionally longer chains are formed, but the lower ATP production might also decrease the overall performance, as was seen in incubations of *C. kluyveri* without *C. autoethanogenum* (Diender et al., 2016).

3.8 Problems with pertraction system caused decreased performance

The efficiency of the pertraction system in R1 was low at pH 6. At a loading rate of 10 g COD/L/d (Phase IV) the efficiencies for *n*-caproic and *n*-caprylic acid removal were 64.8 ± 13.7 % and 94.4 ± 6.6 %, respectively. Problems with mineral oil recirculation and a short-circuit affected the reactor performance (see section 2.4). Also, the short-circuit may have influenced the extraction rate by decreasing the flow rate of the broth in the forward pertraction unit. These problems decreased the extraction efficiencies when the loading rate was increased (Table 4.3). In principle a removal efficiency of *n*-caproic and *n*-caprylic acid above 95% can be

obtained with the pertraction system, when operated at pH 5.5 (Ge et al., 2015). At pH 6 only 6.6% of the caproic acid is present in the protonated form, while this increases to 18.3% at pH 5.5. A new acid-tolerant chain elongating isolate, or the acid-tolerant *C. kluyveri* isolate described by Weimer and Stevenson (2012), should be considered as biocatalyst.

4. Future perspectives

This is the first long-term continuous reactor study using *C. kluyveri* as the biocatalyst for chain elongation. A proof-of-concept for upgrading syngas fermentation effluent with a pure culture of *C. kluyveri* was demonstrated. Two reactors, one with and one without in-line product removal, were operated and we showed that both reactor operation modes are possible. In mixed culture studies the pertraction system proved effective for product recovery, increased production rates and inhibition of methanogens (Agler et al., 2012). In our study, the low pH (5.50) required for efficient product recovery was detrimental to *C. kluyveri* and we operated the system at a pH of 6, which is not ideal for extraction. However, we did not test a gradual decrease of the pH from 7 to 5.50, which might be a feasible strategy to adapt the culture to a lower pH. The use of an acid-tolerant isolate is another strategy for pure culture reactor operation (Weimer & Stevenson, 2012).

Through our reactor operation, we gained a better insight regarding the role of *C. kluyveri* in mixed culture studies. If a mixed culture reactor system is operated at a low SRT and low pH, *C. kluyveri* would likely play an insignificant role since cells would be washed out of the system due to sporulation and growth inhibition of *C. kluyveri*. High *n*-caproic acid production rates, and production of *n*-caprylic acid, have been obtained in reactors with both high and low enrichments of *C. kluyveri*, which suggests their presence may not be required to produce MCCAs using the carboxylate platform. Other strains indeed possess MCCA production pathways and might have a more versatile physiology, but thus far *C. kluyveri* is the only known microbe with the ability to use ethanol as the electron donor (Angenent et al., 2016). We did not yet investigate if and how *n*-caprylic acid production can be enhanced. Strategies could include: i) an increased availability of reducing equivalents; ii) an increased loading rate; and iii) an optimized in-line product extraction.

Coupling the syngas platform and carboxylate platform was feasible, without the addition of expensive growth factors such as yeast extract. We propose a system with two separate reactors for the initial syngas fermentation and the chain elongation process. This would allow a specific steering of the reactor conditions to optimize production rates of each process and a higher selectivity. From a practical point of view the coupling of the syngas and carboxylate platform in sequence is feasible, at their respective process temperatures (35°C and 30°C).

Obtaining a high rate chain elongation process will be crucial for a successful coupling of the syngas platform and the carboxylate platform. If methanogenesis and other competing pathways can successfully be inhibited in mixed culture fermentations, this fermentation strategy would, at first sight, be more advantageous than a pure culture process. Mixed culture chain elongations have been extensively studied on real and synthetic substrates, including syngas fermentation effluent. The study presented here was, however, a first proof-of-concept that a pure culture of *C. kluyveri* can act as the catalyst in this process. Follow-up studies should focus on the influence of pH on the metabolism of *C. kluyveri* in continuous processes or the selection of a different, acid-tolerant, biocatalyst, as well as the influence of product extraction with an optimized design at higher OLR.

Acknowledgements

S.G. is supported by the Special Research Fund (BOF) from Ghent University. The research stay of S.G. at Cornell University was financed with a travel grant from the FWO (Research Foundation – Flanders) and supported with a donation from ArcelorMittal (Ghent, Belgium) to K.R. and L.A.. B.M. is funded through a postdoctoral research fellowship from the German Research Foundation (DFG, MO2933/1-1). K.R. was supported by the ERC Starter Grant ELECTROTALK. L.T.A. was supported by the NSF SusChEM Program (Award # 1336186). The authors thank Tim Lacoere for drawing the reactor scheme. The input of Ramon Ganigué on the manuscript draft was greatly appreciated.

CHAPTER 5 – GENERAL DISCUSSION

This thesis work focused on the development of a reactor technology for the electricity-driven production of biochemicals from CO_2. The main findings are:

1) Biocathodic systems suffer from larger overpotentials than bioanodic systems. This is probably due to the indirect electron transfer mechanism that takes place at biocathodes for MES. Indeed, thermodynamically H_2 production cannot be excluded, even for studies that claimed DET.
2) By integrating product extraction in an MES reactor system, increased concentrations of acetic acid (up to 13.5 g/L, 225 mM) from CO_2 could be obtained. Compared to systems without product extraction, higher rates and efficiencies were obtained (13.8 g/m²/d with extraction *vs.* 9.3 g/m²/d without extraction in direct comparison; up to 24 g/m²/d in best experiment). The acetic acid is furthermore recovered as a clean acidified stream that can be directly upgraded, to ethyl acetate for example. This highly volatile compound can be more easily recovered than the highly water soluble acetic acid.
3) *C. kluyveri* can upgrade syngas fermentation effluents to MCCAs in a continuous process, without addition of yeast extract. The chain elongation process could be steered toward a carbon conversion efficiency of 90.1 ± 0.7 % at a caproic acid production rate of 35.3 ± 2.7 mM/d (4.1 g/L/d). Caprylic acid production by *C. kluyveri* is reported for the first time in this study. In a two-step process, CO and CO_2 can thus be converted to C6 and C8 products.

Using CO_2 as a carbon source for bioproduction is challenging for several reasons. First, it is the most oxidized form of carbon. Any transformation to a useful product thus requires a large input of electrons. Especially if fuel production is targeted, a relatively reduced form of carbon has to be obtained as product output (Desloover et al., 2012b; Aresta et al., 2013). If the energy for reduction does not come from a renewable source, then the technology as a whole will not be sustainable. Second, a suitable source of CO_2 must be found. The biocatalysts used in anaerobic fermentations are sensitive, to oxygen for example, but also to some extent to contaminants (H_2S, nitric oxide, tars) that might be present in waste gases (Daniell et al., 2012).

Besides the challenge in the production process, there is the challenge of bringing CO_2-derived products to the market. Still, the transition toward a CO_2-based economy is gaining momentum. A diversity of technologies is being developed and marketed. This diversity contrasts with the carbon economy that relies solely on fossil fuel resources. There are two driving forces for transition that can be considered: the technology development itself and the market demand. These two driving forces, “the push” and “the pull” side, need to be aligned further. In this general discussion, the MES and biological chain elongation technology are discussed from this point of view.

For a good understanding of this chapter, the current production methods for acetic acid and caproic acid are shortly explained. Acetic acid is mostly produced from fossil fuel resources (90%); only 10% is obtained through oxidation of aqueous ethanol (López-Garzón & Straathof, 2014). The most implemented fossil fuel based process (65% of the market) is the Monsanto process, a methanol carbonylation process, that is followed by distillation to purify the acetic acid (Clark, 2015). Natural fatty acids (such as caproic and caprylic acids) are obtained from palm, palm kernel oils, and coconut. Triglycerides present in these oils are hydrolyzed to obtain a mixture of saturated and unsaturated fatty acids, that are separated *via* fractional distillation (TMR, 2016).

1. "The push side": technology development

1.1 Microbial electrosynthesis and the syngas platform

An increasing number of articles on MES are published in peer reviewed journals each year (Figure 5.1). The research in this thesis was carried out in the context of this expanding research field. This research focused on the production of acetic acid from CO_2 in a new reactor system with *in-situ* product extraction. Developments needed for CO_2 based production in the context of this research and the broader MES field are discussed first.

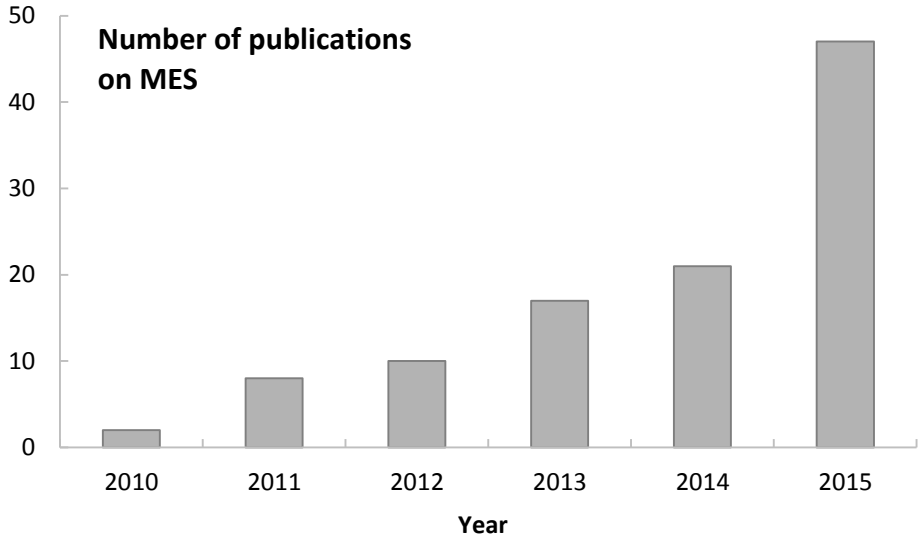

Figure 5.1 - Number of publications on the topic "microbial electrosynthesis" (MES) published per year. The number is a sum of research articles and review articles. Data obtained from ISI Web of Science.

What products should we make through MES?

In this section, gas fermentations (H_2/CO_2 or $CO/H_2/CO_2$) and MES combined are discussed, because all these processes rely on the same microorganisms and pathways. The production rates thus far are ~200 g/L/d for ethanol in syngas fermentations (Molitor et al., 2016), a

maximum of 150 g/L/d for acetic acid in H_2/CO_2 fermentations (Kantzow et al., 2015) and 42 g/m²/d (total surface area; 0.03 g/L/d) for MES (Jourdin et al., 2016a). Homoacetogenic organisms, which are the key players in MES and (syn)gas fermentation, use the Wood-Ljungdahl pathway for autotrophic metabolism. Of all CO_2 fixation pathways in bacteria, this is the most efficient one, but it currently limits the product spectrum to biochemicals derived from Acetyl-CoA (Berg et al., 2010). Acetic acid is the main product outcome, and several wild-type strains have the ability to produce ethanol as well (Drake et al., 2006). Both acetic acid and ethanol can be produced at high rates, which is a prerequisite to obtain a cost-effective process (Daniell et al., 2016). Ethanol production, rather than acetic acid, is a strategy to increase the usage of reducing equivalents in nutrient-limited conditions (Richter et al., 2016). Fermentation can thus be steered toward the desired product to obtain high specificity by controlling the process conditions. Other products that can be obtained in wild-type homoacetogenic strains are butanol, *n*-butyric acid and 2,3-butanediol (Liou et al., 2005; Henstra et al., 2007; Tracy et al., 2012; Latif et al., 2014). These products are however detected as side-products during fermentation. Production rates and titers remain too low compared to acetic acid and ethanol, but their market value makes them products of interest for commercialization (Liou et al., 2005; Köpke et al., 2011b; Shen et al., 2014).

To increase production rates of these higher value products, genetic modification of homoacetogenic species has been proposed (Schiel-Bengelsdorf & Dürre, 2012; Rosenbaum & Henrich, 2014; Liew et al., 2016). Using a gene knockout technique, competing pathways can be disrupted, which was first demonstrated in *Clostridium ljungdahlii* (Leang et al., 2013). Deletion of several genes diminished the capacity to produce ethanol, with an equivalent increased capacity to produce acetic acid. The same organism was successfully modified with plasmids *via* electroporation, introducing new pathways to produce butanol (Köpke et al., 2010). Production of biochemicals with genetically modified electrocatalysts *via* MES has not yet been accomplished. Other CO_2 fixation pathways could be introduced to diversify the product outcome beyond derivatives of Acetyl-CoA (Berg et al., 2010). For MES specifically, modifying the metabolic pathways of an electroactive microorganism is more likely to be successful than the addition of an electroactive pathway in a chosen biocatalyst, because the latter implies that the electron transfer mechanism must be fully understood, which is not yet the case (Jensen et al., 2010; Rosenbaum et al., 2011).

A better understanding of possible bioproduction routes can also be gained *via* thermodynamic and energetic models. In Chapter 2, a simple calculation method was proposed to assess the thermodynamic efficiency of existing systems. To gain new knowledge on microbe-electrode interactions or production pathways, more complex models are needed, that take into account the kinetics and enzymatics of production reactions (Gonzalez-Cabaleiro et al., 2013;

Kracke et al., 2015). *Via* these models, insights on reactor conditions needed to steer production of desired products can be gained.

Other strategies to obtain higher value products or higher rates of production include: i) the use of co-cultures of selected strains; ii) adaptive evolution; and iii) the selective enrichment of natural mixed cultures. In the first case, a strain able to convert H_2/CO_2 or syngas is combined with a culture that has the ability to metabolize the products of this first fermentation step (usually acetic acid and ethanol). A co-culture of *C. autoethanogenum* and *C. kluyveri* was used to produce *n*-butyric acid, butanol, *n*-caproic acid, and hexanol from syngas (Diender et al., 2016). To obtain one specific product, this co-culture technology should be combined with a selective extraction technique, such as stripping in the case of alcohols (Richter et al., 2012). In co-cultures, the reaction conditions cannot be optimized toward each specific strain, while it is known that reaction conditions can highly influence the product outcome (e.g. H_2 or acetic acid production depending on the pH in MES (LaBelle et al., 2014)). In the case of syngas conversions one has to additionally take into account that CO is toxic to many organisms, including *C. kluyveri* to some extent, decreasing the applicability (Diender et al., 2016). The second strategy, adaptive evolution, focusses on increasing production rates by naturally altering the microbial metabolism. *S. ovata* was adapted using methanol as substrate for growth. This increased the production of acetic acid at least 5 times compared to a non-adapted culture, both with H_2 and an electrode serving as electron donor (Tremblay et al., 2015). Thirdly, the selective enrichment of mixed cultures, is an effective strategy to obtain high-rate production *via* MES (Patil et al., 2015a). This was also studied in the context of this work: several natural populations were enriched under H_2/CO_2 atmosphere to select autotrophic, acetic acid producing microorganisms, with varying success (see Appendix 1.1). The use of unenriched cultures in reactor systems was unsuccessful due to the presence of competing metabolic pathways. A pre-enrichment allows a quick screening of a variety of natural populations. Conditions favoring high-rate production can then be selected for further reactor enrichments.

The new routes to broaden the product spectrum and increase the production rates require further exploration. MES will on the short-term remain limited to acetic acid production. This is not surprising as it is the sole product that can be generated at elevated rates and selectivity thus far. In syngas fermentation reactor conditions can be altered to obtain a high selectivity toward ethanol. This selectivity is beneficial for downstream processing. For new metabolic routes that are yet to be explored and will lead to a diversification of the product portfolio on the mid-term, the production rate and selectivity will be the criteria determining their success.

Technology developments needed for MES

The reactor technology and design can have a major impact on MES production (Chapter 3). The new reactor design presented in this work included *in-situ* extraction of acetic acid. This resulted in higher production rates compared to systems without extraction, and increased product titers (13.5 g/L), while guaranteeing high selectivity toward acetic acid (up to 98.4% of carbon in products). The produced acetic acid could directly be converted to ethyl acetate using an innovative esterification technique. A pure product can as such be obtained *via* evaporation of the volatile ester (Andersen et al., 2016). *In-situ* product recovery has in many cases been a key approach to decrease product inhibition, a problem also frequently occurring in acidifying MES reactors (Agler et al., 2012; Marshall et al., 2013b). The reactor with *in-situ* extraction allows production at high rates without the input of chemicals to balance the pH, a major improvement for the MES technology (Chapter 3). The reactor technology has a growth margin for its efficiency. Three key elements are (Figure 5.2): i) cathode materials; ii) resistance losses; and iii) extraction efficiency. The first two elements thus relate to electrochemical losses, the third to improved reactor design.

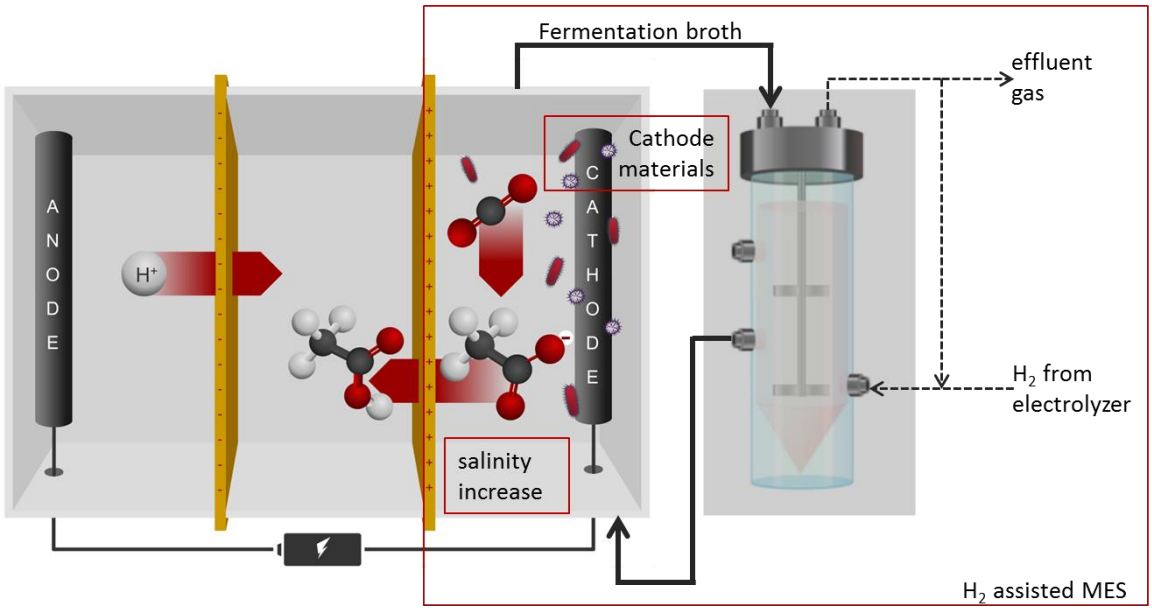

Figure 5.2 - Strategies proposed to improve microbial electrosynthesis (MES) technology: i) improved cathode materials; ii) decreased resistance losses *via* increased salinity; and iii) improved extraction efficiency through coupling with an external fermenter.

The energy input is at this early stage of reactor development 19 kWh/kg acetic acid extracted. Decreasing electrochemical losses in the reactor system is crucial to increase efficiency (Clauwaert et al., 2008a). In that perspective, the development of MES technology shows similarities with bioanodic BESs. Losses are generally more important for cathodic MES systems than for bioanodic systems, most likely due to the electron transfer mechanism at the

cathode, which takes place *via* indirect H_2 production, rather than DET (see Chapter 2). A cathode material that efficiently allows H_2 evolution, but also has a biocompatible surface for biofilm formation could thus be a considerable advantage. The biofilm could as such efficiently metabolize the H_2. Functionalization of carbon materials with positive charges, biopolymers or metal particles were advantageous strategies to increase the acetic acid production rate (Zhang et al., 2013c). No definite proof was, however, given in that study for the claimed DET process. Production rates furthermore remained low (14 g/m²/d) compared to rates obtained with unmodified carbon materials in other studies (e.g. this study: 24 g/m²/d). Much higher rates were obtained with 3D carbon materials, coated with carbon nanotubes, and an enriched mixed culture (42 g/m²/d; (Jourdin et al., 2016a)). A combination with *in-situ* extraction could possibly further increase production rates, as a low end product concentration increases the Gibbs energy change (see Chapter 2).

The energy input required for acetic acid production *via* the conventional Monsanto process is only 57 Wh/kg electricity, and 400 Wh/kg as steam for distillation of the acetic acid (Ecoinvent, 2007). The resulting product is 98% acetic acid. If the energy required for methanol production from natural gas is also considered, the energy input increases to 4 kWh/kg acetic acid (Ecoinvent, 2007). The MES system presented here required, in the best case of several experimental runs, 19 kWh/kg, for the production of 1.35% acetic acid. While this is a proof-of-concept study only, several improvements will be needed to decrease the energy input. The combination of a bioanode and biocathode has been proposed in that perspective (Gong et al., 2012). Oxidation of organics takes place at a lower potential than water electrolysis. In this thesis work the use of a bioanode and chemical anode were compared in the context of NH_4^+ recovery from synthetic waste streams (see Appendix 1.2). Bioanodes are prone to disturbances and have a longer startup time. For industrial applications, requiring constant high current densities, operation with a bioanode would involve too much risk, which does not compensate for the lower energy input.

Secondly, the energy input can be decreased by increasing the conductivity of the electrolytes (Schröder & Harnisch, 2010). A 10 times higher applied current density, a prerequisite for increased production rates, would lead to a 10 times higher ohmic drop. A combined effect of decreased distance between the electrodes and increased salinity, could compensate for this ohmic drop. A saline catholyte would require the use of halotolerant species for acetic acid production. Only very few halotolerant or halophilic homoacetogenic strains have been isolated to date (Drake et al., 2006). Two haloalkaliphilic species, *Natroniella acetigena* and *Natronincola histinovorans*, cannot grow on H_2/CO_2 or CO, which would limit their applicability for MES (Zhilina et al., 1996; Zhilina et al., 1998). *Acetohalobium arabaticum* is the only autotrophic halotolerant homoacetogen isolated to date (Zhilina & Zavarzin, 1990).

Homoacetogenic organisms play an important role in the geochemical cycles in the sea and sediments (Küsel et al., 1999; Drake et al., 2006). Enrichment of these species for technological applications requires an adapted strategy, including the use of defined saline media (see Appendix 1.1). The higher salinity will impact *in-situ* product extraction. The molar ratio of acetate will decrease compared to other charged species in media with higher salinity. This is a drawback of this strategy, as the extraction efficiency of acetate will probably decrease.

To decrease the energy input, while still allowing *in-situ* product recovery, utilization of the extraction reactor as secondary microbial electrochemical technology (MET) should be considered as third strategy. As secondary MET, the extraction would support a H_2/CO_2 fermentation by: i) extracting the acetic acid; ii) balancing the pH of the fermentation broth; and iii) provide additional H_2. The acetate extraction efficiency, thus far, limited to 12.5% of the charge balancing, could as such be increased through the extraction of acetic acid (as acetate) produced in the external fermenter. This would allow much higher production and extraction rates at a lower energy input: commercially available alkaline electrolyzers require only 1.8-2V energy input for applied current densities as high as 300 A/m² (Zeng & Zhang, 2010). The extraction cell can thus be coupled to a fermenter converting either off-gas or H_2 produced through electrolysis. Using a control system, the extraction cell could furthermore be switched on intermittently, when pH stabilization is needed, or acetic acid accumulates above a set concentration, to optimize the energy investment.

1.2 Chain elongation and product recovery

For the development of the carboxylate platform, key challenges are identified in the context of this work: i) the substrate; ii) the biocatalyst; iii) specificity; and iv) product extraction. This last topic will be covered in a separate section.

Perspectives for the carboxylate platform

The carboxylate platform originally focused on the valorization of organic waste streams *via* mixed culture fermentations (Agler et al., 2011). Such waste streams are available in large quantities in the food and biofuel industries, where they are currently transformed to low-value products such as biogas or animal feed. In the carboxylate platform, organic matter is first catabolized to SCCAs and ethanol as intermediates. When using biomass waste streams, part of this undefined matrix is not broken down biologically to the building block (SCCAs and ethanol). In contrast, when these building blocks are obtained through autotrophic gas fermentations, a clean matrix for chain elongation is obtained. Independently of the substrate, the further conversion to caproic acid and caprylic acid, which are the target products of the carboxylate platform, requires an efficient reducing agent. As reduction with H_2 is thermodynamically not

possible, sufficient ethanol, or alternatively lactic acid, must be available as reducing agent for this conversion (Gonzalez-Cabaleiro et al., 2013; Kucek et al., 2016). Complex substrates that can be efficiently converted are residues from bio-ethanol production, as these typically contain a high fraction of easily convertible organics, and sufficient reducing equivalents (Andersen et al., 2015; Ge et al., 2015). Production of carboxylic acids from organic waste streams that do not have these characteristics might require the addition of an external ethanol sources to obtain an efficient process. Undistilled ethanol obtained from biomass or syngas fermentation seems to be a most obvious choice. This research furthermore showed that syngas fermentation effluent can be directly used for chain elongation as well. It must be noted that to date, the highest production rates for caproic acid (2.3 g/L/h) have been obtained in synthetic medium, with excess ethanol available (Grootscholten et al., 2013d). Research using real streams is essential to push development of this technology.

The conversion of biomass waste streams to bioproducts is often carried out with mixed cultures, as sterilization can as such be avoided (Agler et al., 2011). Methanogens are naturally present in these anaerobic mixed communities and inhibition of methanogenic metabolism is crucial to ensure high specificity toward the desired MCCAs (Steinbusch et al., 2009). Operation at low pH (≤ 5.50), addition of a specific methanogenic inhibitor or heat-shocks are common strategies to reduce methanogenesis (Agler et al., 2011). The last two strategies are not sustainable at large scale. Operation at low pH does not always lead to a complete inhibition of the methanogenesis and requires an in-situ recovery strategy to avoid inhibition of the fermenting culture by the produced carboxylic acids (Agler et al., 2014). In specific cases, such as the conversion of syngas fermentation effluent studied here, a pure culture process might be advantageous to avoid competing pathways (see Chapter 4). This first continuous reactor study with *C. kluyveri* could not show the full potential of this organism yet. Operation coupled to pertraction, which requires a low pH that is detrimental for the chosen culture, must be optimized. Operation at higher loading rates should clarify the potential production rates and associated conversion efficiencies. The development of genetic tools and a better understanding of the metabolism of *C. kluyveri* can contribute to better strategies to steer the production toward desired products (Seedorf et al., 2008). Developments of genetic tools are opportunities for linking the syngas and carboxylate platform with *C. kluyveri*. On the other hand, mixed cultures undoubtedly remain the first choice for chain elongation at the moment, because of the resilience and versatility of the community and the associated ability to handle varying input streams (Werner et al., 2011).

A challenge for fermentations is to steer the process toward one specific product that can be recovered at a relatively low energy input (Agler et al., 2014; Schievano et al., 2016). Specificity can be obtained either: i) in the fermentation process itself; or ii) *via* a selective recovery step.

To steer the fermentation process itself, a high input of reducing equivalent is beneficial for the production of longer chain carboxylic acids (caproic acid and caprylic acid; (Angenent et al., 2016)). As mentioned before, the use of a pure culture decreases the number of pathways available in the fermentation process and can be beneficial to obtain a higher specificity. Secondly, a recovery technique targeting a specific fermentation product is beneficial, since removing an end product is thermodynamically favorable. Reactor operation at high dilution rates, without product recovery, might lead to higher overall production rates because the end-product is removed but: i) does not provide a selective removal of an end-product; and ii) negatively affects product recovery due to the low product concentrations, as has been discussed for MES (see Chapter 3). Both pertraction (membrane based liquid-liquid extraction) and ME have been proposed in this work to recover carboxylic acids directly from the broth (see further). Alternatively, an additional conversion of carboxylic acids to alcohols using syngas, and subsequent stripping of the alcohols is a possible strategy (Richter et al., 2012; Richter et al., 2013a). A complex substrate can as such be converted into fuels in a two-step conversion, where the recovery technique ensures product specificity. This is also a characteristic of the *in-situ* recovery techniques discussed next.

Extracting products: electrochemical techniques *vs.* pertraction

In contrast to biogas production, where the gaseous product readily separates from the broth, downstream processing accounts for 30-40% of the production cost of most carboxylic acids (López-Garzón & Straathof, 2014). Recovery strategies for carboxylic acids mostly comprise adsorption techniques, such as ion exchangers, and extraction techniques, such as a solvent extraction. For mixed culture fermentations and new processes, such as MES, that are now being developed, an appropriate recovery method must be designed. In this work two product recovery strategies are put forward for the recovery of carboxylic acids from fermentation broths: membrane electrolysis and pertraction.

Membrane electrolysis (ME) extracts charged molecules from the fermentation broth through an AEM, driven by electrical current. The molar concentration of the different charged species in the diluate stream, their diffusivity, and hydrophobicity determine the extraction efficiency (Andersen et al., 2014). For example, at an equimolar concentration of acetate and caproate, the smaller, more hydrophilic, acetate molecules will preferentially be extracted (Andersen et al., 2015). In this study, ME was proposed as a recovery strategy for MES. One of the main advantages of the MES system over chain elongating fermenters is that a very high production selectivity (> 95%) toward acetic acid, which is a small hydrophilic molecule, can be obtained (see Chapter 3). An extraction method with lower selectivity, but targeting smaller, charged, hydrophilic molecules in general, can then be applied to MES. Furthermore, acid (H^+)

and base (OH^-) are generated *in-situ* during ME. This decreases the input of chemicals, and makes treatment of a salt by-product otherwise created through their addition unnecessary (López-Garzón & Straathof, 2014; Andersen et al., 2015). The obtained acetic acid stream still contains salts, but a pure product can be obtained *via* a subsequent esterification, and the evaporation of ethyl acetate (Andersen et al., 2016). When MCCAs are extracted, it is possible to apply phase separation of the carboxylic acids following ME (Xu et al., 2015). The extracted carboxylic acids are obtained in their protonated form, which is advantageous, as the solubility of both caproic acid and caprylic acid are low (10.82 g/L and 0.68 g/L respectively) compared to other shorter chain carboxylic acids, such as butyric acid. Phase separation results in increased specificity when the non-water soluble compounds are recovered; salts remain in the aqueous phase (Angenent et al., 2016). The use of ME directly on the fermentation broth could be difficult since membrane fouling is likely to occur. Even if a filter is used to retain biomass, soluble organics can cause membrane fouling, increasing the operational cost of the system (Strathmann et al., 2013).

In this work, caproic acid production was coupled to pertraction, a membrane based liquid-liquid extraction, as recovery technique. A pH gradient and a preferential extraction of the longer chain, hydrophobic, carboxylic acids drive this extraction system. Pertraction can thus be considered a semi-selective extraction technique, targeting hydrophobic products. The continuous reactor operation with *C. kluyveri* showed that it is crucial to operate the system at a pH of 5.50 (or lower) to obtain efficient extraction. A culture that can tolerate this lower pH, either pure or mixed, is an important prerequisite for successful operation. Reactor operation at pH 5.50 comprises an operational risk (product inhibition) in case the pertraction system fails, but redundancy can be built into the system with several extraction tanks. Operation of the *C. kluyveri* reactor with ME would have resulted in a less selective extraction of the longer chain products, especially caprylic acid, which was produced at a low rate compared to butyric and caproic acid. Operation at a neutral pH combined with electrochemical product extraction could have had a positive impact on production by *C. kluyveri*, but these assumptions need to be verified experimentally.

In fact, a combined approach using both pertraction and ME provides more advantages than either method alone. The pertraction system selectively removes the most valuable, but also most toxic carboxylic acids: caproic acid and caprylic acid. Application of an ME system on the stripping solution then results in extraction and acidification of these products. Due to the low solubility of caproic and caprylic acid, they can be recovered *via* phase separation. Butyric acid that will still be extracted to some extent with the pertraction system, will not phase-separate in the anolyte of the ME system. A concentrated product containing 92% caproic and caprylic acid

was obtained in a first study combining pertraction and ME in this way (Xu et al., 2015). Future experiments will have to confirm if these advantages outweigh the higher capital cost.

2. "The pull side": the market for CO_2-based products

Positioning CO_2-based products on the market is a second important aspect, besides technology development. Fossil fuel based processes have the advantage that they are implemented on a large scale, thus, decreasing production costs. These processes have been improved over long time use toward higher efficiency and sustainability. To position existing chemicals, but produced from CO_2, on the market, these have to be: i) cheaper; ii) of equal or better quality; and iii) substantially more sustainable than the fossil fuel based products, and the market for these products must furthermore not yet be saturated (Otto et al., 2015). Legislation can play a crucial role in the expansion of a CO_2-based economy, including through subsidy mechanisms.

2.1 Biological and (electro)chemical approaches: which platform to choose?

Biological approaches are usually not considered when reviewing approaches to capture and transform CO_2 to chemicals (Lim, 2015; Styring & Armstrong, 2015). Microbial platforms clearly do not compete yet with (electro)chemical technologies. Algal technologies are often mentioned, but not considered applicable at large scale due to land use issues, technical challenges regarding sufficient exposure to sunlight, and difficulties harvesting the biomass or intracellular lipids. This renders the algal technology too costly at the moment (Hunt et al., 2010). On the other hand, processes involving chemical or electrochemical reductions of CO_2 are already implemented at large scale.

Chemical processes mainly involve the low-cost transformation of CO_2 to (poly)carbonates and urea. The market for carbonates (calcium carbonate as building material, polycarbonates as plastics) is, however, limited. One Japanese company, Asahi Kasei Chemicals, produces 660 000 tons of polycarbonate from CO_2 on a yearly basis, which corresponds to 14% of the worldwide polycarbonate market (Lim, 2015). Urea production uses 120 Mton CO_2 on a yearly basis. Both the NH_3 and CO_2 used in the production of urea are, however, obtained from coal, so no sequestration of CO_2 takes places. A sustainable process would require an alternative NH_3 source and waste CO_2 (Aresta et al., 2013).

The real challenge is to produce hydrocarbons from CO_2, which requires a larger energy input, but has a market value about 12 to 14 times larger than the products described above (Aresta et al., 2013). A successful example is Carbon Recycling International, an Icelandic

company that uses geothermal energy for H_2 production *via* water electrolysis. The H_2 is then used for reduction of CO_2 to methanol, a liquid product that can be exported (CRI, 2016). The CO_2 is obtained from carbonate rocks on Iceland, but could also be obtained from point sources in industry. The availability of large amounts of cheap geothermal power makes this conversion economically attractive in the Icelandic case. Indeed, the electricity price should decrease by a factor 10, from the actual reference price of €95/MWh to €9/MWh, to make methanol production from CO_2 economically attractive in the broader European context (EC, 2016c). This economic challenge also applies to MES, which is an electricity-driven biological conversion.

Chemical production routes have another limitation: conversions are usually restricted to C1 carbon molecules and in most cases the specificity is quite limited. This could be seen as an opportunity for the production of short-chain hydrocarbons, such as acetic acid from CO_2 instead of fossil fuel resources. Currently 65% of the acetic acid worldwide is produced *via* methanol carbonylation by the Monsanto processes (Clark, 2015). The methanol required for the process could be produced from CO_2, and the CO obtained from waste gas effluents, and thus totally eliminating the need for fossil fuel resources.

This limitation to C1 products creates an opening for alternative biological production routes toward added value products that separate more easily. The microbial pathways discussed already lead to at least C2 products, when Acetyl-CoA acts as intermediate. The versatility of microbial metabolism enables production of specific biochemicals with a variety of functional groups (Rabaey et al., 2011), and longer chain products can be obtained through subsequent biological conversions. Several possibilities for doing this sustainably could be considered. For example, reducing equivalents can be obtained from renewable electricity as well (electrolysis for H_2 production), or from dilute product and biomass streams (*e.g.* ethanol). Biological production routes can be linked with chemical production platforms. Another advantage for biological conversions from CO_2 is their lower sensitivity gas composition and purity. The ratio of $H_2/CO/CO_2$ in the waste gas if also of lower importance for biological conversions, whereas chemical conversion processes such as the Fischer-Tropsch process require a fixed H_2/CO ratio of 2/1 (Liew et al., 2016). Metal catalysts are prone to poisoning when the off-gas used is of too low purity (Whipple & Kenis, 2010; Wang et al., 2011). Biological catalysts have a higher versatility; small concentrations of H_2S (up to 100 ppm) or tars do not negatively affect the biocatalysts (Molitor et al., 2016). Use of polluted gases would, however, require a gas treatment step, projected to cost €10/ton CO_2 (€15/ton acetic acid; (Xu et al., 2014)). Cleaner combustion processes could contribute to an efficient and possibly direct usage of waste gases in biological based technologies (Markewitz et al., 2012).

The key for biological processes, not to remain a niche application, is to produce compounds at high rate, relatively high selectivity, and high purity. Production rates will most likely increase when technology improves. Biological routes should be linked with the chemical industry platform to make use of established purification technology. The market potential of the different production routes proposed in this work is evaluated next.

2.2 *Toward a techno-economic assessment of microbial electrosynthesis, syngas fermentation and the carboxylate platform*

To assess the potential of the different routes to produce chemicals from CO_2, one has to consider several factors: i) the CO_2 reduction obtained with the alternative production route; ii) the purity obtained; iii) the production cost; iv) the market value and market capacity of the product; and v) the integration of a new process in the existing chemical industry pipeline (Styring et al., 2011; Otto et al., 2015). An overview is given of the processes and products that can be obtained *via* the three studied processes: MES, syngas fermentation and chain elongation (Figure 5.3). For each approach, opportunities and disadvantages are discussed below. Several of these products (ethanol, and the derived ethyl acetate, as well as jet fuels) are listed on the "top 12 building blocks" list published by the U.S. Department of Energy. These are the key platform chemicals for which biomass-based routes must be developed (DOE, 2016). Commercialization of biomass-based routes has been achieved for most of these bioproducts (Choi et al., 2015). Production from CO_2 should now follow the same trajectory.

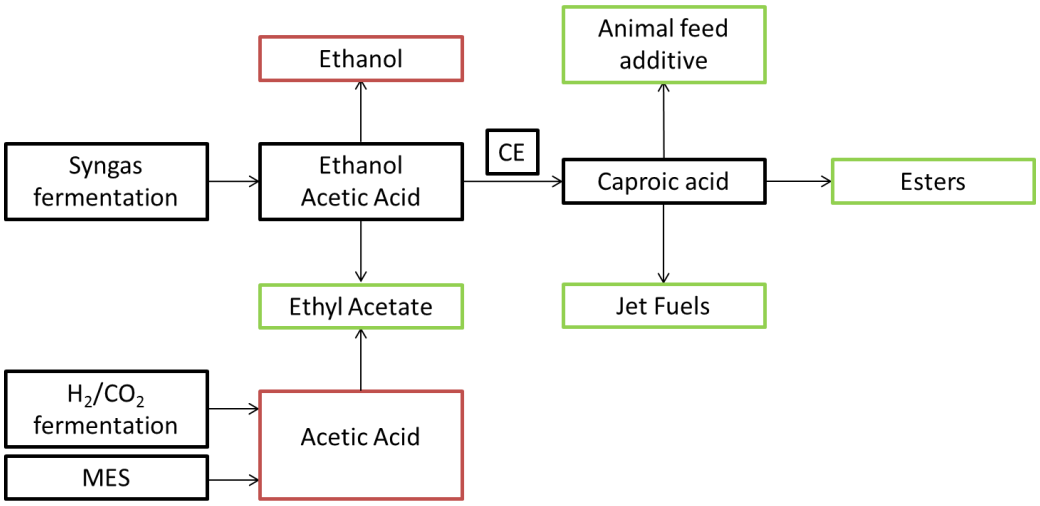

Figure 5.3 - The biological conversion processes studied (microbial electrosynthesis (MES), chain elongation (CE), syngas fermentation, H_2/CO_2 fermentation) can result in a variety of products with different market potential.

Gas fermentations

The MES process presented, with an integrated product recovery step, resulted in acetic acid concentrations up to 13.5 g/L (225 mM). This is a higher concentration than what is usually

obtained in MES, and the product is obtained in a clean and acidified form. It is not unlikely that MES or a combination of MES and H_2/CO_2 fermentations would lead to concentrations as high as 6% (1 M) in the near future. An azeotropic distillation is needed to purify mixtures of acetic acid and water, which would require a very large energy input[1]. At a current market price of $370/ton (Lee, 2015), even an improved reactor system could not compete on the acetic acid market[2]. Acetic acid produced *via* MES would, furthermore, have to compete with other clean production strategies. Production could for example become a sink for CO_2 *via* the Monsanto technology as well, as described in the previous section. This process has the benefit of the economy of scale, with high rates and efficiencies that can be obtained. Although the electricity cost also impacts methanol production from CO_2 thus far, the easy integration of the chemical CO_2-based route forms a competitive advantage.

Ethyl acetate production *via* esterification has a greater potential of application, given the higher market price of $1100/ton (Pafford, 2016), and the low boiling point of this chemical. It can be produced from dilute acetic acid and low-grade bio-ethanol in a water excluding solvent such as an ionic liquid (Andersen et al., 2016). The ionic liquid technology proposed is still in its infancy, so cost estimations are difficult, but the high cost for ionic liquids certainly make the recycling of this solvent crucial. The advantage of an esterification step is that low-grade products are transformed into chemicals that can be purified easily using existing techniques due to their volatility, resulting in the required 99.99% purity for high-tech applications.

The second process studied here, syngas fermentation, now focusses on ethanol production from waste gas. Pilot and demonstration plants are being built at several test sites. Ethanol can be mixed with gasoline fuels, which is heavily promoted to decrease GHG emissions in the transportation sector. Ethanol has a variable market value, between €400 - €600/ton (Ellis, 2016). Subsidies currently only concern biomass-based ethanol (see further). Lanzatech, the leader in syngas fermentation, also foresees the production of 2,3-butanediol, which is a niche chemical with higher value than ethanol. Both ethanol and 2,3-butanediol are difficult to extract due to their chemical properties, such as their high hydrophilicity and low boiling point (Molitor et al., 2016). Ethanol distillation to 95% ethanol requires approximately 2 kWh/kg, an input

[1] Heating (from 25°C to 100°C) and evaporation of water would require 11.2 kWh/kg at 6% acetic acid

[2] Assuming a system with a 1 m² electrode runs at 100 A/m² and 75% CE, 500 kg of acetic acid is produced daily. Assuming the energetic efficiency can be doubled (energy input of 9.5 kWh/kg; current labscale system requires 19 kWh/kg extracted), the system demands 4.8 MWh/d. At the current European energy price (€95/MWh), this corresponds roughly to an input of €900/ton ($1000/ton), solely for the production of a dilute acetic acid stream.

doubled to obtain 99.7% ethanol (Jungbluth et al., 2007). The economic viability of ethanol production from syngas still has to be proven (GreentechMedia, 2014).

Caproic acid production

In this work, a new conversion route for syngas fermentation effluent was proposed, the fermentation to caproic acid *via* chain elongation. The high ethanol/acetic acid ratio's (20/1) make the effluent a suitable substrate for chain elongating bacteria (Angenent et al., 2016). The technical aspects of this process, including the type of biocatalyst and extraction technique, have been discussed earlier. Three possible routes can be envisioned for the caproic acid product (Figure 5.3): i) as an ester after esterification; ii) as feed additive in animal feed; iii) as a jet fuel after Kolbe electrosynthesis.

The first route follows the same strategy as the esterification of acetic acid, resulting in ethyl hexanoate, an aroma component in for example strawberries and Chinese liquor, which has a relatively small market (2000 ton/year) (Xu et al., 2002). In the case of acetic acid synthesis, the advantage of esterification is that a dilute product can be upgraded *via* a reaction in a water-excluding solvent, forming a product with low boiling point (77.1°C). In contrast, ethyl hexanoate has a low volatility (boiling point 168°C). Esterification might, thus, not be the most ideal route for caproic acid valorization.

Caproic acid itself, however, has a low solubility in water and it can be easily recovered *via* phase separation. The oil product that is as such obtained has a high purity and has direct market value, as feed additive for animal feed for example (Devi & Kim, 2014; Xu et al., 2015). Caproic acid has probiotic and antimicrobial properties, an important aspect now that antibiotics use in animal farming is highly regulated in the EU. Caproic acid for the animal feed market is now obtained from palm kernel and coconut oil, which is not considered sustainable because of the way tropical forests are managed. The crude oil intake price is about €1000/ton, making it a valuable product. This study proposed caproic aid from syngas fermentation effluent. If all ethanol produced from steel mill syngas in Europe (projection: 380 x 10^6 L/year; (Molitor et al., 2016)) would, however, be converted to caproic acid, this would correspond to current market size of caproic acid (25kton/year)[3]. As caproic acid can also be produced from biomass waste, a saturation of the market can be expected, even when considering the projected expansion of the animal feed market.

[3] Assuming a 100% efficient conversion to caproic acid, at a ratio of 3.33 mol caproic acid per mol ethanol (Angenent et al., 2016).

A much bigger market opportunity is the production of jet fuels *via* Kolbe electrolysis (Levy et al., 1981). Caproic acid is then transformed to *n*-decane. Kerosene-type jet fuels currently have a market price of $1.33/gallon ($0.34/L), which is about half the price from the period 2011-2014 (DOE, 2016). The U.S. market alone is projected to increase to a value of $84 billion in 2030 (Frost & Sullivan, 2008). Accounting for 3% of the total GHG emissions in the EU, the aviation sector is a major contributor to climate change (EC, 2016b). The aviation business is counting on government support for the transition to the more expensive bio-based fuels (De Guzman, 2011). Public perception regarding the use of CO_2-based caproic acid as animal feed additive might be negative, but should not be problematic for the production of fuels.

Of all presented approaches, the production of ethyl acetate and *n*-decane probably has most potential, based on the 5 factors described at the beginning of this section. The market value or market size of both products is high and integration with the established chemical industry can be foreseen, which will allow to obtain high-quality products. In both cases, the production rates and efficiencies of the biological conversions will be crucial. Once pilot studies have proven the potential of these technologies, regulatory aspects will be an important driver to penetrate the competitive fossil fuel based market.

2.3 Legislation for CO_2-based products

The European Union (EU) currently does not support CO_2-based chemicals *via* subsidies or specific labeling. The legislation and support is limited to three fields related to the context of this work: i) biofuels and biochemicals made from biomass; ii) carbon capture and storage (CCS); and iii) advanced fossil fuel power generation (EC, 2016a).

Ethanol produced *via* the fermentation of syngas originating from fossil fuel based processes does not fit the definition used by the EU, which details that only biomass-based chemicals are considered as biochemicals or green chemicals. For biofuels a specific CO_2-reduction norm is added to the definition: bioethanol and biodiesel need to represent a reduction of CO_2 emissions of at least 35% compared to conventional fuels, a number that will be increased to 50% in 2017 (EC, 2016a). Although production of biochemicals from CO_2 also represents a decrease in CO_2-emissions, this value is currently not recognized by the EU and no subsidies support the development of CO_2-based production. The biofuels market receives €8.4 billion subsidies from the EU yearly (EC, 2016a). The different pipelines proposed for production based on CO_2 can be easily integrated in the chemical industry in Europe and represent a true decrease in CO_2 emissions as besides the capture of CO_2 from, for example, power plants or steel mills, more emissions are avoided by not using fossil fuel resources for the production of these chemicals and fuels.

Research on CCS is supported by the EU, as well as projects to implement the technology at large scale. An example of a subsidized project is the White Rose project in the UK. It concerns the re-injection of CO_2 in off-shore reservoirs. There are several arguments against CCS: there's no added value creation (in fact, CCS doubles the cost for electricity production (Rubin & Zhai, 2012)), the negative perception from the general public is difficult to overcome and the system requires a vast network of pipelines to transport CO_2 to a centralized reservoir (EC, 2016c).

CCS is, however, the technology of choice to also increase the sustainability of fossil fuel power plants. The EU projects that in 2030 about 40 to 50% of our electricity will still be generated from fossil fuel, a number that would only decrease to 31% in 2050. Therefore the EU strives to combine these power plants with CCS, by retrofitting existing power plants to render them more efficient and producing cleaner CO_2. The combination of retrofitting power plants with decentralized production of biochemicals from CO_2 is currently not considered as an option (EC, 2016c).

The absence of subsidies and a clear legislation background make investments difficult. The added value of carbon capture and utilization (CCU) for the European economy is not yet recognized. A shift in the EU policy has recently been made as several calls for research grants in the framework of the Horizon 2020 are now specifically for CCU techniques (EC, 2016a). A long term vision on the role of CCU is now needed, including a strategy to deal with the variability of the CO_2 cost. This is needed to create a positive investment climate that will allow the EU to diversify its economy, decreasing the dependency on fossil fuel resources. A clear support from policymakers is also needed to increase public awareness and support for CO_2-based chemicals. (Bio)production from CO_2 will not become the sole strategy to replace fossil-fuel based production. Biomass-based routes and even fossil-fuel based routes will continue to exist. Side products from agriculture will keep on requiring treatment, for example. The key is, however, to recognize the real opportunity of each route and to provide a fair legislational and subsidiary system for each technology.

Conclusions

The future carbon-neutral economy will utilize a variety of feedstocks for the production of biochemicals. Low-grade biomass and CO_2 streams will be upgraded to added-value products. The energy required for CO_2 reduction must be obtained from sustainable sources.

Reduction of CO_2 can be achieved *via* MES. The high specificities toward acetic acid are an advantage of this technology, but this requires a pH control strategy at neutral pH to avoid product diversification or end-product inhibition. A new reactor design was proposed in this PhD thesis, allowing: i) *in-situ* extraction of the produced acetic acid (as acetate); ii) pH control of the catholyte without chemicals dosing, thus avoiding product inhibition; and iii) concentration of the acetic acid as a clean product stream in a separate reactor compartment. An acetic acid concentration of 13.5 g/L was as such obtained at an energy input of 19 kWh/kg. To fully use the extraction capacity of the system, this technology would be more efficient as secondary microbial electrochemical technology, assisting H_2/CO_2 fermentation. This would allow a better steering of the process conditions, rendering them thermodynamically more favorable. Besides design improvements for the reactor system presented here, the MES technology would also benefit from the further development of electrode materials and selection or modification of the homoacetogenic biocatalysts. These steps will result in higher production rates, necessary to increase the economic viability of the technology.

Another CO_2 conversion technique, syngas fermentation, now results in a dilute ethanol stream. This study aimed at increasing the product value of this stream. Instead of distillation, chain elongation of this syngas fermentation effluent has been shown to be a good and efficient way to do this. Addition of yeast extract was not necessary, which is an important outcome for future technology development. A pure culture of *C. kluyveri* was used as biocatalyst. Caprylic acid was for the first time detected as product of chain elongation for this species. This first continuous bioreactor study with *C. kluyveri* was inconclusive about the advantages and disadvantages of the use of a pure culture for upgrading syngas fermentation effluent. Mixed cultures will in any case remain the best choice for the conversion of complex biomass streams. For chain elongation too, *in-situ* product recovery is an efficient strategy to avoid product inhibition and, to concentrate and purify the products, caproic and caprylic acid.

When developing the sustainable technologies of the future, it is important to be aware of the market. Fermentation technology is not the only new production route, and will compete with other technologies for the market of CO_2-based products. Conversion of the fermentation products acetic and caproic acid to chemicals with a higher market potential, such as ethyl acetate and *n*-decane must be considered. To be competitive, the quality of the products, the

production rates, and cost will be important benchmarks. Legislation will be a crucial factor to aid the development of new technologies. Subsidies should not solely take into account the feedstock, but especially the CO_2-emmission reduction achieved.

ABSTRACT - SAMENVATTING

Abstract

Our current economic model highly depends on fossil fuel resources for energy and production of materials. A shift toward a carbon-neutral economy is necessary to decrease the impact of the usage of fossil fuel resources on climate change. One strategy that will gain importance in the future carbon-neutral economy is carbon capture and utilization. Emitted CO_2 can be directly reused for the production of fuels and materials. Syngas fermentation and microbial electrosynthesis (MES) are emerging as two microbial technologies, for the autotrophic production of organics such as ethanol and acetic acid, respectively. Syngas fermentation relies on H_2 or CO as energy source, while in MES electricity is the driver for microbial metabolism. In the case of CO, microbial production avoids CO_2 emissions after the typical conversion to electric power.

The goal of this research was to contribute to the development of a reactor technology platform for the production of biochemicals , short- and medium-chain carboxylic acids from CO_2. The work focused on three key aspects:

i) A theoretical understanding of primary fermentation. A thermodynamic assessment of bioproduction systems, especially the electricity-driven systems, was performed to gain a better understanding in losses and thermodynamic limits **(Chapter 2)**.

ii) An improvement of the primary autotrophic fermentation. It was hypothesized that an MES system with *in-situ* product extraction would be beneficial in terms of production rates and titers. A new reactor system was thus developed and compared with systems without *in-situ* product extraction **(Chapter 3)**.

iii) The valorization of primary fermentation effluents in a secondary fermentation. To upgrade the low-value ethanol and acetic acid from syngas fermentation, a pure culture continuous bioreactor system was designed for the production of caproic acid **(Chapter 4)**.

A new calculation method was proposed to assess the efficiency of electrode reactions **(Chapter 2)**. This method utilizes the *degree of reduction* as the central parameter for evaluating the overpotential of half-reactions. It was calculated that bioanode reactions generally suffer from lower overpotentials than biocathode reactions. We concluded that this difference is based on the electron transfer mechanisms; while there is a good understanding of how microorganisms can donate electrons to an electrode (the terminal electron acceptor), there is very little understanding of how a cathode can serve as electron donor. Most likely, and although many biocathode studies claim this is not the case, H_2 is formed as an intermediate, and no direct electron transfer takes place. This is an important aspect for MES, as it results in

the production of better electrode materials that have a low overpotential for the production of H_2, but are biocompatible, thus allowing for a rapid uptake of H_2 by the biofilm.

To improve MES, a new reactor system was designed **(Chapter 3)**. The design consisted of a reactor with three compartments and two membranes, and operated with an enriched mixed culture at a fixed current density of 5 A/m². The new reactor design allowed *in-situ* extraction of the produced acetic acid, as acetate, over an anion exchange membrane (AEM). The electric current thus drove three processes in this reactor system: i) the production of acetic acid by homoacetogenic organisms, as is the case in classic reactor systems; ii) the extraction of the charged acetate into the middle compartment over an AEM, thus balancing part of the charge in the system by the extraction of the product; and iii) the acidification of the product stream through the production of protons at the anode; protons that transferred to the middle compartment over a cation exchange membrane (CEM) to balance the charge. A first reactor study resulted in acetic acid production up to a concentration of 13.5 g/L, the highest reported thus far for MES, at an electron efficiency of 61%, a production rate of 20 g/m²/d, and an energy input of 19 kWh/kg acetic acid extracted. In a second study the performance of the system was compared to systems without *in-situ* extraction. It was hypothesized that the reactor with *in-situ* extraction would have: i) a higher production efficiency; ii) a more stable cathode pH; and iii) higher product concentration than the systems without extraction. Two of the three hypotheses were demonstrated: the system with extraction produced acetic acid at an efficiency of 41%, *vs.* 25% and 28% in systems without extraction. The catholyte pH was stable and high in the system with extraction (8.15 ± 0.15), while it dropped several times below 5.50 in systems without extraction. Addition of NaOH was required to balance the pH. Due to a water flux from the cathode to the extraction compartment, the concentration of acetic acid was limited to 9 g/L, while a concentration of 10.5 g/L was in a classic reactor configuration with two compartments and a CEM. However, the stable pH in the reactor with *in-situ* extraction allowed for a stable production, unhindered by production inhibition, and the production of a clean acetic acid stream that could be directly upgraded to ethyl acetate in a water excluding solvent such as an ionic liquid. The key challenges for this reactor technology are: i) decreasing the energy input for the production of acetic acid; ii) increasing the extraction efficiency (now limited to 12.5% of the charge balancing); and iii) increasing the production rates. In **Chapter 5**, several strategies were proposed for this, including the use of an external fermenter to which the electrochemical system could be coupled.

Acetic acid and ethanol, the two major products of autotrophic fermentation, have a low market value. Their distillation from an aqueous stream is furthermore energy intensive. In **Chapter 3** and **Chapter 5**, esterification was proposed as strategy to upgrade acetic acid produced *via* MES. For syngas fermentation effluent, a different route was developed in **Chapter**

4. For the first time, a pure culture of *C. kluyveri*, a known chain elongating organism, was used as biocatalyst in a continuous reactor study, for the conversion of ethanol and acetic acid to caproic and caprylic acid. A system with and without membrane-based liquid-liquid extraction (pertraction) were compared, both with synthetic medium and real medium. Pertraction requires a low operating pH (5.50), but it was found that this pH is detrimental to *C. kluyveri*. The organic loading rate of the system was gradually increased from 6 g COD/L/d to 15 g COD/L/d. The ethanol/acetic acid ratio of the synthetic medium was changed from 10/1 at the beginning of the test (a usual outcome of syngas fermentation), to 3/1 at the end of the test, to match with the ratio of the syngas fermentation effluent available. Operation on synthetic medium resulted in caproic acid production rates as high as 40 mM/d at a loading rate of 15 g COD/L/d, which corresponds to a conversion efficiency into caproic acid of 65%. No differences in performance were found between the system with and without pertraction, but it is expected that at a higher loading rate, the toxicity of the produced carboxylic acids would render an extraction system essential. Two additional findings from this research are highlighted. First, it was found that the conversion of syngas fermentation effluent by *C. kluyveri* does not require the addition of yeast extract as source of growth factors, which can substantially decrease operating costs. Second, for the first time, caprylic acid production by *C. kluyveri* was shown. While the specificity toward caprylic acid was limited to a maximum of about 10% of the input carbon, the production of this compound was not yet steered. To increase the general reactor performance, an acid-tolerant pure culture should be used for upgrading syngas fermentation effluent at high rate.

This thesis showed the potential of microbial platforms to produce biochemicals from CO_2. In **Chapter 5**, the challenges to bring these products on the market were discussed. High production rates must be obtained, and it is important to target products with a high market value. In that perspective, an *in-situ* extraction coupled to a chemical modification to a product that can be obtained at high titer and selectivity, is the most likely route for CO_2 based bioproduction. Pilot scale studies now have to show the potential of the different bioproduction routes. Next, legislation will play an important role in creating a stable investment climate, and a fair subsidy system for bioproducts produced from CO_2.

Samenvatting

Het huidig economisch model is sterk afhankelijk van fossiele grondstoffen voor energie en de productie van materialen. Een verschuiving naar een koolstof-neutrale economie is noodzakelijk om de impact van het gebruik van fossiele brandstoffen op het klimaat in te dijken. Een strategie die aan belang zal winnen in de toekomstige koolstof-neutrale economie is het kortsluiten van CO_2 kringlopen door "carbon capture and utilization": het opvangen en direct hergebruiken van CO_2. Uitgestote CO_2 kan direct hergebruikt worden voor de productie van brandstoffen en materialen. Syngasfermentatie en microbiële elektrosynthese (MES) zijn als microbiële productiestrategieën op de voorgrond aan het treden voor de autotrofe productie van organische moleculen zoals respectievelijk ethanol en azijnzuur. Syngas fermentatie gebruikt H_2 of CO als energiebron, terwijl elektriciteit de drijver is voor het microbieel metabolisme in MES. In het geval CO wordt gebruikt als energiebron, vermijdt men door microbiële productie de uitstoot van CO_2 die plaatsvindt na de conventionele conversie van CO naar elektrische energie.

Het doel van dit thesiswerk was bij te dragen aan de ontwikkeling van een reactortechnologie platform voor de productie van biochemicaliën, korte- en middellange-keten carbonzuren uit CO_2. Het werk focuste op drie belangrijke aspecten:

i) Een theoretisch begrip van primaire fermentaties. Hiervoor werd een thermodynamische beoordeling van bioproductiesystemen, in het bijzonder van elektriciteits-gedreven systemen, uitgevoerd om een beter inzicht te verwerven in de verliezen en thermodynamische limieten **(Hoofdstuk 2)**.

ii) Een verbetering van de primaire, autotrofe fermentatie. Er werd verondersteld dat een MES systeem met *in-situ* productextractie voordelig zou zijn in termen van productiesnelheden en productconcentraties. Een nieuw reactorsysteem werd dus ontworpen en getest in vergelijking met systemen zonder *in-situ* extractie **(Hoofdstuk 3)**.

iii) De opwaardering van effluent van primaire fermentaties in een secundaire fermentatie. Om de laagwaardige ethanol en azijnzuur afkomstig van syngasfermentatie op te waarderen, werd een pure cultuur, continu bioreactorsysteem ontworpen voor de productie van capronzuur **(Hoofdstuk 4)**.

Een nieuwe berekeningsmethode werd voorgesteld, om de efficiëntie van elektrodereacties te bepalen **(Hoofdstuk 2)**. Deze methode gebruikt de *reductiegraad* als centrale parameter voor de evaluatie van overpotentialen van halfreacties. Er werd berekend dat verliezen algemeen beperkter zijn voor bioanodes dan voor biokathodes. Er werd geconcludeerd dat dit verschil een gevolg is van het elektron transfer mechanisme. Het is al beschreven hoe micro-organismen elektronen kunnen overdragen op een elektrode (die dienst doet als terminale

elektronacceptor), maar er is weinig inzicht over hoe een kathode als elektrondonor kan optreden. Hoewel heel wat studies een vorm van directe elektron transfer claimen, wordt waarschijnlijk H_2 gevormd als intermediair. Dit is een belangrijk aspect voor MES, omdat het kan resulteren in de productie van betere kathodematerialen, die een lage overpotentiaal hebben voor de productie van H_2, maar uit een biocompatibel materiaal vervaardigd zijn om biofilmvorming, en dus een snelle opname van H_2, te verzekeren.

Om MES te verbeteren werd een nieuw reactorsysteem ontworpen **(Hoofdstuk 3)**. Een reactor met drie compartimenten en twee membranen werd ontworpen en geopereerd met een aangerijkte mengcultuur aan een vaste stroomdensiteit van 5 A/m². Het nieuwe design laat *in-situ* extractie van het geproduceerde azijnzuur toe, als acetaat, over een anion uitwisselingsmembraan. De elektrische stroom dreef dus 3 verschillende processen: i) de productie van azijnzuur door homoacetogene micro-organismen, zoals ook het geval is in klassieke reactorsystemen; ii) de extractie van de geladen acetaat moleculen naar het middencompartiment over een anion uitwisselingsmembraan, waarbij de ladingsbalans gedeeltelijk hersteld werd door acetaat transfer; en iii) de verzuring van de productstroom door productie van protonen aan de anode, die naar het middencompartiment werden getransporteerd over een kationuitwisselingsmembraan om de ladingsbalans te herstellen. Een eerste reactorstudie resulteerde in de productie van azijnzuur tot een concentratie van 13.5 g/L, de hoogst gerapporteerde voor MES, aan een elektronenefficiëntie van 61%, een productiesnelheid van 20 g/m²/d, en een energie-input van 19 kWh/kg geëxtraheerd azijnzuur. In een tweede studie werd de prestatie van het nieuwe ontwerp vergeleken met systemen zonder *in-situ* extractie. Er werd verondersteld dat de reactor met *in-situ* extractie: i) een hogere productie-efficiëntie; ii) een stabielere katholyt-pH; en iii) hogere productconcentratie zou opleveren dan systemen zonder extractie. Twee van de drie hypotheses werden aangetoond. Het systeem met extractie produceerde azijnzuur aan een efficiëntie van 41%, *vs.* 25% en 28% in systemen zonder extractie. De pH van het katholyt was stabiel en relatief hoog in het systeem met extractie (8.15 ± 0.15), maar daalde meerdere keren onder de 5.50 in systemen zonder extractie. Dosering van NaOH was nodig om de pH te stabiliseren. Omwille van een waterflux van de kathode naar het extractiecompartiment, was de concentratie azijnzuur beperkt tot 9 g/L, waar een concentratie van 10.5 g/L werd bereikt in een klassiek reactorsysteem met twee compartimenten en een kation uitwisselingsmembraan. De stabiele pH in het systeem met *in-situ* extractie liet echter een stabiele productie toe, ongehinderd door productinhibitie, en de productie van een zuivere azijnzuurstroom, die meteen kon opgewaardeerd worden naar ethylacetaat door verestering in een ionische vloeistof. De belangrijkste uitdagingen voor deze reactortechnologie zijn nu: i) het verlagen van de energie-input voor de productie van azijnzuur; ii) het verhogen van de extractie-efficiëntie voor azijnzuur (nu beperkt tot 12.5% van de

ladingsbalans); en iii) het verhogen van de productiesnelheden. In **Hoofdstuk 5** werden verschillende strategieën voorgesteld om dit te bereiken, waaronder het gebruik van een externe fermenter waaraan de elektrochemische cel zou kunnen worden gekoppeld.

Azijnzuur en ethanol, de twee belangrijkste producten van autotrofe fermentaties, hebben een lage marktwaarde. Het distilleren van deze producten uit een waterige stroom is bovendien energie-intensief. In **Hoofdstuk 3** en **Hoofdstuk 5** werd verestering voorgesteld als strategie om laagwaardig azijnzuur uit MES op te waarderen. Voor syngas fermentatie effluent werd een andere route ontwikkeld in **Hoofdstuk 4**. Een pure cultuur van *C. kluyveri* werd voor de eerste maal gebruikt als biokatalysator in een continu reactorsysteem, voor de omzetting van ethanol en azijnzuur in capronzuur en caprylzuur. Een systeem met en zonder membraan- gebaseerde vloeistof-vloeistof extractie (pertractie) werden vergeleken, zowel met synthetisch medium, als syngas fermentatie effluent. Pertractie vereist een lage reactor-pH (5.50), maar er werd vastgesteld dat deze pH nadelig is voor *C. kluyveri*. De organische belasting werd gradueel verhoogd van 6 g CZV/L/d naar 15 g CZV/L/d. De ethanol/azijnzuur ratio van het synthetische medium veranderde van 10/1 bij de start van de test (een typische ratio voor syngas fermentatie effluent), naar 3/1 op het einde van de test, de ratio in het beschikbare syngas fermentatie effluent. Dit resulteerde in capronzuur productiesnelheden tot 40 mM/d met synthetisch medium (15 g CZV/L/d), wat overeenkomt met een conversie-efficiëntie van 65%. Er was geen verschil in prestatie tussen het systeem met en zonder pertractie, maar er wordt verondersteld dat bij een hogere organische belasting een extractiesysteem essentieel zou worden om de toxiciteit van de gevormde vetzuren te elimineren. Twee bijkomende vaststellingen van dit onderzoek worden uitgelicht. Ten eerste werd aangetoond dat toevoeging van gistextract aan syngas fermentatie effluent niet nodig is voor ketenverlenging met *C. kluyveri*, wat de bedrijfskosten substantieel kan verlagen. Ten tweede werd voor de eerste keer productie van caprylzuur door een pure cultuur van *C. kluyveri* aangetoond. De specificiteit van caprylzuur productie bedroeg maximaal 10%, maar was niet gestuurd om die productie te maximaliseren. Om de algemene performantie van de reactor te verhogen zou een zuur-tolerante pure cultuur moeten worden gebruikt voor het opwaarderen van syngas fermentatie effluent aan hoge productiesnelheden.

Deze doctoraatsthesis toonde het potentieel aan van microbiële platformen voor de productie van biochemicaliën uit CO_2. In **Hoofdstuk 5** werden de uitdagingen om deze producten op de markt te brengen besproken. Hoge productiesnelheden moeten worden gehaald, en het is van belang producten met een hoge marktwaarde te selecteren. In dat perspectief is een *in-situ* extractie gekoppeld aan een chemische modificatie tot een product dat aan hoge concentratie en selectiviteit kan worden bekomen, de meest waarschijnlijke route voor CO_2 gebaseerde bioproductie. Pilootschaal studies moeten nu het potentieel van de verschillende routes

aanonen. Vervolgens zal een wetgevend kader een belangrijke rol spelen in het creëren van een stabiel investeringsklimaat en een billijk subsidiesysteem voor biochemicaliën geproduceerd uit CO_2.

BIBLIOGRAPHY

Agler, M., Spirito, C., Usack, J., Werner, J., Angenent, L. 2014. Development of a highly specific and productive process for *n*-caproic acid production: applying lessons from methanogenic microbiomes. *Water Science & Technology*, **69**(1), 62-68.

Agler, M.T., Wrenn, B.A., Zinder, S.H., Angenent, L.T. 2011. Waste to bioproduct conversion with undefined mixed cultures: the carboxylate platform. *Trends in biotechnology*, **29**(2), 70-78.

Agler, M.T., Spirito, C.M., Usack, J.G., Werner, J.J., Angenent, L.T. 2012. Chain elongation with reactor microbiomes: upgrading dilute ethanol to medium-chain carboxylates. *Energy & Environmental Science*, **5**(8), 8189-8192.

Alberty, R.A. 2003. *Thermodynamics of biochemical reactions*. John Wiley & Sons, New York.

Alberty, R.A. 2006. Thermodynamic properties of weak acids involved in enzyme-catalyzed reactions. *The Journal of Physical Chemistry B*, **110**(10), 5012-5016.

Albrecht, J., Laleman, R. 2015. Hoe sterk stijgt de CO_2-uitstoot na de kernuitstap?, Universiteit Gent.

Amend, J.P., Shock, E.L. 2001. Energetics of overall metabolic reactions of thermophilic and hyperthermophilic archaea and bacteria. *FEMS Microbiology Review*, **25**(2), 175-243.

Andersen, S.J., Hennebel, T., Gildemyn, S., Coma, M., Desloover, J., Berton, J., Tsukamoto, J., Stevens, C., Rabaey, K. 2014. Electrolytic membrane extraction enables production of fine chemicals from biorefinery sidestreams. *Environmental Science & Technology*, **48**(12), 7135-7142.

Andersen, S.J., Candry, P., Basadre, T., Khor, W.C., Roume, H., Hernandez-Sanabria, E., Coma, M., Rabaey, K. 2015. Electrolytic extraction drives volatile fatty acid chain elongation through lactic acid and replaces chemical pH control in thin stillage fermentation. *Biotechnology for biofuels*, **8**(1).

Andersen, S.J., Berton, J.K.E.T., Naert, P., Gildemyn, S., Rabaey, K., Stevens, C.V. 2016. Extraction and Esterification of Low-Titer Short-Chain Volatile Fatty Acids from Anaerobic Fermentation with Ionic Liquids. *ChemSusChem*, **9**(16), 2059-2063.

Angenent, L.T., Karim, K., Al-Dahhan, M.H., Wrenn, B.A., Domiguez-Espinosa, R. 2004. Production of bioenergy and biochemicals from industrial and agricultural wastewater. *Trends Biotechnol.*, **22**(9), 477-485.

Angenent, L.T., Richter, H., Buckel, W., Spirito, C.M., Steinbusch, K.J.J., Plugge, C.M., Strik, D.P.B.T.B., Grootscholten, T.I.M., Buisman, C.J.N., Hamelers, H.V.M. 2016. Chain elongation with reactor microbiomes: open-culture biotechnology to produce biochemicals. *Environmental Science & Technology*, **50**(6), 2796-2810.

Arends, J.B.A., Desloover, J., Puig, S., Verstraete, W. 2012. Principles and technology of microbial fuel cells. *Fuel Cell Science and Engineering: Materials, Processes, Systems and Technology*, 147-184.

Arends, J.B.A., Verstraete, W. 2012. 100 years of microbial electricity production: three concepts for the future. *Microbial Biotechnology*, **5**(3), 333-346.

Aresta, M., Dibenedetto, A., Angelini, A. 2013. Catalysis for the valorization of exhaust carbon: From CO_2 to chemicals, materials, and fuels. Technological use of CO_2. *Chemical reviews*, **114**(3), 1709-1742.

Atkins, P., De Paula, J. 2012. *Elements of physical chemistry*. Oxford University Press.

Aulenta, F., Canosa, A., Reale, P., Rossetti, S., Panero, S., Majone, M. 2009. Microbial reductive dechlorination of trichloroethene to ethene with electrodes serving as electron donors without the external addition of redox mediators. *Biotechnology and Bioengineering*, **103**(1), 85-91.

Aulenta, F., Tocca, L., Reale, P., Rossetti, S., Majone, M. 2010. Bioelectrochemical dechlorination of trichloroethene: From electron transfer mechanisms to process scale-up. *Journal of Biotechnology*, **150**(Supplement 1), 34-35.

Bagastyo, A.Y., Radjenovic, J., Mu, Y., Rozendal, R.A., Batstone, D.J., Rabaey, K. 2011. Electrochemical oxidation of reverse osmosis concentrate on mixed metal oxide (MMO) titanium coated electrodes. *Water Research*, **45**(16), 4951-4959.

Balch, W.E., Fox, G., Magrum, L., Woese, C., Wolfe, R. 1979. Methanogens: reevaluation of a unique biological group. *Microbiological reviews*, **43**(2), 260-296.

Bard, A.J., Parsons, R., Jordan, J. 1985. Standard potentials in aqueous solution, Marcel Dekker. New York.

Bard, A.J., Faulkner, L.R. 2001. *Electrochemical methods: fundamentals and applications*. *2nd ed*. John Wiley & Sons, New York.

Barker, H., Taha, S. 1942. *Clostridium kluyverii*, an organism concerned in the formation of caproic acid from ethyl alcohol. *Journal of bacteriology*, **43**(3), 347-363.

Barker, H., Kamen, M., Bornstein, B. 1945. The synthesis of butyric and caproic acids from ethanol and acetic acid by *Clostridium kluyveri*. *Proceedings of the National Academy of Sciences*, **31**(12), 373-381.

Batlle-Vilanova, P., Puig, S., Gonzalez-Olmos, R., Balaguer, M.D., Colprim, J. 2015. Continuous acetate production through microbial electrosynthesis from CO_2 with microbial mixed culture. *Journal of Chemical Technology and Biotechnology*, **91**(4), 921-927.

Berg, I.A., Kockelkorn, D., Ramos-Vera, W.H., Say, R.F., Zarzycki, J., Hügler, M., Alber, B.E., Fuchs, G. 2010. Autotrophic carbon fixation in archaea. *Nature Reviews Microbiology*, **8**(6), 447-460.

Bertsch, J., Müller, V. 2015. Bioenergetic constraints for conversion of syngas to biofuels in acetogenic bacteria. *Biotechnology for biofuels*, **8**(1), 1.

Blanchet, E., Duquenne, F., Rafrafi, Y., Etcheverry, L., Erable, B., Bergel, A. 2015. Importance of the hydrogen route in up-scaling electrosynthesis for microbial CO_2 reduction. *Energy & Environmental Science*, **8**(12), 3731-3744.

Block, M., Spiegler, K.S. 1963. Transport of Bicarbonate, Carbonate, and Chloride Ions through Ion Exchange Membranes. *Journal of The Electrochemical Society*, **110**(6), 577-580.

Bond, D.R., Lovley, D.R. 2003. Electricity production by *Geobacter sulfurreducens* attached to electrodes. *Applied and Environmental Microbiology*, **69**(3), 1548-1555.

BP. 2012. Statistical Review of World Energy.

BP. 2015. Statistical Review of World Energy.

Bretschger, O., Gorby, Y.A., Nealson, K. 2010. A survey of direct electron transfer transfer from microbes to electronically active surfaces. in: *Bioelectrochemical systems: from extracellular electron transfer to biotechnological application*, (Eds.) K. Rabaey, L.T. Angenent, U. Schroder, J. Keller, IWA Publishing. London, UK, pp. 81-100.

Breznak, J.A., Switzer, J.M. 1986. Acetate synthesis from H_2 plus CO_2 by termite gut microbes. *Applied and Environmental Microbiology*, **52**(4), 623-630.

Buckel, W., Thauer, R.K. 2013. Energy conservation via electron bifurcating ferredoxin reduction and proton/Na^+ translocating ferredoxin oxidation. *Biochimica et Biophysica Acta Bioenergetics*, **1827**(2), 94-113.

Butler, C.S., Clauwaert, P., Green, S.J., Verstraete, W., Nerenberg, R. 2010. Bioelectrochemical perchlorate reduction in a microbial fuel cell. *Environ. Sci. Technol.*, **44**(12), 4685-4691.

Chaudhuri, S.K., Lovley, D.R. 2003. Electricity generation by direct oxidation of glucose in mediatorless microbial fuel cells. *Nature biotechnology*, **21**(10), 1229-1232.

Chen, S., He, G., Liu, Q., Harnisch, F., Zhou, Y., Chen, Y., Hanif, M., Wang, S., Peng, X., Hou, H. 2012. Layered corrugated electrode macrostructures boost microbial bioelectrocatalysis. *Energy & Environmental Science*, **5**(12), 9769-9772.

Cheng, S., Logan, B.E. 2007. Sustainable and efficient biohydrogen production via electrohydrogenesis. *Proceedings of the National Academy of Sciences*, **104**(47), 18871-18873.

Cheng, S.A., Xing, D.F., Call, D.F., Logan, B.E. 2009. Direct biological conversion of electrical current into methane by electromethanogenesis. *Environmental Science & Technology*, **43**(10), 3953-3958.

Choi, S., Song, C.W., Shin, J.H., Lee, S.Y. 2015. Biorefineries for the production of top building block chemicals and their derivatives. *Metabolic Engineering*, **28**, 223-239.

Clark, B. 2015. Acetic Acid. *ICIS Chemical Business*, **2-8 March**, 34.

Clarke, K.G., Hansford, G.S., Jones, D.T. 1988. Nature and significance of oscillatory behavior during solvent production by *Clostridium acetobutylicum* in continuous culture. *Biotechnology and Bioengineering*, **32**(4), 538-544.

Clauwaert, P., Rabaey, K., Aelterman, P., De Schamphelaire, L., Ham, T.H., Boeckx, P., Boon, N., Verstraete, W. 2007a. Biological denitrification in microbial fuel cells. *Environmental Science & Technology*, **41**(9), 3354-3360.

Clauwaert, P., Van der Ha, D., Boon, N., Verbeken, K., Verhaege, M., Rabaey, K., Verstraete, W. 2007b. Open air biocathode enables effective electricity generation with microbial fuel cells. *Environmental Science & Technology*, **41**(21), 7564-7569.

Clauwaert, P., Aelterman, P., Pham, T.H., De Schamphelaire, L., Carballa, M., Rabaey, K., Verstraete, W. 2008a. Minimizing losses in bio-electrochemical systems: the road to applications. *Applied Microbiology and Biotechnology*, **79**(6), 901-913.

Clauwaert, P., Tolêdo, R., Van der Ha, D., Crab, R., Verstraete, W., Hu, H., Udert, K.M., Rabaey, K. 2008b. Combining biocatalyzed electrolysis with anaerobic digestion. *Water Science and Technology*, **57**(4), 575-579.

Coma, M., Puig, S., Pous, N., Balaguer, M.D., Colprim, J. 2013. Biocatalysed sulphate removal in a BES cathode. *Bioresource technology*, **130**, 218-223.

Costentin, C., Robert, M., Savéant, J.-M. 2013. Catalysis of the electrochemical reduction of carbon dioxide. *Chemical Society Reviews*, **42**(6), 2423-2436.

CRI. Carbon Recycling International. http://carbonrecycling.is/. 2016, May 30th

Daniell, J., Köpke, M., Simpson, S.D. 2012. Commercial biomass syngas fermentation. *Energies*, **5**(12), 5372-5417.

Daniell, J., Nagaraju, S., Burton, F., Köpke, M., Simpson, S.D. 2016. Low-carbon fuel and chemical production by anaerobic gas fermentation, Springer Berlin Heidelberg. Berlin, Heidelberg, pp. 1-29.

Danks, M.A. 2012. Gut-retention time in mycophagous mammals: a review and a study of truffle-like fungal spore retention in the swamp wallaby. *Fungal Ecology*, **5**(2), 200-210.

Datar, R.P., Shenkman, R.M., Cateni, B.G., Huhnke, R.L., Lewis, R.S. 2004. Fermentation of biomass-generated producer gas to ethanol. *Biotechnology and Bioengineering*, **86**(5), 587-594.

Dawson, T.J., Hulbert, A. 1970. Standard metabolism, body temperature, and surface areas of Australian marsupials. *American Journal of Physiology--Legacy Content*, **218**(4), 1233-1238.

De Guzman, D. 2011. Aviation industry aims to use more alternative fuel. *ICIS Chemical Business*, **November 21 - December 4**, 22.

De Roy, K., Clement, L., Thas, O., Wang, Y., Boon, N. 2012. Flow cytometry for fast microbial community fingerprinting. *Water Research*, **46**(3), 907-919.

Deloitte. Opportunities for the fermentation-based chemical industry: an analysis of the market potential and competitiveness of North-West Europe. http://www2.deloitte.com/global/en/pages/manufacturing/articles/opportunities-for-fermentation-based-chemical-industry.html. 2016, April 12th

Demler, M., Weuster-Botz, D. 2011. Reaction engineering analysis of hydrogenotrophic production of acetic acid by *Acetobacterium woodii*. *Biotechnology and Bioengineering*, **108**(2), 470-474.

Dennis, P.G., Harnisch, F., Yeoh, Y.K., Tyson, G.W., Rabaey, K. 2013. Dynamics of cathode-associated microbial communities and metabolite profiles in a glycerol-fed bioelectrochemical system. *Applied and Environmental Microbiology*, **79**(13), 4008-4014.

Desloover, J., Puig, S., Virdis, B., Clauwaert, P., Boeckx, P., Verstraete, W., Boon, N. 2011. Biocathodic nitrous oxide removal in bioelectrochemical systems. *Environmental Science & Technology*, **45**(24), 10557-10566.

Desloover, J., Abate Woldeyohannis, A., Verstraete, W., Boon, N., Rabaey, K. 2012a. Electrochemical resource recovery from digestate to prevent ammonia toxicity during anaerobic digestion. *Environmental Science & Technology*, **46**(21), 12209-12216.

Desloover, J., Arends, J.B.A., Hennebel, T., Rabaey, K. 2012b. Operational and technical considerations for microbial electrosynthesis. *Biochemical Society Transactions*, **40**(6), 1233-1238.

Desloover, J., De Vrieze, J., Van de Vijver, M., Mortelmans, J., Rozendal, R., Rabaey, K. 2015. Electrochemical nutrient recovery enables ammonia toxicity control and biogas desulfurization in anaerobic digestion. *Environmental Science & Technology*, **49**(2), 948-955.

Deutzmann, J.S., Sahin, M., Spormann, A.M. 2015. Extracellular enzymes facilitate electron uptake in biocorrosion and bioelectrosynthesis. *MBio*, **6**(2), e00496-15.

Devi, S.M., Kim, I. 2014. Effect of medium chain fatty acids (MCFA) and probiotic (*Enterococcus faecium*) supplementation on the growth performance, digestibility and blood profiles in weanling pigs. *Veterinarni Medicina*, **59**(11), 527-535.

Diender, M., Stams, A.J., Sousa, D.Z. 2016. Production of medium-chain fatty acids and higher alcohols by a synthetic co-culture grown on carbon monoxide or syngas. *Biotechnology for biofuels*, **9**(82).

Długołęcki, P., Nymeijer, K., Metz, S., Wessling, M. 2008. Current status of ion exchange membranes for power generation from salinity gradients. *Journal of Membrane Science*, **319**(1), 214-222.

DOE. U.S. Department of energy, energy efficiency and renewable energy. www.fueleconomy.gov. 2016, May 22th

Dolfing, J., Janssen, D.B. 1994. Estimates of Gibbs free energies of formation of chlorinated aliphatic compounds. *Biodegradation*, **5**(1), 21-28.

Dolfing, J., Xu, A.P., Head, I.M. 2010. Anomalous energy yields in thermodynamic calculations: importance of accounting for pH-dependent organic acid speciation. *ISME J.*, **4**(4), 463-464.

Dolfing, J. 2014. Thermodynamic constraints on syntrophic acetate oxidation. *Applied and Environmental Microbiology*, **80**(4), 1539-1541.

Dominguez-Faus, R., Powers, S.E., Burken, J.G., Alvarez, P.J. 2009. The water footprint of biofuels: A drink or drive issue? *Environmental Science & Technology*, **43**(9), 3005-3010.

Donovan, C., Dewan, A., Heo, D., Lewandowski, Z., Beyenal, H. 2013. Sediment microbial fuel cell powering a submersible ultrasonic receiver: New approach to remote monitoring. *Journal of Power Sources*, **233**, 79-85.

Drake, H.L., Küsel, K., Matthies, C. 2006. Acetogenic prokaryotes. in: *The prokaryotes*, Springer, pp. 354-420.

Drake, H.L., Gößner, A.S., Daniel, S.L. 2008. Old acetogens, new light. *Annals of the New York Academy of Sciences*, **1125**(1), 100-128.

Duboc, P., von Stockar, U. 1998. Systematic errors in data evaluation due to ethanol stripping and water vaporization. *Biotechnology and bioengineering*, **58**(4), 428-439.

Dunn, B., Kamath, H., Tarascon, J.-M. 2011. Electrical energy storage for the grid: a battery of choices. *Science*, **334**(6058), 928-935.

Dürre, P. 2014. Physiology and sporulation in Clostridium. *Microbiology spectrum*, **2**(4), TBS-0010-2012.

Dürre, P., Eikmanns, B.J. 2015. C1-carbon sources for chemical and fuel production by microbial gas fermentation. *Current Opinion in Biotechnology*, **35**, 63-72.

EC. Strategic energy technologies information system. setis.ec.europa.eu/. 2016, May 24th

EC. Climate Action. http://ec.europa.eu/clima/policies/transport/aviation/index_en.htm. 2016, May 25th

EC. 2016c. Carbon Capture Utilisation and Storage. in: *SETIS Magazine*, Vol. 11, European Commission.

Ecoinvent. 2007. Life cycle inventories of chemicals v2.0. Swiss Center for Life Cycle Inventories.

Ellis, V. 2016. Ethanol. *ICIS Chemical Business*, **9-15 May**, 35.

EPA. Global greenhouse gas emissions. https://www3.epa.gov/climatechange/science/indicators/ghg/global-ghg-emissions.html. 2016, April 19th

Feng, C.H., Li, F.B., Mai, H.J., Li, X.Z. 2010. Bio-electro-fenton process driven by microbial fuel cell for wastewater treatment. *Environmental Science & Technology*, **44**(5), 1875-1880.

Fornero, J.J., Rosenbaum, M., Cotta, M.A., Angenent, L.T. 2008. Microbial Fuel Cell Performance with a Pressurized Cathode Chamber. *Environmental Science & Technology*.

Fornero, J.J., Rosenbaum, M., Cotta, M.A., Angenent, L.T. 2010. Carbon Dioxide Addition to Microbial Fuel Cell Cathodes Maintains Sustainable Catholyte pH and Improves Anolyte pH, Alkalinity, and Conductivity. *Environmental Science & Technology*, **44**(7), 2728-2734.

Freguia, S., Rabaey, K., Yuan, Z., Keller, J. 2007. Electron and carbon balances in microbial fuel cells reveal temporary bacterial storage behavior during electricity generation. *Environmental Science & Technology*, **41**(8), 2915-2921.

Freguia, S., Rabaey, K., Yuan, Z., Keller, J. 2008. Syntrophic processes drive the conversion of glucose in microbial fuel cell anodes. *Environmental Science & Technology*, **42**(21), 7937-7943.

Frost, Sullivan. 2008. Global commercial aviation alternative fuel market: A strategic overview

Ganigué, R., Puig, S., Batlle-Vilanova, P., Balaguer, M., Colprim, J. 2015. Microbial electrosynthesis of butyrate from carbon dioxide. *Chemical Communications*, **51**(15), 3235-3238.

Gao, S., Lin, Y., Jiao, X., Sun, Y., Luo, Q., Zhang, W., Li, D., Yang, J., Xie, Y. 2016. Partially oxidized atomic cobalt layers for carbon dioxide electroreduction to liquid fuel. *Nature*, **529**(7584), 68-71.

Gapes, J.R., Nimcevic, D., Friedl, A. 1996. Long-term continuous cultivation of *Clostridium beijerinckii* in a two-stage chemostat with on-line solvent removal. *Applied and Environmental Microbiology*, **62**(9), 3210-3219.

Ge, S., Usack, J.G., Spirito, C.M., Angenent, L.T. 2015. Long-term *n*-caproic acid production from yeast-fermentation beer in an anaerobic bioreactor with continuous product extraction. *Environmental Science & Technology*, **49**(13), 8012-8021.

Geelhoed, J.S., Stams, A.J.M. 2011. Electricity-assisted biological hydrogen production from acetate by *Geobacter sulfurreducens*. *Environmental Science & Technology*, **45**(2), 815-820.

Ghyselbrecht, K., Huygebaert, M., Van der Bruggen, B., Ballet, R., Meesschaert, B., Pinoy, L. 2013. Desalination of an industrial saline water with conventional and bipolar membrane electrodialysis. *Desalination*, **318**, 9-18.

Giddings, C.G., Nevin, K.P., Woodward, T., Lovley, D.R., Butler, C.S. 2015. Simplifying microbial electrosynthesis reactor design. *Frontiers in microbiology*, **6**(468).

Gildemyn, S., Luther, A.K., Andersen, S.J., Desloover, J., Rabaey, K. 2015a. Electrochemically and bioelectrochemically induced ammonium recovery. *JoVE*(95), e52405.

Gildemyn, S., Verbeeck, K., Slabbinck, R., Andersen, S.J., Prévoteau, A., Rabaey, K. 2015b. Integrated production, extraction, and concentration of acetic acid from CO_2 through microbial electrosynthesis. *Environmental Science & Technology Letters*, **2**(11), 325-328.

Gong, Y., Ebrahim, A., Feist, A.M., Embree, M., Zhang, T., Lovley, D., Zengler, K. 2012. Sulfide-driven microbial electrosynthesis. *Environmental Science & Technology*, **47**(1), 568-573.

Gonzalez-Cabaleiro, R., Lema, J.M., Rodriguez, J., Kleerebezem, R. 2013. Linking thermodynamics and kinetics to assess pathway reversibility in anaerobic bioprocesses. *Energy & Environmental Science*, **6**(12), 3780-3789.

Gorby, Y.A., Yanina, S., McLean, J.S., Rosso, K.M., Moyles, D., Dohnalkova, A., Beveridge, T.J., Chang, I.S., Kim, B.H., Kim, K.S. 2006. Electrically conductive bacterial nanowires produced by *Shewanella oneidensis* strain MR-1 and other microorganisms. *Proceedings of the National Academy of Sciences*, **103**(30), 11358-11363.

Graedel, T.E., Harper, E.M., Nassar, N.T., Nuss, P., Reck, B.K. 2015. Criticality of metals and metalloids. *Proceedings of the National Academy of Sciences*, **112**(14), 4257-4262.

Graves, T., Narendranath, N.V., Dawson, K., Power, R. 2006. Effect of pH and lactic or acetic acid on ethanol productivity by *Saccharomyces cerevisiae* in corn mash. *Journal of Industrial Microbiology and Biotechnology*, **33**(6), 469-474.

Greenberg, A.E., Clesceri, L.S., Eaton, A.D. 1992. *Standard methods for the examination of water and wastewater*. American Public Health Association.

Greening, R., Leedle, J. 1989. Enrichment and isolation of *Acetitomaculum ruminis, gen. nov., sp. nov.*: acetogenic bacteria from the bovine rumen. *Archives of microbiology*, **151**(5), 399-406.

GreentechMedia. LanzaTech, a waste-gas-to-fuel startup, tops off a $112M funding round. http://www.greentechmedia.com/articles/read/Can-Lanza-Khosla-Solve-the-Biofuels-Conversion-Riddle. 2016, June 6th

Gregory, K.B., Bond, D.R., Lovley, D.R. 2004. Graphite electrodes as electron donors for anaerobic respiration. *Environmental Microbiology*, **6**(6), 596-604.

Gregory, K.B., Lovley, D.R. 2005. Remediation and recovery of uranium from contaminated subsurface environments with electrodes. *Environmental Science & Technology*, **39**(22), 8943-8947.

Grootscholten, T., dal Borgo, F.K., Hamelers, H., Buisman, C. 2013a. Promoting chain elongation in mixed culture acidification reactors by addition of ethanol. *Biomass and Bioenergy*, **48**, 10-16.

Grootscholten, T.I.M., Steinbusch, K.J.J., Hamelers, H.V.M., Buisman, C.J.N. 2013b. Chain elongation of acetate and ethanol in an upflow anaerobic filter for high rate MCFA production. *Bioresource Technology*, **135**, 440-445.

Grootscholten, T.I.M., Steinbusch, K.J.J., Hamelers, H.V.M., Buisman, C.J.N. 2013c. High rate heptanoate production from propionate and ethanol using chain elongation. *Bioresource Technology*, **136**, 715-718.

Grootscholten, T.I.M., Steinbusch, K.J.J., Hamelers, H.V.M., Buisman, C.J.N. 2013d. Improving medium chain fatty acid productivity using chain elongation by reducing the hydraulic retention time in an upflow anaerobic filter. *Bioresource Technology*, **136**, 735-738.

Guo, K., Donose, B.C., Soeriyadi, A.H., Prévoteau, A., Patil, S.A., Freguia, S., Gooding, J.J., Rabaey, K. 2014a. Flame oxidation of stainless steel felt enhances anodic biofilm formation and current output in bioelectrochemical systems. *Environmental Science & Technology*, **48**(12), 7151-7156.

Guo, K., Soeriyadi, A.H., Patil, S.A., Prévoteau, A., Freguia, S., Gooding, J.J., Rabaey, K. 2014b. Surfactant treatment of carbon felt enhances anodic microbial electrocatalysis in bioelectrochemical systems. *Electrochemistry Communications*, **39**, 1-4.

Hamelers, H.V.M., ter Heijne, A., Stein, N., Rozendal, R.A., Buisman, C.J.N. 2010. Butler-Volmer-Monod model for describing bio-anode polarization curves. *Bioresource Technology*, **102**(1), 381-387.

Harnisch, F., Schröder, U., Scholz, F. 2008. The suitability of monopolar and bipolar ion exchange membranes as separators for biological fuel cells. *Environmental Science & Technology*, **42**(5), 1740-1746.

Harnisch, F., Schröder, U. 2009. Selectivity versus mobility: separation of anode and cathode in microbial bioelectrochemical systems. *ChemSusChem*, **2**(10), 921-926.

Harnisch, F., Rabaey, K. 2012. The diversity of techniques to study electrochemically active biofilms highlights the need for standardization. *Chemsuschem*, **5**(6), 1027-1038.

Havlík, P., Schneider, U.A., Schmid, E., Böttcher, H., Fritz, S., Skalský, R., Aoki, K., Cara, S.D., Kindermann, G., Kraxner, F., Leduc, S., McCallum, I., Mosnier, A., Sauer, T., Obersteiner, M. 2011. Global land-use implications of first and second generation biofuel targets. *Energy Policy*, **39**(10), 5690-5702.

Hays, S., Zhang, F., Logan, B.E. 2011. Performance of two different types of anodes in membrane electrode assembly microbial fuel cells for power generation from domestic wastewater. *Journal of Power Sources*, **196**(20), 8293-8300.

He, W., Zhang, X., Liu, J., Zhu, X., Feng, Y., Logan, B.E. 2016. Microbial fuel cells with an integrated spacer and separate anode and cathode modules. *Environmental Science: Water Research & Technology*, **2**(1), 186-195.

Heidrich, E., Curtis, T., Dolfing, J. 2010. Determination of the internal chemical energy of wastewater. *Environmental Science & Technology*, **45**(2), 827-832.

Heijnen, J.J. 1999. Bioenergetics of microbial growth. in: *Encyclopedia of Bioprocess Technology: Fermentation, Biocatalysis, and Bioseparation*, (Eds.) M.C. Flickinger, S.D. Drew, John Wiley & Sons. Chicester, UK, pp. 267-291.

Heise, R., Müller, V., Gottschalk, G. 1989. Sodium dependence of acetate formation by the acetogenic bacterium *Acetobacterium woodii*. *Journal of bacteriology*, **171**(10), 5473-5478.

Henry, C.S., Broadbelt, L.J., Hatzimanikatis, V. 2007. Thermodynamics-based metabolic flux analysis. *Biophysical journal*, **92**(5), 1792-1805.

Henstra, A.M., Sipma, J., Rinzema, A., Stams, A.J. 2007. Microbiology of synthesis gas fermentation for biofuel production. *Current Opinion in Biotechnology*, **18**(3), 200-206.

Hernandez, M., Newman, D. 2001. Extracellular electron transfer. *Cellular and Molecular Life Sciences CMLS*, **58**(11), 1562-1571.

Holmes, D.E., Chaudhuri, S.K., Nevin, K.P., Mehta, T., Methe, B.A., Liu, A., Ward, J.E., Woodard, T.L., Webster, J., Lovley, D.R. 2006. Microarray and genetic analysis of electron transfer to electrodes in *Geobacter sulfurreducens*. *Environmental Microbiology*, **8**(10), 1805-1815.

Holtzapple, M.T., Granda, C.B. 2009. Carboxylate platform: the MixAlco process part 1: comparison of three biomass conversion platforms. *Applied Biochemistry and Biotechnology*, **156**(1-3), 95-106.

Huang, L., Cheng, S., Chen, G. 2011. Bioelectrochemical systems for efficient recalcitrant wastes treatment. *Journal of Chemical Technology & Biotechnology*, **86**(4), 481-491.

Hungate, R. 1969. A roll tube method for cultivation of strict anaerobes. *Methods in microbiology, 3B*, 117-132.

Hunt, A.J., Sin, E.H.K., Marriott, R., Clark, J.H. 2010. Generation, capture, and utilization of industrial carbon dioxide. *ChemSusChem*, **3**(3), 306-322.

IPCC. 2014. Climate change 2014: Mitigation of climate change. Contribution of working group III to the fifth assessment report of the Intergovernmental Panel on Climate Change.

Jensen, H.M., Albers, A.E., Malley, K.R., Londer, Y.Y., Cohen, B.E., Helms, B.A., Weigele, P., Groves, J.T., Ajo-Franklin, C.M. 2010. Engineering of a synthetic electron conduit in living cells. *Proceedings of the National Academy of Sciences*, **107**(45), 19213-19218.

Jiang, Y., Su, M., Zhang, Y., Zhan, G.Q., Tao, Y., Li, D.P. 2013. Bioelectrochemical systems for simultaneously production of methane and acetate from carbon dioxide at relatively high rate. *International Journal of Hydrogen Energy*, **38**(8), 3497-3502.

Johnston, S.L. 2013. Role of elemental sulfur and polysulfide in corrosion mediated by sulfate reducing bacteria. in: *Department of Biological Sciences*, Vol. Doctor in Philosophy, University of Calgaray. Calgary, Alberta.

Jones, D.T., Woods, D.R. 1986. Acetone-butanol fermentation revisited. *Microbiological reviews*, **50**(4), 484.

Jourdin, L., Freguia, S., Donose, B.C., Chen, J., Wallace, G.G., Keller, J., Flexer, V. 2014. A novel carbon nanotube modified scaffold as an efficient biocathode material for improved microbial electrosynthesis. *Journal of Materials Chemistry A*, **2**(32), 13093-13102.

Jourdin, L., Grieger, T., Monetti, J., Flexer, V., Freguia, S., Lu, Y., Chen, J., Romano, M., Wallace, G.G., Keller, J. 2015. High acetic acid production rate obtained by microbial electrosynthesis from carbon dioxide. *Environmental Science & Technology*, **49**(22), 13566-13574.

Jourdin, L., Freguia, S., Flexer, V., Keller, J. 2016a. Bringing high-rate, CO_2-based microbial electrosynthesis closer to practical implementation through improved electrode design and operating conditions. *Environmental Science & Technology*, **50**(4), 1982-1989.

Jourdin, L., Lu, Y., Flexer, V., Keller, J., Freguia, S. 2016b. Biologically induced hydrogen production drives high rate/high efficiency microbial electrosynthesis of acetate from carbon dioxide. *ChemElectroChem*, **3**(4), 581-591.

Jungbluth, N., Chudacoff, M., Dauriat, A., Dinkel, F., Doka, G., Faist Emmenegger, M., Gnansounou, E., Kljun, N., Schleiss, K., Spielmann, M. 2007. Life cycle inventories of bioenergy. *Final report ecoinvent data v2.0*, **17**.

Kantzow, C., Mayer, A., Weuster-Botz, D. 2015. Continuous gas fermentation by *Acetobacterium woodii* in a submerged membrane reactor with full cell retention. *Journal of biotechnology*, **212**, 11-18.

Katuri, K.P., Scott, K. 2010. Electricity generation from the treatment of wastewater with a hybrid up-flow microbial fuel cell. *Biotechnology and Bioengineering*, **107**(1), 52-58.

Kenealy, W.R., Waselefsky, D.M. 1985. Studies on the substrate range of *Clostridium kluyveri*; the use of propanol and succinate. *Archives of Microbiology*, **141**(3), 187-194.

Kerckhof, F.-M., Courtens, E.N., Geirnaert, A., Hoefman, S., Ho, A., Vilchez-Vargas, R., Pieper, D.H., Jauregui, R., Vlaeminck, S.E., Van de Wiele, T. 2014. Optimized cryopreservation of mixed microbial communities for conserved functionality and diversity. *PloS one*, **9**(6), e99517.

Kleerebezem, R., Van Loosdrecht, M.C.M. 2010. A generalized method for thermodynamic state analysis of environmental systems. *Critical Reviews in Environmental Science and Technology*, **40**(1), 1-54.

Köpke, M., Held, C., Hujer, S., Liesegang, H., Wiezer, A., Wollherr, A., Ehrenreich, A., Liebl, W., Gottschalk, G., Dürre, P. 2010. *Clostridium ljungdahlii* represents a microbial production platform based on syngas. *Proceedings of the National Academy of Sciences*, **107**(29), 13087-13092.

Köpke, M., Mihalcea, C., Bromley, J.C., Simpson, S.D. 2011a. Fermentative production of ethanol from carbon monoxide. *Current Opinion in Biotechnology*, **22**(3), 320-325.

Köpke, M., Mihalcea, C., Liew, F., Tizard, J.H., Ali, M.S., Conolly, J.J., Al-Sinawi, B., Simpson, S.D. 2011b. 2, 3-Butanediol production by acetogenic bacteria, an alternative route to chemical synthesis, using industrial waste gas. *Applied and Environmental Microbiology*, **77**(15), 5467-5475.

Kracke, F., Krömer, J.O. 2014. Identifying target processes for microbial electrosynthesis by elementary mode analysis. *BMC bioinformatics*, **15**(1), 1.

Kracke, F., Vassilev, I., Krömer, J.O. 2015. Microbial electron transport and energy conservation – the foundation for optimizing bioelectrochemical systems. *Frontiers in Microbiology*, **6**(575).

Kucek, L.A., Nguyen, M., Angenent, L.T. 2016. Conversion of L-lactate into *n*-caproate by a continuously fed reactor microbiome. *Water research*, **93**, 163-171.

Kuntke, P., Smiech, K.M., Bruning, H., Zeeman, G., Saakes, M., Sleutels, T.H.J.A., Hamelers, H.V.M., Buisrnan, C.J.N. 2012. Ammonium recovery and energy production from urine by a microbial fuel cell. *Water Research*, **46**(8), 2627-2636.

Küsel, K., Pinkart, H.C., Drake, H.L., Devereux, R. 1999. Acetogenic and sulfate-reducing bacteria inhabiting the rhizoplane and deep cortex cells of the sea grass *Halodule wrightii*. *Applied and Environmental Microbiology*, **65**(11), 5117-5123.

LaBelle, E.V., Marshall, C.W., Gilbert, J.A., May, H.D. 2014. Influence of acidic pH on hydrogen and acetate production by an electrosynthetic microbiome. *PloS one*, **9**(10), e109935.

Lam, F.H., Ghaderi, A., Fink, G.R., Stephanopoulos, G. 2014. Engineering alcohol tolerance in yeast. *Science*, **346**(6205), 71-75.

Latif, H., Zeidan, A.A., Nielsen, A.T., Zengler, K. 2014. Trash to treasure: production of biofuels and commodity chemicals via syngas fermenting microorganisms. *Current Opinion in Biotechnology*, **27**, 79-87.

Leang, C., Ueki, T., Nevin, K.P., Lovley, D.R. 2013. A genetic system for *Clostridium ljungdahlii*: a chassis for autotrophic production of biocommodities and a model homoacetogen. *Applied and Environmental Microbiology*, **79**(4), 1102-1109.

Leclerc, M., Bernalier, A., Donadille, G., Lelait, M. 1997. H_2/CO_2 metabolism in acetogenic bacteria isolated from the human colon. *Anaerobe*, **3**(5), 307-315.

Lee, H.-J., Sarfert, F., Strathmann, H., Moon, S.-H. 2002. Designing of an electrodialysis desalination plant. *Desalination*, **142**(3), 267-286.

Lee, H. 2015. Acetic acid steady on lower output in China. *ICIS Chemical Business*, **19-25 October**, 17.

Lefebvre, O., Moletta, R. 2006. Treatment of organic pollution in industrial saline wastewater: a literature review. *Water research*, **40**(20), 3671-3682.

Levy, P., Sanderson, J., Kispert, R., Wise, D. 1981. Biorefining of biomass to liquid fuels and organic chemicals. *Enzyme and Microbial Technology*, **3**(3), 207-215.

Li, F.F., Lau, J., Licht, S. 2015. Sungas instead of syngas: Efficient coproduction of CO and H_2 with a single beam of sunlight. *Advanced Science*, **2**(11).

Liao, J.C., Mi, L., Pontrelli, S., Luo, S. 2016. Fuelling the future: microbial engineering for the production of sustainable biofuels. *Nature Reviews Microbiology*, **14**(5), 288-304.

Liew, F., Martin, M.E., Tappel, R.C., Heijstra, B.D., Mihalcea, C., Köpke, M. 2016. Gas fermentation - A flexible platform for commercial scale production of low-carbon-fuels and chemicals from waste and renewable feedstocks. *Frontiers in microbiology*, **7**(694).

Lim, X. 2015. How to make the most of carbon dioxide. *Nature*, **526**(7575), 628-630.

Liou, J.S.-C., Balkwill, D.L., Drake, G.R., Tanner, R.S. 2005. *Clostridium carboxidivorans sp. nov.*, a solvent-producing clostridium isolated from an agricultural settling lagoon, and reclassification of the acetogen *Clostridium scatologenes* strain SL1 as *Clostridium drakei sp. nov. International journal of systematic and evolutionary microbiology*, **55**(5), 2085-2091.

Liu, H., Logan, B.E. 2004. Electricity generation using an air-cathode single chamber microbial fuel cell in the presence and absence of a proton exchange membrane. *Environmental Science & Technology*, **38**(14), 4040-4046.

Liu, H., Cheng, S., Logan, B.E. 2005a. Power generation in fed-batch microbial fuel cells as a function of ionic strength, temperature, and reactor configuration. *Environmental Science & Technology*, **39**(14), 5488-5493.

Liu, H., Cheng, S.A., Logan, B.E. 2005b. Production of electricity from acetate or butyrate using a single-chamber microbial fuel cell. *Environmental Science & Technology*, **39**(2), 658-662.

Liu, H., Grot, S., Logan, B.E. 2005c. Electrochemically assisted microbial production of hydrogen from acetate. *Environmental Science & Technology*, **39**(11), 4317-4320.

Liu, Y., Kim, H., Franklin, R.R., Bond, D.R. 2011. Linking spectral and electrochemical analysis to monitor c-type cytochrome redox status in living *Geobacter sulfurreducens* biofilms. *ChemPhysChem*, **12**(12), 2235-2241.

Ljungdahl, L. 1986. The autotrophic pathway of acetate synthesis in acetogenic bacteria. *Annual Reviews in Microbiology*, **40**(1), 415-450.

Logan, B., Cheng, S., Watson, V., Estadt, G. 2007. Graphite fiber brush anodes for increased power production in air-cathode microbial fuel cells. *Environmental Science & Technology*, **41**(9), 3341-3346.

Logan, B.E., Murano, C., Scott, K., Gray, N.D., Head, I.M. 2005. Electricity generation from cysteine in a microbial fuel cell. *Water Res.*, **39**(5), 942-952.

Logan, B.E., Hamelers, B., Rozendal, R., Schröder, U., Keller, J., Freguia, S., Aelterman, P., Verstraete, W., Rabaey, K. 2006. Microbial fuel cells: methodology and technology. *Environmental Science & Technology*, **40**(17), 5181-5192.

Logan, B.E., Call, D., Cheng, S., Hamelers, H.V., Sleutels, T.H., Jeremiasse, A.W., Rozendal, R.A. 2008. Microbial electrolysis cells for high yield hydrogen gas production from organic matter. *Environmental Science & Technology*, **42**(23), 8630-8640.

Logan, B.E. 2009. Exoelectrogenic bacteria that power microbial fuel cells. *Nature Reviews Microbiology*, **7**(5), 375-381.

Logan, B.E., Rabaey, K. 2012. Conversion of wastes into bioelectricity and chemicals by using microbial electrochemical technologies. *Science*, **337**(6095), 686-690.

Lonkar, S., Fu, Z., Holtzapple, M. 2016. Optimum alcohol concentration for chain elongation in mixed-culture fermentation of cellulosic substrate. *Biotechnology and bioengineering*.

López-Garzón, C.S., Straathof, A.J. 2014. Recovery of carboxylic acids produced by fermentation. *Biotechnology advances*, **32**(5), 873-904.

Lovley, D.R., Phillips, E.J.P. 1988. Novel mode of microbial energy metabolism: organic carbon oxidation coupled to dissimilatory reduction of iron or manganese. *Applied and Environmental Microbiology*, **54**(6), 1472-1480.

Lovley, D.R. 2011. Powering microbes with electricity: direct electron transfer from electrodes to microbes. *Environmental Microbiology Reports*, **3**(1), 27-35.

Lovley, D.R., Malvankar, N.S. 2015. Seeing is believing: novel imaging techniques help clarify microbial nanowire structure and function. *Environmental microbiology*, **17**(7), 2209-2215.

Mambrini, M., Peyraud, J. 1997. Retention time of feed particles and liquids in the stomachs and intestines of dairy cows. Direct measurement and calculations based on faecal collection. *Reproduction Nutrition Development*, **37**(4), 427-442.

Marcus, A.K., Torres, C.I., Rittmann, B.E. 2007. Conduction-based modeling of the biofilm anode of a microbial fuel cell. *Biotechnology and Bioengineering*, **98**(6), 1171-1182.

Markewitz, P., Kuckshinrichs, W., Leitner, W., Linssen, J., Zapp, P., Bongartz, R., Schreiber, A., Müller, T.E. 2012. Worldwide innovations in the development of carbon capture technologies and the utilization of CO_2. *Energy & Environmental Science*, **5**(6), 7281-7305.

Marshall, C.W., Ross, D.E., Fichot, E.B., Norman, R.S., May, H.D. 2012. Electrosynthesis of commodity chemicals by an autotrophic microbial community. *Applied and Environmental Microbiology*, **78**(23), 8412-8420.

Marshall, C.W., LaBelle, E.V., May, H.D. 2013a. Production of fuels and chemicals from waste by microbiomes. *Current Opinion in Biotechnology*, **24**(3), 391-397.

Marshall, C.W., Ross, D.E., Fichot, E.B., Norman, R.S., May, H.D. 2013b. Long-term operation of microbial electrosynthesis systems improves acetate production by autotrophic microbiomes. *Environmental Science & Technology*, **47**(11), 6023-6029.

Martin, M.E., Richter, H., Saha, S., Angenent, L.T. 2015. Traits of selected Clostridium strains for syngas fermentation to ethanol. *Biotechnology and Bioengineering*, **113**(3), 531-539.

Martin, W.F. 2012. Hydrogen, metals, bifurcating electrons, and proton gradients: the early evolution of biological energy conservation. *FEBS letters*, **586**(5), 485-493.

McGlade, C., Ekins, P. 2015. The geographical distribution of fossil fuels unused when limiting global warming to 2 [deg] C. *Nature*, **517**(7533), 187-190.

Menzel, U., Gottschalk, G. 1985. The internal pH of *Acetobacterium wieringae* and *Acetobacter aceti* during growth and production of acetic acid. *Archives of microbiology*, **143**(1), 47-51.

MIRA-VMM. Milieurapport Vlaanderen. www.milieurapport.be. 2016, April 19th

Mock, J., Zheng, Y., Mueller, A.P., Ly, S., Tran, L., Segovia, S., Nagaraju, S., Köpke, M., Dürre, P., Thauer, R.K. 2015. Energy conservation associated with ethanol formation from H_2 and CO_2 in *Clostridium autoethanogenum* involving electron bifurcation. *Journal of bacteriology*, **197**(18), 2965-2980.

Molenaar, S.D., Mol, A.R., Sleutels, T.H., Ter Heijne, A., Buisman, C.J. 2016. The microbial rechargeable battery: Energy storage and Rrecovery through acetate. *Environmental Science & Technology Letters*, **3**(4), 144-149.

Molitor, B., Richter, H., Martin, M.E., Jensen, R.O., Juminaga, A., Mihalcea, C., Angenent, L.T. 2016. Carbon recovery by fermentation of CO-rich off gases–turning steel mills into biorefineries. *Bioresource Technology*, **215**, 386-396.

Mu, Y., Rabaey, K., Rozendal, R.A., Yuan, Z., Keller, J. 2009a. Decolourization of azo dyes in bio-electrochemical systems. *Environmental Science & Technology*, **43**(13), 5137-5143.

Mu, Y., Rozendal, R.A., Rabaey, K., Keller, J. 2009b. Nitrobenzene removal in bioelectrochemical systems. *Environ. Sci. Technol.*, **43**(22), 8690-8695.

Müller, V. 2003. Energy conservation in acetogenic bacteria. *Applied and environmental microbiology*, **69**(11), 6345-6353.

Munasinghe, P.C., Khanal, S.K. 2010. Biomass-derived syngas fermentation into biofuels: opportunities and challenges. *Bioresource Technology*, **101**(13), 5013-5022.

Myers, C.R., Nealson, K.H. 1988. Bacterial manganese reduction and growth with manganese oxide as the sole electron acceptor. *Science*, **240**(4857), 1319-1321.

Nagarale, R., Gohil, G., Shahi, V.K. 2006. Recent developments on ion-exchange membranes and electro-membrane processes. *Advances in colloid and interface science*, **119**(2), 97-130.

Nevin, K.P., Woodard, T.L., Franks, A.E., Summers, Z.M., Lovley, D.R. 2010. Microbial electrosynthesis: feeding microbes electricity to convert carbon dioxide and water to multicarbon extracellular organic compounds. *mBio*, **1**(2), e00103-10

Nevin, K.P., Hensley, S.A., Franks, A.E., Summers, Z.M., Ou, J., Woodard, T.L., Snoeyenbos-West, O.L., Lovley, D.R. 2011. Electrosynthesis of organic compounds from carbon dioxide is catalyzed by a diversity of acetogenic microorganisms. *Applied and Environmental Microbiology*, **77**(9), 2882-2886.

Newman, D.K., Kolter, R. 2000. A role for excreted quinones in extracellular electron transfer. *Nature*, **405**(6782), 94-97.

Nie, H., Zhang, T., Cui, M., Lu, H., Lovley, D.R., Russell, T.P. 2013. Improved cathode for high efficient microbial-catalyzed reduction in microbial electrosynthesis cells. *Physical Chemistry Chemical Physics*, **15**(34), 14290-14294.

Okada, T., Møller-Holst, S., Gorseth, O., Kjelstrup, S. 1998. Transport and equilibrium properties of Nafion® membranes with H^+ and Na^+ ions. *Journal of Electroanalytical Chemistry*, **442**(1–2), 137-145.

Otto, A., Grube, T., Schiebahn, S., Stolten, D. 2015. Closing the loop: captured CO_2 as a feedstock in the chemical industry. *Energy & Environmental Science*, **8**(11), 3283-3297.

Pafford, J. 2016. Ethyl Acetate. *ICIS Chemical Business*, **18-24 January**, 32.

Park, D.H., Laivenieks, M., Guettler, M.V., Jain, M.K., Zeikus, J.G. 1999. Microbial utilization of electrically reduced neutral red as the sole electron donor for growth and metabolite production. *Applied Environmental Microbiology*, **65**(7), 2912-2917.

Patil, S.A., Arends, J.B.A., Vanwonterghem, I., van Meerbergen, J., Guo, K., Tyson, G.W., Rabaey, K. 2015a. Selective enrichment establishes a stable performing community for microbial electrosynthesis of acetate from CO_2. *Environmental Science & Technology*, **49**(14), 8833-8843.

Patil, S.A., Gildemyn, S., Pant, D., Zengler, K., Logan, B.E., Rabaey, K. 2015b. A logical data representation framework for electricity-driven bioproduction processes. *Biotechnology Advances*, **33**(6), 736-744.

Peters, V., Janssen, H.P., Conrad, R. 1999. Transient production of formate during chemolithotrophic growth of anaerobic microorganisms on hydrogen. *Current Microbiology*, **38**(5), 285-289.

Pham, T.H., Aelterman, P., Verstraete, W. 2009. Bioanode performance in bioelectrochemical systems: recent improvements and prospects. *Trends in biotechnology*, **27**(3), 168-178.

Picioreanu, C., Head, I.M., Katuri, K.P., van Loosdrecht, M.C.M., Scott, K. 2007. A computational model for biofilm-based microbial fuel cells. *Water Research*, **41**(13), 2921-2940.

Picot, M., Lapinsonnière, L., Rothballer, M., Barrière, F. 2011. Graphite anode surface modification with controlled reduction of specific aryl diazonium salts for improved microbial fuel cells power output. *Biosensors and Bioelectronics*, **28**(1), 181-188.

Pikaar, I., Rozendal, R.A., Yuan, Z., Rabaey, K. 2011. Electrochemical caustic generation from sewage. *Electrochemistry Communications*, **13**(11), 1202-1204.

Plugge, C.M. 2005. Anoxic media design, preparation, and considerations. *Methods in enzymology*, **397**, 3-16.

Potter, M.C. 1911. Electrical effects accompanying the decomposition of organic compounds. *Proceedings of the Royal Society of London. Series B, Containing Papers of a Biological Character*, **84**(571), 260-276.

Puig, S., Serra, M., Coma, M., Cabré, M., Dolors Balaguer, M., Colprim, J. 2011. Microbial fuel cell application in landfill leachate treatment. *Journal of Hazardous Materials*, **185**(2), 763-767.

Qiao, J., Liu, Y., Hong, F., Zhang, J. 2014. A review of catalysts for the electroreduction of carbon dioxide to produce low-carbon fuels. *Chemical Society Reviews*, **43**(2), 631-675.

Rabaey, K., Lissens, G., Siciliano, S.D., Verstraete, W. 2003. A microbial fuel cell capable of converting glucose to electricity at high rate and efficiency. *Biotechnology Letters*, **25**(18), 1531-1535.

Rabaey, K., Boon, N., Höfte, M., Verstraete, W. 2005. Microbial phenazine production enhances electron transfer in biofuel cells. *Environmental Science & Technology*, **39**(9), 3401-3408.

Rabaey, K., Rodriguez, J., Blackall, L.L., Keller, J., Gross, P., Batstone, D., Verstraete, W., Nealson, K.H. 2007. Microbial ecology meets electrochemistry: electricity-driven and driving communities. *ISME J.*, **1**(1), 9-18.

Rabaey, K., Butzer, S., Brown, S., Keller, J., Rozendal, R.A. 2010. High current generation coupled to caustic production using a lamellar bioelectrochemical system. *Environmental Science & Technology*, **44**(11), 4315-4321.

Rabaey, K., Rozendal, R.A. 2010. Microbial electrosynthesis - revisiting the electrical route for microbial production. *Nature Reviews Microbiology*, **8**(10), 706-716.

Rabaey, K., Girguis, P., Nielsen, L.K. 2011. Metabolic and practical considerations on microbial electrosynthesis. *Current Opinion in Biotechnology*, **22**, 1-7.

Ragsdale, S.W., Pierce, E. 2008. Acetogenesis and the Wood-Ljungdahl pathway of CO_2 fixation. *Biochimica Et Biophysica Acta-Proteins and Proteomics*, **1784**(12), 1873-1898.

Reguera, G., McCarthy, K.D., Mehta, T., Nicoll, J.S., Tuominen, M.T., Lovley, D.R. 2005. Extracellular electron transfer via microbial nanowires. *Nature*, **435**(7045), 1098-1101.

Rey, F.E., Faith, J.J., Bain, J., Muehlbauer, M.J., Stevens, R.D., Newgard, C.B., Gordon, J.I. 2010. Dissecting the in vivo metabolic potential of two human gut acetogens. *Journal of biological chemistry*, **285**(29), 22082-22090.

Richardson, D.J. 2000. Bacterial respiration: a flexible process for a changing environment. *Microbiology*, **146**(3), 551-571.

Richter, H., Qureshi, N., Heger, S., Dien, B., Cotta, M.A., Angenent, L.T. 2012. Prolonged conversion of *n*-butyrate to *n*-butanol with *Clostridium saccharoperbutylacetonicum* in a two-stage continuous culture with *in-situ* product removal. *Biotechnology and Bioengineering*, **109**(4), 913-921.

Richter, H., Loftus, S.E., Angenent, L.T. 2013a. Integrating syngas fermentation with the carboxylate platform and yeast fermentation to reduce medium cost and improve biofuel productivity. *Environmental Technology*, **34**(13-14), 1983-1994.

Richter, H., Martin, M., Angenent, L. 2013b. A two-stage continuous fermentation system for conversion of syngas into ethanol. *Energies*, **6**(8), 3987-4000.

Richter, H., Molitor, B., Wei, H., Chen, W., Aristilde, L., Angenent, L.T. 2016. Ethanol production in syngas-fermenting *Clostridium ljungdahlii* is controlled by thermodynamics rather than by enzyme expression. *Energy & Environmental Science*, **9**, 2392-2399.

Rodríguez, J., Lema, J.M., Kleerebezem, R. 2008. Energy-based models for environmental biotechnology. *Trends in biotechnology*, **26**(7), 366-374.

Rosenbaum, M., Aulenta, F., Villano, M., Angenent, L.T. 2011. Cathodes as electron donors for microbial metabolism: Which extracellular electron transfer mechanisms are involved? *Bioresource technology*, **102**(1), 324-333.

Rosenbaum, M.A., Franks, A.E. 2013. Microbial catalysis in bioelectrochemical technologies: status quo, challenges and perspectives. *Applied microbiology and biotechnology*, **98**(2), 509-518.

Rosenbaum, M.A., Henrich, A.W. 2014. Engineering microbial electrocatalysis for chemical and fuel production. *Current opinion in biotechnology*, **29**, 93-98.

Rozendal, R.A., Hamelers, H.V.M., Buisman, C.J.N. 2006a. Effects of membrane cation transport on pH and microbial fuel cell performance. *Environmental Science & Technology*, **40**(17), 5206-5211.

Rozendal, R.A., Hamelers, H.V.M., Euverink, G.J.W., Metz, S.J., Buisman, C.J.N. 2006b. Principle and perspectives of hydrogen production through biocatalyzed electrolysis. *International Journal of Hydrogen Energy*, **31**(12), 1632-1640.

Rozendal, R.A., Hamelers, H.V.M., Rabaey, K., Keller, J., Buisman, C.J.N. 2008a. Towards practical implementation of bioelectrochemical wastewater treatment. *Trends in biotechnology*, **26**(8), 450-459.

Rozendal, R.A., Jeremiasse, A.W., Hamelers, H.V.M., Buisman, C.J.N. 2008b. Hydrogen production with a microbial biocathode. *Environmental Science & Technology*, **42**(2), 629-634.

Rozendal, R.A., Jeremiasse, A.W., Hamelers, H.V.M., Buisman, C.J.N. 2008c. Hydrogen production with a microbial biocathode. *Environ. Sci. Technol.*, **42**, 629-634.

Rozendal, R.A., Sleutels, T., Hamelers, H.V.M., Buisman, C.J.N. 2008d. Effect of the type of ion exchange membrane on performance, ion transport, and pH in biocatalyzed electrolysis of wastewater. *Water Science and Technology*, **57**(11), 1757-1762.

Rozendal, R.A., Leone, E., Keller, J., Rabaey, K. 2009. Efficient hydrogen peroxide generation from organic matter in a bioelectrochemical system. *Electrochemistry Communications*, **11**(9), 1752-1755.

Rubin, E.S., Zhai, H. 2012. The cost of carbon capture and storage for natural gas combined cycle power plants. *Environmental Science & Technology*, **46**(6), 3076-3084.

Schiel-Bengelsdorf, B., Dürre, P. 2012. Pathway engineering and synthetic biology using acetogens. *FEBS Letters*, **586**(15), 2191-2198.

Schievano, A., Pepé Sciarria, T., Vanbroekhoven, K., De Wever, H., Puig, S., Andersen, S.J., Rabaey, K., Pant, D. 2016. Electro-fermentation - Merging electrochemistry with fermentation in industrial applications. *Trends in Biotechnology*, Accepted, in press.

Schink, B. 1997. Energetics of syntrophic cooperation in methanogenic degradation. *Microbiol. Mol. Biol. Rev.*, **61**(2), 262-&.

Schoberth, S., Gottschalk, G. 1969. Considerations on the energy metabolism of *Clostridium kluyveri*. *Archiv für Mikrobiologie*, **65**(4), 318-328.

Schröder, U. 2007. Anodic electron transfer mechanisms in microbial fuel cells and their energy efficiency. *Physical Chemistry Chemical Physics*, **9**(21), 2619-2629.

Schröder, U., Harnisch, F. 2010. Electrochemical losses. in: *Bioelectrochemical Systems: from extracellular electron transfer to biotechnological application*, (Eds.) K. Rabaey, L.T. Angenent, U. Schröder, J. Keller, IWA Publishing. London.

Schröder, U. 2011. Discover the possibilities: microbial bioelectrochemical systems and the revival of a 100-year–old discovery. *Journal of Solid State Electrochemistry*, **15**(7), 1481-1486.

Schröder, U., Harnisch, F., Angenent, L.T. 2015. Microbial electrochemistry and technology: terminology and classification. *Energy & Environmental Science*, **8**, 513-519.

Schuchmann, K., Müller, V. 2013. Direct and reversible hydrogenation of CO_2 to formate by a bacterial carbon dioxide reductase. *Science*, **342**(6164), 1382-1385.

Seedorf, H., Fricke, W.F., Veith, B., Brüggemann, H., Liesegang, H., Strittmatter, A., Miethke, M., Buckel, W., Hinderberger, J., Li, F. 2008. The genome of *Clostridium kluyveri*, a strict anaerobe with unique metabolic features. *Proceedings of the National Academy of Sciences*, **105**(6), 2128-2133.

Shafiee, S., Topal, E. 2009. When will fossil fuel reserves be diminished? *Energy policy*, **37**(1), 181-189.

Sharma, M., Bajracharya, S., Gildemyn, S., Patil, S.A., Alvarez-Gallego, Y., Pant, D., Rabaey, K., Dominguez-Benetton, X. 2014. A critical revisit of the key parameters used to describe microbial electrochemical systems. *Electrochimica Acta*, **140**, 191-208.

Shen, Y., Brown, R., Wen, Z. 2014. Syngas fermentation of *Clostridium carboxidivorans* P7 in a hollow fiber membrane biofilm reactor: Evaluating the mass transfer coefficient and ethanol production performance. *Biochemical Engineering Journal*, **85**, 21-29.

Sleutels, T.H., Molenaar, S.D., Heijne, A.T., Buisman, C.J. 2016. Low substrate loading limits methanogenesis and leads to high coulombic efficiency in bioelectrochemical systems. *Microorganisms*, **4**(1), 7.

Sleutels, T.H.J.A., Hamelers, H.V.M., Rozendal, R.A., Buisman, C.J.N. 2009. Ion transport resistance in microbial electrolysis cells with anion and cation exchange membranes. *International Journal of Hydrogen Energy*, **34**(9), 3612-3620.

Smith, G.M., Kim, B.W., Franke, A.A., Roberts, J.D. 1985. 13C NMR studies of butyric fermentation in *Clostridium kluyveri*. *Journal of Biological Chemistry*, **260**(25), 13509-13512.

Snider, R.M., Strycharz-Glaven, S.M., Tsoi, S.D., Erickson, J.S., Tender, L.M. 2012. Long-range electron transport in *Geobacter sulfurreducens* biofilms is redox gradient-driven. *Proceedings of the National Academy of Sciences*, **109**(38), 15467-15472.

Sørensen, J., Christensen, D., Jørgensen, B.B. 1981. Volatile fatty acids and hydrogen as substrates for sulfate-reducing bacteria in anaerobic marine sediment. *Applied and Environmental Microbiology*, **42**(1), 5-11.

Soussan, L., Riess, J., Erable, B., Delia, M.-L., Bergel, A. 2013. Electrochemical reduction of CO_2 catalysed by *Geobacter sulfurreducens* grown on polarized stainless steel cathodes. *Electrochemistry Communications*, **28**, 27-30.

Spirito, C.M., Richter, H., Rabaey, K., Stams, A.J.M., Angenent, L.T. 2014. Chain elongation in anaerobic reactor microbiomes to recover resources from waste. *Current Opinion in Biotechnology*, **27**, 115-122.

Stams, A.J.M., De Bok, F.A.M., Plugge, C.M., Van Eekert, M.H.A., Dolfing, J., Schraa, G. 2006. Exocellular electron transfer in anaerobic microbial communities. *Environmental Microbiology*, **8**(3), 371-382.

Steinbusch, K.J., Hamelers, H.V., Plugge, C.M., Buisman, C.J. 2011. Biological formation of caproate and caprylate from acetate: fuel and chemical production from low grade biomass. *Energy & Environmental Science*, **4**(1), 216-224.

Steinbusch, K.J.J., Hamelers, H.V.M., Buisman, C.J.N. 2008. Alcohol production through volatile fatty acids reduction with hydrogen as electron donor by mixed cultures. *Water Research*, **42**(15), 4059-4066.

Steinbusch, K.J.J., Arvaniti, E., Hamelers, H.V.M., Buisman, C.J.N. 2009. Selective inhibition of methanogenesis to enhance ethanol and n-butyrate production through acetate reduction in mixed culture fermentation. *Bioresource Technology*, **100**(13), 3261-3267.

Steinbusch, K.J.J., Hamelers, H.V.M., Schaap, J.D., Kampman, C., Buisman, C.J.N. 2010. Bioelectrochemical ethanol production through mediated acetate reduction by mixed cultures. *Environmental Science & Technology*, **44**(1), 513-517.

Strathmann, H. 2010. Electrodialysis, a mature technology with a multitude of new applications. *Desalination*, **264**(3), 268-288.

Strathmann, H., Grabowski, A., Eigenberger, G. 2013. Ion-exchange membranes in the chemical process industry. *Industrial & Engineering Chemistry Research*, **52**(31), 10364-10379.

Strycharz, S.M., Woodard, T.L., Johnson, J.P., Nevin, K.P., Sanford, R.A., Loffler, F.E., Lovley, D.R. 2008. Graphite electrode as a sole electron donor for reductive dechlorination of tetrachlorethene by *Geobacter lovleyi*. *Applied and Environmental Microbiology*, **74**(19), 5943-5947.

Styring, P., Jansen, D., De Coninck, H., Reith, H., Armstrong, K. 2011. *Carbon Capture and Utilisation in the green economy*. Centre for Low Carbon Futures.

Styring, P., Armstrong, K. 2015. Assessing the potential of utilisation and storage strategies for post-combustion CO_2 emissions reduction. *Frontiers in Energy Research*, **3**(8), 1-9.

Su, M., Jiang, Y., Li, D. 2013. Production of acetate from carbon dioxide in bioelectrochemical systems based on autotrophic mixed culture. *Journal of Microbiology and Biotechnology*, **23**(8), 1140-1146.

Subramanian, P., Pirbadian, S., El-Naggar, M.Y., Jensen, G.J. 2016. Electron Cryo-Tomography of Nanowires in *Shewanella Oneidensis* MR-1. *Biophysical Journal*, **110**(3), 23a.

Tchobanoglous, G., Burton, F.L., Stensel, H.D. 2003. *Wastewater engineering: treatment and reuse*. *3rd ed*. Metcalf & Eddy, McGraw-Hill, New York.

Ter Heijne, A., Liu, F., van der Weijden, R., Weijma, J., Buisman, C.J.N., Hamelers, H.V.M. 2010. Copper recovery combined with electricity production in a microbial fuel cell. *Environmental Science & Technology*, **44**(11), 4376-4381.

Thauer, R., Jungermann, K., Henninger, H., Wenning, J., Decker, K. 1968. The energy metabolism of *Clostridium kluyveri*. *European Journal of Biochemistry*, **4**(2), 173-180.

Thauer, R.K., Jungermann, K., Decker, K. 1977. Energy conservation in chemotrophic anaerobic bacteria. *Bacteriol. Rev.*, **41**(1), 100-180.

Thrash, J.C., Van Trump, J.I., Weber, K.A., Miller, E., Achenbach, L.A., Coates, J.D. 2007. Electrochemical stimulation of microbial perchlorate reduction. *Environmental Science & Technology*, **41**(5), 1740-1746.

TMR. 2016. Palm kernel oil and coconut oil based natural fatty acids market for detergents, personal care, plastics, rubber, and other end-users - global industry analysis, size, share, growth, trends and forecast, 2015 - 2023.

Tomlinson, N., Barker, H. 1954. Carbon dioxide and acetate utilization by *Clostridium kluyveri* i. Influence of nutritional conditions on utilization patterns. *Journal of Biological Chemistry*, **209**(2), 585-595.

Tracy, B.P., Jones, S.W., Fast, A.G., Indurthi, D.C., Papoutsakis, E.T. 2012. Clostridia: the importance of their exceptional substrate and metabolite diversity for biofuel and biorefinery applications. *Current Opinion in Biotechnology*, **23**(3), 364-381.

Tremblay, P.-L., Höglund, D., Koza, A., Bonde, I., Zhang, T. 2015. Adaptation of the autotrophic acetogen *Sporomusa ovata* to methanol accelerates the conversion of CO_2 to organic products. *Scientific Reports*, **5**(16168).

Tremblay, P.L., Zhang, T., Dar, S.A., Leang, C., Lovley, D.R. 2013. The Rnf complex of *Clostridium ljungdahlii* is a proton-translocating ferredoxin: NAD^+ oxidoreductase essential for autotrophic growth. *mBio*, **4**(1), e00406-12

Van Nevel, S., Koetzsch, S., Weilenmann, H.-U., Boon, N., Hammes, F. 2013. Routine bacterial analysis with automated flow cytometry. *Journal of microbiological methods*, **94**(2), 73-76.

Vanoppen, M., Bakelants, A.F.A.M., Gaublomme, D., Schoutteten, K.V.K.M., Bussche, J.V., Vanhaecke, L., Verliefde, A.R.D. 2014. Properties governing the transport of trace organic contaminants through ion-exchange membranes. *Environmental Science & Technology*, **49**(1), 489-497.

Varcoe, J.R., Atanassov, P., Dekel, D.R., Herring, A.M., Hickner, M.A., Kohl, P.A., Kucernak, A.R., Mustain, W.E., Nijmeijer, K., Scott, K. 2014. Anion-exchange membranes in electrochemical energy systems. *Energy & Environmental Science*, **7**(10), 3135-3191.

Vasudevan, D., Richter, H., Angenent, L.T. 2014. Upgrading dilute ethanol from syngas fermentation to *n*-caproate with reactor microbiomes. *Bioresource Technology*, **151**, 378-382.

Villano, M., Aulenta, F., Ciucci, C., Ferri, T., Giuliano, A., Majone, M. Bioelectrochemical reduction of CO_2 to CH_4 via direct and indirect extracellular electron transfer by a hydrogenophilic methanogenic culture. *Bioresource Technology*, **101**(9), 3085-3090.

Villano, M., Monaco, G., Aulenta, F., Majone, M. 2011. Electrochemically assisted methane production in a biofilm reactor. *Journal of Power Sources*, **196**(22), 9467-9472.

Virdis, B., Rabaey, K., Yuan, Z., Rozendal, R.A., Keller, J. 2009. Electron fluxes in a microbial fuel cell performing carbon and nitrogen removal. *Environmental Science & Technology*, **43**(13), 5144-5149.

Virdis, B., Read, S.T., Rabaey, K., Rozendal, R.A., Yuan, Z., Keller, J. 2011. Biofilm stratification during simultaneous nitrification and denitrification (SND) at a biocathode. *Bioresource Technology*, **102**(1), 334-341.

VITO. 2015. Energiebalans Vlaanderen 1990-2014.

Wagner, R.C., Call, D.I., Logan, B.E. 2010. Optimal set anode potentials vary in bioelectrochemical systems. *Environmental Science & Technology*, **44**(16), 6036-6041.

Wang, W., Wang, S., Ma, X., Gong, J. 2011. Recent advances in catalytic hydrogenation of carbon dioxide. *Chemical Society Reviews*, **40**(7), 3703-3727.

Weber, K.A., Achenbach, L.A., Coates, J.D. 2006. Microorganisms pumping iron: anaerobic microbial iron oxidation and reduction. *Nature Reviews Microbiology*, **4**(10), 752-764.

Webster, D.P., TerAvest, M.A., Doud, D.F., Chakravorty, A., Holmes, E.C., Radens, C.M., Sureka, S., Gralnick, J.A., Angenent, L.T. 2014. An arsenic-specific biosensor with genetically engineered Shewanella oneidensis in a bioelectrochemical system. *Biosensors and Bioelectronics*, **62**, 320-324.

Weimer, P.J., Stevenson, D.M. 2012. Isolation, characterization, and quantification of *Clostridium kluyveri* from the bovine rumen. *Applied Microbiology and Biotechnology*, **94**(2), 461-466.

Werner, J.J., Knights, D., Garcia, M.L., Scalfone, N.B., Smith, S., Yarasheski, K., Cummings, T.A., Beers, A.R., Knight, R., Angenent, L.T. 2011. Bacterial community structures are unique and resilient in full-scale bioenergy systems. *Proceedings of the National Academy of Sciences*, **108**(10), 4158-4163.

Whipple, D.T., Kenis, P.J. 2010. Prospects of CO_2 utilization via direct heterogeneous electrochemical reduction. *The Journal of Physical Chemistry Letters*, **1**(24), 3451-3458.

Widdel, F., Hansen, T., Balows, A., Truper, H., Dworkin, M., Harder, W., Schleifer, K. 1992. The dissimilatory sulfate-and sulfur-reducing bacteria. *The prokaryotes: a handbook on the biology of bacteria: ecophysiology, isolation, identification, applications, vol. I.*(Ed. 2), 582-624.

Wood, H. 1991. Life with CO or CO_2 and H_2 as a source of carbon and energy. *The FASEB journal*, **5**(2), 156-163.

Xu, G., Liang, F., Yang, Y., Hu, Y., Zhang, K., Liu, W. 2014. An improved CO_2 separation and purification system based on cryogenic separation and distillation theory. *Energies*, **7**(5), 3484-3502.

Xu, J., Guzman, J.J., Andersen, S.J., Rabaey, K., Angenent, L.T. 2015. In-line and selective phase separation of medium-chain carboxylic acids using membrane electrolysis. *Chemical Communications*, **51**(31), 6847-6850.

Xu, T. 2005. Ion exchange membranes: State of their development and perspective. *Journal of Membrane Science*, **263**(1–2), 1-29.

Xu, Y., Wang, D., Mu, X.Q., Zhao, G.A., Zhang, K.C. 2002. Biosynthesis of ethyl esters of short-chain fatty acids using whole-cell lipase from *Rhizopus chinesis* CCTCC M201021 in non-aqueous phase. *Journal of Molecular Catalysis B: Enzymatic*, **18**(1–3), 29-37.

Yip, N.Y., Vermaas, D.A., Nijmeijer, K., Elimelech, M. 2014. Thermodynamic, Energy Efficiency, and Power Density Analysis of Reverse Electrodialysis Power Generation with Natural Salinity Gradients. *Environmental Science & Technology*, **48**(9), 4925-4936.

Yoo, J.S., Christensen, R., Vegge, T., Nørskov, J.K., Studt, F. 2015. Theoretical insight into the trends that guide the electrochemical reduction of carbon dioxide to formic acid. *ChemSusChem*, **9**(4), 358-363.

Zaybak, Z., Pisciotta, J.M., Tokash, J.C., Logan, B.E. 2013. Enhanced start-up of anaerobic facultatively autotrophic biocathodes in bioelectrochemical systems. *Journal of Biotechnology*, **168**(4), 478-485.

Zeng, K., Zhang, D. 2010. Recent progress in alkaline water electrolysis for hydrogen production and applications. *Progress in Energy and Combustion Science*, **36**(3), 307-326.

Zhang, F., Ding, J., Shen, N., Zhang, Y., Ding, Z., Dai, K., Zeng, R.J. 2013a. *In situ* hydrogen utilization for high fraction acetate production in mixed culture hollow-fiber membrane biofilm reactor. *Applied microbiology and biotechnology*, **97**(23), 10233-10240.

Zhang, F., Ding, J., Zhang, Y., Chen, M., Ding, Z.-W., van Loosdrecht, M.C., Zeng, R.J. 2013b. Fatty acids production from hydrogen and carbon dioxide by mixed culture in the membrane biofilm reactor. *Water research*, **47**(16), 6122-6129.

Zhang, T., Gannon, S.M., Nevin, K.P., Franks, A.E., Lovley, D.R. 2010. Stimulating the anaerobic degradation of aromatic hydrocarbons in contaminated sediments by providing an electrode as the electron acceptor. *Environmental Microbiology*, **12**(4), 1011-1020.

Zhang, T., Nie, H., Bain, T.S., Lu, H., Cui, M., Snoeyenbos-West, O.L., Franks, A.E., Nevin, K., Russell, T.P., Lovley, D. 2013c. Improved cathode materials for microbial electrosynthesis. *Energy & Environmental Science*, **6**(1), 217-224.

Zhilina, T.N., Zavarzin, G.A. 1990. Extremely halophilic, methylotrophic, anaerobic bacteria. *FEMS Microbiology Reviews*, **7**(3-4), 315-321.

Zhilina, T.N., Zavarzin, G.A., Detkova, E.N., Rainey, F.A. 1996. *Natroniella acetigena gen. nov. sp. nov.*, an extremely haloalkaliphilic, homoacetic bacterium: a new member of Haloanaerobiales. *Current microbiology*, **32**(6), 320-326.

Zhilina, T.N., Detkova, E.N., Rainey, F.A., Osipov, G.A., Lysenko, A.M., Kostrikina, N.A., Zavarzin, G.A. 1998. *Natronoincola histidinovorans gen. nov., sp. nov.*, a new alkaliphilic acetogenic anaerobe. *Current microbiology*, **37**(3), 177-185.

APPENDIX

Appendix 1 - Technical Notes

1. A method for the enrichment of H_2/CO_2 utilizing microorganisms as biocatalyst for microbial electrosynthesis

1.1 Background

Microbial electrosynthesis (MES) from CO_2 relies on homoacetogens as biocatalysts. Carbon fixation into organics, in the first place acetic acid, occurs *via* the Wood-Ljungdahl pathway (see Chapter 1). A good biocatalyst for MES would be an organism or a culture of various microorganisms that can efficiently convert CO_2 and electrons, or H_2 into a single desired product. One could use pure cultures or genetically engineer microorganisms to match these requirements, but it is known that homoacetogens can be found in several natural anaerobic environments. Mixed cultures are often preferred over pure cultures for their resilience and robustness. The use of pure cultures on the other hand ensures a limited number of metabolic pathways is available. Anaerobic mixed cultures indeed contain microorganisms that compete with homoacetogens, especially on rich media: methanogens and sulfate reducing bacteria can also utilize H_2 as electron donor, or CO_2 as carbon source (methanogens) (Sørensen et al., 1981; Angenent et al., 2004). A selective enrichment procedure is therefore needed to obtain a culture for MES of acetic acid from CO_2. In the case of MES, the interaction with the electrode material is another important feature needed for the biocatalyst. The organism or culture must efficiently take up electrons or H_2 produced at the electrode. Enrichment in a bioelectrochemical system has therefore mostly been applied, but in order to screen a large number of environmental samples and conditions, a pre-enrichment under H_2/CO_2 atmosphere in culture tubes might be more feasible in terms of practical work in the lab. Using a serial dilution method and incubation under different conditions, 5 different environmental samples were thus enriched to obtain active homoacetogenic cultures that could potentially be used for MES at the cathode.

1.2 Materials and methods

Inoculum selection

Five environmental samples and reactor samples were collected: i) a fermenter effluent sample; ii) a marine sediment sample; iii) a human fecal sample; iv) a cow rumen sample; and v) a wallaby fecal sample. Selection of the samples was based on literature reports (Drake et al., 2006): a presence of homoacetogenic organisms in these samples was expected.

The fermenter sample was the effluent of a lab-scale upflow anaerobic sludge blanket (UASB) reactor fermenting molasses, operating at 34°C. Marine samples had been collected in the

Atlantic Ocean from the coastal areas of Lisbon. The upper layer of the sediment was collected (0-2 cm) at a sea deepness of approximately 1000 m (Alberto Scoma, CMET, personal communication). Human fecal samples were donated by a healthy, non-smoking individual who did not use antibiotics in the 6 months preceding donation. The cow rumen samples were collected from a low CH_4-emitting cow from ILVO (Thijs Demulder, ILVO, personal communication). The wallaby sample was a freshly collected sample from a swamp Wallaby from the Planckendael Zoo (Mechelen, Belgium). The samples were enriched according to the serial dilution method at 8 different conditions for pH and temperature (4 for the Wallaby fecal sample, Table App. 1.1).

Table App. 1.1 - Five samples were selected for enrichment of homoacetogenic organisms. Eight different conditions were tested at different dilution levels.

Sample	Dilutions	pH	Temperature	Transfer
UASB effluent	10^{-3} – 10^{-13}	6/7.5	20°/28°/37°/55°	Fast/Slow
Marine sediment	10^{-2} – 10^{-12}	6/7.5	20°/28°/37°/55°	Fast/Slow
Human fecal sample	10^{-3} – 10^{-13}	6/7.5	20°/28°/37°/55°	Fast/Slow
Cow rumen	10^{-3} – 10^{-13}	6/7.5	20°/28°/37°/55°	Fast/Slow
Wallaby fecal sample	10^{0} – 10^{-11}	6/7.5	28°C/37°C	Fast

Medium preparation

Samples were enriched in general homoacetogenic medium (see Chapter 3 and Gildemyn et al. (2015b)). For enrichment purposes yeast extract was added to the medium at a concentration of 0.5 g/L and resazurine (0.01%) was used as redox indicator. Medium was prepared under strict anaerobic conditions according to the method of Plugge (Plugge, 2005) and Hungate (Hungate, 1969). The medium containing salts, yeast extract and resazurine was boiled and consequently cooled in an ice bath under N_2/CO_2 atmosphere. At this point the pH was adjusted using 1M NaOH and 1M HCl. The medium was anaerobically dispensed into Balch growth tubes (9 mL medium). Tubes were closed with butyl rubber stoppers. Before use, vitamins, bicarbonate, tungstate-selenium and trace-elements were added to the medium from sterile anaerobic stock solutions (Chapter 3 and Appendix 3). The headspace was manually replaced by H_2/CO_2, reaching a final pressure of 270±30 kPa (n=3). Sodium sulfide (final concentration 2 mM) was added before inoculation to reduce the medium. It must be noted that after the additions, the pH differed from the targeted pH values. The medium at pH 6 increased to 6.5 while the medium at pH 7.5 decreased to 7.3.

Sample preparation

Inoculum samples were either directly used or stored at -80°C until use. A cryoprotectant (DMSO-Threhalose-Tryptic Soy broth; DMSO-TT) was used for storage, as described by the

procedure of Kerckhof et al. (2014). Revival of the samples was conducted according to the same protocol. All buffers and solutions used were sterile and anaerobic.

The fresh fermenter sample was centrifuged twice at 1500 g for 10 min. After the first centrifugation the pellet was resuspended in phosphate buffer (50 mM KH_2PO_4, 50 mM K_2HPO_4, 1 g/L sodium thyoglycolate). After a second centrifugation step, the resuspended pellet was used as inoculum.

Marine sediment samples and cow rumen samples were revived from the -80°C stock according to the procedure from Kerckhof et al. (2014). Marine samples were washed with 3.5% NaCl instead of phosphate buffer.

The human fecal sample and wallaby sample were kept anaerobic after collection using an anaeroGen bag (Oxoid, AN0035A), and treated within 8 hours. A 40% (w/v) solution of fecal material in phosphate buffer was prepared and homogenized using a stomacher (LabBlender 400, LEDTechno). After 5 minutes the homogenized solution was centrifuged at 500 g (2 min). The supernatant was used as inoculum. The wallaby fecal sample was prepared according to the same procedure, but using general homoacetogenic medium as buffer.

Inoculation and cultivation strategy

The prepared sample was used as inoculum for a series of hungate tubes. The sample was used for inoculation of the first tube and then increasingly diluted by transferring a small volume (0.1 mL) into the next 10 mL tube (1% transfer). A maximal dilution of 10^{-13} compared to the prepared inoculum was used. Per condition tested, 1 series of dilutions was prepared. The first transfer into fresh medium took place after either 4 days (“fast” cultures) or 11 days (“slow” cultures) of incubation at the selected temperature. Transfers (1%) took place under sterile anaerobic conditions. For each condition, the culture with the highest dilution that showed growth and production (based on visual inspection, optical density (OD) measurements and carboxylic acid measurement) was transferred, as well as the 1 time more and 1 time less diluted cultures. In any case the lowest dilution was transferred after 4 days and 11 days as well. After the initial fast or slow transfer, all cultures were transferred weekly for 3 or 4 consecutive weeks and incubated at the selected condition. Cultivation was considered successful if the total COD of the soluble products was higher than the COD of the original medium (0.8 g/L). The pH was not controlled during the enrichments.

Analytical methods

Before a transfer, samples were taken for analysis of the OD, carboxylic acids and pH. The OD was measured at a wave length of 620 nm using a multi-well plate reader (spectrophotometer,

Tecan infinite M200 Pro, Magellan software; Tecan, Switzerland). No calibration curve or blanks were included and therefore the OD was only a relative indication of growth. Carboxylic acids and pH were measured as described in Chapter 3. Gas measurements included a measurement of the headspace pressure (handheld tensiometer, WIKA, The Netherlands) and gas composition using a gas chromatograph (as described in Chapter 3).

1.3 Results and discussion

Acetic acid production was targeted in the enrichment experiments. Only results from the lowest dilution will be discussed. This dilution was always transferred for each condition and furthermore gave the best results for all 5 inocula tested. The presence of homoacetogens in the original samples and their growth yield had thus been overestimated. All figures in the following sections are marked with a same code to identify the sampling times. The "S" indicates a subculture (with x the number of transfers), "D" stands for day and indicates that the culture was not transferred since the previous measurement (with x the number of days since the start of the enrichment). Thus, the code S*x* on the horizontal axis means that the culture has been subcultured after the previous measurement such that in one week the concentration had been building up from near zero (1% transfer) to the apparent value. Indication of D*x* means that the concentrations had been building up during the time indicated by the number x, as no transfer took place in between. If results or trends were very similar for the fast as for the slow growing cultures, data for the slow growing cultures are omitted.

Fermenter effluent

Growth was initially observed at several conditions, for dilutions up to 10^{-7}. On the longer term, acetic acid was only detected in cultures initially diluted at 10^{-3}. For the "fast cultures" the best results were obtained at 37°C, for both pH values (Figure App. 1.1 and Figure App 1.2). Concentrations up to 2 g/L acetic acid were obtained, which corresponds to 2.1 g/L COD. The proportion of acetic acid and the concentration of acetic acid increased over the subsequent transfers (Table App. 1.2). Methane was not produced throughout any of the fermenter enrichments.

The original sample was obtained from a fermenter operating at 34°C, close to the temperature of 37°C at which the best results were obtained during the enrichment. The UASB fermenter was in fact already an enriched system, pushed toward the production of MCCAs. The absence of methanogenesis in that reactor system was beneficial for the enrichment procedure. Homoacetogenesis is a pathway typically present in anaerobic production fermentation environments (Angenent et al., 2004). High rate production could thus be expected for this enrichment strategy. A similar enrichment procedure had been used by Patil et al. (2015a),

however, faster transfers (every 2 days) were needed to eliminate methanogenic activity, as the original sample was obtained from a methanogenic UASB reactor. The experimental results presented here confirm that fermenter samples are a good source of inoculum. Several MES studies using this type of inoculum have already been published, but without pre-enrichment the use of methanogenic inhibitors was needed to promote acetic acid production (Marshall et al., 2012; Su et al., 2013).

Pre-enrichment of the culture could also lead to the elimination of other competitive pathways such as sulfate reduction. In MES reactor experiments with unenriched fermenter samples (setup and operation as described by Patil et al. (2015a)), SCCA concentrations were steadily decreasing over time (data not shown). No H_2 was detected in those experiments, whereas H_2 evolution was expected based on abiotic experiments and CV analysis. It was hypothesized that sulfate reducing bacteria (SRB) present in the unenriched fermenter inoculum utilized the SCCA and H_2 as electron donor and carbon source for reduction of sulfate and growth. Although no SO_4^{2-} is added to the general homoatogenic medium, cross-over of the Na_2SO_4 used as anolyte had occurred over the CEM. The hypothesis of presence of SRB was not confirmed by sequencing, but the medium had turned yellow during the experiment, a color typical for polysulfide (Johnston, 2013). Furthermore, sulfate reduction with a biocathode has been described (Coma et al., 2013). Patil and co-workers did not detect metabolic activity that could be associated with SRB (Patil et al., 2015a)). These results show that pre-enrichment in sulfate-free medium could be a good strategy to eliminate SRB.

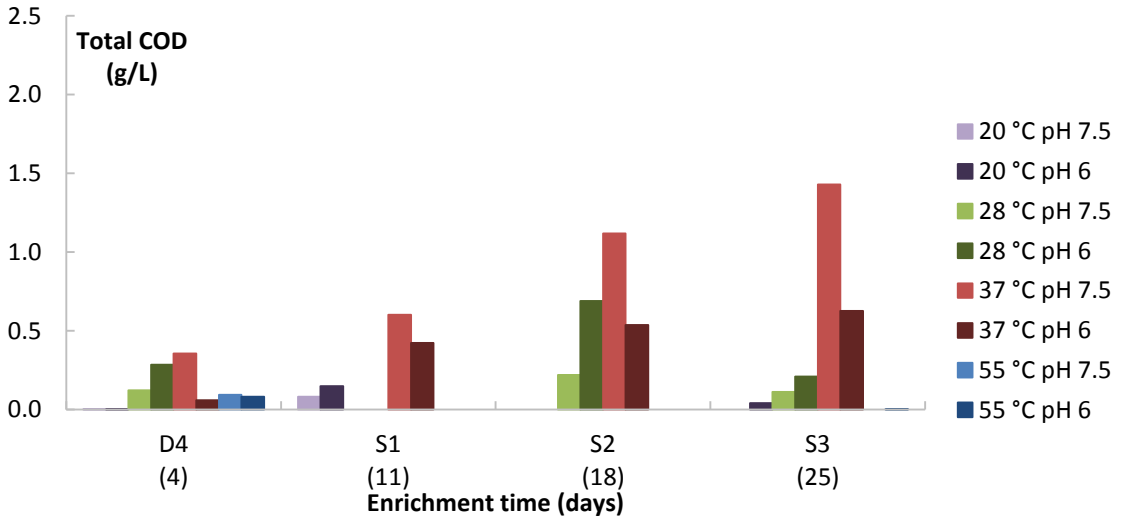

Figure App. 1.1 - Enrichment of the "fast" growing fermenter inoculum resulted in successful enrichment for cultures at 37°C

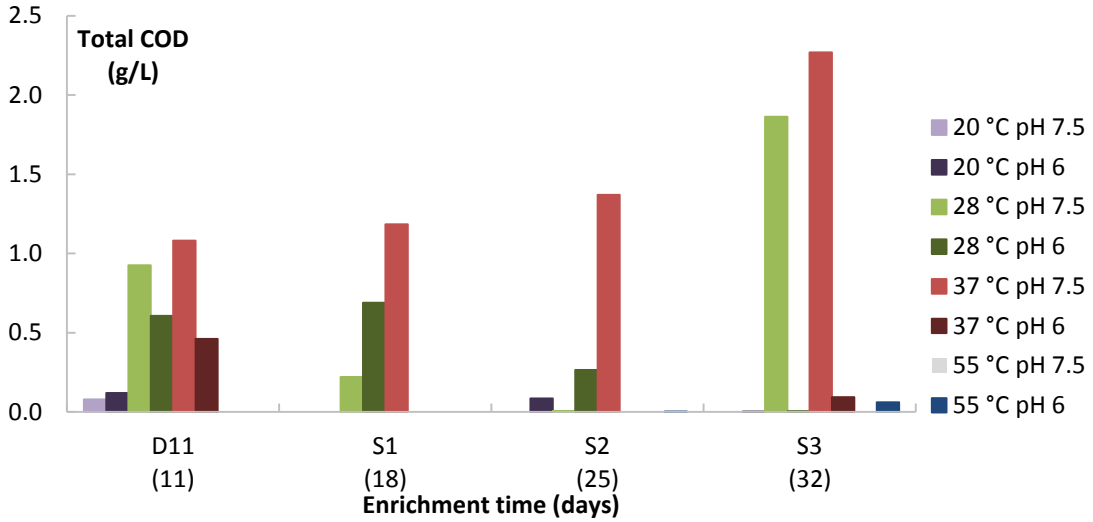

Figure App. 1.2 - Enrichment of the "slow" growing fermenter inoculum resulted in successful enrichment for cultures at 37°C, pH 7.5 and 28°C, pH 7.5

Table App. 1.2 - Acetic acid concentrations and proportions increased throughout the enrichment. Both for the "fast" and "slow" cultures the three best enrichment conditions are represented.

Successful enrichment condition	Acetic acid (% COD and concentration), D4	Acetic acid (% COD and concentration), S3, fast	Acetic acid (% COD and concentration), S3, slow
37°C, pH 7.5	92 (309 mg/L)	95 (1279 mg/L)	97 (2059 mg/L)
37°C, pH 6	85 (47 mg/L)	91 (532 mg/L)	52 (46 mg/L)
28°C, pH 7.5	57 (66 mg/L)	-	97 (1689 mg/L)
28°C, pH 6	49 (132 mg/L)	78 (154 mg/L)	-

Marine sediment sample

No successful enrichment of homoacetogens could be obtained from the chosen marine sediment sample, under the tested conditions (data not shown). A lower initial dilution had been chosen (10^{-2}) because of the low biomass density of the sediment sample. After the initial 4 days of incubation, growth was visually detected in two conditions: 20°C and 28°C at pH 7.5. These cultures were transferred to obtain fast growing cultures, however, SCCAs were not detected in the cultures, neither after 4 nor after 11 days of incubation, nor in the subcultures. The samples at the lowest dilution were further incubated for 5 months, without positive outcome. Methane was not detected in the gas phase.

Marine samples are of interest for MES because microorganisms in this environment are tolerant to low temperatures and high salinities. MES operation at low temperature can decrease the operational cost. The tolerance to high salinity would allow the use of highly conductive media for MES, decreasing overpotentials. It is clear that the conditions tested do

not reflect the natural environment of the samples. The use of a medium with a higher salinity, closer to the composition of seawater should be considered, as well as the use of a higher biomass concentration for the initial incubation. The use of fresh marine samples (rather than samples stored at -80°C) should further increase the chance of a successful enrichment.

Human fecal sample

Some production was obtained throughout the enrichment of the human fecal samples, but none of the conditions tested resulted in production above the COD concentration of the original medium (Figure App. 1.3 and Figure App. 1.4). A prolonged incubation of the D11 cultures and S4 cultures did not result in increased product output. The product spectrum was broader compared to the fermenter sample: also propionate and succinate were produced, while acetic acid accounted for approximately 50% of the soluble COD on D4. The proportion of acetic acid did not increase throughout the enrichment (data not shown). Propionate and succinate could be products of interest if produced from CO_2. Due to the low product concentrations it can, however, not be concluded if CO_2-based production took place, or if the yeast extract was metabolized.

Fermenting organisms are a key player in the human gut. All metabolic components for H_2/CO_2 utilization are present in the microbial community (Rey et al., 2010). It is therefore surprising that results of this enrichment were negative. The sample preparation method is generally used for experimental work with fecal material and is therefore most likely not responsible for the low productivity of the cultures. Possibly a lower dilution of the original sample could have improved the product outcome.

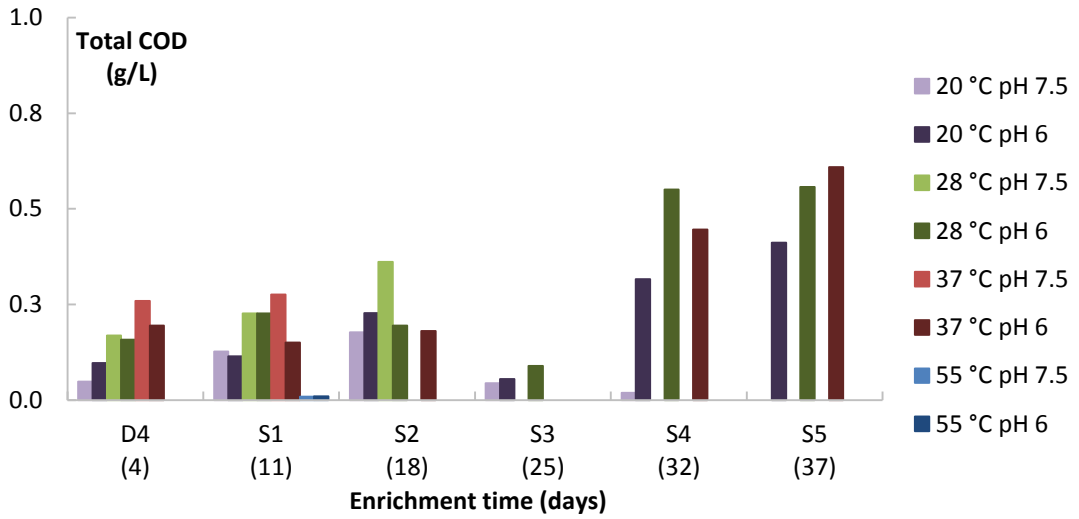

Figure App. 1.3 - Enrichments of the "fast" growing human fecal sample did not result in successful enrichment even after prolonged subculturing. Probably the yeast extract was mainly metabolized.

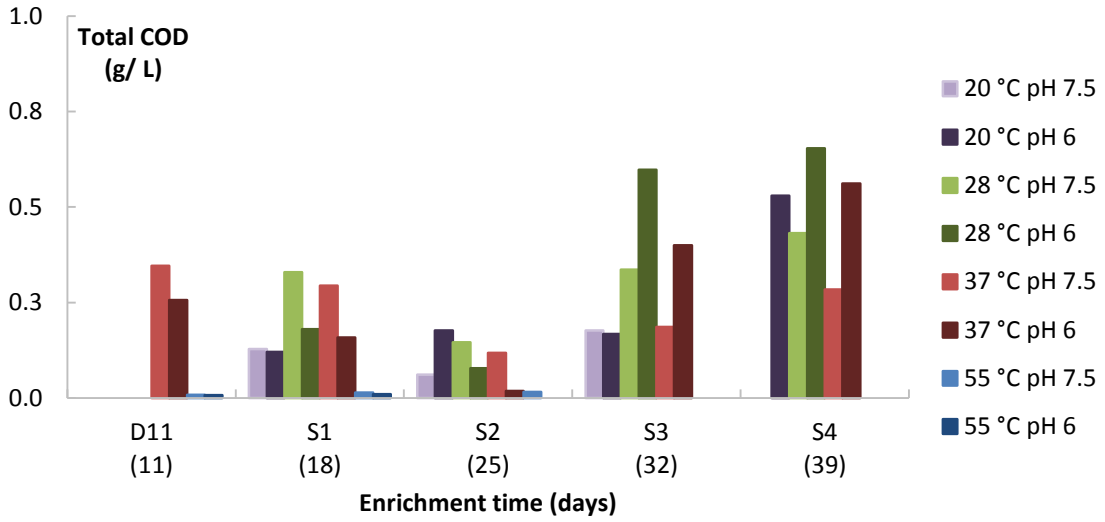

Figure App. 1.4 - Enrichments of the "slow" growing human fecal sample did not result in successful enrichment of homoacetogens.

Cow rumen sample

The cow rumen sample used for enrichment had been stored at -80°C prior to use. Production remained below the COD concentration of the original medium (Figure App. 1.5). A general trend of decreasing productivity was observed in the subsequent subcultures. Similar to the human fecal sample, succinate was also produced. A four-day follow-up experiment on S4 cultures (started on day 25) showed that most production took place within one day (data not shown). This suggests that the easily assimilable COD of the yeast extract was converted to products, and that little or no autotrophic production took place. Two subcultures were kept for prolonged incubation (28°C, pH 7.5, culture S3 and S4). Acetic acid concentrations in these samples increased to 1893 and 2026 mg/L after 3 months. The selectivity toward acetic acid was high as acetic acid COD accounted for more than 95% of the soluble COD in the sample. A subsequent transfer did not show rapid acetic acid production (rate below 0.1 g COD/L/d). Possibly the storage at -80°C had negatively affect the culture, resulting in low production rates and decreased activity. As for other unsuccessful enrichments, a lower dilution might contribute to improved results. Although methanogens are typically present in the gastro-intestinal tract of cows, no CH_4 was detected during the enrichments. In case fresh inoculum would be used at lower dilutions a strategy involving rapid transfers to wash out methanogens might be necessary.

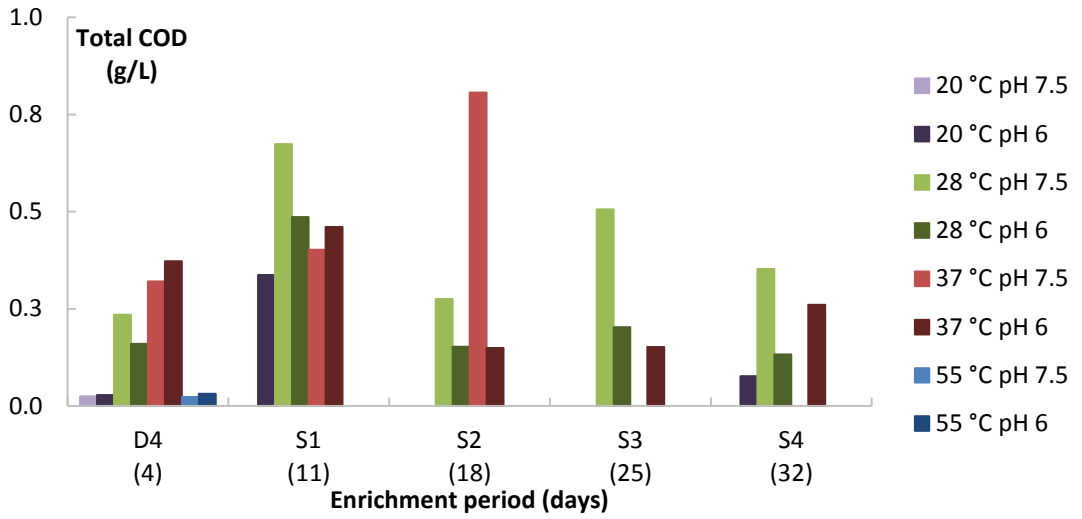

Figure App. 1.5 - Enrichments of the "fast" growing cow rumen sample did not result in successful enrichment. Data for the slow growing cultures were similar and are therefore omitted.

Wallaby fecal sample

Wallaby fecal samples were only enriched at 28°C and 37°C, the two temperatures closest to the body temperature of Wallabies (36°C) (Dawson & Hulbert, 1970). Wallabies and cows eat the same type of food (mainly grass), but in contrast to cows, the residence time in the gastro-intestinal tract of wallabies is short (cows > 40h, wallaby < 35h; (Mambrini & Peyraud, 1997; Danks, 2012). It was therefore hypothesized that fermenting organisms would be more abundant than the slower-growing methanogens. To increase the probability of successful enrichments, additional low dilutions (10^{0} – 10^{-1} – 10^{-2}) were tested and only fast-growing cultures (initial transfer after 4 days) were considered. Methane production took place in 3 initial cultures (37°C): at pH 7.5 for the cultures 10^{0} and 10^{-1}, and pH 6 for the 10^{0} culture. In these cultures the H_2 was almost completely consumed after 4 days. The 10^{0}, 10^{-1}, and 10^{-3} cultures were transferred and subcultures according to the same protocol as for the other enrichments. The subcultures obtained from the 10^{-3} dilution were less successful than the subcultures obtained from lower dilutions (Figure App. 1.6 and Figure App. 1.7). Methanogenic activity was not detected in the subcultures within the 7 day incubation period but instead the production of SCCAs increased. A prolonged incubation of subcultures for 21 days resulted in CH_4 production (data not shown). The methanogens were thus not completely removed after 4 1% transfers. Possibly, faster transfers could lower the concentration of methanogens in the culture. Homoacetogens, however, showed a higher activity as acetic acid was the dominant product after 7 days of incubation.

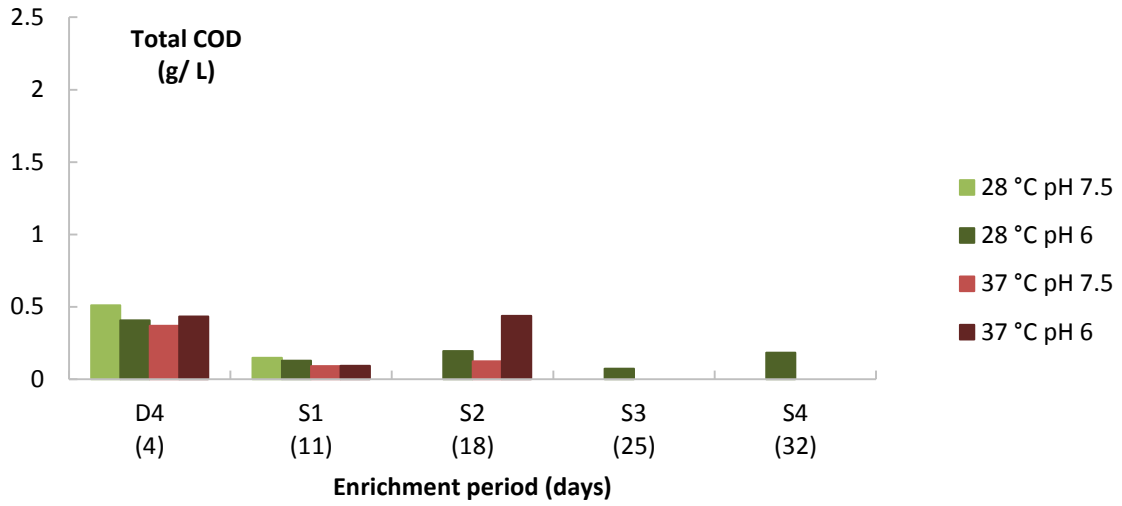

Figure App. 1.6 - Enrichments of the "fast" growing wallaby fecal sample did not result in successful enrichment when starting from a 10^{-3} dilution.

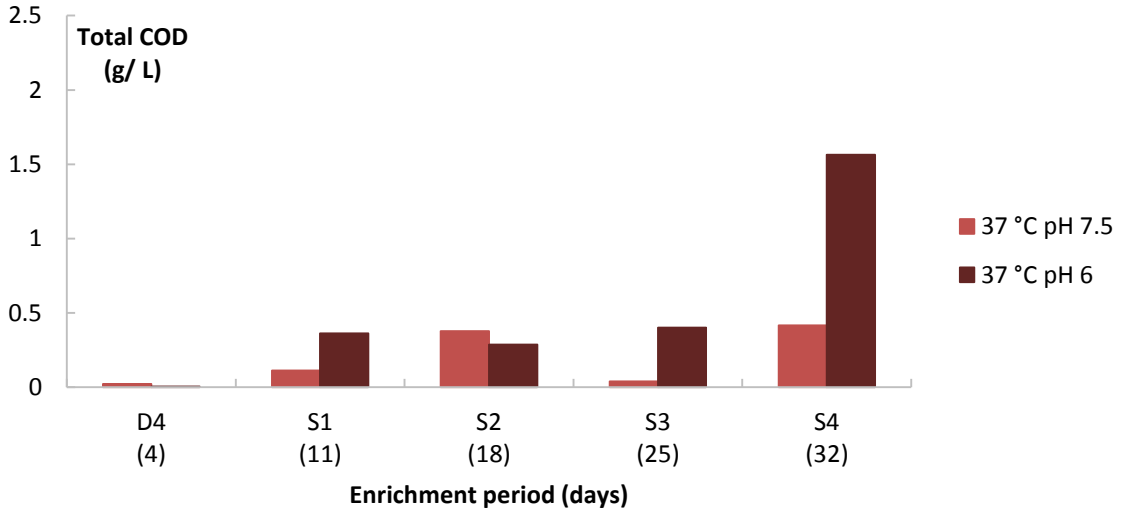

Figure App. 1.7 - Enrichments of the "fast" growing wallaby fecal sample was successful enrichment when starting from a 10^{0} dilution. In the initial incubation methane was produced instead of acetic acid. Acetic acid production increased over subsequent transfers.

1.4 Recommendations for future enrichments

Homoacetogens could be successfully enriched in several environmental samples. In the fermenter sample, homoacetogenic activity was expected and a culture producing acetic acid at high selectivity could be obtained. The wallaby fecal sample also showed high homoacetogenic activity. Enrichment at conditions close to the original environment was beneficial in both cases. For the marine sediment sample the tested conditions were most likely too different from the environmental conditions. As the use of high conductivities is of interest, an adapted enrichment strategy using marine media should be considered.

Storage of the samples at -80°C was detrimental for the enrichment procedure. Preferably fresh inoculum samples should be used. The storage procedure proposed by Kerckhof et al. (2014) was tested on three different environmental samples in that study and the activity of the cultures could be preserved over storage. This is in contrast to the results presented here, where stored samples did not result in successful enrichments. Undoubtedly microorganisms do suffer from this procedure. The enrichment medium and conditions are furthermore very different from the original environment. A concentration step before storage and the use of lower dilutions after reviving could increase the chance of successful enrichments in case storage is required.

The use of lower dilutions might in all cases be required to increase the success rate. It should be pointed out, however, that the competition between the different microbial pathways present in the inoculum will also be higher in that case. Increasing the selective pressure will then be necessary. Competition with the slower growing methanogens can be decreased by quickly transferring the culture several times. A single additions of the inhibitor 2-bromo-ethane sulphonate could also be considered to inhibit methanogenic activity (Patil et al., 2015a). When possible, SO_4^{2-} can be omitted from the medium to avoid competition with SRB. In the case of marine media this would be challenging, as SO_4^{2-} is an important component of seawater. Sodium molybdate is an effective inhibitor of SRB, that has little or no effect on fermenting bacteria (Sørensen et al., 1981). Adding the inhibitor during enrichment is a more sustainable alternative to additions during reactor operation.

Also new sources of inoculum, such as termites, should be considered. It is estimated that up to 33% of the acetic present in the termite gut is produced through H_2/CO_2 fermentation (Breznak & Switzer, 1986). The high selective pressure in these natural environments, as well as engineered environments such as fermenters is beneficial to the enrichment of targeted pathways.

2. The use of a bioanode *vs.* an electrochemical anode: summary of advantages and disadvantages using urine treatment as example

This section was redrafted after: "Gildemyn, S., Luther, A.K., Andersen, S.J., Desloover, J. and Rabaey, K. (2015) Electrochemically and Bioelectrochemically Induced Ammonium Recovery. JoVE (95), e52405."

2.1 Background

In BESs, the anodic oxidation reaction and cathodic reduction reaction are physically separated. One of these reactions, at least, is catalyzed by electroactive microorganisms, either producing electricity (MFC) or consuming electricity (MEC). When focusing on MECs, three types of configurations can be distinguished: i) a bioanode coupled to an abiotic cathode; ii) a biocathode coupled to an abiotic anode; or iii) the combination of a bioanode and biocathode (see Chapter 1).

In scenario i), the oxidation reaction catalyzed by the microorganisms, e.g. the treatment of wastewater, is coupled to an electrochemical reduction which can result in the production of H_2, caustic, or H_2O_2. Scenario ii) is the configuration most usually selected for MES. The combination of one electrochemical reaction and one biological reaction, as for scenario i), lowers the number of operational parameters that need to be actively controlled. Configuration iii) has been tested for MES, by combining sulfide oxidation and acetic acid production ((Gong et al., 2012); Chapter 1, Chapter 3).

While in scenario i) some of the products obtained cannot be produced biologically and therefore require the use of a chemical cathode, the biocathode reaction in ii) can in principle be coupled to any reaction at the anode.

In this technical note, the use of either a bioanode or electrochemical anode for the recovery of ammonium from ammonium-rich streams such as urine is studied. In this case, the electrochemical system consists of an anode chamber, a cathode chamber and an ion selective membrane to separate the compartments. A voltage is applied across the cell to produce a current flow from anode to cathode. To close the circuit and maintain the charge balance, a charged species must migrate between the electrodes for each electron generated. Ammonium transport from the anode chamber to the cathode chamber across a CEM can compensate the flux of electrons. The cell potential applied to drive this reaction can be generated by an external power source to drive water oxidation and reduction reactions. Alternatively the anodic oxidation, e.g., of organics, can be catalyzed by electroactive bacteria, requiring less overall

power input. In both cases the abiotic cathodic reduction leads to the production of H_2 and OH^-. The increased pH (to levels at or above the pKa of NH_4^+, 9.25) results in the formation of ammonia, that can be stripped and recovered (Desloover et al., 2012a). The advantages and disadvantages of the use of a bioanode or chemical anode to drive water reduction and ammonia recovery were investigated.

2.2 Materials and Methods

An electrochemical cell with a stripping unit attached, was constructed as described by Desloover et al. (2012a) and Gildemyn et al. (2015a). In short, the (bio)electrochemical cell consisted of Perspex frames and end-plates, with a CEM (64 cm², Membranes International, USA) separating the anode and cathode chamber. Graphite felt was used as anode material in the bioelectrochemical cell, while a stable anode (titanium-coated TiO_2/IrO_2 (35/65%) mesh, Magneto Special Anodes, the Netherlands), was used for the electrochemical system. Stainless steel mesh was used as cathode (Solana, Belgium). A reference electrode (Ag/AgCl, Bio-Logic, France) was placed in each anode compartment. The system was connected to a potentiostat (VSP, Bio-Logic, France). The catholyte was recirculated through a spray nozzle over a stripping column packed with Raschig rings (4 x 4 mm, Saillart, Belgium); gas was recirculated from the bottom of the column. The ammonia loaded gas was subsequently bubbled through an absorption solution (1 M sulfuric acid), resulting in the formation of ammonium sulfate (Figure App 1.8). The gas was recirculated either in an open loop or closed loop (Desloover et al., 2012a; Gildemyn et al., 2015a).

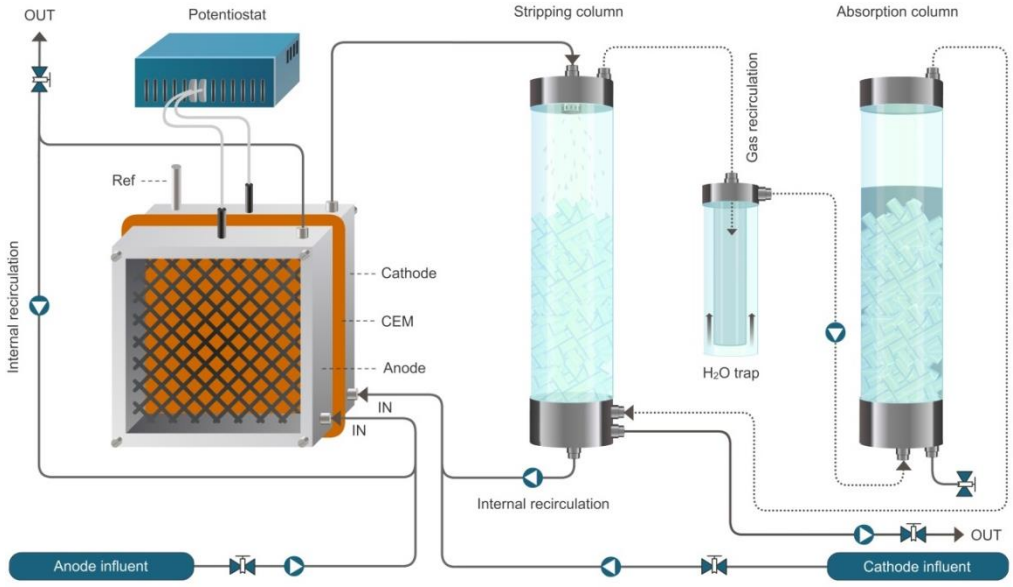

Figure App. 1.8 - Scheme of the setup used for electrochemical recovery of ammonium from ammonium-rich streams. The ammonium extracted over the cation exchange membrane (CEM) is stripped out of the solution and recovered as ammonium sulfate. The bioelectrochemical cell is similar, but with a graphite felt anode instead of iridium oxide mesh. Ref: reference electrode.

To allow caustic production, 0.1 M NaCl was used as catholyte in both systems. The anolyte for bioelectrochemical extraction of ammonium was a modified M9 medium with sodium acetate as carbon source, as described in Gildemyn et al. (2015a). The nitrogen content (as ammonium bicarbonate) was increased gradually to mimic a nitrogen-rich waste stream (Table App. 1.3). The acetate concentration was increased as well, in order not to limit the current production and supply enough electrons to extract all ammonium. The anolyte for the electrochemical extraction consisted of synthetic wastewater and is described in Desloover et al. (2012a). No chloride was added to avoid Cl_2 production at the anode. Nitrogen was added as ammonium sulfate to obtain a final concentration of 1, 3 or 5 g N/L.

Table App. 1.3 - Amount of ammonium bicarbonate added to the anolyte of the bioelectrochemical cell to mimic a nitrogen-rich waste stream

Time	Amount of NH_4HCO_3 added to the anode feed (g/L)	Phase
Day 0 – Day 16	2.26	I
Day 16 – Day 26	4.5	II
Day 26 – Day 33	9	III
Day 33 – Day 40	14.1	IV
Day 40 – Day 47	20	V
Day 47 – Day 54	25.4	VI
Day 54 – Day 63	31	VII

The following parameters were measured as described by Gildemyn et al. (2015a) and Desloover et al. (2012a): current density (A/m²), electrode potentials (V *vs.* Ag/AgCl), cell potential, total ammonia nitrogen (TAN) concentration in the anode and cathode effluent, and absorption column, and pH and conductivity of the electrolytes and absorption column.

2.3 Calculations

To evaluate the systems several parameters are calculated based on the measured variables.

The current production by the bioreactor

This is best represented as current density, which is calculated as follows (Equation 1, (Harnisch & Rabaey, 2012)):

$$j\left(\frac{A}{m^2}\right) = \frac{I\,(A)}{A_e\,(m^2)} \quad \text{EQ. 1}$$

with j as the current density, I the absolute current, and A_e the projected surface area of the electrode.

The nitrogen flux

Nitrogen flux (g N /m²/d) is normalized to the membrane surface area recalculated to a current density (I_N). This value is then used to calculate the current efficiency (CE; Equation 2, 3, and 4):

$$J_N = \frac{(C_{An,in} - C_{An,out}) \times Q}{A_m} \quad \text{EQ. 2}$$

where $C_{An,in}$ (g N/L) and $C_{An,out}$ (g N/L) are the measured ammonium concentrations coming in and out the anode compartment, respectively. Q (L/d) is the anode flow rate and A_m (m^2) is the membrane surface area (equal to projected anode and cathode surface area).

The nitrogen flux presented as current density

The nitrogen flux can be presented as a current density (I_N, A/m²):

$$I_N = \frac{J_N \times z_{NH_4^+} \times F}{M \times 86400 \text{ s d}^{-1}} \quad \text{EQ. 3}$$

where z_{NH4+} (-) is the charge of NH_4^+, F the Faraday constant (96485 C/mol) and M the molecular weight of nitrogen (14 g/mol).

The current efficiency then follows as:

$$CE = \frac{I_N}{I_{Applied}} \times 100 \quad \text{EQ. 4}$$

where $I_{Applied}$ (A/m²) is the applied (electrochemical extraction) or measured (bioelectrochemical extraction) current density.

The theoretical nitrogen flux

The maximum theoretical nitrogen flux ($J_{N,Max}$, g N/m²/d) can be calculated for a given applied current and membrane surface area (Equation 5) and is calculated as:

$$J_{N,max} = \frac{I_{Applied} \times z_{NH_4^+} \times M \times 86400 \text{ s d}^{-1}}{F \times A} \quad \text{EQ. 5}$$

The nitrogen removal efficiency (RE, %)

The percentage of ammonium that is removed from the anolyte is referred to as the removal efficiency. This is calculated from the anode influent and effluent TAN concentrations (Equation 6).

$$RE = \frac{C_{AN,in} - C_{AN,out}}{C_{AN,in}} \times 100 \quad \text{EQ. 6}$$

The maximum theoretical nitrogen removal efficiency (RE_{max}, %).

This can be calculated for a given influent TAN load and applied current (Equation 7):

$$RE_{max} = \frac{J_{N,applied} \times A}{C_{An,in} \times Q} \times 100 \quad \text{EQ. 7}$$

where $J_{N,applied}$ (g N m^{-2} d^{-1}) is the applied current density expressed as a nitrogen flux.

The gas/liquid ratio

The gas/liquid ratio influences the stripping efficiency and is calculated as (Equation 8)

$$\left(\frac{G}{L}\right) = \frac{\text{Gas flow rate } (\frac{m^3}{h})}{\text{Liquid flow rate } (\frac{m^3}{h})} \quad \text{EQ. 8}$$

The maximal capacity of the absorption column.

The maximum theoretical N load to the absorption column can be calculated from the maximum theoretical nitrogen flux J_{Nmax}, the TAN concentration in the influent (mol/L), the time of operation t, the membrane surface area A, and the volume of absorbent V (Equation 9):

$$H_2SO_4 \text{ (mol/L)} = \frac{J_{Nmax} \times \frac{TAN}{14} \times A \times t}{\frac{2}{V}} \quad \text{EQ. 9}$$

The stripping efficiency SE (%)

The liquid recirculation rate and the air pump performance can be adjusted in order to obtain higher stripping efficiency. The choice of an open or closed air circulation loop will also have an effect on the stripping efficiency. An open air stream is favorable when the absorption efficiency is high and all the NH_3 gas is trapped during its passage through the acid. The open air system ensures that the air going through the stripping column is free of ammonia, resulting in a higher

driving force for the conversion of dissolved NH_3 to gaseous NH_3. In case of a low absorption efficiency the closed system will prevent ammonia losses. The ammonia gas captured in the gas flow must be absorbed into an acid solution to make the stripping process thermodynamically favorable, as expressed by the principle of Le Chatelier (Atkins & De Paula, 2012). When the pH of the absorbent starts to rise it must be replaced, as this indicates that there are no longer protons available to protonate the ammonia. The absorption capacity can be estimated beforehand. For every mole of H_2SO_4, 2 moles of N from NH_3 can be captured.

The stripping efficiency (SE, %) is calculated based on the ammonia nitrogen removed from the anode, and the cathode effluent concentration ($C_{CAT,out}$). This method is more accurate than methods using the measured TAN from the absorption column as these are subject to evaporation/precipitation. It is important to note that Equation 10 is only valid for equal flow rates of the anolyte and catholyte.

$$\mathrm{SE} = \frac{\mathrm{C_{AN,in}} - \mathrm{C_{AN,out}} - \mathrm{C_{CAT,out}}}{\mathrm{C_{AN,in}}} \mathrm{x}\ 100 \quad \text{EQ. 10}$$

Energy input

The energy input for ammonium extraction through the CEM (E_N, expressed as kWh/kg N) (Equation 11)

$$\mathrm{E_N} = \frac{\mathrm{j} * \mathrm{A} * \Delta\mathrm{V} * 24 / 1000}{(\mathrm{C_{An,in}} - \mathrm{C_{An,out}})\ \mathrm{x}\ \mathrm{Q}} \quad \text{EQ. 11}$$

With ΔV the measured potential difference between anode and cathode. In the case of the bioreactor, ΔV was calculated as the average for the sampling period, for the electrochemical reactor the average for the entire run is taken.

2.4 Results

Chronoamperometry results for the bioreactor

The chronoamperometry results, calculated according to Equation 1, show a typical graph for a continuous reactor (Figure App. 1.9). At the start of the experiment, the anode and cathode were operated in recirculation mode. This allows a biofilm to develop and the onset of the current production. After 5 days of operation, the current density reached a maximum, followed by a decrease in current production. This is an indication that the biofilm lacked a carbon/electron source (e.g., acetate) to produce current. The change to continuous operation on day 6, using an HRT of 6 hours, resulted in a continuous increase in current production until a

plateau was reached at 3.5 A/m² between day 12 and 16. A plateau was necessary to obtain sufficient data on ammonium extraction for a certain current density. The effect of the temperature was clearly visible in the bioelectrochemical test presented here. Daily variations between night (cold, low current) and day (warm, high current) can be seen, in particular between day 42 and 46, when no other factors such as low availability of carbon source were inhibiting the bacterial activity (Liu et al., 2005a; Clauwaert et al., 2008a).

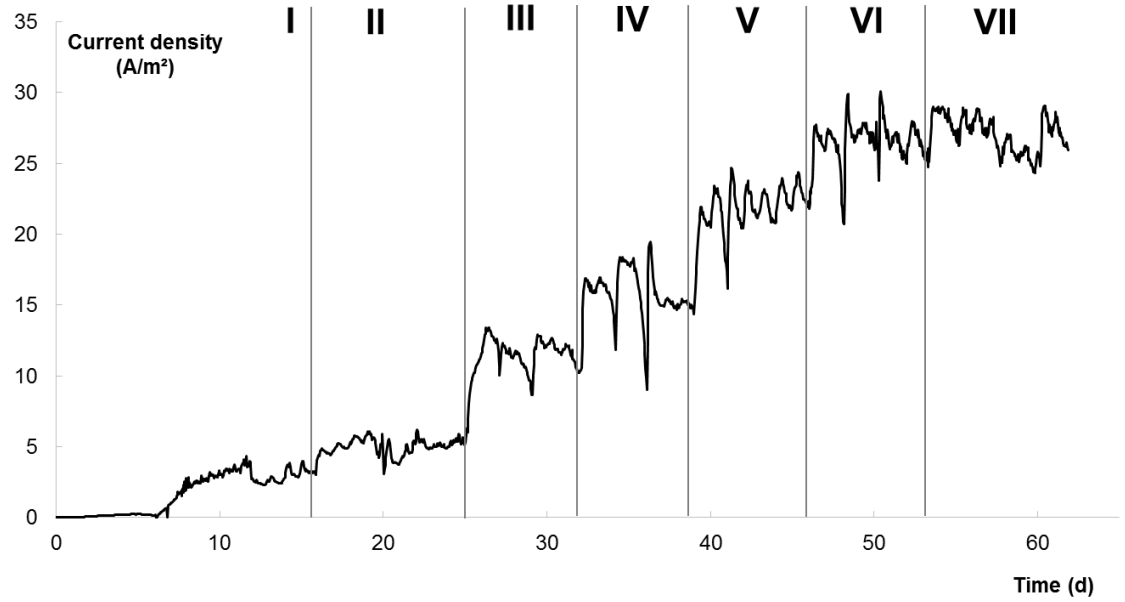

Figure App. 1.9 - Current production (A/m²) for the bioreactor over time. The current density increased for increasing ammonium concentrations when acetate concentrations where not limiting.

The ammonium concentration in the feed was increased in several steps from 2.26 g/L NH_4CO_3 to 31 g/L NH_4CO_3. Each step resulted in an increase of the current density that ultimately reached an average current of 27 A/m². This current increase was linked to an increased conductivity of the anode feed, in which the addition of ammonium bicarbonate increased the concentration of ions and thus the conductivity. A higher conductivity decreases ohmic resistance and thus favors current production (Clauwaert et al., 2008a).

Acetate measurements showed the complete removal of the carbon source by the anodic biofilm from day 27 to 37. During this period, the current density produced by the biofilm decreased prior to medium change. As the medium was not kept in sterile conditions, the acetate concentration in the feed dropped over time due to consumption by non-electroactive microorganisms in the feed bottle. The current density increased again as soon as the medium was replenished. This indicated that the current production by the biofilm was limited by the carbon source concentration in the feed. Several increases in acetate concentration were necessary to prevent carbon limitation in the second half of the test.

Cell potential

The cell potential is calculated based on the difference between the anode and cathode potential, the overpotentials at the electrodes and the Ohmic resistance. The cell potential relates to the total energy necessary to drive the electrochemical cell. For equations and elaboration on this topic, we refer to the review paper by Clauwaert and co-workers (Clauwaert et al., 2008a).

In the case of the biological ammonium extraction, the anode potential was fixed at -200 mV *vs.* Ag/AgCl and the biofilm produced the current. As a consequence, the cathode potential varied in order to sustain the current produced by the biofilm. In this case, the resistance across the cell affected the cathode potential. On day 16 the cell potential of the bioreactor started to increase although no increase in current was observed and the anode potential remained fixed at -200 mV *vs.* Ag/AgCl. This was a consequence of an increased resistance in the system, which may be a result of membrane resistance (e.g., scaling on the membrane) or diffusional limitations caused by poor mixing between the anode and the membrane. The reactor was carefully emptied and opened, and the membrane was replaced. The anode was placed further away from the membrane to improve mixing. The anode compartment was filled again with the anolyte that had been previously removed. This operation restored the cell potential to the same level as at the start of the continuous experiment (0.5 V), with the cathode potential stable around -700 mV *vs.* Ag/AgCl, indicating that the system performance was restored.

In the abiotic electrochemical extraction experiments, the cell potential is calculated similarly as for the bioelectrochemical extraction, including overpotentials and ohmic resistance. Both the anode and cathode potential were subject to variations. The cell voltage for the electrochemical system is higher than for the bioreactor (Table App. 1.4). This is mainly due to the higher anode potential required for electrochemical oxidation of water to oxygen. Specific anode and cathode potentials for the conditions tested are described by Desloover et al. (2012a).

Table App. 1.4 - Comparison of the cell potentials (V) for the bioreactor and electrochemical system at different current densities. The results for the bioreactor are calculated from steady state periods were the current density value reached between the indicated current density value ± 2 A/m². For the bioreactor the anolyte feed concentration increased from 1.62 g N/L (10 A/m²) to 5.1 g N/L (30/m²) across this range of currents. All values for the electrochemical system were calculated for a system operating at 5 g N/L in the anolyte feed. n.d.: not determined.

Current density	Bioanode (V)	Electrochemical system (V)
0 A/m²	n.d.	n.d.
10 A/m²	1.69 ± 0.05	2.73 ± 0.06
20 A/m²	2.20 ± 0.11	2.99 ± 0.08
30 A/m²	2.32 ± 0.14	3.35 ± 0.21

The electrochemical parameters presented in the two previous sections are the factors that determine the efficiency of ammonium extraction through the CEM. The following parameters are calculated in order to compare the performances of the biotic and abiotic systems in terms of ammonium extraction.

Nitrogen flux (J_N) and current efficiency (CE) of extraction

Ammonium ions cross the CEM to restore the charge balance over the cell. For each electron being released at the anode, one positive charge must be displaced from the anode to the cathode compartment. If ammonium restored 100% of the charge balance, one would obtain a current efficiency of 100%.

The nitrogen flux for the bioreactor was higher than for the electrochemical system (Figure App. 1.10). Comparison of the data is not straightforward as the nitrogen concentration in the anolyte was not the same for both systems. The last data points on the graph, however, allow a comparison. The bioreactor was treating an influent at 4.5 g N/L and 5.1 g N/L while producing an average current of 27 A/m². These conditions are similar those of the electrochemical cell where the applied current and influent nitrogen concentration were 30 A/m² and 5 g N/L respectively. This higher flux for the bioreactor can be explained by the difference in anolyte pH between the two systems. The higher pH in the case of the bioreactor anolyte resulted in less competition with protons for transport across the membrane. More ammonium cations were proportionally available to restore the charge balance compared to protons (0.2 ± 0.05 M NH_4^+ in anolyte *vs.* 10^{-7} M H^+). The well-buffered anolyte of the bioreactor is necessary to maintain stable conditions for electricity production by the electroactive bacteria, and is also an advantage for the ammonium extraction. This explains the higher current efficiency in the bioreactor as compared to the electrochemical system.

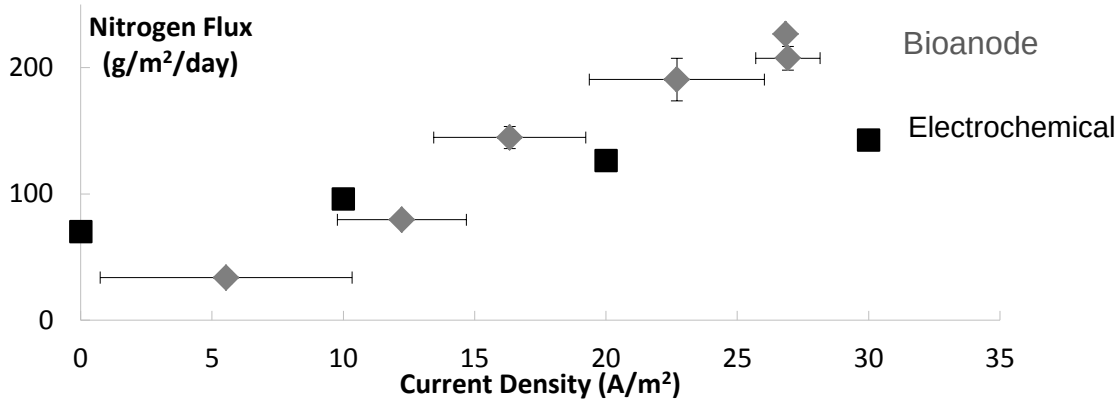

Figure App. 1.10 - The nitrogen flux for the bioreactor compared to the nitrogen flux for the electrochemical system for different current densities. The flux for the bioreactor is calculated for a range of total ammonia nitrogen concentration in the anode influent; for the electrochemical system the flux is given only for a concentration of 5 g N/L. The error bars (stdev) for the electrochemical system are smaller than the symbols.

Overall comparison of the biotic and abiotic systems

The bioreactor and the electrochemical system are compared for the most similar conditions of the test: a concentration of 5.1 g N/L for the bioreactor anolyte, which resulted in a current density of 27 A/m² and a concentration of 5 g N/L combined with an applied current density of 30 A/m² in the case of the electrochemical system (Table App. 1.5).

Table App. 1.5 - Overall comparison of the bioreactor and electrochemical system. The bioreactor was operating at steady state at 5.1 g N/L feed concentration, resulting in an average current density of 27 A/m². The electrochemical system was operated at 30 A/m² for a nitrogen feed concentration of 5 g/L.

Parameter	Bioanode	Electrochemical system
Current efficiency (%)	67.1 ± 0.28	38 ± 0.6
Removal efficiency (%)	51 ± 0.5	41 ± 2
Nitrogen flux (g N/m²/d)	226 ± 1	143 ± 7
Cell voltage (V)	2.12 ± 0.09	3.35 ± 0.21
Energy input (kWh/kg N removed)	6.04 ± 1.78	16.8 ± 1.4
Anolyte pH	7.39 ± 0.13	1.56 ± 0.14
Catholyte pH	12.53 ± 0.07	12.92 ± 0.08

2.5 Discussion

The bioelectrochemical and electrochemical system are similar in setup and function. The main operational difference between the two systems is the choice of a fixed anode potential for the bioelectrochemical setup *vs.* a fixed current for the electrochemical cell. For the BES, a fixed anode potential of -200 mV *vs.* Ag/AgCl was chosen to enable electron transfer to the electrode (Logan, 2009). The fixed current for the abiotic setup, on the other hand, is necessary to drive the electrode reactions and allows also allows for regulation of the processes in the bulk phase, thus leading to steady state conditions. The two-compartment electrochemical cell allows the extraction of ammonium over a membrane, driven by an electrical current. Each system presents certain advantages over the other.

The BES offers several advantages with regards to the cost of the system. The cost of the graphite felt anode is much lower than the cost for the stable anode used in the electrochemical system. For a 1 m² electrode surface, the capital costs of the anode is decreased by a factor of 10, from $1000 to $100 per m² (Korneel Rabaey, personal communication; Guo et al. (2014a)). The electroactive bacteria catalyze the anodic reaction at a lower potential as opposed to the electrochemical oxidation of water, which substantially reduces the operational cost of the bioreactor. Ammonia is also more efficiently extracted. In the electrochemical cell the extraction requires an energy input of 16.8 kWh/kg N extracted, while for the bioanode operating under the same conditions the energy input is more than halved to 6.04 kWh/kg N extracted. Other operational costs such as power for pumps and stripping and absorption are not included, but

are anticipated to be similar for both systems. An even lower energy input is obtained when using an MFC instead of an MEC. The low extraction rates obtained with an MFC (3.29 g/m²/d compared to > 140 g/m²/d in this study) make the investment of electrical energy in the case of the MEC attractive (Kuntke et al., 2012).

While cost favors the BES, operational stability and reproducibility is an advantage of the electrochemical cell. As a biological system, the electroactive biofilm is sensitive to the environment and can be easily be disrupted. The biofilm is sensitive to changes in pH, concentration of toxic compounds and changes in temperature. The influent should be well buffered to maintain the pH around 7. The anode reaction will enforce a pH decrease if the anolyte is not sufficiently buffered. This is a critical point to address when using the bioreactor for the treatment of real wastewater. To avoid influence of temperature, it is best to place the reactor in a temperature-controlled environment to exclude the influence of temperature on bacterial kinetics but this seems unlikely to be feasible at larger scale.

Another disadvantage is that the bioreactor requires a longer startup time. The biofilm develops over a few days on the electrode, but changes to the feed characteristics such as the TAN concentration must be applied gradually in order to reduce stress to the microbial biofilm. It thus took approximately 50 days to reach a stable system operated at a TAN concentration of 5 g/L. The electrochemical system only requires 24 h of polarization and 3 HRTs (total of 42 hours) to reach stable operating conditions.

An electrochemical system allows a greater degree of control over operational parameters. For example, the current density can be controlled to obtain an optimal ratio between product recovery and power input (Desloover et al., 2012a). Current densities higher than those presented here (over 30 A/m²) can be used, while for a BES the current production cannot be controlled in the present state-of-the-art. Limiting the carbon source, or providing excess carbon can alter the current output of the biological system, but as discussed in the results section more factors affect current production by the biofilm, thus making it difficult to optimize process parameters.

The conclusions above are also valid for an MES system, in the scenario (iii) where a bioanode would be coupled to a biocathode. The additional challenge would be to couple two biological reactions. The rate of these two reactions would have to be synchronized in order not to limit the kinetics of either the oxidation or reduction. If MES is the main aim of the process (rather than e.g. wastewater treatment at the anode), then the anode should be operated in such a way that enough reducing equivalents are continuously supplied for the reductive bioproduction, even if this would require a less efficient wastewater treatment. The risk associated to this

configuration probably makes its implementation less likely, as the two reactions are prone to failure, which would increase the time for recovery after a disturbance. Furthermore, if extraction is envisioned in a system as presented in Chapter 3, proton production at the anode is critical to produce acetic acid in the middle compartment. As operation at a pH around 7 is optimal for a bioanode, insufficient proton transfer to the middle compartment would hamper the acetate extraction, unless an acid-tolerant culture would be enriched.

Appendix 2 - Supplementary information for Chapter 2

Table App. 2.1 - Degree of reduction (γ) and Gibbs energy per electron $\Delta G_e^{0'}$ of specific compounds as defined in the Growth Reference System (biochemical standard conditions: 1 atm, 298.15 K, 1 mol/L, pH 7). Data from Heijnen (Heijnen, 1999) unless otherwise indicated.

Chemical Compound	Chemical Formula	γ (electrons)	$\Delta G_e^{0'}$ (kJ/e-mol)
Reference compounds			
Bicarbonate	HCO_3^-	0	0
Sulfate	SO_4^{2-}	0	0
Nitrate	NO_3^-	0	0
Water	H_2O	0	0
Proton	H^+	0	0
Halide ions	(F^-, Cl^-, Br^-, I^-)	0	0 [a]
Fe^{3+}	Fe^{3+}	0	0
Alkanes			
Methane	CH_4	8	22.925
Ethane	C_2H_6	14	25.404
Propane	C_3H_8	20	25.948
Carboxylic acids			
Formate	CHO_2^-	2	39.186
Acetate	$C_2H_3O_2^-$	8	26.801
Propionate	$C_3H_5O_2^-$	14	26.939
Butyrate	$C_4H_7O_2^-$	20	27.000
Oxalate	$C_2HO_4^-$	2	52.522
Citrate	$C_6H_7O_7^-$	18	32.282
Fumarate	$C_4H_3O_4^-$	12	33.662
Succinate	$C_4H_5O_4^-$	14	28.405
Lactate	$C_3H_5O_3^-$	12	31.488
Pyruvate	$C_3H_3O_3^-$	10	34.129
Gluconate	$C_6H_{11}O_7^-$	22	39.106
β-hydroxybutyrate	$C_4H_7O_3^-$	18	30.220 [a]
Carbohydrates			
Glucose	$C_6H_{12}O_6$	24	39.744
Fructose	$C_6H_{12}O_6$	24	39.820
Galactose	$C_6H_{12}O_6$	24	39.481

Sucrose	$C_{12}H_{22}O_{11}$	48	40.690
Glycogen (per glucose unit)	$C_6H_{10}O_5$	24	40.482
Alcohols			
Methanol	CH_4OH	6	36.032
Ethanol	C_2H_5OH	12	30.353
n-Propanol	C_3H_7OH	18	29.144
n-Butanol	C_4H_9OH	24	28.466 [a]
Ethylene glycol	$C_2H_6O_2$	10	37.292
Propanediol	$C_3H_8O_2$	16	33.177
Butanediol	$C_4H_{10}O_2$	22	31.374
Glycerol	$C_3H_8O_3$	14	37.625
Ketones/Aldehydes			
Formaldehyde	CH_2O	4	45.326
Acetone	C_3H_6O	16	28.718
Acetoin	$C_4H_8O_2$	20	32.625
Amino acids			
Aspartate	$C_4H_6NO_4^-$	20	5.313 [a]
Cysteine	$C_3H_7NO_2S$	26	8.926 [a]
Cystine	$C_6H_{12}N_2O_4S_2$	50	7.941 [a]
Glutamate	$C_5H_8NO_4^-$	26	10.056 [a]
Phenyl alanine	$C_9H_{11}NO_2$	48	17.862 [a]
Tryptophane	$C_{11}H_{12}N_2O_2$	62	12.582 [a]
Halogenated compounds			
Ethylene	C_2H_4	12	32.520 [b]
Chloroethylene	C_2H_3Cl	10	45.964 [b]
1,1-Dichloroethylene	$C_2H_2Cl_2$	8	65.426 [b]
cis-1,2-Dichloroethylene	$C_2H_2Cl_2$	8	64.873 [b]
trans-1,2-Dichloroethylene	$C_2H_2Cl_2$	8	65.405 [b]
Trichloroethylene	C_2HCl_3	6	101.296 [b]
Tetrachloroethylene	C_2Cl_4	4	175.286 [b]
Inorganic compounds			
Hydrogen	H_2	2	39.870
Carbon monoxide	CO	2	47.477
Sulfite	SO_3^{2-}	2	50.296
Sulfur	S^0	6	19.146
Thiosulfate	$S_2O_3^{2-}$	8	23.584
Polysulfide	S_5^{2-}	32	20.003 [c]
Bisulfide	HS^-	8	20.850
Nitrite	NO_2^-	2	-41.650

Nitric oxide	NO	3	-38.989 [d]
Nitrous oxide	N_2O	8	-57.540
Ammonium	NH_4^+	8	-35.109
Nitrogen	N_2	10	-72.194
Oxygen	O_2	-4	-78.719
Hydrogen peroxide	H_2O_2	-2	-130.23 [a]
Chlorate	ClO_3^-	-6	-59.424 [e]
Perchlorate	ClO_4^-	-8	-84.220 [e]
Fe^{2+}	Fe^{2+}	1	-74.270

[a] Calculated using Eq. (2) (Chapter 2) and thermodynamic data from Thauer et al. (1977).

[b] Calculated using Eq. (2) (Chapter 2) and thermodynamic data from Dolfing and Janssen (1994) and Thauer et al. (1977).

[c] Calculated using Eq. (2) (Chapter 2) and thermodynamic data from Bard et al. (1985) and Thauer et al. (1977).

[d] Corrected by authors from Heijnen (1999) using data from Thauer et al. (1977) and verified using Bard et al. (1985).

[e] Calculated from Weber et al. (2006)

Table App. 2.2 - Gibbs energy change $\Delta G_r^{0'}$ and equilibrium potential $E_r^{0'}$ of specific half reactions with bicarbonate as the electron acceptor. Calculated using the Growth Reference System (biochemical standard conditions: 1 atm, 298.15 K, 1 mol/L, pH 7). Data from Heijnen (Heijnen, 1999) unless otherwise indicated.

Half reaction (e-acceptor + x e^- ⇆ e-donor)	$\Delta G_r^{0'}$ (kJ/mol)	$E_r^{0'}$ (V)
Alkanes		
HCO_3^- + 9 H^+ + 8 e^- ⇆ Methane + 3 H_2O	183	-0.238
2 HCO_3^- + 16 H^+ + 14 e^- ⇆ Ethane + 6 H_2O	356	-0.263
3 HCO_3^- + 23 H^+ + 20 e^- ⇆ Propane + 9 H_2O	519	-0.269
Carboxylic acids		
HCO_3^- + 2 H^+ + 2 e^- ⇆ Formate + H_2O	78	-0.406
2 HCO_3^- + 9 H^+ + 8 e^- ⇆ Acetate + 4 H_2O	214	-0.278
3 HCO_3^- + 16 H^+ + 14 e^- ⇆ Propionate + 7 H_2O	377	-0.279
4 HCO_3^- + 23 H^+ + 20 e^- ⇆ Butyrate + 10 H_2O	540	-0.280
2 HCO_3^- + 3 H^+ + 2 e^- ⇆ Oxalate + 2 H_2O	105	-0.544
6 HCO_3^- + 23 H^+ + 18 e^- ⇆ Citrate + 11 H_2O	581	-0.335
4 HCO_3^- + 15 H^+ + 12 e^- ⇆ Fumarate + 8 H_2O	404	-0.349
4 HCO_3^- + 17 H^+ + 14 e^- ⇆ Succinate + 8 H_2O	398	-0.294
3 HCO_3^- + 14 H^+ + 12 e^- ⇆ Lactate + 6 H_2O	378	-0.326
3 HCO_3^- + 12 H^+ + 10 e^- ⇆ Pyruvate + 6 H_2O	341	-0.354
6 HCO_3^- + 27 H^+ + 22 e^- ⇆ Gluconate + 11 H_2O	860	-0.405
4 HCO_3^- + 21 H^+ + 18 e^- ⇆ β-hydroxybutyrate + 9 H_2O	544	-0.313
Carbohydrates		
6 HCO_3^- + 30 H^+ + 24 e^- ⇆ Glucose + 12 H_2O	954	-0.412
6 HCO_3^- + 30 H^+ + 24 e^- ⇆ Fructose + 12 H_2O	956	-0.413
6 HCO_3^- + 30 H^+ + 24 e^- ⇆ Galactose + 12 H_2O	948	-0.409
12 HCO_3^- + 60 H^+ + 48 e^- ⇆ Sucrose + 25 H_2O	1953	-0.422
6 HCO_3^- + 30 H^+ + 24 e^- ⇆ Glycogen + 13 H_2O	972	-0.420
Alcohols		
HCO_3^- + 7 H^+ + 6 e^- ⇆ Methanol + 2 H_2O	216	-0.373
2 HCO_3^- + 14 H^+ + 12 e^- ⇆ Ethanol + 5 H_2O	364	-0.315
3 HCO_3^- + 21 H^+ + 18 e^- ⇆ n-Propanol + 8 H_2O	525	-0.302
4 HCO_3^- + 28 H^+ + 24 e^- ⇆ n-Butanol + 11 H_2O	683	-0.295
2 HCO_3^- + 12 H^+ + 10 e^- ⇆ Ethylene glycol + 4 H_2O	373	-0.387
3 HCO_3^- + 19 H^+ + 16 e^- ⇆ Propanediol + 7 H_2O	531	-0.344
4 HCO_3^- + 26 H^+ + 22 e^- ⇆ Butanediol + 10 H_2O	690	-0.325
3 HCO_3^- + 17 H^+ + 14 e^- ⇆ Glycerol + 6 H_2O	527	-0.390
Ketones/Aldehydes		
HCO_3^- + 5 H^+ + 4 e^- ⇆ Formaldehyde + 2 H_2O	181	-0.470
3 HCO_3^- + 19 H^+ + 16 e^- ⇆ Acetone + 8 H_2O	459	-0.298

4 HCO_3^- + 24 H^+ + 20 e^- ⇆ Acetoin + 10 H_2O	653	-0.338
Amino acids		
4 HCO_3^- + NH_4^+ + 14 H^+ + 12 e^- ⇆ Aspartate + 8 H_2O	387	-0.334
3 HCO_3^- + NH_4^+ + SO_4^{2-} + 22 H^+ + 18 e^- ⇆ Cysteine + 11 H_2O	513	-0.295
6 HCO_3^- + 2 NH_4^+ + 2 SO_4^{2-} + 42 H^+ + 34 e^- ⇆ Cystine + 22 H_2O	959	-0.292
5 HCO_3^- + NH_4^+ + 21 H^+ + 18 e^- ⇆ Glutamate + 11 H_2O	542	-0.312
9 HCO_3^- + NH_4^+ + 48 H^+ + 40 e^- ⇆ Phenyl alanine + 25 H_2O	1138	-0.295
11 HCO_3^- + 2 NH_4^+ + 55 H^+ + 46 e^- ⇆ Tryptophane + 31 H_2O	1342	-0.302

Table App. 2.3 - Gibbs energy change $\Delta G_r^{0'}$ and equilibrium potential $E_r^{0'}$ of specific half reactions with an organic electron acceptor. Calculated using the Growth Reference System (biochemical standard conditions: 1 atm, 298.15 K, 1 mol/L, pH 7). Data from Heijnen (Heijnen, 1999) unless otherwise indicated.

Half reaction (e-acceptor + x e^- ⇆ e-donor)	$\Delta G_r^{0'}$ (kJ/mol)	$E_r^{0'}$ (V)
Reduction of carboxylic acids to alcohols		
Formate + 5 H^+ + 4 e^- ⇆ Methanol + H_2O	138	-0.357
Acetate + 5 H^+ + 4 e^- ⇆ Ethanol + H_2O	150	-0.388
Propionate + 5 H^+ + 4 e^- ⇆ Propanol + H_2O	147	-0.382
Butyrate + 5 H^+ + 4 e^- ⇆ Butanol + H_2O	143	-0.371
Reduction of alcohol groups		
Methanol + 2 H^+ + 2 e^- ⇆ Methane + H_2O	-33	0.170
Ethanol + 2 H^+ + 2 e^- ⇆ Ethane + H_2O	-9	0.044
Propanol + 2 H^+ + 2 e^- ⇆ Propane + H_2O	-6	0.029
Glycerol + 2 H^+ + 2 e^- ⇆ Propanediol + H_2O	4	-0.021
Double bond saturation		
Fumarate + 2 H^+ + 2 e^- ⇆ Succinate	-6	0.033
Dehalogenation		
Tetrachloroethylene + 4 H^+ + 8 e^- ⇆ Ethylene + 4 Cl^-	-311	0.403
Tetrachloroethylene + H^+ + 2 e^- ⇆ Trichloroethylene + Cl^-	-93	0.484
Trichloroethylene + H^+ + 2 e^- ⇆ 1,1-Dichloroethylene + Cl^-	-84	0.437
Trichloroethylene + H^+ + 2 e^- ⇆ cis-1,2-Dichloroethylene + Cl^-	-89	0.460
Trichloroethylene + H^+ + 2 e^- ⇆ trans-1,2-Dichloroethylene + Cl^-	-85	0.438
1,1-Dichloroethylene + H^+ + 2 e^- ⇆ Chloroethylene + Cl^-	-64	0.330
cis-1,2-Dichloroethylene + H^+ + 2 e^- ⇆ Chloroethylene + Cl^-	-59	0.307
trans-1,2-Dichloroethylene + H^+ + 2 e^- ⇆ Chloroethylene + Cl^-	-64	0.330
Chloroethylene + H^+ + 2 e^- ⇆ Ethylene + Cl^-	-69	0.360

Table App. 2.4 - Gibbs energy change $\Delta G_r^{0'}$ and equilibrium potential $E_r^{0'}$ of specific half reactions with an inorganic electron acceptor. Calculated using the Growth Reference System (biochemical standard conditions: 1 atm, 298.15 K, 1 mol/L, pH 7). Data from Heijnen (Heijnen, 1999) unless otherwise indicated.

Half reaction (e-acceptor + x e^- ⇆ e-donor)	$\Delta G_r^{0'}$ (kJ/mol)	$E_r^{0'}$ (V)
Nitrogen species		
$NO_3^- + 6\ H^+ + 5\ e^- \leftrightarrows 0.5\ N_2 + 3\ H_2O$	-361	0.748
$NO_2^- + 4\ H^+ + 3\ e^- \leftrightarrows 0.5\ N_2 + 2\ H_2O$	-278	0.959
$NO_3^- + 2\ H^+ + 2\ e^- \leftrightarrows NO_2^- + H_2O$	-83	0.432
$NO_2^- + 2\ H^+ + 1\ e^- \leftrightarrows NO + H_2O$	-34	0.349
$NO + H^+ + e^- \leftrightarrows 0.5\ N_2O + 0.5\ H_2O$	-113	1.173
$0.5\ N_2O + H^+ + e^- \leftrightarrows 0.5\ N_2 + 0.5\ H_2O$	-131	1.356
$NO_3^- + 10\ H^+ + 8\ e^- \leftrightarrows NH_4^+ + 3\ H_2O$	-281	0.364
$NO_2^- + 8\ H^+ + 6\ e^- \leftrightarrows NH_4^+ + 2\ H_2O$	-198	0.341
Sulfur species		
$SO_4^{2-} + 9\ H^+ + 8\ e^- \leftrightarrows HS^- + 4\ H_2O$	167	-0.216
$SO_3^{2-} + 7\ H^+ + 6\ e^- \leftrightarrows HS^- + 3\ H_2O$	66	-0.114
$S_2O_3^{2-} + 4\ H^+ + 4\ e^- \leftrightarrows HS^- + 1.5\ H_2O$	72	-0.188
$S^0 + H^+ + 2\ e^- \leftrightarrows HS^-$	52	-0.269
$SO_4^{2-} + 8\ H^+ + 6\ e^- \leftrightarrows S^0 + 4\ H_2O$	115	-0.198
$SO_4^{2-} + 2\ H^+ + 2\ e^- \leftrightarrows SO_3^{2-} + H_2O$	101	-0.521
$S_5^{2-} + 5\ H^+ + 8\ e^- \leftrightarrows 5\ HS^-$	194	-0.251
$5\ S^0 + 2\ e^- \leftrightarrows S_5^{2-}$	66	-0.341
Other		
$2\ H^+ + 2\ e^- \leftrightarrows H_2$	80	-0.413
$O_2 + 4\ H^+ + 4\ e^- \leftrightarrows 2\ H_2O$	-345	0.816
$O_2 + 2\ H^+ + 2\ e^- \leftrightarrows H_2O_2$	-54	0.282
$H_2O_2 + 2\ H^+ + 2\ e^- \leftrightarrows 2\ H_2O$	-260	1.350
$ClO_3^- + 6\ H^+ + 6\ e^- \leftrightarrows Cl^- + 3\ H_2O$	-357	0.616 [a]
$ClO_4^- + 8\ H^+ + 8\ e^- \leftrightarrows Cl^- + 4\ H_2O$	-674	0.873 [a]
$Fe^{3+} + e^- \leftrightarrows Fe^{2+}$	-74	0.770
$Fe(CN)_6^{3-} + e^- \leftrightarrows Fe(CN)_6^{4-}$	35	0.361 [b]

[a] Value obtained from Weber et al. (2006)

[b] Value obtained from Bard et al. (1985)

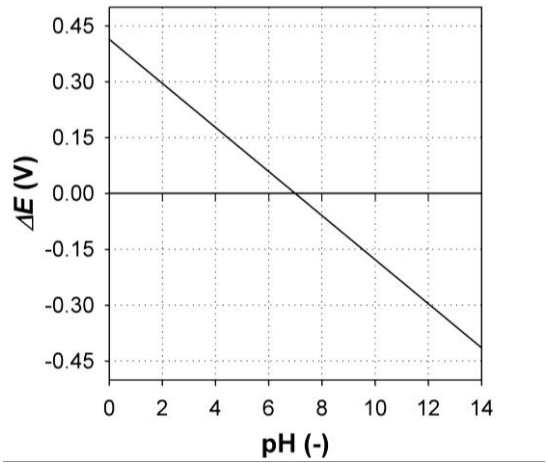

Figure App. 2.1 - A shift of one unit in the pH results in a shift of 0.059 V in the equilibrium potential for half reactions that involve as many protons in the reaction as electrons (i.e., ν_H=n) at 298.15 K.

Appendix 3 - Supplementary information for Chapter 3

1. Homoacetogenic growth medium: composition of the trace metal solution, vitamins and tungstate-selenium.

*Composition of trace metal solution (Balch et al., 1979)	g/L
Nitrilotriacetic acid (dissolve with KOH; pH 6.5)	1.5
$Mg_2Cl_2.6H_2O$	3.0
$MnCl_2.2H_2O$	0.5
NaCl	1
$FeCl_2$	0.1
$CoCl_2$	0.1
$CaCl_2.2H_2O$	0.1
$ZnCl_2$	0.1
$CuCl_2$	0.01
$AlCl_3.6H_2O$	0.01
H_3BO_3	0.01
$Na_2MoO_4.2H_2O$	0.01

**Composition of vitamin solution 123 (Greening & Leedle, 1989)	mg/L
Sodium ascorbate	10
Biotin	4
Folic acid	4
Pyridoxine hydrochoride	20
Thiamine hydrocloride	10
Riboflavin	10
Nicotinic acid	10
DL-calcium pantothenate	10
Vitamin B12	0.2
p-aminobenzoic acid	10
Lipoic (thioctic) acid	10
Myo-inositol	10
Choline chloride	10
Niacinamide	10
Pyridoxal hydrochloride	10

***Composition of tungstate-selenium solution: 0.1mM Na_2WO_4 + 0.1mM Na_2SeO_3 in 20mM NaOH

2. Carboxylic acid content per compartment in experiment 1

Table App. 3.1 and Table App. 3.2 show the final concentrations and total amount of organic carbon in each compartment at the end of the first and second batch cycle. Due to osmosis of water from the catholyte to the more saline middle compartment the total volumes in each compartment changed over time. Catholyte was periodically added to the cathodic buffer vessel to ensure enough medium would be present to obtain a good recirculation flow. The amount of carbon (mmol C) was calculated based on the final volumes and final concentrations for each cycle. For cycle two, the data are also represented as the mass of acetate in each compartment over time (Figure App. 3.1). This allows a better evaluation of the production and extraction rates, as volumes of medium in each compartment were changing over time.

Table App. 3.1 - Products at the end of cycle 1 (43 days). SCCA: short-chain carboxylic acid.

	Catholyte (mg SCCA/L – mmol C)	Extraction (mg SCCA/L – mmol C)	Anolyte (mg SCCA/L – mmol C)
Formic acid	0 – 0	143 – 1.7	39 – 0.30
Acetic acid*	1430 – 9.69	11900 – 222	6890 – 81.7
Propionic acid	0 – 0	262 – 5.92	197 – 2.83
Final volume (mL)	230	550	350

* Acetic acid represented 96.2% of all organic carbon contained in dissolved SCCAs at the end of the first batch cycle. Recovery in the extraction compartment was 73% efficient.

Table App. 3.2 - Products at the end of cycle 2 (43 days). SCCA: short-chain carboxylic acid.

	Cathode (mg SCCA/L – mmol C)	Extraction (mg SCCA/L – mmol C)	Anode (mg SCCA/L – mmol C)
Formic acid	0 – 0	176 – 2.10	57 – 0.43
Acetic acid*	2206 – 16.9	13528 – 323	9654 – 147
Propionic acid	0 – 0	95 – 3.41	97 – 2.21
Final volume (mL)	255	500	350

* Acetic acid represented 98.4% of all organic carbon contained in dissolved SCCAs at the end of the second batch cycle. Recovery in the extraction compartment was 65% efficient

Losses through volatilization were estimated to 4.4% of all acetate produced. This was calculated based on the mass of acetate retained in the 1M NaOH trap placed on the gas effluent of the extraction compartment.

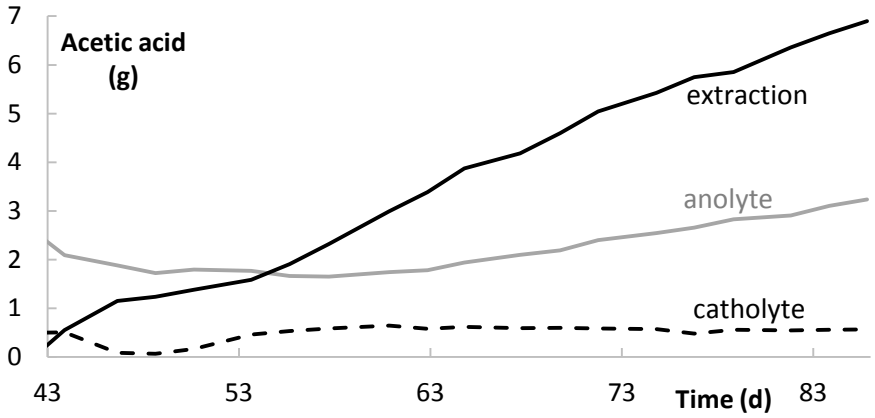

Figure App. 3.1 - Mass of acetic acid in each compartment (extraction black line, anode gray line, cathode black dotted line) during the second cycle (day 43 – 86).

3. Carboxylic acid content per compartment in experiment 2

Table App. 3.3 - Products in the reactor with extraction at the end of the 43 day production cycle. SCCA: short-chain carboxylic acid.

	Catholyte (mg SCCA/L – mmol C)	Extraction (mg SCCA/L – mmol C)	Anolyte (mg SCCA/L – mmol C)
Formic acid	0 – 0	470 – 5.90	56 – 0.34
Acetic acid*	540 – 2.47	8881 – 85.05	2583 – 12.04
Propionic acid	0 – 0	100 – 0.78	20 – 0.07
Butyric acid	0 – 0	0 – 0	0 – 0
Ethanol	0 – 0	0 – 0	0 – 0
Final volume (mL)	270	565	275

* Acetic acid represented 95.8% of all organic carbon contained in dissolved products at the end of the batch cycle.

Table App. 3.4 - Products in the reactor with CEM at the end of the 43 day production cycle. SCCA: short-chain carboxylic acid.

	Catholyte (mg SCCA/L – mmol C)	Anolyte (mg SCCA/L – mmol C)
Formic acid	0 – 0	0 – 0
Acetic acid*	10389 – 61.63	37.5 – 0.21
Propionic acid	72.16 – 0.35	0 – 0
Butyric acid	69.96 – 0.28	0 – 0
Ethanol	18.96 – 0.41	0 – 0
Final volume (mL)	270	275

* Acetic acid represented 97.6% of all organic carbon contained in dissolved products at the end of the batch cycle.

Table App. 3.5 - Products in the reactor with BPM at the end of the 43 day production cycle. SCCA: short-chain carboxylic acid.

	Catholyte (mg SCCA/L – mmol C)	Anolyte (mg SCCA/L – mmol C)
Formic acid	0 – 0	0 – 0
Acetic acid*	8092 – 63.01	767 – 4.16
Propionic acid	97 – 0.61	0 – 0
Butyric acid	70 – 0.37	14 – 0.05
Ethanol	3.59 – 0.08	0 – 0
Final volume (mL)	270	275

* Acetic acid represented 97.3% of all organic carbon contained in dissolved products at the end of the batch cycle.

4. Electron balance for experiment 2

Table App. 3.6- Electron balance for the three reactor types in experiment 2. For the reactor with cation exchange membrane (CEM), values in italic are estimations. H_2 concentrations increased above the theoretical maximum after day 32. Acetic acid was not further produced, so probably this additional H_2 was produced *via* biomass fermentation. AEM: anion exchange membrane; BPM: bipolar membrane.

Electron sink (%)	AEM reactor	CEM reactor	BPM reactor
Acetic acid	41	25	28
Other organics	1.3	0.8	0.9
H_2	28	*56.9*	52
Other (e.g. biomass)	29.7	*17.3*	19.1

5. Control experiments and biological replicate for experiment 1

To show that no acetic acid production would occur when either the catholyte was not inoculated or when no current was provided, two control experiments were carried out.

The first one, a control without inoculation, was performed using the same three-compartment setup as described, polarized at a current density of – 5 A/m². Neither vitamins nor culture were added to the catholyte. After 8 days of operation, which is longer than the lag-phase observed in the reactor experiments, no products were detected *via* ion chromatography in the catholyte. This confirms previous research on electrochemical production from CO_2 that, under the conditions in the reactor (electrode material, electrolyte and current density applied), no abiotic electrochemical reduction of CO_2 into SCCAs can be obtained (Qiao et al., 2014).

In the second control experiment, the mixed microbial community was incubated in the catholyte containing vitamins and trace-elements, but without addition of any electron donor. The incubation was performed in triplicate in serum flasks, under and N_2/CO_2 (90%/10%) atmosphere, the same gas used to sparge the catholyte. At the start of the incubation and after two weeks, samples were taken for flow cytometry analysis and measurement of SCCAs. The cell concentration (viable cells) at the start of the control experiment was (3.12 ± 0.40) × 10^6 cells/mL, similar to the reactor experiments, while this decreased to (2.02 ± 0.61) × 10^6 cells/mL after two weeks of incubation. In contrast a serum flask with electron donor (H_2/CO_2 headspace (70%/30%) showed an increase of viable cells to 1.15 × 10^8 cells/ml over the same period of time. Measurement of SCCAs showed stable concentrations between the start and the end of the incubation without electron donor (36 ± 1 mg/L *vs.* 36 ± 2 mg/L), while the parallel incubation with H_2/CO_2 produced over 1 g/L of acetic acid.

An independent experiment was performed to show the reproducibility of the technology. This experiment was run using the exact same setup and enriched mixed culture. Acetic acid production started within 3 days, a similar lag-phase as observed in the first experiment (Figure App. 3.2). The concentration in the catholyte quickly stabilised around 1 g/L while the concentration in the extraction compartment increased to 11 g/L over 43 days. This includes a short period where the culture was exposed to a pH higher than 10, on day 20. Similar to the experiment described in the main article, this pH shock did not affect the culture. The shorter exposure to a high pH can explain the faster recovery. Overall, the catholyte pH was 8.3 ± 0.6. Acetic acid was the main product, corresponding to 98.7% of all dissolved organic carbon produced at the end of the experiment. The production parameters are compared to the first two cycles in Table S3. Notice that the event resulting in pH increase falls within the period for which calculations are performed (day 6 – 43). The results of this independent experiment confirm that the reactor can be operated stably, keeping the product concentrations low in the catholyte thus avoiding product inhibition, while increased concentrations can be obtained in the extraction compartment.

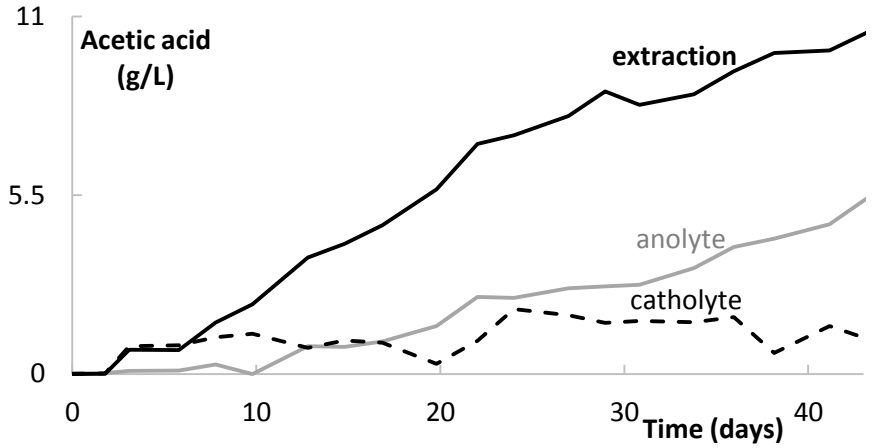

Figure App. 3.2 – Acetic acid concentration (g/L) for the cathode compartment (black dotted line), extraction compartment (full black line) and anode (gray line) compartment over a 43 days replication experiment.

Table App. 3.7 - Production parameters and average values for the three production cycles during stable operation show the good reproducibility of the proposed approach for simultaneous production and extraction of acetate. For batch 2, cycle 1 (day 6 – day 43) this includes a short period (24h, day 20) where the reactor was exposed to pH 10. CE: coulombic efficiency.

Parameter	Batch 1, cycle 1	Batch 1, cycle 2	Batch 2, cycle 1	Average ± stdev
Production rate (g/m2/d)	24.3	22.4	21.3	22.7 ± 1.5
Extraction rate (g/m^2/d)	24.2	21.2	21.3	22.2 ± 1.7
CE (%)	72.6	67.0	64.6	68.1 ± 4.1
Extraction efficiency (%)	99.5	94.3	100	97.9 ± 3.2

6. Electrochemical analysis of the cathodic process (experiment 1)

To understand the cathodic process, a CV was performed weekly with the cathode as working electrode (Figure App. 3.3).

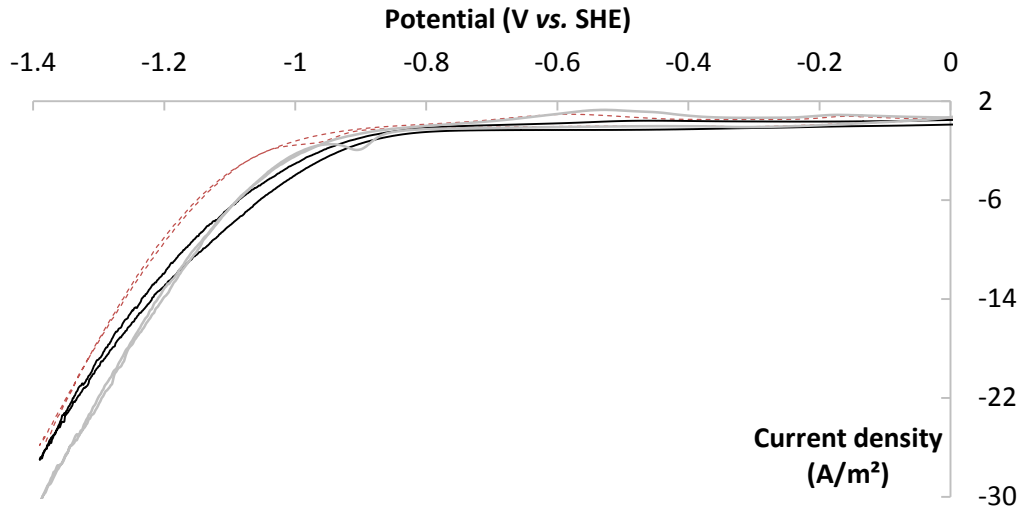

Figure App. 3.3 - CVs of the cathode recorded in abiotic conditions (black) and after 42 (gray) and 74 (red dotted) days of operation at 2 mV/s. Forward scans are negative starting from 0 V. Only the second of two successive CVs are presented. Scans are representative for cycle 1 and cycle 2.

To better understand the significance of the redox peaks observed during routine CV, a deeper investigation was carried out on day 78 and 79 of the biocathode experiment.

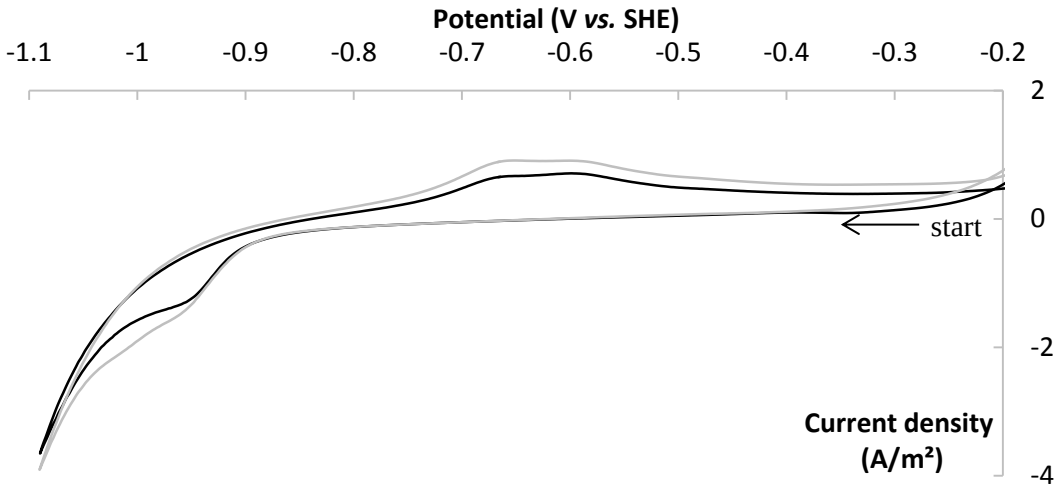

Figure App. 3.4 - Cyclic voltammograms (CVs) recorded a 2 mV/s in stagnant conditions (gray) and under convection (pumping and gas sparging, black). The two CVs were recorded immediately after eachother.

In addition to the exponential increase in the current of H_2 evolution at low potential, the CVs presented two additional zones of redox activity (Figure App. 3.4). A reduction peak appears

around - 0.96 V *vs.* SHE and an oxidative zone combining at least two peaks is visible for potentials higher than – 0.8 V. The CVs recorded under convection presented lower absolute peak currents than the ones recorded just previously under stagnant condition, proving that the peaks were related to adsorbed species rather than dissolved one(s) (and suggesting that a fraction of them may have been washed out by the convection). Furthermore, the positive back scans from the lowest potential (from – 1.1 V) showed no sign of the reductive peak mentioned above, but only the exponential shape of the abiotic H_2 evolution. This finding shows that the specie(s) associated with the negative peak were not involved in the electrocatalytic reduction, or with such a sluggish kinetics that no typical plateau-like (bio)electrocatalysis could be detected at a scan rate already as slow as 2 mV/s.

To confirm this finding, a serial of two successive experiments was performed. In the first one, eight successive CVs were recorded in the negative zone (between – 0.9 V and – 1.15 V), avoiding the oxidative zone (Figure App. 3.5). The negative peak was visible in the first negative scan, disappeared on the seven following CVs showing excellent reproducibility with only an exponential shape. It proves that none of the specie(s) involved in the reductive peak have been re-oxidized in the time scale of the measurement, oppositely to the behaviour of an electrocatalyst in presence of its substrate. Furthermore, a polarization curve showing the steady state currents recorded by chronoamperometry at different potentials (see squares on graph) showed no substantial difference with the stable successive CVs previously recorded, confirming the purely transient nature of the reductive peak and the non-involvement of the associated specie(s) in the electrocatalysis.

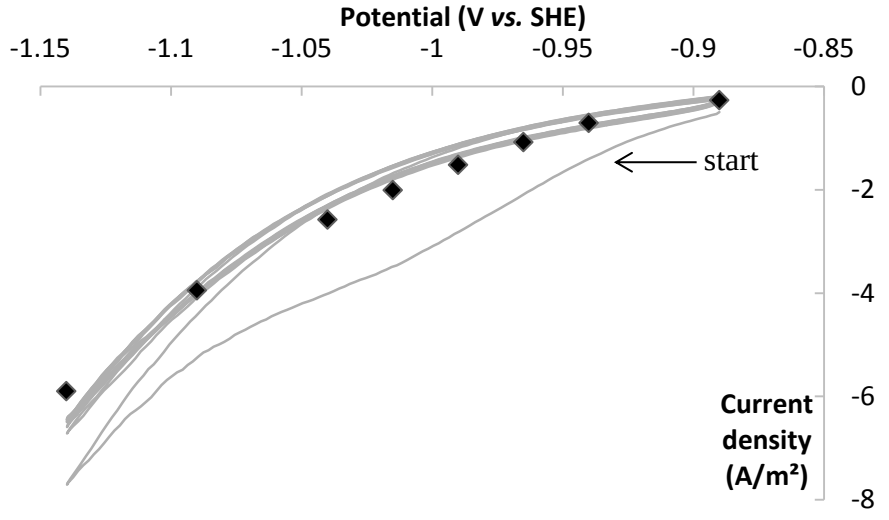

Figure App. 3.5 - Disappearance of the negative redox peak when the potential of the zone of the oxidative peaks is not reached. The apparent thick line is superposition of 7 successive CVs recorded to ascertain their stability. CVs recorded at 10 mV/s, convection (gas sparging). The squares show the steady state currents recorded by chronoamperometry at different potentials.

The third experiment shows again successive CVs, that time recorded in the range of potential including both reductive and oxidative peaks (Figure App. 3.6). In particular, the first negative scan started at – 0.9 V in a situation where all the electroactive specie(s) involved in the reductive peak are initially reduced (immediately after the experiment presented in Figure 2). This time, no reduction peak is observed for the first negative scan, but the reduction peak re-appeared in the following CVs after the oxidative zone had been reached. This interdependence between both oxidative and reductive peaks occurrence, as well as their similar surface area, confirmed that the same specie(s) were associated with both peaks zones. The large peaks to peaks separation (ΔEp) also demonstrates that a sluggish electron transfer kinetics occurs between these electroactive specie(s) and the electrode. The nature of these species remains open for discussion i.e. biological residues, adsorption of trace elements, *etc*.

More importantly, these findings support the fact that no DET was involved in the biocatalytic acetic acid production with this acetogenic mixed culture, whose reducing power was only provided indirectly *via* H_2 "abiotic " electrosynthesis.

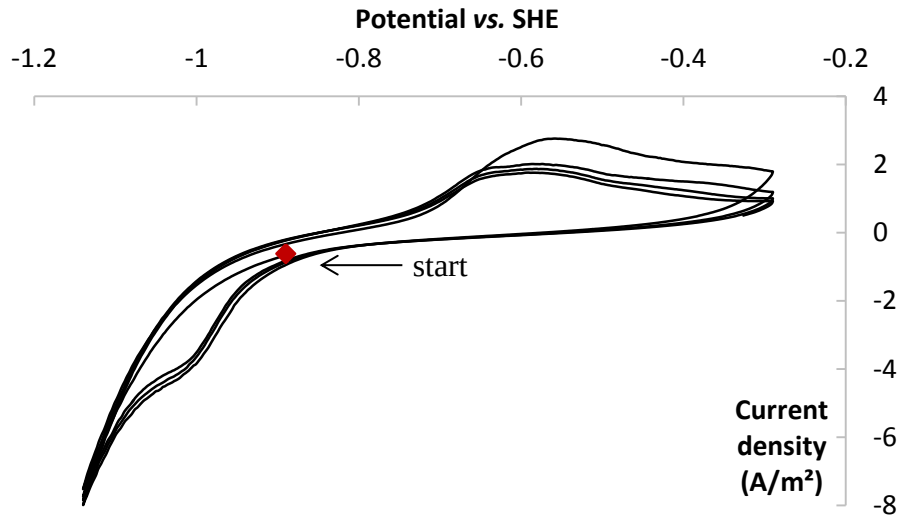

Figure App. 3.6 - CVs successively recorded in the range of potential including both reductive and oxidative peaks. The first CV starts at – 0.9 V (red square), in a situation where all the electroactive specie(s) involved in the reductive peak are initially reduced (immediately after the experiment presented in Figure 2). A scan rate of 10 mV/s was used.

Appendix 4 - Supplementary information for Chapter 4

1. Media used for syngas fermentation

1.1 P7 medium

A 2 times concentrated adapted P7 medium was used. Besides the minerals, trace elements and vitamins below, 1 mM cysteine and 1 mM Na_2S were added to the medium.

Mineral solution for 2x P7 medium (60 mL/L):

Sodium chloride	80 g/L
Ammonium chloride	100 g/L
Potassium chloride	10 g/L
Potassium phosphate monobasic	10 g/L
Magnesium chloride	16 g/L
Calcium chloride	4 g/L

100x Vitamin solution for 2x P7 medium (20 mL/L):

Pyridoxine	0.01 g/L
Thiamine	0.005 g/L
Riboflavin	0.005 g/L
Calcium pantothenate	0.005 g/L
Thioctic acid	0.005 g/L
Amino benzoic acid	0.005 g/L
Nicotinic acid	0.005 g/L
Vitamin B12	0.005 g/L
Biotin	0.002 g/L
Folic acid	0.002 g/L
Mercaptoethanesulfonic acid sodium salt	0.01 g/L

100x Trace metals solution for 2x P7 medium (20 mL/L):

Nitrilo triacetic acid	2 g/L
Manganese chloride	0.833 g/L
Ferrous ammonium sulfate	0.8 g/L
Cobalt chloride	0.2 g/L
Zinc sulfate x 7 H_2O	0.356 g/L
Copper chloride	0.02 g/L
Nickel chloride	0.02 g/L
Sodium molybdate	0.02 g/L
Sodium selenite	0.018 g/L
Sodium tungstate x 2 H_2O	0.022 g/L

1.2 "Mock" medium

A medium adapted from Mock et al. (2015) was used in a second syngas fermentation experiment. This medium was also a 2x concentrated medium. The second batch of effluent was obtained from this experiment.

Mineral solution (60 mL/L):

Sodium chloride	0 g/L (added separately, 0.24 g/L final concentration in medium)
Ammonium chloride	100 g/L
Potassium chloride	5 g/L
Potassium phosphate monobasic	27.23 g/L
Magnesium chloride x 6 H_2O	13.33 g/L
Calcium chloride	9.8 g/L

100x Vitamin solution (20 mL/L):

Pyridoxine	0.01 g/L
Thiamine	0.05 g/L
Riboflavin	0.05 g/L
Calcium pantothenate	0.05 g/L
Thioctic acid = alpha-lipoic acid	0.05 g/L
Amino benzoic acid	0.05 g/L
Nicotinic acid	0.05 g/L
Vitamin B12	0.05 g/L
Biotin	0.02 g/L
Folic acid	0.02 g/L

Mercaptoethanesulfonic acid sodium salt	0.01 g/L

100x Trace metals solution (20 mL/L):

Nitrilo triacetic acid	2 g/L
Manganese chloride	0.0252 g/L (200 µM)
Ferrous ammonium sulfate	2.84 g/L (10 mM)
Cobalt chloride	0.0476 g/L (200 µM)
Zinc sulfate x 7 H2O	0.2 g/L (700 µM)
Nickel chloride x 6 H2O	0.119 g/L (500 µM)
Sodium molybdate	0.0484 g/L (200 µM)
Sodium selenite	0.0346 g/L (200 µM)
Sodium tungstate x 2 H2O	0.0660 g/L (200 µM)

2. Visual observation of the sporulation behavior of *C. kluyveri*

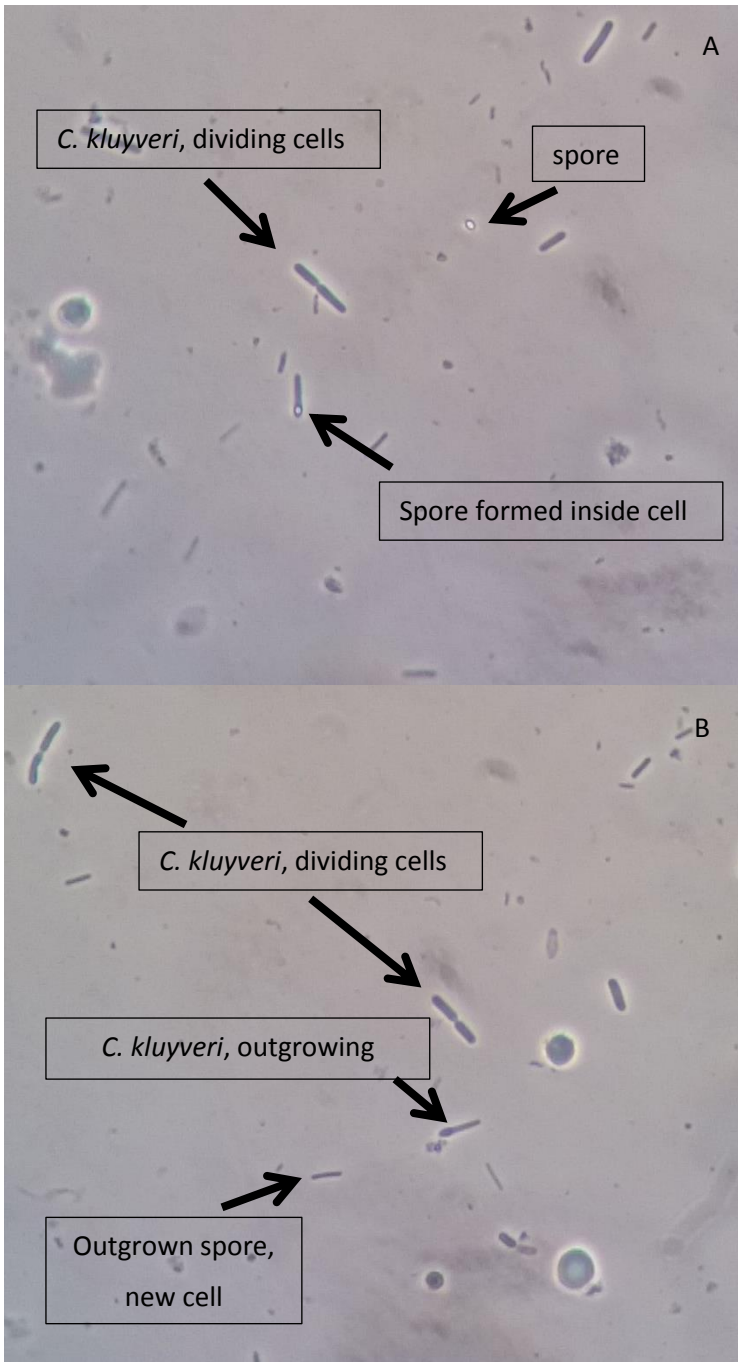

Figure App. 4.1 - Light microscopy pictures of reactor R1 (with pertraction), day 64, to illustrate the different stages of sporulation of *C. kluyveri*. Photo A: Active dividing cells; spore being formed inside a cell; free spore. Photo B: Active cells dividing; outgrowing spore; new cell (from outgrown spore).

3. Batch growth experiment: pH profile

Eight different media types (main text, Table 4.2) were used as growth medium of *C. kluyveri*. The pH of the different media did not decrease below 6 (Figure App. 4.2).

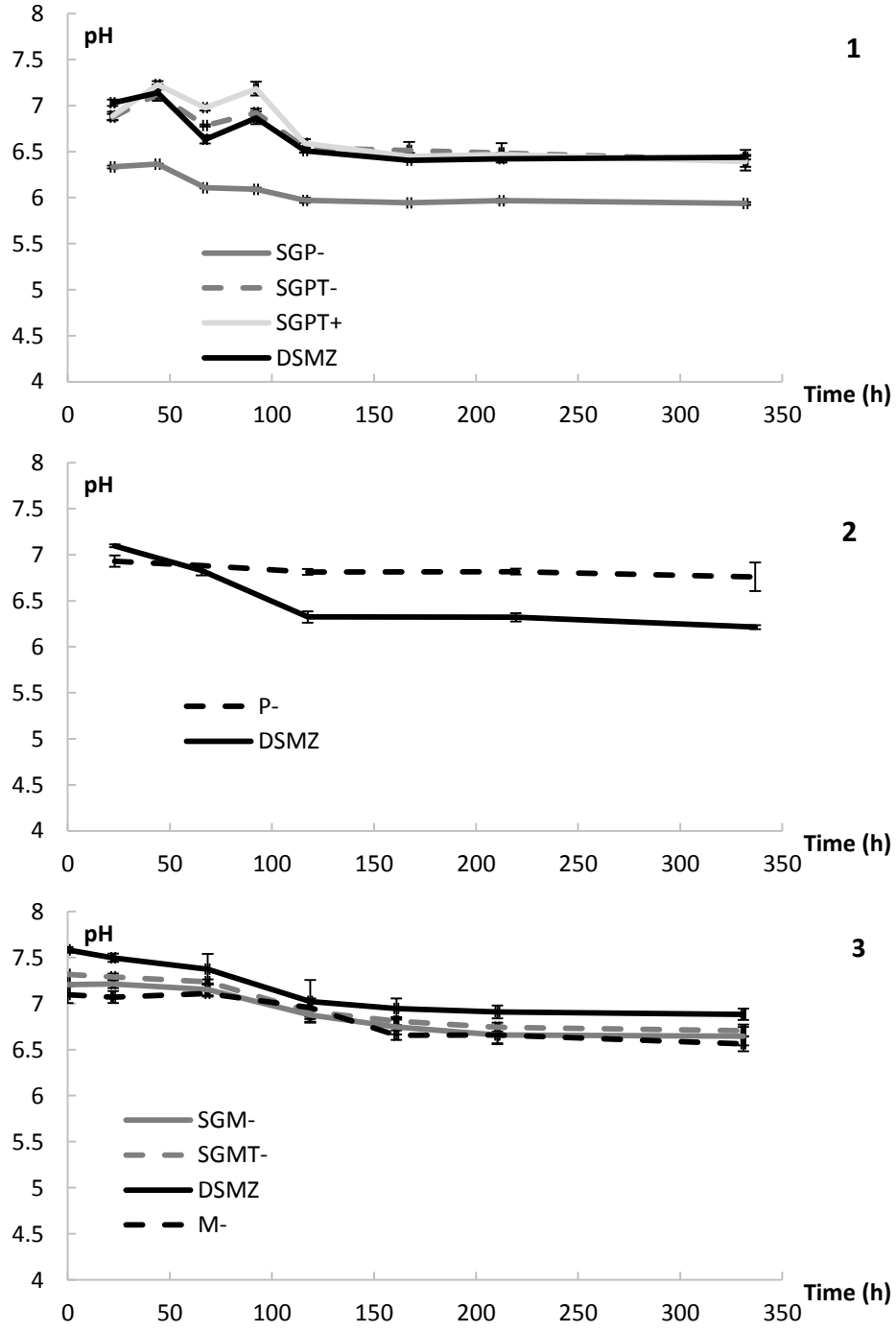

Figure App. 4.2 - pH profile of 8 media tested for chain elongation. The standard DSMZ 52 medium was each time used as control. SG: syngas fermentation effluent; P: 2 x P7 medium; M: 2 x Mock medium; T: additions (trace elements, vitamins, selenite-tungstate); -: no yeast extract; +: yeast extract added; DSMZ: standard DSMZ52 medium.

4. Optical density

The reactor with pertraction (R1) consistently had a lower OD than the reactor without pertraction (R2) (Figure App. 4.3). In the reactor without pertraction the OD_{600} was influenced by the formation of a black precipitate. This precipitate dissolved at lower pH; as such no precipitate was formed in the reactor with pertraction, operating at pH 5.50 or 6.00. In batch experiments precipitates were not formed. The composition of the precipitate was not determined. From day 80 on, the validity of OD measurements was checked by dissolving the precipitate in acid. Viability of the cells was checked with microscopy. OD was from then on always measured after dissolving the precipitate. A short-circuit was furthermore detected in the reactor with pertraction, which caused washout of biomass.

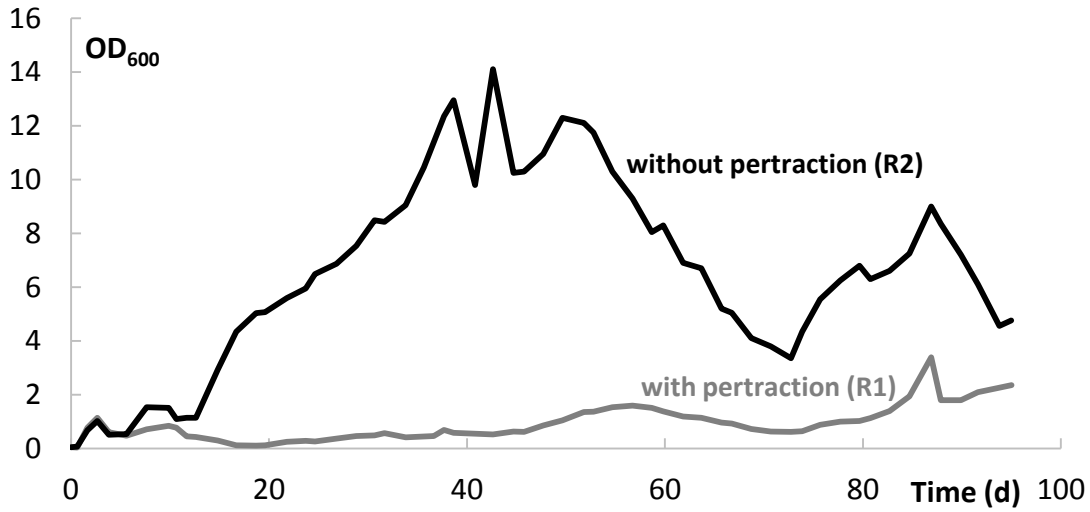

Figure App. 4.3 - Optical density (measured at 600 nm) for both bioreactors.

5. Concentrations of carboxylic acids in the reactor broth

Carboxylic acid concentrations for the reactor with (R1, Figure 4.4) and without (R2, Figure 4.5) pertraction. In the reactor with pertraction (R1), carboxylic acids were extracted from day 11 on, when the extraction modules were switched on. Part of the produced acids, mainly the MCCAs, was extracted. Due to the higher pH in the reactor (6 instead of 5.5) and problems with the pertraction unit, the extraction efficiency remained below the expected levels and (see main text Chapter 4, Table 4.3).

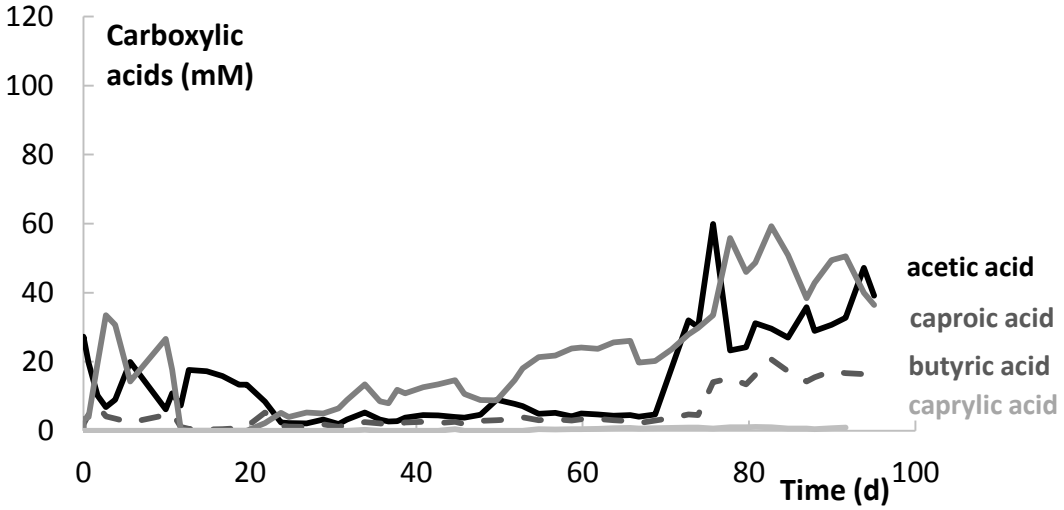

Figure App. 4.4 - Concentrations of the carboxylic acids in the reactor broth, for the reactor with pertraction (operating pH 6 from day 20 on). The low broth concentrations are due to extraction of the products in the pertraction system.

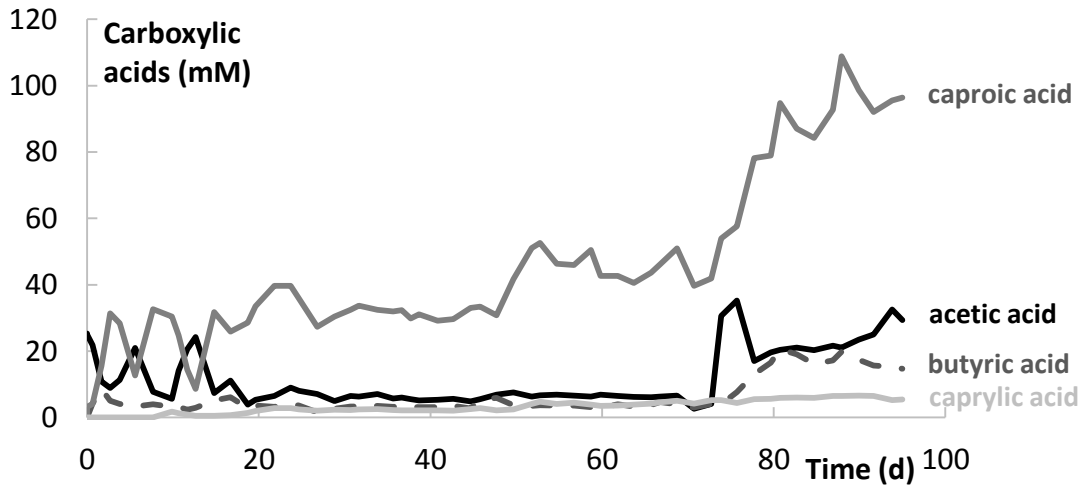

Figure App. 4.5 - Concentrations of the carboxylic acids in the reactor broth, for the reactor without pertraction (operating at pH 7).

6. Ethanol concentrations in the reactors

Figure App. 4.6 - Ethanol concentration in the reactor broth, for both bioreactors.

7. Conversion efficiency

Conversion efficiencies were calculated on a carbon basis. The ethanol and acetic acid were considered as input carbon, the butyric acid, caproic acid and caprylic acid produced, as output carbon. Biomass production and CO_2 were not taken into account for the balance.

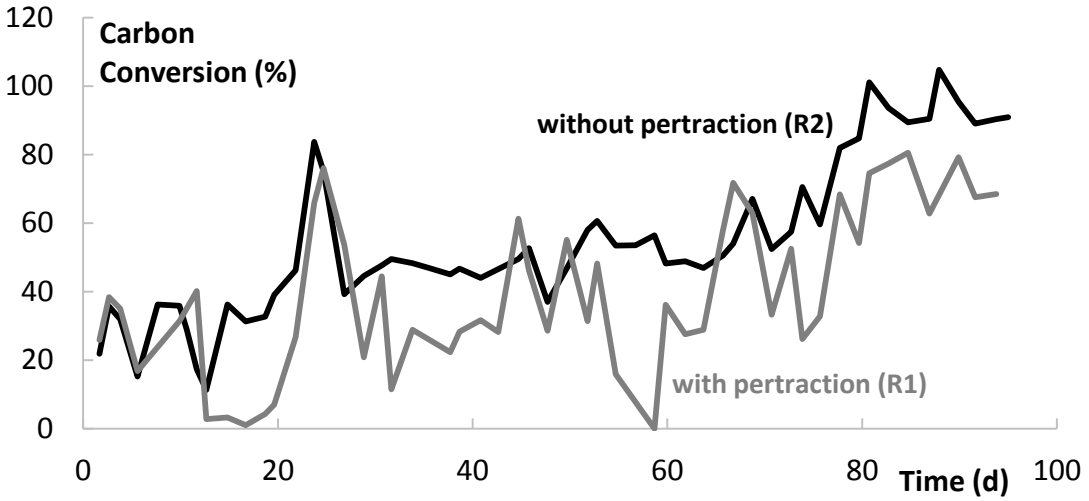

Figure App. 4.7 - Conversion of carbon in the substrate (ethanol and acetic acid) to carbon in products (butyric acid, caproic acid and caprylic acid), expressed as carbon conversion efficiency (%).

Curriculum Vitae Sylvia Gildemyn

Date and place of birth:	19th March 1989, Gent, Belgium
Nationality:	Belgian
Email:	Sylvia.Gildemyn@ugent.be
Phone:	+32497143722
Affiliation:	Ghent University, Faculty of Bioscience Engineering, Center for Microbial Ecology and Technology (CMET, http://www.cmet.ugent.be/users/ir-sylvia-gildemyn)
Workplace address:	Coupure Links 653, 9000 Gent, Belgium

Education

2012 – 2016 PhD Candidate

- Doctor of Applied Biological Sciences & Doctoral Training Programme
- Title: "Technology and tools for bioelectrochemical production of short- and medium-chain carboxylic acids from CO_2"
- Promoter: Prof. Korneel Rabaey

October 2015 – March 2016 Visiting Scientist

- The Angenent Lab, Cornell University, USA
- Advisor: Prof. Lars Angenent

2010 – 2012 Master of Science in Bioscience Engineering, Environmental Technology

- Ghent University
- Master thesis: "Valorization of biorefinery waste streams using electrochemically assisted anaerobic digestion". Center for Microbial Ecology and Technology. Promoter: Prof. Korneel Rabaey
- Institute of Chemical Technology, Prague. Czech Republic. September 2010 – January 2011. Erasmus Exchange Programme

2007 – 2010 Bachelor of Science in Bioscience engineering, Environmental Technology

- Ghent University

Publications

Articles on ISI Web of Science (published, A1)

1. Andersen, S.*, Berton, J.K.E.T.*, Naert, P.*, Gildemyn, S., Rabaey, K., Stevens, C. (2016). **Extraction and esterification of low-titer short-chain volatile fatty acids from anaerobic fermentation with ionic liquids.** ChemSusChem, 9(16): 2059–2063. (IF: 7.116. Rank 20/163). *Equal contributions.

2. Gildemyn, S., Verbeeck, K., Slabbinck, R., Andersen, S.J., Prévoteau A., Rabaey, K. (2015). **Integrated production, extraction and concentration of acetic acid from CO_2 through microbial electrosynthesis.** Environmental Science and Technology Letters, 2(11): 325–328. (IF: 4.839. Rank: 6/50).

3. Patil, S. A., Gildemyn S., Pant D., Zengler K., Logan B. and Rabaey K. (2015). **A logical data representation framework for electricity-driven bioproduction processes.** Biotechnology Advances, 33(6): 736-744. (IF: 9.848. Rank 6/161).

4. Gildemyn, S., Luther, A., Andersen, S., Desloover, J., Rabaey, K. (2015). **Electrochemical and bioelectrochemical recovery of ammonium using an electrolysis cell.** Journal of Visualized Experiments, 95, doi: 10.3791/52405. (IF: 1.113. Rank 24/62).

5. De Vrieze, J., Gildemyn, S., Vilchez-Vargas, R., Jáuregui, R., Pieper, D., Verstraete, W., Boon N. (2015). **Inoculum selection is crucial to ensure operational stability in anaerobic digestion**. Applied Microbiology and Biotechnology, 99(1): 189-199. (IF: 3.376. Rank 41/161).

6. Andersen, S.J.*, Hennebel, T.*, Gildemyn, S., Coma, M., Desloover, J., Berton, J., J., T., Stevens, C., Rabaey, K. (2014). **Electrolytic membrane extraction enables fine chemical production from biorefinery sidestreams**. Environmental Science and Technology, 48 (12): 7135-7142. (IF: 5.393. Rank 3/50). * Equal contributions

7. Sharma, M., Bajracharya, S., Gildemyn, S., Patil, S.A., Alvarez-Gallego, Y., Pant, D., Rabaey, K., Bergel, A., Dominguez-Benetton, X. (2014). **A critical revisit of the key parameters used to describe microbial electrochemical systems**. Electrochimica Acta, 140: 191-208. (IF: 4.803. Rank 3/27).

8. De Vrieze, J.*, Gildemyn, S.*, Arends, J.B.A.*, Vanwonterghem, I., Verbeken, K., Boon, N., Verstraete, W., Tyson, G.W., Hennebel, T., Rabaey, K. (2014). **Biomass retention on**

electrodes rather than electrical current enhances methane production in anaerobic digestion. Water Research, 54: 211-221. (IF: 5.991. Rank 2/50). * Equal contributions.

Articles intended for ISI Web of Science (submitted)

1. Gildemyn, S., Rozendal, R., Rabaey, K. (2016). **A thermodynamic assessment of microbial electrocatalysis.** Submitted to Trends in Biotechnology

2. Gildemyn, S.*, Verbeeck, K.*, Jansen, R., Rabaey, K. (2016). **The type of ion selective membrane determines stability and production levels of microbial electrosynthesis**. Submitted to Bioresource Technology. *Equal contributions.

Scientific Awards

ISMET Innovation Award for Best Technological Advancement, 2016, for the first author publication and reactor technology described in Gildemyn et. al. (2015): **Integrated production, extraction and concentration of acetic acid from CO_2 through microbial electrosynthesis.**

Best Oral Presentation, 2nd prize, 1st IWA Resource Recovery Conference, August 30th – September 2nd, 2015, Gent, Belgium. **Integrated production, extraction, and concentration of acetic acid from CO_2 through microbial electrosynthesis.**

Best Pitch Award, 2nd EU-ISMET *International Society for Microbial Electrochemistry and Technology Meeting*, September 3rd-5th, 2014, Alcala, Spain. **Simultaneous production and extraction of acetate from CO_2 during microbial electrosynthesis**.

EUREC Awards 2012, 2nd prize, for the Master Thesis "**Valorization of biorefinery waste streams using electrochemically assisted anaerobic digestion**".

ArcelorMittal Environmental Award 2012, nomination, for the Master Thesis "**Valorization of biorefinery waste streams using electrochemically assisted anaerobic digestion**".

IE-prijzen 2012, Public Prize "most ingenious project", for the Master Thesis "**Valorization of biorefinery waste streams using electrochemically assisted anaerobic digestion**".

Presentations at international conferences

Presenting author is underlined

1. Gildemyn, S., Verbeeck, K., Jansen, R., Rabaey, K. In-situ membrane electrolysis enables high-rate production and electrochemical pH control in microbial electrosynthesis of acetic acid from carbon dioxide. At: *3rd EU-ISMET International Society for Microbial Electrochemistry and Technology Meeting*, September 26th-28th, 2016, Rome, Italy.

2. Rabaey, K., Verbeeck, K., Patil, S.A., Arends, J.B.A., Gildemyn, S. **From electro-fermentation to microbial electrosynthesis: rapid production of carboxylic acids at high titer.** At: 3rd *AP-ISMET International Society for Microbial Electrochemistry and Technology Meeting*, August 31st- September 2nd, 2016, Busan, South-Korea.

3. Gildemyn, S., Verbeeck, K. , Patil, S.A., Slabbinck, R., Andersen, S.J., Prévoteau, A., Arends, J.B.A., Rabaey K. **Integrated production, extraction and concentration of acetic acid from CO_2 through microbial electrosynthesis.** At: *5th international ISMET International Society for Microbial Electrochemistry and Technology Meeting,* October 1st-4th, 2015, Tempe, Arizona, USA.

4. Rabaey, K., Gildemyn, S., Verbeeck, K., Arends, J.B.A., Guo, K., Patil, S.A., Prevoteau, A. **How useful is electricity as driver for microbial processes?** At: *5th international ISMET International Society for Microbial Electrochemistry and Technology Meeting,* October 1st-4th, 2015, Tempe, Arizona, USA.

5. Arends, J.B.A, Ameril, C., Gildemyn, S., Patil, S., Roume, H., Rabaey, K. **Cathodic polarization in a BES allows efficient conversion of glycerol into 1.3 propanediol and VFAs compared to addition of other electron donors**. At: *4th IWA-Young Water Professionals Benelux,* September 28th-29th, 2015, Leeuwarden, The Netherlands.

6. Christiaens, M., Gildemyn, S., D'hooge, R., Rabaey, K. **Fermentation of urine results in electrochemical production of industrial resources**. At: *4th IWA-Young Water Professionals Benelux,* September 28th-29th, 2015, Leeuwarden, The Netherlands.

7. Gildemyn, S., Verbeeck, K., Slabbinck, R., Andersen, S.J., Prévoteau A., Rabaey, K. **Integrated production, extraction and concentration of acetic acid from CO_2 through microbial electrosynthesis.** At: *1st IWA Resource Recovery conference*, August 30th-September 2nd 2015, Ghent, Belgium.

8. Gildemyn, S., Verbeeck, K., Andersen, S., Rabaey, K. **Microbial electrosynthesis - electricity driven bioproduction and extraction**. At: *2nd EU-ISMET International Society for Microbial Electrochemistry and Technology Meeting*, September 3rd-5th, 2014, Alcala, Spain.

9. Arends, J.B.A., De Vrieze, J., Gildemyn, S., Vanwonterghem, I., Verbeken, K., Boon, N., Verstraete, W., Tyson, G., Hennebel, T., Rabaey, K. **Biomass retention on electrodes rather than electrical current enhances stability in anaerobic digestion**. At: *2nd EU-ISMET International Society for Microbial Electrochemistry and Technology Meeting*, September 3rd-5th, 2014, Alcala, Spain.

10. Gildemyn, S., Verbeeck, K., Andersen, S., Rabaey, K. **Microbial electrosynthesis - electricity driven bioproduction and extraction**. At: *2nd AP-ISMET International Society for Microbial Electrochemistry and Technology Meeting*, July 21st-23rd, 2014, Singapore.

11. Andersen, S., Hennebel, T., Gildemyn, S., Coma, M., Berton, J., Stevens, C., Rabaey, K. **Electrolytic membrane extraction enables fine chemical production from biorefinery side streams**. At: *11th IWA Leading Edge Technology Conference on Water and Wastewater Technology*, 26th-29th May, 2014, Abu Dhabi, United Arab Emirates.

12. Andersen, S., Hennebel, T., Gildemyn, S., Coma, M., Berton, J., Stevens, C., Rabaey, K. **Electrolytic membrane extraction enables fine chemical production from biorefinery side streams**. At: *Francqui Symposium: Recent advances in microbial and enzymatic electrocatalysis*, November 22nd, 2013, Ghent, Belgium.

13. Gildemyn, S., Guo, K., Rabaey, K. ***In-situ*** **extraction of microbial electrosynthesis products**. At: *Young Water Professionals BeNeLux*, October 4th, 2013, Belval, Luxemburg.

14. De Vrieze, J., Gildemyn, S., Arends, J.B.A., Braems, A., Vanwonterghem, I., Boon, N., Verstraete, W., Tyson, G.W., Hennebel, T., Rabaey, K. **A bioelectrochemical system in anaerobic digestion: Stabilization and remediation**. At: *4th International MFC Conference*, September 4th, 2013, Cairns, Australia.

15. Patil, S.A., Arends, J.B.A., Gildemyn, S., Silva, J., Rabaey, K. **Microbial electrosynthesis with an enriched mixed homoacetogenic culture**. At: *4th International MFC Conference*, September 3rd, 2013, Cairns, Australia.

16. De Vrieze, J., Gildemyn, S., Arends, J.B.A., Boon, N., Verstraete, W., Hennebel, T., Rabaey, K. **A Bioelectrochemical System as Stabilizing and Remediating Agent in Anaerobic Digestion**. At: *13th World Congress on Anaerobic Digestion*, June 25th – 28th, 2013, Santiago de Compostela, Spain.

17. De Vrieze, J., Gildemyn, S., Arends, J.B.A., Boon, N., Verstraete, W., Hennebel, T., Rabaey, K. **A Bioelectrochemical System as Stabilizing and Remediating Agent in Anaerobic Digestion**. At: *1st EU-ISMET European International Society for Microbial Electrochemistry and Technology Meeting*, September 26th – 28th, 2012, Ghent, Belgium.

18. De Vrieze, J., Gildemyn, S., Verstraete, W., Boon, N. **Variation and Inoculum Selection Induces Functional Stability In Anaerobic Digestion**. At: *ISWA World Solid Waste Congress*, September 17th – 19th, 2012, Firenze, Italy.

Other relevant experience

Organizational

1. Organizing committee *1st IWA Resource Recovery conference*, August 30th-September 2nd 2015, Ghent, Belgium.
2. Organizing committee 1st EU-ISMET European International Society for Microbial Electrochemistry and Technology Meeting, September 26th – 28th, 2012, Ghent, Belgium.

Educational

1. Teaching of the calculation excercices for the course “Biotechnological Processes in Environmental Sanitation”. 2012, 2013, 2014.
2. Guidance of 1 bachelor project and 6 master thesis students. 2012-2016

Completed courses

1. Francqui lectures and master class “Water 4.0”. Instructor: professor David Sedlak (University of California, Berkley)
2. Effective Scientific Communication. Instructor: Dr. Jean-Luc Doumont
3. Effective Graphical Displays. Instructor: Dr. Jean-Luc Doumont

Dankwoord – Acknowledgements

Na vier jaar doctoreren moeten er nog enkele bladzijden tekst geschreven worden. Telkens de laatste waar een doctorandus aan begint, en de eerste die door iedereen worden gelezen, na het titelblad dan. Voor de laatste keer staar ik dus naar een wit blad, vooraleer ik aan dit dankwoord begin. Want na vier jaar doctoreren wil ik graag heel wat mensen, die van dichtbij of van ver aan dit doctoraat hebben bijgedragen, bedanken. Er komen waarschijnlijk drie talen aan te pas, u bent gewaarschuwd!

Korneel, in de eerste plaats wil ik jou bedanken voor jouw fantastische rol als promotor. Tijdens mijn masterthesis sprak ik je nog aan als “professor Rabaey”, dat is vervolgens gelukkig snel veranderd. Dank om mij de kans te geven dit onderzoek bij CMET uit te voeren. Misschien startte ik met een naïef idee van wat onderzoek inhield, maar door de jaren heen ben ik met jouw input enorm gegroeid in mijn rol als onderzoeker. Ik heb de kans gekregen om veel bij te leren, onder andere door samen te werken met onderzoeksgroepen in het buitenland en ik heb kunnen kennismaken met belangrijke spelers in de industrie. Wanneer het moeilijk ging en ik de moed verloor was mijn manier om dat duidelijk te maken misschien niet altijd even subtiel, maar je slaagde er telkens in het volgende concreet doel te herdefiniëren om stap voor stap vooruitgang te boeken, en mij opnieuw te motiveren. Je zal me vooral bijblijven als een prof met een uitgebreid netwerk, met een grote interesse voor onderzoek, maar die ook steeds op zoek gaat naar samenwerking met de industrie. Een prof die er, ondanks de soms beperkte beschikbare tijd, sterk op toeziet dat iedereen van het team zich goed in de groep voelt. Jammer dat ik vanaf nu het mecat weekend zal moeten missen, maar ik kijk al uit naar de volgende barbecue!

Ook de andere proffen van CMET wil ik graag bedanken. Prof. Verstraete, Willy, u was de eerste die mij over doctoreren sprak en me aanmoedigde na m’n master aan onderzoek te doen. Ook in de afgelopen vier jaar kruisten we elkaar vaak, en telkens polste u naar de vooruitgang van mijn onderzoek en mijn toekomstige plannen. Het is fijn te weten dat u uw oud-studenten zo blijft volgen en steunen. Nico, Tom en Siegfried, ondanks het groeiend aantal mensen op het labo, vroegen jullie ook telkens met oprechte interesse naar mijn progressie en plannen, wat ik enorm apprecieerde. Nico, ik zal niet vergeten dat je me persoonlijk naar het UZ Gent bracht toen ik in mijn aangezicht verbrand raakte bij het maken van anaeroob medium. Tom, het was heel fijn dat je je buitenlandervaring deelde tijdens de kajaktocht van de teambuildingactiviteit vorig jaar.

Van bijzonder groot belang, voor het afronden van een doctoraat, is de input van de jury op het finale werk. Annemiek, na jou ontmoet te hebben tijdens de voorbije ISMET congressen, waar er steeds een open discussie rond ons onderzoek was, was het een genoegen je als jurylid te hebben. Jouw vragen hebben tot verdere reflectie geleid, waardoor ik verschillende aspecten van mijn onderzoekswerk nog verder heb kunnen verduidelijken. Lars, na het verblijf in jouw labo in Cornell University, was het evident dat je deel zou uitmaken van deze jury. Je kritische kijk op mijn werk heeft het zeker naar een hoger niveau getild. Maar ik kon ook zeker de complimenten die je bij de

evaluatie neerschreef bijzonder appreciëren! Marjan en Monica, van jullie beiden kreeg ik bijzonder constructieve commentaar, waardoor mijn doctoraat (hopelijk) ook voor het bredere publiek van deze faculteit bio-ingenieurswetenschappen een hapklare brok wetenschappelijk onderzoek werd. Pascal, bedankt om de verdedigingen in goede baan te leiden, waardoor de voorverdediging ook veel korter werd dan ik me ooit had kunnen inbeelden.

Terug naar het labo… Vier jaar geleden, bij de start va mijn doctoraatsonderzoek, kon men de leden van de groep die rond bio-elektrochemische systemen werkte nog op één hand tellen. Als nieuweling kreeg ik meteen de taak de toenmalige BES-clusters in goede banen te leiden. Enkele maanden later werd de groep omgedoopt tot de mecat-groep, werd de structuur van de clusters overhoop gehaald, en werden de wekelijkse mecat meetings geïntroduceerd. Intussen is de groep zodanig gegroeid dat de Kleine Academieraadzaal uit z'n voegen barst bij voltallige aanwezigheid. The input of the mecat group has been essential to succeed in this PhD research, and I'd like to thank every member of the group for their input along the way. Whether it was during cluster presentations, a coffee break, while working in the Technology Hall, or even after working hours, the discussions and exchanges have been extremely valuable. The diverse expertise and background of all group members is a real asset. So, thank you to all of you, my colleagues, and in particular the MESS-cluster. Jan, hoewel ik meer dan eens gewoon mijn eigen weg opging, heb ik het altijd enorm geapprecieerd dat ik steeds om raad kon vragen. Je bent een wandelend vat BES-kennis! Stephen, it was great to have someone else struggling with extractions and anion exchange membranes at the beginning of my PhD as well. Thank you for all the scientific input and proofreading of manuscripts. There's no doubt all the discussions and collaborative labwork have been extremely important for my PhD thesis. Soupi, I'd like to thank you for the numerous hours you helped me trying to figure out why the overpotential in my reactor was so high, or what electron-transfer mechanisms could take place in my reactor. Kristof, dank voor het vele samenwerken, vooral bij de start van de experimenten met de "drie-compartimenten-reactor", en in het afgelopen jaar. Het mag zeker een succes genoemd worden!

I also want to thank the six master students that I guided during the last four years: João, Kristof, Esther, Rik, Tess, and Robbe. You'll probably see that many of the results that we generated together are now part of this PhD thesis. Het doet me ook enorm veel plezier, Kristof en Esther, dat jullie er voor gekozen hebben een doctoraat te starten, ondanks de soms harde realiteit van het onderzoek waar jullie tijdens jullie thesis mee geconfronteerd werden. Ik wens jullie heel veel succes de komende jaren en kijk er al naar uit aanwezig te zijn op jullie verdediging.

Een doctoraatsthesis op CMET (ik moet toegeven dat LabMET nog steeds natuurlijker klinkt), kan niet tot stand komen zonder de bijdrage van het ATP. Het staat in elk dankwoord dat geschreven wordt bij het afsluiten van een doctoraat bij CMET, en ik kan met zekerheid zeggen dat dit telkens zeer gemeend is. Inderdaad, Christine en Regine, jullie verzetten bergen werk voor ons, staan altijd

meteen klaar met raad en daad om ons te helpen, of het nu gaat om een bestelling die we na de officiële termijn tóch nog willen plaatsen, papierwerk voor het doctoraat, of het halen van, alweer, een nieuwe toner voor de printer. Sarah, ik heb m'n best gedaan om telkens de tallying op tijd in te vullen, en was heel blij dat je me afgelopen zomer kon melden dat ik nog net voldoende budget had om de allerlaatste analyses voor mijn doctoraat uit te voeren. Jana, jou wil ik enorm hard bedanken: je leerde me anaerobe pure culturen opkweken, ik kon tijdens vakantieperiodes op jou rekenen om de anaerobe culturen te onderhouden, je zorgde voor stockoplossingen, en zoveel meer. Allemaal zaken die het onderzoek vooruithielpen en versnelden! Tim, dankzij jou staan er op mijn posters, in mijn papers, en nu ook in mijn doctoraat prachtige figuren, die onderzoeksresultaten zoveel duidelijker maken. Mike, een labo als CMET draaiende houden is geen sinecure, dank daarvoor. Greet, dank om mijn stalen af en toe wat voorrang te geven tijdens de IC-analyses! Robin, zonder jouw reactor-building skills hadden we gegarandeerd (nog) meer lekkende reactoren, en dank ook om me te leren hoe de reusachtige boor in de workshop veilig kan worden gebruikt.

During my PhD, I also had the chance to visit several labs abroad to learn new techniques, or work on different topics. Un grand merci à Fréderic Barrière et Laure Lapinsonnière de m'avoir accueilli à Rennes en 2012. La semaine passée dans votre labo m'a permis d'apprendre énormément, aussi bien sur l'électrochimie que la chimie des surfaces. In January 2014 I had the opportunity to spend a week at the Novo Nordisk Foundation for Biosustainability in Copenhagen, to learn more on anaerobic culturing techniques. I'd like to thank Tian Zhang for the week spent there, and I must say I'm still jealous about the hydrogen gas lines in the lab, having to walk from the microbial lab to the TechHall with a gas bag to get hydrogen gas, each time I transferred my culture. My longest, and undoubtedly most interesting stay abroad, was the six months I spent in the Angenent Lab at Cornell University. Lars, the welcome in your group, your guidance, your critical follow-up of the experiments, and the opportunities you gave me to work together with several people of the group, made this stay a great success for me. It was very enriching to focus on a different topic, biological chain elongation, for six months, after having spent most of my PhD working on microbial electrosynthesis. I think all my colleagues here in Gent know as well how valuable this experience was, as I am now, even more than before, a great advocate of international mobility. I hope I'll have the chance to visit you in Tübingen one day, and I wish you good luck setting up the new lab.

Dit is het punt in het dankwoord waar heel wat collega's al denken, "wanneer gaat ze nu iets "interessants" zeggen?". Inderdaad, ik moet m'n collega's stuk voor stuk bedanken, want het succesvol afronden van een doctoraat, doe je ook dankzij de steun van collega's. Thank you, all my CMET colleagues! The fact that I now realize how different it will be when I leave the lab, is definitely because at CMET, colleagues very often become friends over the years. First, I want to thank the office colleagues. In 2012 moesten we nog afscheid nemen van ons gezellig bureautje met prachtig zicht op de binnentuin van de faculteit, maar we konden het uitzicht behouden en kregen een grote

bureau met internationale collega's in de plaats. Ik hou enorm goede herinneringen over aan de Rotonde 1.0, van de frietclusters, tot het ineensteken van onze nieuwe stoelen en bureaus… Joachim, in het eerste anderhalf jaar van m'n doctoraat stond je altijd paraat om me aan te moedigen, ik denk dat je onderschat hoe belangrijk dat is geweest. Willem, "den bompa", altijd bereid om klassiekers, weetjes, en quizvragen met ons te delen, net als Simon trouwens. Sam, de avonturier met ongelooflijke photoshop skills, dankzij jou hebben we allemaal een prachtige trui en koffietas. Joeri and Stephen, the two "old-Rotonderos" who'd always be present at the beer-cluster for some afterwork fun. En natuurlijk Emilie en Synthia, twee fantastische collega's waarmee ik lief en leed heb kunnen delen, heb gelachen en gefluisterd (al bleek dat ook soms voor teveel lawaai te zorgen in het bureau); ik hou er ongelooflijk goede herinneringen aan over, en het is super dat we alle-drie de eindmeet hebben gehaald. And then the "new" Rotonde 2.0, with Marta, Eleni, Francis, Oliver, Kun, Benjamin, Dries, Sunil, Antonin, Alberto, Cristina C., Naya, Way, Hugo, Mélanie, Charlotte, Chiara, Tom, Wendy, Delphine, Ruben, Lorenzo, Amanda, Erika, Elephteria, Ioanna, Jeet, and the many visiting scientists that spent some time in the office… Great to share an office with so many great people! I hope some of the traditions such as the Friday lunches will survive. And there are of course more people to mention, for the lunch breaks, the CMET running club, and the Fridays at Koepuur: Jo, Jan, Jana, Marlies, Eline, Annelies, Curro, Ralph, Gio, Samuel, Cristina P., Tim, Ramiro, Pieter, Pieter, Mathias, Kim, Floor, Wim, FM, Alessia, Victoria, Ramon… Thank you for all the great moments! In particular: Benjamin, ¡Muchas gracias!, voor het jaartje Spaanse les samen. Dank aan Jana, Annelies en Eline voor de ladies-nights. Tim, geef maar een seintje als je nog eens fietsbegeleiding naar het station nodig hebt. Kun, I enjoyed our week eating (non-spicy!) crêpes in Rennes. Het Belval & Ikea dinner team: prachtige herinneringen! The whole Sicily-trip team: that was an amazing week, in particular the Etna-climb! Pieter, dank voor de steun tijdens het schrijven en afronden, het is me veel waard geweest, meer dan je misschien zelf beseft. En proficiat ook, dat je je stempel kon drukken op de Koepuur avonden, met de introductie van de nu alomtegenwoordige Rodenbach. Je voorgangers (Joachim – Ename Blond; Ramiro – Vedett; Joeri – Witkap) zijn intussen opgenomen in de Galerij der Groten van de Vrijdagen in de Koepuur. Stephen, we became really good friends over the years, following the same timing between starting and ending our PhD. I can already say I'll miss your "Can I ask you a science question?", but I'm looking forward to many more coffees together, discussing life, work, science and dreams. And we'll both be Dr. then, congrats to you too! Soupi, véritable ambassadeur de la culture française et du cinéma international, je sais qu'on se croisera encore souvent et ce sera un véritable plaisir à chaque fois.

And then there's this other group of colleagues and friends that I, of course, want to mention in these acknowledgements. To everyone I met in Ithaca, or the USA, and I could share this amazing experience with: thank you! Everyone from the Angenent Lab, and in particular Juan, Bastian, Joe, Hanno, Catherine and Lauren: thank you for the amazing welcome, the help, and the corridor-beers. And then after working hours: Cassi, Matt, Francis, Koenraad, Pria, Krissy, Michele and of course,

Bianca… It's been an unforgettable experience and I hope to see many of you back some day, somewhere in the world.

Er is gelukkig ook tijd voor een leven naast een doctoraat, en daarvoor wil ik ook heel wat mensen bedanken. Aan de boerekot-bende, Sacha, Marieke, Elina, Pieter, Elien, Maurine, Kristien; al blijven we na vier jaar met niet zoveel achter in Gent, jullie zijn een fantastische bende vrienden, ik kijk altijd uit naar het volgend weerzien. In 2017 moeten we zeker weer een weekend plannen! Elina, dank om met jou de frustraties van het doctoreren te kunnen ventileren! De Bavo-bende, die ik dan misschien wel zonder vaste frequentie kruiste, ik heb heel goede herinneringen aan etentjes, veel te kleine disco's op de Gentse Feesten, en gezellige reünies. Et puis la bande de Sainte-Colette et le staff AV1, pleins de bons moments passés avec vous tous, même maintenant qu'on n'est plus des chefs actifs. Je suis certaine que beaucoup de barbecues et kroegentochten suivront encore! Cédric, un tout grand merci d'avoir créé la couverture de mon doctorat, et aussi de toujours partager tes projets avec tant d'enthousiasme. Louis, altijd een plezier om je te kruisen op het boerekot of in de Koepuur, en ik hoop van harte ergens rond 2020 of 2022 naar jouw doctoraatsverdediging te mogen komen.

Et aussi, bien sûr, un grand merci à ma famille. Je sais que vous pensez que votre rôle dans cette réussite est trop petit pour valoir une mention dans ce mot final, mais ça n'est sûrement pas vrai. Marie-Pascale, tu as été la première avant moi de faire un doctorat, et je te remercie de m'avoir soutenu, sachant qu'il y a des moments difficiles, à côté de la réussite. Je garde de très bons souvenirs de notre séjour à Philadelphie. Maman, Papa, Delphine, Thomas et Maïté, merci d'avoir été là, même si mes bactéries, mon vinaigre, et jus de chèvre n'étaient pas toujours votre sujet de conversation préféré. Mais j'ai pu partager avec vous mes moments de frustrations et de grande joie, merci, ça a été très important pour moi. Papa, j'apprécie énormément que tu aies relu mon premier manuscrit, et merci à toi et maman d'avoir traversé l'océan pour me rendre visite à New York. Delphine, Thomas et Maïté, je ne pense pas que vous allez avoir le courage de lire ce livre, mais il y a un compte-rendu (en néerlandais, s'il vous plait), pour que vous compreniez enfin à quoi j'ai bien pu m'occuper pendant ces 4 ans ;-) Merci à tous!

Sylvia, September 2016

"Be micro-ambitious. Put your head down and work with pride on whatever is in front of you… you never know where you might end up." – Tim Minchin